2002

Mechanisms of somatostatin-induced paradoxical increase in insulin secretion in the presence of arginine vasopressin in clonal [beta]-cell HIT-T15

Henrique Cheng
Iowa State University

INFORMATION TO USERS

This manuscript has been reproduced from the microfilm master. UMI films the text directly from the original or copy submitted. Thus, some thesis and dissertation copies are in typewriter face, while others may be from any type of computer printer.

The quality of this reproduction is dependent upon the quality of the copy submitted. Broken or indistinct print, colored or poor quality illustrations and photographs, print bleedthrough, substandard margins, and improper alignment can adversely affect reproduction.

In the unlikely event that the author did not send UMI a complete manuscript and there are missing pages, these will be noted. Also, if unauthorized copyright material had to be removed, a note will indicate the deletion.

Oversize materials (e.g., maps, drawings, charts) are reproduced by sectioning the original, beginning at the upper left-hand corner and continuing from left to right in equal sections with small overlaps.

Photographs included in the original manuscript have been reproduced xerographically in this copy. Higher quality 6" x 9" black and white photographic prints are available for any photographs or illustrations appearing in this copy for an additional charge. Contact UMI directly to order.

ProQuest Information and Learning
300 North Zeeb Road, Ann Arbor, MI 48106-1346 USA
800-521-0600

UMI®

Mechanisms of somatostatin-induced paradoxical increase in insulin secretion in the presence of arginine vasopressin in clonal β-cell HIT-T15

by

Henrique Cheng

A dissertation submitted to the graduate faculty

in partial fulfillment of the requirements for the degree of

DOCTOR OF PHILOSOPHY

Major: Physiology (Pharmacology)

Program of Study Committee:
Walter H. Hsu, Major Professor
Franklin A. Ahrens
Lloyd L. Anderson
Janice E. Buss
Donald C. Dyer
Srdija Jeftinija
Etsuro Uemura

Iowa State University

Ames, Iowa

2002

ProQuest Information and Learning Company
300 North Zeeb Road
P.O. Box 1346
Ann Arbor, MI 48106-1346

Graduate College

Iowa State University

This is to certify that the doctoral dissertation of

Henrique Cheng

has met the dissertation requirements of Iowa State University

Signature was redacted for privacy.

Major Professor

Signature was redacted for privacy.

For the Major Program

TABLE OF CONTENTS

LIST OF ABBREVIATIONS

AVP	Arginine vasopressin
BK	Bradykinin
$[Ca^{2+}]_i$	Intracellular calcium concentration
cAMP	Cyclic adenosine monophosphate
DAG	Diacylglycerol
DHP	Dihydropyridines
ER	Endoplasmic reticulum
GDP	Guanosine diphosphate
G-protein	Guanine nucleotide-binding protein
GPCR	G-protein coupled receptor
Grb-2	Growth factor receptor-binding protein 2
GTP	Guanosine triphosphate
IBMX	3-isobutyl-1-methylxanthine
IGF-1	Insulin-like growth factor-1
IP_3	Inositol 1,4,5-trisphosphate
IP_4	Inositol 1,3,4,5-tetrakisphosphate
IRS-1	Insulin receptor substrate-1
MAPK	Mitogen-activated protein kinase
PH	Pleckstrin homology
PI	Phosphatidylinositol
PIP, PI4P, PI5P	Phosphatidylinositol 4- or 5-phosphate
PIP_2	Phosphatidylinositol 4,5-bisphosphate
PIP_3	Phosphatidylinositol 3,4,5-trisphosphate
PKA	Protein kinase A
PKC	Protein kinase C
PLA	Phospholipase A
PLC	Phospholipase C
PLD	Phospholipase D
PTX	Pertussis toxin
ROC	Receptor-operated Ca^{2+} channel
SHC	Src homology 2-containing protein

SHPTP-2	Src homology 2 domain-containing protein-tyrosine phosphatase
SRIF	Somatostatin
TG	Thapsigargin
VDCC	Voltage-dependent Ca^{2+} channel

ABSTRACT

We investigated the mechanism underlying somatostatin-induced increase in $[Ca^{2+}]_i$ leading to insulin release in the presence of arginine vasopressin (AVP) in clonal β-cell HIT-T15. Somatostatin increased $[Ca^{2+}]_i$ and insulin release in a biphasic pattern, characterized by a sharp and transient increase followed by a rapid decline to the sub-basal level. Pretreatment with pertussis toxin, which inactivates Gi/Go, abolished the effects of somatostatin. U-73122, an inhibitor of phospholipase C, antagonized somatostatin-induced increase in $[Ca^{2+}]_i$. In Ca^{2+}-free environment, somatostatin still increased $[Ca^{2+}]_i$, whereas depletion of intracellular Ca^{2+} stores with thapsigargin, a microsomal Ca^{2+} ATPase inhibitor, abolished somatostatin's effect. In the presence of bradykinin, another Gq-coupled receptor agonist, somatostatin also increased $[Ca^{2+}]_i$, but not in the presence of isoproterenol (a Gs-coupled receptor agonist) or medetomidine (a Gi/Go-coupled receptor agonist). Utilizing selective agonists for each somatostatin receptor subtype (SSTR1-5) and PRL-2903, a specific SSTR2 antagonist, we characterized the receptor mediating the somatostatin signaling. In the presence of AVP, treatment with the SSTR2 agonist L-779,976 resulted in responses similar to those seen with somatostatin. L-779,976 increased both $[Ca^{2+}]_i$ and insulin release in a dose-dependent manner. Treatment with L-779,976 alone did not alter $[Ca^{2+}]_i$ or basal insulin release. In the presence of AVP, all other somatostatin receptor agonists failed to increase $[Ca^{2+}]_i$ and insulin release. The effects of somatostatin and L-779,976 were abolished by PRL-2903. Administration of antibody against the β subunit of Gi/Go into single cells inhibited the increase in $[Ca^{2+}]_i$ by somatostatin, but antibodies against Giα1/Giα2 and Giα3/Goα failed to do so. Somatostatin increased PIP_2 synthesis from PIP in the presence and absence of AVP, whereas an increase in IP_3 synthesis was observed only in the presence of AVP. Taken together, our study strongly suggests that activation of the SSTR2 coupled to Gi/Go by somatostatin increases PIP_2 synthesis through the βγ dimer. The PIP_2 generated by somatostatin serves as additional substrate for preactivated PLC-β, which hydrolyzes PIP_2 to form IP_3, leading to Ca^{2+} release from the endoplasmic reticulum and insulin release in clonal β-cell HIT-T15. The increases in $[Ca^{2+}]_i$ and insulin release are due to a cross-talk between Gq and Gi/Go, although not limited to the AVP and somatostatin receptors.

CHAPTER I GENERAL INTRODUCTION

Dissertation Organization

This dissertation is written in an alternative thesis format. It contains a general introduction, three research papers, a general discussion, a list of references cited in the general introduction and discussion, and acknowledgments. The general introduction includes a research objective, background information, and literature review. Chapter II, "Somatostatin-induced paradoxical increase in intracellular Ca^{2+} concentration and insulin secretion in the presence of arginine vasopressin in clonal β-cells HIT-T15", and Chapter III, "SSTR2 mediates the somatostatin-induced increase in intracellular Ca^{2+} concentration and insulin secretion in the presence of arginine vasopressin in clonal β-cell HIT-T15", have been accepted for publication in the *Biochemical Journal and Life Sciences*, respectively. Chapter IV, "Somatostatin increases phosphatidylinositol 4,5-bisphosphate formation via βγ dimer of Gi/Go in clonal β-cells HIT-T15: mechanisms for its paradoxical increase in insulin release" has been submitted for publication in the *Journal of Biological Chemistry*.

This dissertation contains the experimental results obtained by the author during his graduate study under the supervision of his major professor, Dr. Walter H. Hsu.

Research Objective

The hormone insulin is synthesized and released from pancreatic β-cells, and is the most important regulator of elevated blood glucose levels. The mechanisms that regulate insulin secretion are rather complex from an endocrine point of view. Although an increase in blood glucose levels is one of the most potent stimulators for insulin release, several hormones act directly or indirectly in the pancreas to stimulate or inhibit its release. Inhibition of insulin secretion by somatostatin (SRIF) has been well characterized in studies utilizing the whole pancreas, pancreatic islets and several β-cell lines. Arginine vasopressin (AVP), a hormone normally found in the posterior pituitary gland, is also present in the pancreas. We previously demonstrated AVP's ability to stimulate the release of glucagon and insulin from the rat pancreas, in the α-cell line InR1G9 and β-cell line RINm5F.

The research presented in this dissertation focuses on a novel response to SRIF in an insulin secreting cell line HIT-T15, in which SRIF induces a paradoxical increase in $[Ca^{2+}]_i$, leading to insulin release in the presence of AVP. The objectives of this study are: 1) Characterize the SRIF receptor subtype that mediates the increase in $[Ca^{2+}]_i$ and insulin release, 2) Characterize which subunit of Gi/Go mediates the intracellular signaling by SRIF, and 3) Measure PIP_2 and IP_3 mass formation by SRIF in the presence of AVP. In these studies we have characterized a novel mechanism by which SRIF stimulates insulin release in the presence of AVP, through a cross-talk between Gq and Gi/Go.

Background and Literature Review

This section provides background information related to the studies that are presented in the dissertation: 1) Regulation of insulin secretion; 2) Heterotrimeric G-proteins; and 3) Signal transduction by AVP and SRIF.

The endocrine pancreas

During development, the pancreas arises from the gut endoderm as two buds, the duodenal and the hepatic diverticula. The dorsal bud develops from the dorsal wall of the duodenum and later forms the entire body, tail, and part of the head of the pancreas. The remaining posterior portion of the head is derived from the ventral bud, which arises from the primitive bile-duct. The glandular tissue of the pancreas is developed by budding and branching of the primordial epithelial cell cords. This budding result from cell division in a plane perpendicular to the axis of the lumen of the forming ducts, disrupting tight-junction complexes and promoting cell separation. The endocrine pancreas is formed by the islets of Langerhans, which were first described in 1869 by Paul Langerhans. The islets originate from specialized buds of the same epithelial tissue that gives rise to the pancreatic ducts and acinar cells. The endocrine cells generally separate at an early stage and undergo independent differentiation, although some retain their original connection with the ducts.

The islets constitute 1-2 % of the pancreas and the main cell types present are β-cells (secreting insulin), α-cells (secreting glucagon), δ-cells (secreting SRIF) and PP-cells (secreting pancreatic polypeptide), occurring in the ratio 68:20:10:2 % (Rahier, 1988). During embryonic development, α-cells usually are the first to develop and the PP-cells the last. The core of each islet consists primarily of β-cells surrounded by a cortex of α- and δ-

cells or, in the posterior region of the head, of PP-cells (Orci, 1985). The cell types of islets can be distinguished by various histological stains, such as safranin and methyl green (α-cells red and β-cells green), Gomori's aldehyde fuchsin trichrome (β-cells deep violet, α-cells red, and δ-cells green), or by silver impregnation methods of Grimelius (α-cells) and Davenport (δ-cells). In addition to histological techniques, electron-microscopy of secretory granules, specific immunocytochemical stains and *in situ* hybridization for hormone products have been developed.

Islets are innervated by a complex network of sympathetic and parasympathetic nerves, and are vascularized by direct arteriolar blood flow. Although they constitute only 1-2 % of the pancreas, they receive approximately 20 % of total pancreatic blood flow (Lifson et al., 1985). Afferent arterioles, arising from branches of the splenic and pancreatic-duodenal arteries, may supply acinar tissue before reaching the islets. Within the islets, the arterioles branch to form a dense mesh of wide, anastomosing capillary, reminiscent of the renal glomerulus. Arterioles enter the core of β-cells to branch into a portal system of capillaries, which carry blood from β-cells to surrounding cells (Bonner-Weir and Orci, 1982). Cortex cells are not only exposed to blood-borne nutrients but also secretory products of β-cells, particularly insulin. In addition to the circulatory route, direct cell-to-cell communications through gap junctions are present. Gap junctions are specialized junctions that can allow passage of electrical impulses, ions, and low molecular weight molecules (<1000) (Meda et al., 1984). The pancreas receives its extrinsic innervation from the coeliac plexus.

Islets play a central role in hormonal control of fuel metabolism and particularly of glucose homeostasis. Maintenance of a normal plasma glucose concentration during periods of food consumption and fasting requires a precise balance between glucose production and utilization. Although control of glucose homeostasis involves many hormonal and neural factors, insulin and glucagon are the major determinants of this control. Insulin is secreted by β-cells in response to nutrients to promote energy storage in targets organs (liver, skeletal muscle, and adipose tissue); glucagon release by α-cells is then inhibited. In the postabsorptive state, while insulin secretion falls, glucagon is stimulated, which activates glycogenolysis and gluconeogenesis; this reciprocal change in plasma insulin-glucagon ratio will favor energy store consumption. Biosynthesis and secretion of

these two hormones must be tightly regulated to match fuel production and delivery to metabolic demands.

Insulin synthesis, secretion and metabolism

Insulin is synthesized and stored within pancreatic β-cells where it is released upon stimulus. In humans, the gene encoding preproinsulin is located on the short arm of chromosome 11 (Bell et al., 1980). It has 1355 base pairs and its coding region consists of three exons: the first encodes the signal peptide at the N-terminus of the preproinsulin, the second the B chain and part of the C peptide, and the third the remaining of the C peptide and the A chain. Transcription and splicing to remove the sequences encoded by introns yields a mRNA of 600 nucleotides, which after translation, gives rise to the preproinsulin (109 amino acids). The preproinsulin is converted to proinsulin after cleavage by proteolytic enzymes in the cisternal space of the rough endoplasmic reticulum. The proinsulin contains the A and B chains (21 and 30 amino acids respectively) of insulin, which are linked by C peptide (30-35 amino acids) (Kemmler et al., 1972). The major function of C peptide is to align the disulfide bridges that link the A and B chains so the molecule is folded properly for cleavage. Proinsulin is transported to the Golgi apparatus (Orci et al., 1987), where it is packed into vesicles. The conversion of proinsulin into insulin begins in the Golgi apparatus and continues within the maturing secretory granules through the sequential action of prohormone convertases 2 and 3, and carboxy peptidase H (Hutton, 1994). The actions of these enzymes on proinsulin cleaves the C peptide chain giving rise to insulin (Fig. 1), which are stored in granules and released upon stimulus.

Insulin secretion occurs in a coordinated matter during exocytosis, in which insulin containing granules move close to the cell membrane, until fusion of granules and membrane promotes the release of insulin into the blood stream (Lacy, 1970). Following incorporation of the granule/membrane, the expanded membrane is partially reabsorbed into the cell by endocytosis and recycled back to the Golgi apparatus. The role of cytoskeletal components, mainly microtubules and microfilaments in the translocation of insulin granules inside the cell has been extensively studied. However, the precise mechanism by which metabolic signals developed during stimulation of insulin secretion are translated into granule movement and exocytosis remains unknown. Treatment of β-cells with microtubule inhibitors such as colchicines, vinblastine and nocodazole inhibits glucose-stimulated insulin secretion (Howell, 1984). Other contractile proteins such as actin and myosin participate in

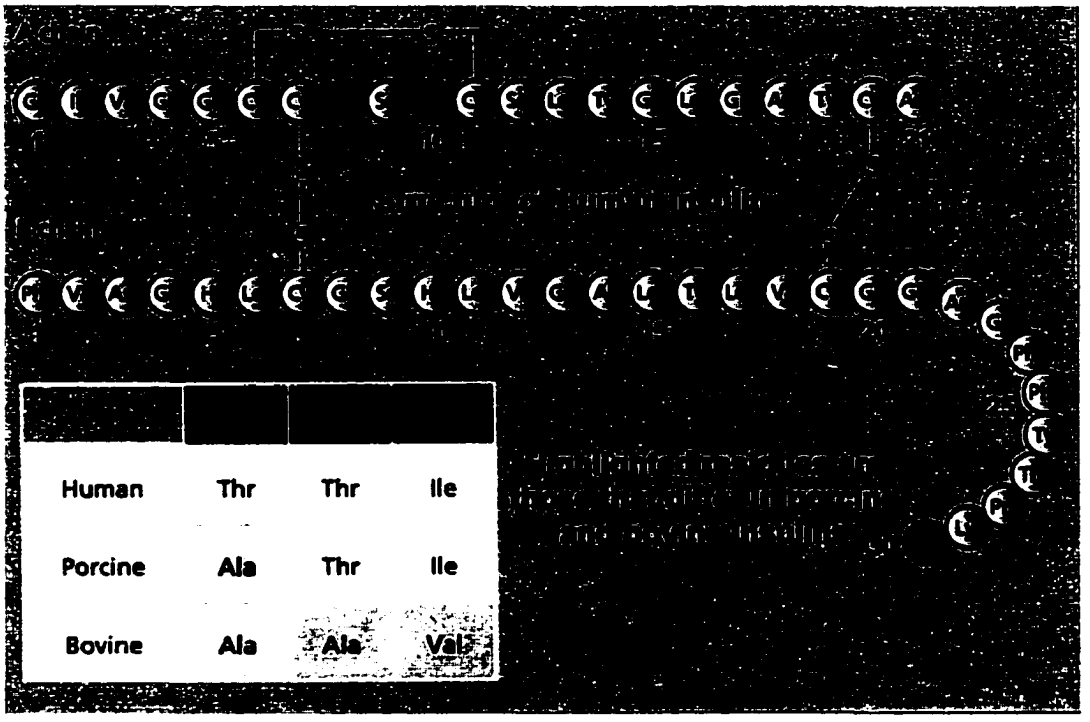

Figure 1. The primary structure of human insulin (Modified from Wood and Gill, 1997).

the insulin secretory pathway. Actin, the component of microfilaments is present in cells in two forms: a globular form of 43 kDa and a filamentous form, which associate to form microfilaments. Involvement of microfilaments in insulin secretion derives partly from observations that insulin secretion is inhibited by cytochalasin B and phalloidin, both of which interfere with microfilament formation (Howell, 1984). Both myosin light chain and heavy chain are found in rat islets at concentrations that are considerably higher than those present in the liver, and have been localized by immunofluorescence to both α- and β-cells. It is possible that microfilaments, microtubules and myosin act together to transport insulin granules along the cytoplasm. Other molecules such as kinesin and dynein may interact with microtubules in the transport of granules, since these proteins are responsible for organelle transport in a variety of cell types.

Insulin is normally degraded within the liver and kidneys, with a plasma half-life of approximately 5 min in humans. The major enzyme responsible for insulin degradation is hepatic glutathione insulin dehydrogenase, which splits the hormone into its A and B chains. Glutathione, a cysteine-containing tripeptide acts as a cofactor for the transhydrogenase to reduce the individual half-cysteine moieties of the disulfide bonds (Duckworth, 1988).

Regulation of insulin secretion

The main physiological determinant for insulin secretion is blood glucose concentration, although metabolic, endocrine, neuronal and pharmacological agents can also promote insulin secretion. Through GLUT-2, glucose is transported into β-cells and phosphorylated by glucokinase to generate glucose 6-phosphate, which undergoes glycolysis to produce ATP. Generation of ATP closes ATP-sensitive K^+ channels in the membrane, causing depolarization, leading to Ca^{2+} influx through voltage-dependent channels. The increase in $[Ca^{2+}]_i$ then triggers insulin secretion (Ashchroft et al., 1984). Glucose-stimulated insulin secretion is biphasic, comprising a rapid first phase lasting 5-10 min, followed by a prolonged second phase, that continues for the duration of the stimulus. The shape of the glucose-response curve is determined by the activity of the glucokinase, which dictates the rate-limiting step for glucose metabolism (Van Schaftingen, 1994).

Amino acids such as leucine and arginine can also stimulate insulin secretion, although the mechanism is not well understood. In the case of arginine, the inward movement of its cationic charge may depolarize the cell membrane and open voltage-dependent Ca^{2+} channels (Hermans et al., 1987). Leucine may generate ATP through its metabolism, and promote closure of ATP-sensitive K^+ channels in a similar manner to glucose (McClenaghan and Flatt, 2000). Several hormones and neurotransmitters can also influence insulin secretion. Secretagogues such as glucagon, arginine vasopressin, gastric inhibitory peptide, cholecystokinin, opioids, vasoactive intestinal peptide and glucagon-like peptides can stimulate insulin secretion, while SRIF, pancreastatin, galanin and neuropeptide Y can inhibit insulin secretion (McClenaghan and Flatt, 1999). The autonomic innervation of pancreatic islets also plays a role with its vagal inputs stimulating, and sympathetic endings and catecholamines present in the circulation inhibiting insulin secretion. The stimulatory effect of the parasympathetic system is mediated by muscarinic cholinergic receptors, while circulatory or locally released catecholamines exert their inhibitory action via α_2 adrenergic receptors (Ahren, 2000; Sivitz et al., 2001). The effect of pharmacological agents such as sulfonylureas, which promotes closure of ATP-sensitive K^+ channels by binding to receptors closely associated to these channels leads to depolarization and subsequent insulin secretion (Zunkler et al., 1988). Atypical sulfonylureas derivative, such as diazoxide, a potent but reversible inhibitor of insulin secretion, act by opening ATP-sensitive K^+ channels (Sturgess et al., 1988).

Development of clonal hamster β-cells (HIT)

In the early 1980s, most of the understanding of insulin biosynthesis and β-cell metabolism was derived from *in vitro* studies utilizing isolated islets, either intact or dissociated in monolayer culture. Such studies were limited by difficulties in the preparation of even small quantities of islets; cellular and hormonal heterogeneity within islets; and rapid loss of insulin production *in vitro*. In rats, the development of a transplantable insulinoma (Chick et al., 1977) resulted in the purification and characterization of preproinsulin mRNA (Duguid et al., 1976), and cloning and sequence analysis of cDNA (Villa-Komaroff et al., 1978). The need for permanent cell lines that possessed functions characteristic of differentiated β-cells that would facilitate *in vitro* studies, lead Robert Santerre and colleagues to develop the clonal hamster β-cell (HIT) (Santerre et al., 1981). This cell line was established by Simian virus 40 transformation of Syrian hamster pancreatic islet cells. Analysis of cytoplasmic insulin by fluorescent antibody staining demonstrated that insulin was present in all cells. Hamster insulin was detected from extracts of HIT cell cultures through radioimmunoassay, radioreceptor assay, and bioassay. Stimulation of insulin secretion was confirmed by exposure to glucose, glucagon and IBMX, where as inhibition of insulin secretion was demonstrated by exposure to SRIF and dexamethasone. Development of the HIT cell line originated a unique model system to study β-cells, due to its ability to provide unlimited material for biochemical studies of membrane receptors or mRNA processing. The HIT cell line became a popular and well-accepted model to investigate mechanisms controlling insulin secretion. The main characteristic of glucose-stimulated insulin release by HIT cells was similar to those of normal islets (Ashcroft et al., 1986).

HIT cells have been extensively used in the study of signal transduction in β-cells, such as the effect of secretagogues on $[Ca^{2+}]_i$ and insulin secretion (Hughes and Ashcroft, 1988), cloning of the α_1 subunit of voltage-dependent Ca^{2+} channels (Seino et al., 1992), regulation of insulin gene transcription by glucose (Olson et al., 1995), regulation of insulin secretion by IGF-1 (Zhao et al., 1997). The role of PKC during AVP-induced insulin secretion has been reported in HIT cells (Hughes et al., 1992). Inhibition of insulin secretion by SRIF is associated with decreases in cAMP and $[Ca^{2+}]_i$ through inhibition of Ca^{2+} influx via L-type voltage-dependent Ca^{2+} channels (Hsu et al., 1991), opening ATP-sensitive K^+ channels (Ribalet and Eddlestone, 1995), and activation of the Ca^{2+}-dependent protein phosphatase calcineurin (Renstrom et al., 1996).

Regulation of insulin secretion by AVP and SRIF

Chemistry and biosynthesis of AVP and SRIF

Arginine vasopressin (AVP) is a nonapeptide hormone (Fig. 2) folded into a ring through a disulfide bridge at positions 1 and 6, leaving a terminal tripeptide side chain. AVP is synthesized within the cell bodies of neurons in the pars nervosa, stored in neurosecretory granules and released from the axonal endings (Russel et al., 1990). A number of AVP-like peptides have been described in different species. All of them contain cysteine residues in positions 1 and 6 and have a disulfide bridge and conserved amino acids (Asn, Pro, Gly) in positions 5, 7 and 9. In mammals, these peptides contain Arg in position 8 and thus the term arginine vasopressin. In addition to AVP, in swine, the arginine can be replaced with lysine, and therefore called lysine vasopressin (LVP). AVP is a product of a preprohormone with 168 amino acids that is synthesized and incorporated into ribosome. During synthesis, a signal peptide (residues -23 to -1) is removed to form pro-AVP, then is translocated through the rough endoplasmic reticulum and incorporated into large membrane-enclosed granules. The prohormone consists of three domains: AVP (residues 1-9), AVP-neurophysin or neurophysin II (residues 13-105) and AVP-glycopeptide or copeptin (residues 107-145). In secretory granules, the prohormone is sequentially cleaved by endopeptidase, exopeptidase, monooxygenase and lyase to form AVP. AVP-neurophysin contains a sequence of more than 90 amino acids that is identical in some species (Land et al., 1983). AVP secretion can be induced by an increase in plasma osmolality, hypovolemia and hypotension, pain, nausea, hypoxia, and agents such as acetylcholine, histamine, dopamine, glutamine, cholecystokinin, and angiotensin II. An increase in plasma osmolality of about 2 % has been shown to cause a two- to three-fold increase in plasma AVP levels. In addition to the pituitary gland, AVP has also been found in the adrenal gland, cerebellum (Richter et al., 1990), ovary (Guldenaar et al., 1984), thymus (Geenan et al., 1986), testis (Guldenaar and Pickering, 1985) and pancreatic islets (Sanchez-Franco et al., 1986).

SRIF, a tetradecapeptide, is synthesized from a large preproSRIF precursor molecule that is processed enzymatically to yield several mature products. cDNAs for preproSRIF molecules were first identified in 1980 followed by elucidation of the structure of rat and human SRIF genes in 1984 (Montminy et al., 1984; Shimon et al.,1997). Mammalian proSRIF consists of 92 amino acids that is processed predominantly at the C-

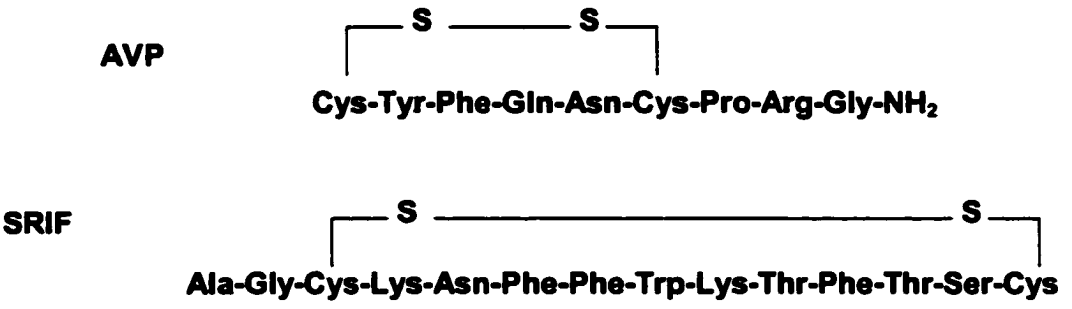

Figure 2. Structures of AVP and SRIF (Modified from Ganong, 1997).

terminal segment to generate two bioactive forms, SRIF-14 and SRIF-28. The two peptides are synthesized in variable amounts by different SRIF-producing cells. SRIF-14 (Fig.2) predominates in pancreatic islets, stomach, neural tissues, and is virtually the only form in retina, peripheral nerves, and enteric neurons. SRIF-28 accounts for 20-30 % of total immunoreactive SRIF in brain, although it is not clear whether it is co-synthesized with SRIF-14 or whether it is produced in separate neurons. SRIF-28 is synthesized as a terminal product of proSRIF processing in intestinal mucosa cells that constitute the largest peripheral source of the peptide. Several genes encoding SRIF-like peptides have been identified (Hobart et al., 1980; Montminy et al., 1984; Shen and Rutter, 1984). The various forms observed in mammals are all derived from differential processing of a common precursor preproSRIF-I. A novel SRIF-like gene called cortistatin (CST), that gives rise to two cleavage products comparable to SRIF-14 and -28 was described in human and rat (De Lecea et al., 1996). These cleavage products consist of human CST-17 and its rat homologue CST-14 and human and rat CST-29. Unlike the broad distribution of the preproSRIF-I gene, expression of CST genes is restricted to the cerebral cortex.

Secretion of SRIF can be influenced by a number of secretagogues ranging from ions and nutrients, to neuropeptides, neurotransmitters, classical hormones, growth factors, and cytokines (Patel, 1992; Reichlin, 1983). Some of these agents exert common effects on SRIF cells in different locations presumably by direct action, where others tend to be tissue-selective. Membrane depolarization stimulates SRIF release from both neurons and peripheral SRIF-secreting cells, suggesting that this mode of release is a fundamental property of all SRIF containing cells (Patel, 1997).

Actions of AVP and receptors

AVP has two major physiological roles: it induces the contraction or relaxation of vascular smooth muscle and promotes water movement across epithelial tissues. In this manner, AVP regulates body fluid volume, osmolality, and maintains normal blood pressure. AVP increases glycogenolysis (Kirk et al., 1979), proliferation of the pituitary gland (McNichol et al., 1990), and secretion of clotting factors (Fuchs and Fuchs, 1984). An increase in adrenocorticotropic hormone (ACTH) (Robinson, 1987), thyroid-stimulating hormone (TSH) (Lumpin et al., 1987), and catecholamine secretion (Grazzini et al., 1996) has also been reported for AVP. In the pancreas, studies have demonstrated AVP's ability to increase glucagon and insulin secretion from α- and β-cells, respectively (Chen et al., 1994; Yibchok-anun et al., 2000). Behavior can be influenced by AVP, where it is involved in acquisition and maintenance of adaptation, and in the learning and memory process (Goodson and Bass, 2001).

AVP receptors are classified according to the second messenger system coupled to them and the affinity of various AVP analogues. There are two types of AVP receptors, the V_1 and V_2 (Guillon et al., 1980). The V_1 receptor posses two subtypes, the V_{1a} and V_{1b}, because the binding properties of V_{1b} to various vasopressin agonists and antagonists differ from those of V_{1a} receptors (Schwartz et al., 1991). The V_{1a} receptor, the most widespread subtype, is present in vascular smooth muscle, myometrium, the bladder, adipocytes, hepatocytes, platelets, renal medullary interstitial cells, vasa recta in the renal microcirculation, epithelial cells in the renal cortical collecting duct, spleen, testis, and many CNS structures (Birnbaumer, 2000). The V_{1b} receptor is present in the adenohypophysis, kidney, thymus, heart, lung, spleen, uterus, breast, as well as in pancreatic islets (Lolait et al., 1995; Saito et al., 1995). The V_{1b} receptors have been pharmacologically characterized in the rat adrenal medulla (Grazzini et al., 1996), rabbit tracheal epithelium (Tamaoki et al., 1998) and rat pancreas (Lee et al., 1995; Yibchok-anun et al., 1999). The V_2 receptor is present mainly in the renal collecting duct system.

AVP receptors belong to the seven-transmembrane family that is coupled to G-proteins, containing seven hydrophobic transmembranes α-helices joined by different intracellular N-terminal and extracellular C-terminal domains. Both V_{1a} and V_{1b} receptors are coupled to Gq and signal through the PLC pathway (Jans et al., 1990), whereas the V_2 receptor is coupled to Gs, which activates adenylyl cyclase, leading to generation of cAMP (Thibonnier, 1992). The second intracellular loop of the V_1 receptor plays a key role in the

selective activation of Gq and the third intracellular loop of the V_2 receptor is responsible for recognition and activation of Gs (Barberis et al., 1998).

Actions of SRIF

SRIF-producing cells are present in high densities throughout the central and peripheral nervous systems, endocrine pancreas, and in the gut. A small number are found in the thyroid, adrenal, and submandibular glands, kidneys, prostate, and placenta (Patel, 1992; Reichlin, 1983). Gastrointestinal SRIF cells are of two types: δ cells in the mucosa and neurons that are intrinsic to the submucous and myenteric plexuses (Hokfelt et al., 1975). In the pancreas, SRIF cells are confined to the islet and found in δ-cells in close proximity to insulin, glucagon, and pancreatic polypeptide-producing cells (Dubois, 1975). Within the thyroid, SRIF coexists with calcitonin in a subpopulation of parafollicular cells (Reichlin, 1983). In the rat, the gut accounts for 65 % of total body SRIF, the brain for 25 %, the pancreas for 5 %, and the remaining organs for 5 % (Patel and Reichlin, 1978).

In the brain, SRIF functions as a neurotransmitter with effects on cognitive, locomotor, sensory, and autonomic functions (Epelbaum et al., 1994). It inhibits the release of dopamine from the midbrain and norepinephrine, thyrotropin-releasing hormone (TRH), corticotropin-releasing hormone, and endogenous SRIF from the hypothalamus. In addition, it inhibits both basal and stimulated secretion of growth hormone, thyroid-stimulating hormone (TSH), and islet hormones (Patel, 1992). In the gastrointestinal tract it inhibits the release of virtually every gut hormone that has been tested. SRIF stimulates migrating motor complex activity (Reichlin, 1983). The effects on the thyroid include inhibition of TSH-stimulated release of thyroid hormones and calcitonin from parafollicular cells. The adrenal effects consist of the inhibition of angiotensin II stimulated aldosterone secretion and the inhibition of acetylcholine-stimulated medullary catecholamine secretion. In the kidneys, SRIF inhibits the release of renin stimulated by hypovolemia and inhibits AVP-mediated water absorption (Patel, 1992). In contrast to its inhibitory action on secretion, the antiproliferative effects of SRIF were later recognized (Weiss et al., 1981) and came about largely through use of long-acting analogs such as octreotide in the early 1980s for treatment of hormone hypersecretion from pancreatic, intestinal, and pituitary tumors (Lamberts et al., 1991; Weckbecker et al., 1993). It was found that SRIF not only blocked hormone hypersecretion from these tumors but also caused variable tumor shrinkage through an additional antiproliferative effect. The antiproliferative effects of SRIF have since

been demonstrated in normal dividing cells, e.g., intestinal mucosal cells (Reichlin, 1983), activated lymphocytes (Aguila et al., 1996), cytokines (Karalis et al., 1994), as well as in tumors (Weckbecker et al., 1993). The diverse effects of SRIF can be explained by its inhibitory effects on two key cellular processes: secretion and cell proliferation.

The pronounced ability of SRIF to block regulated secretion from many different cells is due in part to inhibition of two key intracellular mediators, cAMP and Ca^{2+}. SRIF inhibits secretion stimulated by cAMP, Ca^{2+} ionophores (A23187, ionomycin), the Ca^{2+} channel agonist Bay K 8644, IP_3, and extracellular Ca^{2+} in permeabilized cells (Luini and de Matteis, 1990; Patel, 1992; Patel et al., 1992; Renstrom et al., 1996). These observations suggest that SRIF, independent of any effects on cAMP, Ca^{2+}, or any other known second messenger, is able to inhibit secretion via this distal action. This effect appears to be mediated via a G-protein-dependent inhibition of exocytosis and is induced through SRIF-dependent activation of the protein phosphatase calcineurin (Renstrom et al., 1996). A similar distal effect on the secretory process has been shown for other inhibitory receptors, e.g., α_2-adrenergic and galanine, and suggests that phosphorylation-dephosphorylation events rather than the Ca^{2+} signal play a key role in the distal steps of exocytosis (Renstrom et al., 1996).

Pharmacology of SRIF receptors

The effects of SRIF are mediated through the seven-transmembrane receptor family that signals via Gi/Go and comprise five distinct subtypes (SSTR1-5) that are encoded by separate genes segregated on different chromosomes. The five hSSTR subtypes bind SRIF-14 and -28 with nanomolar affinity (Table 1). hSSTR1-4 bind SRIF-14 $\geq$ -28, whereas hSSTR5 exhibits 10- to 15-fold selectivity for SRIF-28 compared to SRIF-14 (Patel, 1997; Patel and Srikant, 1994). The first clinically useful compound to emerge was the octapeptide analog SMS201-995 (SMS, octreotide), which was introduced into clinical practice in 1983 for treatment of pituitary, pancreatic, and intestinal tumors and has remained the treatment of choice for SRIF analog therapy (Bauer et al., 1982). SMS, along with BIM23014 (Lanreotide), the octapeptide RC160 (Vapreotide), and the hexapeptide MK678 (Seglitide), has been shown to display high affinity for SSTR2 and SSTR5 (Table 1) and moderate affinity for SSTR3 (Bruns et al., 1996; Patel, 1992; Patel et al., 1995).

Table 1. Binding selectivity of endogenous SRIF-like peptides, short peptide analogs, and nonpeptide agonists (Modified from Patel, 1999).

	IC_{50} (nM)				
	SSTR1	**SSTR2**	**SSTR3**	**SSTR4**	**SSTR5**
Endogenous SRIF-like peptides					
SRIF-14	0.1-2.26	0.2-1.3	0.3-1.6	0.3-1.8	0.2-0.9
SRIF-14	0.1-2.2	0.2-4.1	0.3-6.1	0.3-7.9	0.05-0.4
hCST-17	7	0.6	0.6	0.5	0.4
rCST-29	2.8	7.1	0.2	3	13.7
Synthetic peptides					
Octreotide	290-1140	0.4-2.1	4.4-34.5	>1000	5.6-32
Lanreotide	500-2330	0.5-1.8	43-107	66-2100	0.6-14
Vapreotide	>1000	5.4	31	45	0.7
Seglitide	>1000	0.1-1.5	27-36	127- >1000	2-23
BIM23268	18.4	15.1	61.6	16.3	0.37
NC8-12	>1000	0.024	0.09	>1000	>1000
BIM23197	>1000	0.19	26.8	>1000	9.8
CH275	3.2-4.3	>1000	>1000	4.3-874	>1000
Nonpeptides agonists					
L-797, 591	1.4	1875	2240	170	3600
L-779, 976	2760	0.05	729	310	4260
L-796, 778	1255	>10000	24	8650	1200
L-803, 087	199	4720	1280	0.7	3880
L-817, 818	3.3	52	64	82	0.4

The binding affinity of SMS, BIM23014, RC160, and MK678 for SSTR2 and SSTR5 is comparable to that of SRIF-14, indicating that they are neither selective for these subtypes nor more potent than the endogenous ligands (Patel and Srikant, 1994). The analog Des-$AA^{1,2,5}$ [D-Trp^{8} $IAMP^{9}$] SRIF (CH275) binds both SSTR1 and SSTR4 (Liapakis et al., 1996; Patel, 1997). Other than SRIF and some of its derivatives, there are no compounds capable of binding all five subtypes. SRIF peptide antagonists were first described by Bass et al., 1996. One such compound [AC-4-NO_2-Phe-c (d-Cys-Tyr-D-Trp-Lys-Thr-Cys)-D-Tyr-NH_2] binds to hSSTR2 and hSSTR5 with nanomolar affinity. A second peptide, BIM23056, blocks hSSTR5 signaling and appears to be an antagonist for this subtype (Wilkinson et al., 1997). In addition, PRL-2903 (H-Fpa-cyclo(DCys-Pal-DTrp-Lys-Tle-Cys)-Nal-NH_2) has been described as a specific antagonist for the SSTR2 (Hocart et al., 1999; Kawacubo et al., 1999).

Several SRIF analogs have been reported to be selective for one SSTR subtype, e.g., BIM23056 (SSTR3), BIM23052, and L362-855 (SSTR5) (Reisine and Bell, 1995). Due to methodological variations in the binding analyses, however, such claims of subtype selectivity of these and other analogs have not been confirmed by others and remain controversial (Bruns et al., 1996; Patel and Srikant, 1994). In 1998, the Merck Research Group identified a series of nonpeptide agonists (Table 1) for each of the five hSSTRs in combinatorial libraries constructed on the basis of molecular modeling of known peptide agonists (Rohrer et al., 1998). Three of the compounds identified from this screen, L-797591, L-779976, and L-803087, display low nanomolar affinity for hSSTR1 (1.4 nM), hSSTR2 (0.05 nM), and hSSTR4 (0.7 nM). L-796778 binds to hSSTR3 with K_i 24 nM representing 50-fold selectivity and L-817818 displays selectivity for hSSTR5 and hSSTR1 (K_i 0.4 and 3.3 nM, respectively). The availability of these high-affinity subtype-selective agonists for several of the SSTRs represents a major break-through in the field, which should facilitate the direct probing of subtype-selective physiological functions as well as the development of orally active subtype-selective therapeutic compounds.

The insulin receptor

Insulin regulates a number of metabolic processes through binding to receptors in the cell surface of tissues throughout the body. The insulin receptor is a transmembrane glycoprotein complex with a molecular weight of approximately 400 kDa, and consists of two 135-kDa α-subunits and two 95-kDa β-subunits (Fig. 3). Both subunits are derived from a single-chain proreceptor encoded by a single gene located on the short arm of chromosome 19 (Collier and Gorden, 1991; Olson et al., 1988) and are linked by disulfide bonds. The α-subunits are located entirely in the extracellular region and the β-subunits posses an extracellular, transmembrane and intracellular domain. A complex of O- and N-linked carbohydrate side chains and covalently bound fatty acyl residues are attached to the insulin receptor (Mirmira and Tager, 1991). Functionally, the insulin receptor acts as a membrane bound allosteric enzyme and its two subunits perform distinct functions required for transmission of the insulin signal to the interior of the cell. Binding of insulin to the α-subunit

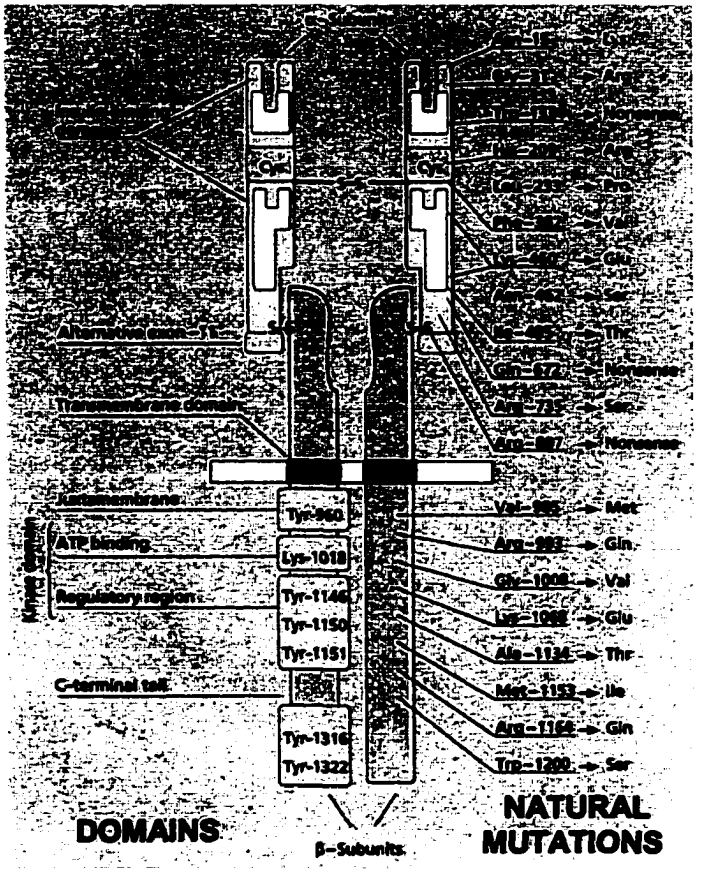

Figure 3. Structure of the insulin receptor (Modified from Maratos-Flier et al., 1997).

activates the receptor, leading to stimulation of the kinase activity of the β-subunit. Once activated, the β-subunit autophosphorylates on at least six tyrosine residues, as well as phosphorylating intracellular substrate proteins (Drake et al., 1996; Tsuruzoe et al., 2001). The best-known substrate for the insulin receptor is the insulin receptor substrate-1 (IRS-1), a cytoplasmic protein with molecular weight of 131 kDa, which undergoes rapid tyrosine phosphorylation following insulin stimulation. This allows non-covalent binding between the phosphorylated sites and specific src homology 2 domains (SH2) on target proteins such as PI3-kinase, growth factor receptor-bound protein 2 (GRB-2) and src homology 2 domain-containing protein-tyrosine phosphatase (SHPTP-2) (Backer et al., 1992; Skolnik et al., 1993). In the case of PI3-K and SHPTP-2, binding of IRS-1 to their SH2 domain results in rapid stimulation of enzymatic activity. GRB-2 does not have intrinsic enzymatic activity, but links IRS-1 with other signaling pathways such as the Ras ($p21^{ras}$), an important protein

involved in regulation of growth and metabolism, and cycles between an active GTP-bound form and an inactive GDP-bound form. Insulin shifts the equilibrium from the GDP-bound to the GTP-bound form, and is mediated by the guanine nucleotide exchange factor, SOS and GRB-2. Activation of $p21^{ras}$ leads to direct activation of Raf-1 kinase and subsequent phosphorylation of MAPK kinase, which in turn phosphorylates MAPK. Activation of enzymes crucial to carbohydrate metabolism such as glycogen synthetase, phosphorylase kinase and glycogen phosphorylase by glycogen-associated protein phosphatases 1 (PPG-1) occur after activation of pp90 S6 kinase (Korn at al., 1987). The signaling mechanisms through the insulin receptor are still largely unknown.

Effects of insulin on metabolism

Blood glucose levels are normally maintained between tight limits by the balance between glucose entry into the blood stream and glucose uptake by peripheral tissues. Insulin lowers blood glucose levels by suppressing hepatic glucose production (inhibits glycogenolysis and restrain gluconeogenesis) and stimulating peripheral glucose uptake, mainly in skeletal muscle and adipose tissue. Glucose uptake is dramatically increased when blood glucose levels rises. This effect is mediated by GLUT-4, which is expressed in insulin-sensitive tissues (Shepherd and Kahn, 1999). Unlike other transporters, GLUT-4 is present in vesicles in the cytoplasm and upon insulin stimulation, promotes translocation of these vesicles to the cell membrane, where they function as pores through which glucose is taken up (Watson and Pessin, 2001). Insulin enhances the activity of individual GLUT-4 and is important in maintaining normal levels of the GLUT-4 in muscle and adipose tissue (Bourey et al., 1990; Holman et al., 1990). In addition, insulin helps maintain the glucose gradient across cell membranes by stimulating enzymes involved in glycogen synthesis and glucose oxidation. Insulin enhances its own action in stimulating glucose uptake into muscle, by suppressing lipolysis and reducing the levels of non-esterified fatty acids that may interfere with glucose uptake and metabolism through the glucose-fatty acid cycle. Lipogenesis is stimulated by insulin, where adipocytes and hepatocytes synthesize triglycerides from non-esterified fatty acids and glycerol-3-phosphate. The activity of lipoprotein lipase, which synthesizes fatty acids from circulating lipoproteins is also increased by insulin. Pyruvate dehydrogenase, an enzyme present in the mitochondria is phosphorylated by insulin to oxidize pyruvate into adipose tissue (Reed and Lane, 1980).

Insulin stimulates the active transport of amino acids into muscle cells, thereby enhancing protein synthesis. Glycolysis and oxidative phosphorylation of glucose derivatives provide the energy required for such metabolic activity (Duckworth, 1988). There is some evidence that insulin may act as a vasodilator, increasing skeletal muscle blood flow and therefore glucose delivery (Baron et al., 1994).

Heterotrimeric G-proteins

The G-protein cycle

G-proteins are made up of three polypeptides: a α subunit that binds and hydrolyzes GTP, a β subunit, and a γ subunit. The β and γ subunits form a dimer that dissociates when its denatured and therefore is a functional monomer. When GDP is bound, the α subunit associates with the $\beta\gamma$ subunit to form an inactive heterotrimer that binds to the receptor. Monomeric, GDP-bound α subunits can interact with receptors, but this association is greatly enhanced by the $\beta\gamma$ subunit. Upon receptor stimulation, it becomes activated and changes its conformation. The GDP-bound α subunit responds with a conformational change that decreases the affinity for GDP, so that GDP is released from the active site. Because the concentration of GTP in cells is much higher than those for GDP, the GDP is replaced with GTP as it leaves the receptor complex (Fig. 4). Once GTP is bound, the α subunit assumes its active conformation and dissociates from the receptor and the $\beta\gamma$ subunit (Gilman, 1987). The activated state lasts until the GTP is hydrolyzed to GDP by the intrinsic GTPase activity of the α subunit. All isoforms of the α subunits are GTPases, although the intrinsic rate of GTP hydrolysis varies from one type of α subunit to another (Carty et al., 1990). After GTP is cleaved to GDP, α and $\beta\gamma$ subunits reassociate, become inactive, and return to the receptor. The free α and $\beta\gamma$ subunits each activate target effectors. The rate of GTP hydrolysis is a timing mechanism that controls the duration of both α and $\beta\gamma$ subunit activation. Reassociation turns off both subunits and primes the system to respond again. Although the $\beta\gamma$ subunit does not bind GTP, its active lifetime depends on the rate of GTP hydrolysis by the α subunit.

G-proteins are classified based on the identity of Gα subunits into four major subfamilies; Gs, Gi/Go, Gq, and G12. Chorela toxin from *Vibrio cholerae* catalyzes the

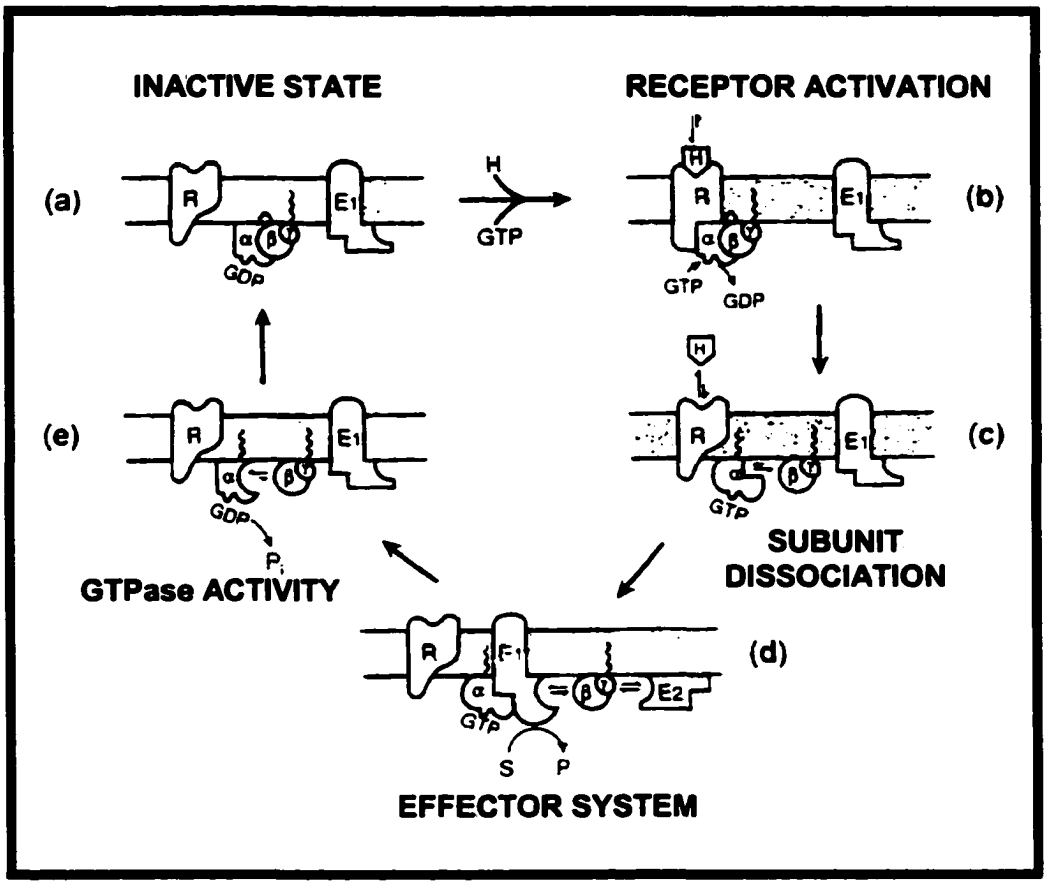

Figure 4. The G-protein cycle (Modified from Hepler and Gilman, 1992).

ADP-ribosylation of a conserved arginine residue (Arg^{202}) on α subunits in the Gs family, which results in inhibition of GTPase activity and interaction with the βγ subunit (Serventi et al., 1992). PTX from *Bordetella pertussis* catalyze the ADP-ribosylation of a cysteine residue at position -4 from the C-terminus of Gα subunits in the Gi/Go family, resulting in inhibition of receptor-G-protein coupling. Gq and G12 lack the cysteine residue that can undergo ADP-ribosylation by PTX, thus is referred as PTX-insensitive G-proteins (Strathmann and Simon, 1990). It has been well established that signaling through Gq is mediated mainly through the PLC pathway (Taylor et al., 1991).

Structure and function of α and βγ subunits

Mammals have over 20 different G-protein α subunits (16 gene products, some with alternatively spliced isoforms). They are divided into four major classes according to the similarity of their amino acid sequences that range from 56 %-95 % identity. With the

exception of G-proteins that are found in sensory organs (such as α_t, α_{gust} or α_{olf}) and a few that are predominantly expressed in hematopoietic cells (α_{16}) or in neurons and β-cells (α_o), most α subunits are widely expressed (Hsu et al., 1990; Kaziro et al., 1991; Marinissen and Gutkind, 2001). Individual cells contain at least four or five types of α subunits, which consist of two domains: a GTPase domain that contains the guanine-nucleotide binding pocket as well as sites for binding receptors, effectors, the βγ subunit, and a helical domain whose function is not clear, Fig. 5 (Coleman et al., 1994; Lambright et al., 1994). Arg^{178} of the α_t subunit may represent a key element in the GTP hydrolysis, where it would help set the GTPase activity (Conklin and Bourne, 1993). The helical domain may also contribute to the effector binding site, along with other regions on the GTPase domain (Coleman et al., 1994). The first 25 amino acids of the α subunit are essential for the βγ subunit binding (Denker et al., 1992). The βγ subunit-binding surface may include the α_2 helix, because a cysteine on this helix (Cys^{215} in α_o) can be chemically cross-linked to the βγ subunit (Thomas et al., 1993). The effector binding site of the α_s includes the α_2 helix, which partially overlaps the putative βγ subunit-binding surface. The C-terminus and parts of the α_5 helix are important sites for interaction with receptors, since an activated receptor triggers the intracellular responses by dramatically decreasing the affinity of the α subunit for GDP. This effect can be replicated by deletion of 14 amino acids from the C-terminus of α_o (Denker et al., 1992).

The βγ subunit is functionally a monomer, where the β subunit is made up of two structurally distinct regions, an amino terminal segment, which is a α helix of approximately 20 amino acids, and a sequence motif that is repeated seven times (Clapham and Neer, 1997). This repeating sequence, called a WD-repeat, is not unique to the β subunit but occurs in approximately 40 other proteins that make up the WD-repeat superfamily (Li et al., 2000). Members of this family are involved in many cellular pathways such as signal transduction, pre-mRNA splicing, transcriptional regulation, assembly of the cytoskeleton, and vesicular traffic.

For many years, the main hypothesis for G-protein mediated signaling was that the GTP-bound α subunit activated the effectors, while the βγ subunit was only a negative regulator. Release of free βγ subunits from the receptor complex was thought to deactivate other α subunits by forming inactive heterotrimers. Indeed, the βγ subunit can block activation of adenylyl cyclase through this mechanism (Gilman, 1987), but this concept was

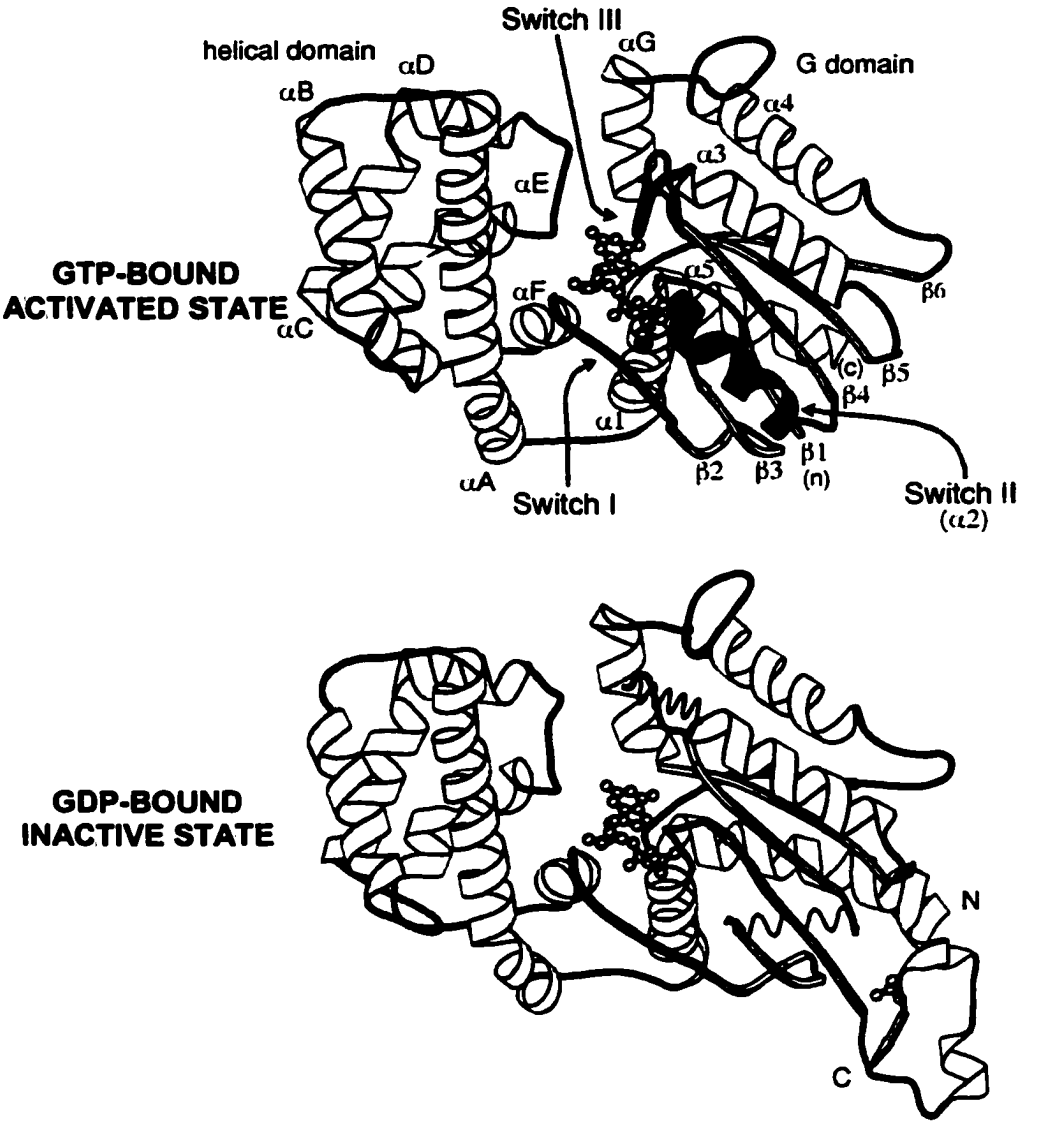

Figure 5. A schematic diagram of Giα1, with switch segments darkened and secondary structure elements labeled. The GTP- and GDP-bound states are represented by a ball and stick model (Modified from Sprang, 1997).

drastically changed after it was discovered that the βγ subunit could activate the muscarinic K^+ channel and that both, α and βγ subunits, could positively regulate effectors (Logothetis et al., 1987). Subsequently, the βγ subunit was shown to activate a large number of effectors, such as adenylyl cyclase, PLC-β, PLA_2, PI3-kinase and β-adrenergic receptor kinase (Clapham and Neer, 1997). It has been suggested that the βγ subunit acts through Ras to activate the MAPK pathway, promoting tyrosine phosphorylation of Src homology 2-

containing protein (SHC), and increasing the functional association among SHC, GRB-2 and SOS (Luttrell et al., 1996).

Receptor G-protein effector interfaces

Cellular responses to external stimuli are sometimes very selective. One example is the heart, which responds accurately to opposing signals. Stimulation of its β-adrenergic receptor increases the rate and force of contraction, while stimulation of muscarinic cholinergic receptors decreases the rate and force of contraction. Each of these receptors is coupled to a different G-protein: the β-adrenergic signals through Gs, while the muscarinic receptors through Gi/Go or Gq. Although cellular responses to hormones are highly specific, they are not always universal. There are several examples of receptors that can interact with more than one G-protein to initiate different signaling pathways (Abou-Samra et al., 1992; Allgeier et al., 1994; Chabre et al., 1994). The parathyroid hormone receptor transfected in COS-7 cells is coupled to two different G-proteins to activate adenylyl cyclase and PLC, while the β_2-adrenergic receptor transfected into the same cell type only activates adenylyl cyclase (Abou-Samra et al., 1992). Effectors discriminate better among G-protein α subunits than do receptors: only α_s activates adenylyl cyclase and only α_q/α_{11} activate PLC-β. In contrast, βγ subunits can also activate effectors equally. Furthermore, the cytoplasmic region of G-protein-coupled receptors is responsible for G-protein selectivity. Specificity depends not only on the presence of a correct G-protein recognition sequence, but also on its proper control by other cytoplasmic regions. The selectivity of a receptor can be greatly diminshed by altering cytoplasmic regions outside the recognition sequence (Wong and Ross, 1994).

Phosphorylation of receptor and G-protein

Exposure of G-protein coupled receptors (GPCRs) to agonists often results in a rapid attenuation of receptor responsiveness. This process, termed desensitization, is the consequence of a combination of different mechanisms. These mechanisms include uncoupling of receptors from heterotrimeric G-proteins in response to receptor phosphorylation (Lohse et al., 1990), internalization (Anborgh et al., 2000), and down-regulation due to reduced receptor mRNA and protein synthesis, as well as both lysosomal and plasma membrane degradation of pre-existing receptors (Jockers et al., 1999; Pak et al., 1999). The time frame over which these processes occur ranges from seconds

(phosphorylation) to minutes (endocytosis) and hours (down-regulation). The extent of receptor desensitization varies from complete termination of signaling, as observed in visual and olfactory systems, to attenuation of agonist potency and maximal responsiveness, such as observed in the β_2 adrenergic receptor (Sakmar, 1998; Zhang et al., 1997). The extent of receptor desensitization is regulated by a number of factors that include receptor structure and cellular environment (Barlic et al., 1999; Menard et al., 1997). Traditionally, GPCR desensitization has been characterized by events that contribute to the uncoupling of receptors from their heterotrimeric G-proteins. GPCR signaling can also be terminated at the level of G-proteins. For example, a family of proteins, termed regulators of G-protein signaling (RGS) act to increase the rate of GTP hydrolysis bound to both α subunits of Gi/Go and Gq, thereby dampening signaling via Gi/Go - and Gq -regulated pathways (Dohlman and Thorner, 1997). The evidence that RGS12 interacts with the carboxyl-terminal PDZ domain binding motif of the interleukin-8 receptor B (CXCR2) suggests that regulation of G-protein signaling by RGS proteins may involve direct interactions with the receptor (Snow et al., 1998). In addition, GPCRs can serve as substrates for PKA, PKC, and G-protein-coupled receptor kinase phosphorylation during desensitization (Budd et al., 2000; Chen et al., 1997; Francesconi and Duvoisin, 2000; Pitcher et al., 1998).

The α subunits can be phosphorylated on serine or threonine residues (Neer, 1997; Rothenberg and Kahn, 1988; Umemori et al., 1997). In most cases, phosphorylation does not change the activity of the protein, but rather changes its localization or association with other proteins (Koch et al., 1991). The first evidence for β subunit phosphorylation was shown in human leukemia HL-60 cells (Wieland et al., 1993). Similarly, the β subunit of the retinal G-protein transducin can be phosphorylated by the GTP analog GTPγS (Wieland et al., 1992). It was suggested that the phosphate group of GTP or the thiophosphate of GTPγS could be transferred from histidine to GDP at α subunits, leading to an alternative pathway for α subunit activation. Phosphorylation can also affect the $\beta\gamma$ subunit function indirectly. Phosphorylation of $G\alpha_z$ or $G\alpha_{12}$ by PKC at a site near the N-terminus inhibits its ability to interact with $\beta\gamma$ subunits (Kozasa and Gilman, 1996). In addition, the $\beta\gamma$ subunit can also undergo direct phosphorylation. The β subunit of yeast (Ste4) is rapidly phosphorylated in response to pheromone (Maeda et al., 1994). The phosphorylation occurs on a sequence that is inserted between the fifth and sixth repeats of Ste4. No homologous sequence is found in other eukaryotic β subunits. Removal of this sequence

does not prevent the βγ subunit from transmitting the mating pheromone signal, but does make yeast expressing the mutant protein more sensitive to pheromone (Cole and Reed, 1991).

Signal transduction by AVP and SRIF

Ca^{2+} signaling

Ionized Ca^{2+} is the most common signal transduction element in cells ranging from bacteria to specialized neurons. Unlike other second messengers, Ca^{2+} is required for life, although exposure to elevated $[Ca^{2+}]_i$ for long periods leads to cell death. Ca^{2+} cannot be metabolized like other second messengers, thus cells regulate very tightly intracellular levels through binding and specialized extrusion proteins. Normal $[Ca^{2+}]_i$ are approximately 100 nM, which is approximately 10000-fold lower than the 1 mM present in the extracellular space. Several proteins bind Ca^{2+} tightly, in some cases simply to buffer or lower free Ca^{2+} levels, and other to trigger second messenger pathways.

The role of Ca^{2+} in insulin exocytosis has been demonstrated by several investigators (Henquin et al., 1998; Qian and Kennedy, 2001; Wollheim and Pozzan, 1984). Basal $[Ca^{2+}]_i$ is maintained by a variety of cellular processes and the major barrier is the plasma membrane that is highly impermeable to Ca^{2+}, and exhibits two energy-dependent processes of Ca^{2+} extrusion. These are the Ca^{2+}-Mg^{2+} ATPase and the Na^+-Ca^{2+} exchange mechanism, which depends on the Na^+ gradient established by the Na^+-K^+ ATPase. Within the cytoplasm, the ER and mitochondria are the major organelles that contribute to the maintenance of low $[Ca^{2+}]_i$. Ca^{2+} is pumped into the ER by the action of membrane-bound Ca^{2+}-Mg^{2+} ATPase, and into the mitochondria by the mitochondrial proton gradient.

Receptor-activated Ca^{2+} mobilization through the IP_3 cascade can involve two phases: 1) Ca^{2+} release from the ER, and 2) a more prolonged phase due to extracellular Ca^{2+} influx (Putney, 1987). In this manner, $[Ca^{2+}]_i$ can increase either through the release from the ER or influx via the plasma membrane. One of the mechanisms of Ca^{2+} influx is through Ca^{2+} release-activated Ca^{2+} influx or so called capacitative Ca^{2+} entry (Birnbaumer et al., 2000; Schofl et al., 1996). The basis for this mechanism is that an increase in $[Ca^{2+}]_i$ by IP_3, evokes Ca^{2+} influx through the opening of Ca^{2+} channels on the plasma membrane (Icrac). Experiments utilizing TG, which inhibits microsomal (but not plasma membrane) Ca^{2+}-ATPase, thereby depleting intracellular Ca^{2+} stores has been utilized to demonstrate this mechanism (Thastrup, 1990). Subsequent addition of Gq agonists in the presence of

TG does not further increase the rate of Ca^{2+} influx (Takemura et al., 1989), suggesting that depletion of the agonist-sensitive intracellular Ca^{2+} stores regulate Ca^{2+} influx at the plasma membrane.

Extracellular Ca^{2+} influx can also be mediated by either the voltage-dependent Ca^{2+} channels (VDCC) or receptor-operated Ca^{2+} channel (ROC). There are three major subtypes of VDCCs: L-type (long-lasting), T-type (transient) and N-type (neither long-lasting nor transient). Activation of VDCCs is controlled by changes in plasma membrane potential, which initiates a number of cellular responses, including muscle contraction and exocytosis in endocrine and nerve cells. The L-type VDCC is characterized by its sensitivity to dihydropyridines (DHP). It is inhibited by the DHP antagonist nimodipine and is activated by the DHP agonist Bay K 8644 (Smith et al., 1993). The T-type VDCC is activated by a membrane potential of ~ - 50 mV, and is important for the pacemaker activity in several tissues. There are no specific blockers for the T-type VDCC, however, Ni^{2+}, tetrandine and felodine can partially block this type of channel. Adenosine, a potent modulator of neurotransmitter release inhibits N-type VDCC (Yawo and Chuhma, 1993) and is mediated by Gi/Go (Mirotznik et al., 2000). Activation of the μ-opioid receptor also inhibits Ca^{2+} influx by selectively inhibiting N-type VDCC (Endo and Yawo, 2000). Agonists that bind plasma membrane receptors activate the ROCs. Their structure and mechanisms are still under investigation. The ROCs provide a number of pathways of Ca^{2+} influx into the cytoplasm and the ER. Store-operated Ca^{2+} channels are a major subfamily of ROCs, and are activated by decreased ER Ca^{2+}. In order to initiate or maintain specific type of Ca^{2+} signal, ROCs, which are non-selective cation channels, can deliver Ca^{2+} directly to specific regions of the cytoplasm. ROCs allow Na^{+} influx, leading to membrane depolarization and opening of VDCCs and Ca^{2+} influx. Store-operated Ca^{2+} channels deliver Ca^{2+} specifically to the ER, thus maintaining oscillating Ca^{2+} signals (Barritt, 1999).

The Gq pathway

The mechanisms by which AVP signals have been investigated in various tissues/cells, such as smooth muscle, endothelium and endocrine cells (Spatz et al., 1994). Insulin release from rat pancreas and clonal β-cell lines RINm5F (Lee et al., 1995) and HIT-T15 (Richardson et al., 1990) are mediated by V_{1b} receptors. AVP binds to Gq-coupled V_1 receptors, leading to PLC-β activation (Thibonnier et al., 1993). Activation of PLC-β promotes PIP_2 hydrolysis, resulting in the generation of IP_3 and DAG. IP_3 stimulates the

release of Ca^{2+} from the ER into the cytoplasm via the IP_3 receptor/Ca^{2+} channel (Berridge, 1993). The IP_3 receptor structure consists of IP_3 binding, coupling and Ca^{2+} channel domains. Upon IP_3 binding, a conformational change of the coupling domain occurs, leading to Ca^{2+} channel opening (Mignery and Sudhof, 1990). Ca^{2+} binds and activates a number of intracellular proteins, including calmodulin, which contribute to many cellular responses, including insulin and glucagon release. DAG, the other product generated from PIP_2 hydrolysis, is known to activate PKC, leading to phosphorylation of key proteins involved in cellular responses. In addition, V_1 receptors can be coupled to other effectors, such as PLD and PLA_2 (Jackson, 1996).

AVP stimulates insulin release through PLC-dependent and -independent pathways (Chen et al., 1994; Li et al., 1992; Richardson et al., 1990). Phosphoinositides consist of a glycerol backbone containing 2 fatty acyl groups (at 1- and 2-positions) and a phosphate group coupled to the suger *myo*-inositol at the 3-position. Phosphorylation of PI to PIP and then to PIP_2 occurs predominantly in the plasma membrane. The PLCs are a family of isozymes that hydrolyze PIP_2 at the 3-position of the phosphodiester bond of the glycerol backbone. Phosphoinositide-specific PLC (PPI-PLC) is a subfamily of PLC that specifically hydrolyzes inositol-containing lipids, but not other phospholipids, such as phosphatidylcholine. PPI-PLC can be classified into three classes; PPI-PLC-β, -γ, and -δ, which are distinct proteins that contain only a small amount of sequence identity (Rhee and Choi, 1992). PLC-β has been further classified into two subtypes: βI and βII, and exhibit a high degree of sequence identity. Both PLC-β and PLC-γ isozymes are involved in receptor-activated PIP_2 hydrolysis, however, their mechanisms of activation are different due to a difference in the primary amino acid sequence. PLC-γ contains SH2 and SH3 domains, and mediates the binding to other proteins that contain phosphorylated tyrosine residues such as growth factor and insulin receptors. Activation of PLC-β is mediated by Gq (Taylor et al., 1991), whereas PLC-γ by receptors that possess intrinsic tyrosine kinase activity (Ullrich and Schlessinger, 1990). Activation of PLC-δ can be mediated by Icrac and PIP_2 (Kim et al., 1999; Lomasney et al., 1996).

The Gi/Go pathway

SRIF receptors (SSTRs) are coupled to Gi/Go proteins and mediate their cellular responses through multiple second messenger systems including adenylyl cyclase, Ca^{2+} and K^+ ion channels, Na^+/H^+ antiporter, guanylate cyclase, PLC, PLA_2, MAPK, and serine,

threonine, and phosphotyrosyl protein phosphatase (Patel et al., 1995; Reisine and Bell, 1995). SSTR1 is coupled to adenylyl cyclase via Gαi3 (Kubota et al., 1994). SSTR2A purified from GH4C1 cells or expressed in CHO cells is capable of associating with Gαi1, Gαi2,Gαi3, and Gαo2 (Gu and Schonbrunn, 1997). SSTR3 can interact with Gαi1, Gαi2, Gαi4, and Gαi6 (Komatsuzaki et al., 1997). The specific G-proteins that associate with other SSTR subtypes have not been determined. Initial studies regarding coupling of Gi/Go to adenylyl cyclase were contradictory, although there is now a general agreement that all five SSTR subtypes inhibits the adenylyl cyclase-cAMP pathway. Three of the SSTR subtypes have been shown to inhibit the MAPK signaling cascade: SSTR2 in neuroblastoma cells, SSTR3 in NIH3T3 cells and mouse insulinoma cells, and SSTR5 in transfected CHO-K1 cells (Cattaneo et al., 1994; Cordelier et al., 1997; Yoshitomi et al., 1997). In contrast, SSTR1 and SSTR4 stimulate MAPK in transfected CHO-K1 cells (Bito et al., 1994; Florio et al., 1999). SSTRs 2-5 activate G-protein-gated inward rectifying K^+ channels in *Xenopus* oocytes, with coupling by SSTR2 being the most efficient (Kreienkamp et al., 1997). In rat insulinoma 1046-38 cells, endogenously expressed SSTR1 and SSTR2 inhibits voltage-dependent Ca^{2+} channels, with the effect of SSTR1 being more pronounced than SSTR2 (Roosterman et al., 1998). SSTR1 also stimulates a Na^+/H^+ exchanger via a PTX-insensitive mechanism (Hou et al., 1994). Studies in cultured mouse hypothalamic neurons have shown that SSTR2 decreases and SSTR1 increases AMPA/kainate receptor-mediated glutamate currents (Lanneau et al., 1998). SSTR4 activates PLA_2-dependent arachidonate production via Gi/Go in transfected CHO-K1 cells (Bito et al., 1994). In addition, a number of reports suggest regulation of the PLC-IP_3 pathway by Gi/Go in both normal and transfected cells (Akbar et al., 1994; Wilkinson et al., 1997). Activation of the SSTR2A and SSTR5 stimulates PLC-dependent IP_3 production in transfected COS-7 and F4C1 pituitary cells (Akbar et al., 1994; Chen et al., 1997). Gi/Go proteins coupled to SSTR5 can inhibit IP_3-mediated Ca^{2+} mobilization in transfected CHO-K1 cells (Bito et al., 1994). The mechanism underlying the selectivity of SSTRs for K^+ and Ca^{2+} channel coupling and the molecular signals in the receptors responsible for activation of various phosphatases and the MAPK pathway remain to be determined.

Cross-talk between Gq and Gi/Go

Signaling via GPCRs can lead to many cellular responses, ranging from regulation of intracellular levels of cAMP to stimulation of gene transcription. Members of this receptor

family are grouped into different categories depending on the particular G-protein that they predominantly interact with. Thus receptors that couple to Gs stimulate adenylyl cyclase in many cells, while Gq-coupled receptors mobilize intracellular Ca^{2+} via activation of PLC. There is compelling evidence that activation of one particular signaling pathway by a GPCR can amplify intracellular signaling within a parallel but separate pathway.

AVP binds the V_{1b} receptor in β-cells (Lee et al., 1995), which is coupled to Gq, thus activating PLC-β through the αq subunit with subsequent hydrolysis of PIP_2 to IP_3 and DAG (Thibonnier, 1992). DAG activates PKC, while IP_3 promotes Ca^{2+} release from the ER, leading to an increase in $[Ca^{2+}]_i$ (Li et al., 1992; Thorn and Petersen, 1991). Activation of Gi/Go-coupled receptors can enhance the inositol phosphate signals generated by Gq-coupled receptors, although in some cases activation of Gi/Go alone does not alter IP_3 formation (Muller and Lohse, 1995; Neer, 1997). Evidence of cross-talk between Gq and Gi/Go has been reported. In human neuroblastoma SH-SY5Y cells, SRIF increases $[Ca^{2+}]_i$ after pretreatment with carbachol, which signals via Gq. SRIF alone fails to increase $[Ca^{2+}]_i$ in SH-SY5Y cells (Connor et al., 1997). In intestinal smooth muscle, SRIF increases IP_3 formation and Ca^{2+} release, leading to muscle contraction through the βγ dimer (Murthy et al., 1996). Stimulation of PLC-β by the βγ dimer of Gi/Go can occur (Offermanns and Simon, 1995). Studies in COS-1 cells have provided support for the βγ dimer mediation of cross-talk between Gq- and Gi/Go-coupled receptors (Quitterer and Lohse, 1999). Enhancement of Gq-dependent signals by Gi/Go-coupled receptors in COS-7 cells requires an activated PLC-β and is mediated by the βγ dimer (Chan et al., 2000). Biochemical assays suggest that the βγ dimer can interact with α subunit from different G-proteins (Muller et al., 1996; Ueda et al., 1994). Although cross-talk between Gq and Gi/Go have been reported, where preactivation of PLC-β by Gq leads to an increase in IP_3 formation and $[Ca^{2+}]_i$ by the βγ dimer from Gi/Go, the precise mechanisms are not fully understood.

Regulation of PIP_2 synthesis

Phosphatidylinositol 4,5-bisphosphate (PIP_2) is a glycerol-phospholipid found predominantly in the inner leaflet of eukaryotic plasma membranes. Although it constitutes less than 0.05 % of total cellular phospholipids, PIP_2 plays a critical role in intracellular signaling. PIP_2 is best known for its ability to serve as a precursor for the second messengers IP_3 and DAG, which are generated from the hydrolysis by PLCs following

agonist stimulation. PIP_2 can be synthesized by two different routes: by phosphorylation of PI4P on the D-5 position of the inositol ring by PIP5Ks or by phosphorylation of PI5P on the D-4 position by PIP4Ks. Although the majority of PIP_2 in cells is produced from PI4P (Hawkins et al., 1992; Stephens et al., 1991), it is likely that some PIP_2 present in cell membranes are synthesized from PI5P. The PIP_2 produced by two different pathways can be hydrolyzed by PLC-β to generate IP_3 and DAG, phosphorylated by PI3-kinase to PIP_3, or dephosphorylated by 5-phosphatase to PIP.

PI4P is synthesized by PI4Ks, through phosphorylation of PI on the D-4 position of the inositol ring. PI4Ks are ubiquitously expressed enzymes that associate with cellular membranes such as the ER, Golgi, plasma membrane, nuclear envelope, lysosomes, and a variety of intracellular vesicles (Pike, 1992). Characteristic features of PI4Ks include a C-terminal catalytic domain homologous to those of PI3-Ks. In addition, there is a phosphoinositide kinase (PIK) domain of unknown function, common to both PI4Ks and PI3Ks (Gehrmann and Heilmeyer, 1998). PI4Ks were originally characterized as a member of a large family of PI kinases, subdivided into three main categories: type I, type II, and type III, based on the biochemical properties of partially purified proteins. The type I kinases were defined as enzymes whose lipid kinase activity is relatively resistant to adenosine and is inhibited by non-ionic detergent (Whitman et al., 1987). Subsequent studies revealed that the type I PI kinases are PI3Ks, based on their ability to phosphorylate the D-3 position of PI (Whitman et al., 1988). In contrast, the type II and type III PI kinases are PI4Ks that require non-ionic detergent for maximal enzyme activity (Whitman et al., 1987). Type II kinases differ from type III in their size and sensitivity to inhibition by adenosine (Endemann et al., 1987). The second step in the conversion of PI to PIP_2 via PI4P requires the action of PIP5Ks. PIP5K activity can be detected in several subcellular compartments, including the plasma membrane, cytoplasm, ER, cytoskeleton, and nucleus (Loijens et al., 1996). PIP5Ks are subdivided into two distinct classes (type I and II), based on their biochemical and immunological properties (Jenkins et al., 1994; Loijens et al., 1996). Several genes encoding the type I and type II PIP5Ks have been cloned and although similar to each other, these enzymes share little homology with other lipid or protein kinases (Boronenkov and Anderson, 1995; Castellino et al., 1997; Ishihara et al., 1996).

An alternative pathway for PIP_2 synthesis is the production from PI5P through the action of PIP4Ks. The mechanism for PI5P synthesis remains unclear and little is known about this lipid. PI5P can be synthesized by PIP5Kα and β, which phosphorylates PI on the

D-5 position (Tolias et al., 1998), however, their preferred substrate is PI4P. The human homologue of Fab1 (p235) can also catalyze the conversion of PI to PI5P *in vitro* (Shisheva et al., 1999). It is possible that this enzyme is responsible for synthesizing PI5P *in vivo*. The second step in the conversion of PI to PIP_2 via PI5P requires the action of PIP4Ks, which are enzymes that phosphorylates the D-4 position of PI5P. PIP4Ks were originally identified as PI4P 5-kinases based on their ability to phosphorylate commercial PI4P (Bazenet et al., 1990). The first cloned PIP4K was characterized as a 47 kDa, type II PI4P 5-kinase and named type IIα PIP5K (Divecha et al., 1995). Following the discovery that this enzyme is actually a PI5P 4-kinase, it has been renamed PIP4Kα. Two genes highly related to PIP4Kα, PIP4Kβ (78 % identical) and PIP4Kγ (61 % identical) have also been cloned (Castellino et al., 1997; Itoh et al., 1998). The PIP4Ks are 35 % identical to the PIP5Ks in their kinase domains, but differ outside this region. PIP4Ks are related to the yeast PIP5Ks, Mss4 (43 %) and Fab1 (28 %) (Loijens and Anderson, 1996). The conserved catalytic domains of the PIP4Ks contain an insert region, which in the case of PIP4Kα and β, is comprised of proline-rich sequences that resembles SH3-domain binding sites (Loijens et al., 1996).

Role of PIP_2 in cellular responses

PIP_2 participates in a number of signaling pathways that regulate cellular function (Fig. 6). It is the precursor of three important second messengers: IP_3, DAG, and PIP_3. PIP_2 can function as a second messenger by interacting with different proteins and regulating their activities and/or localization. PIP_2 plays a direct role in actin cytoskeletal regulation, through binding and regulation of numerous actin-binding proteins *in vitro*, including gelsolin, profilin, and α-actinin (Fukami et al., 1992; Janmey and Stossel, 1987; Lassing and Lindberg, 1988; Takenawa and Miki, 2001). PIP_2 synthesis is correlated with actin assembly, where manipulation of intracellular levels results in altered actin cytoskeletal organization. Overexpression of murine PIP5Ks in COS cells dramatically increases aberrant actin polymerization (Shibasaki et al., 1997), whereas overexpression of PIP_2 - phosphatase synaptojanin decreases actin stress fibers (Sakisaka et al., 1997). Furthermore, yeasts lacking Mss4 display defects in their actin cytoskeleton during polarized cell growth (Homma et al., 1998). PIP_2 is thought to stimulate actin assembly by displacing gelsolin from barbed end of actin filaments, allowing the addition of actin monomers (Hartwig et al., 1995).

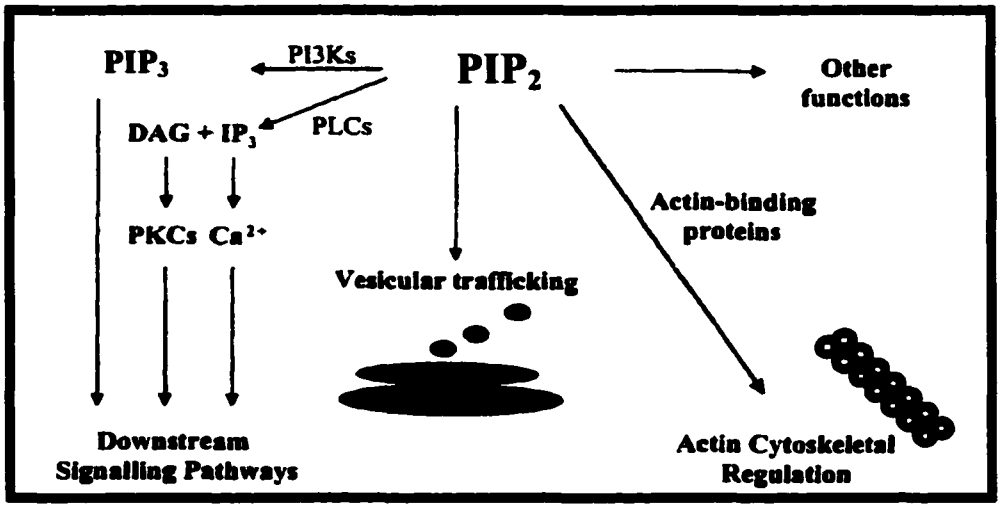

Figure 6. Roles of PIP_2 in cellular function (Modified from Tolias and Carpenter, 2000).

PIP_2 appears to play a role in vesicle trafficking. In permeabilized PC12 cells, PIP5K and phosphatidylinositol transfer protein are required for restoring the 'priming step' of exocytosis, that proceeds Ca^{2+}-activated membrane fusion (Hay et al., 1995). Inhibition of PIP_2 synthesis blocks Ca^{2+}-triggered secretion, suggesting that PIP_2 is necessary for exocytosis. PIP_2 is required for both early and late events in endocytic coated-vesicle formation (Jost et al., 1998). PIP_2 regulates membrane trafficking events by modulating the function of proteins essential for vesicular transport, such as ADP ribosylation factor 1 (ARF1), ARF guanine nucleotide exchange factor (ARNO), PLD, dynamin, and the clathrin adaptor complex AP-2 (Cukierman et al., 1995; Klein et al., 1998; Liscovitch et al., 1994; Randazzo, 1997).

PIP_2 may also function in different pathways by binding pleckstrin homology (PH) domain-containing proteins such as spectrin, pleckstrin, mSOS1, dynamin, and PLC-γ, where PIP_2 binding most likely serves to localize these proteins to the membrane and/or stimulate their activities. Binding of PIP_2 to the PH domain of dynamin activates GTPase activity (Lin and Gilman, 1996). PIP_2 promotes GDP-GTP exchange on the GTPase Cdc42 (Zheng et al., 1996), regulate Na^+-Ca^{2+} exchange and the function of K^+ channels (Hilgemann and Ball, 1996; Huang et al., 1998). In addition, PIP_2 inhibits microtubule assembly by binding to tubulin (Popova et al., 1997). Regulation of mRNA processing and chromatin structure in the nucleus by PIP_2 has also been reported (Boronenkov et al., 1998; Zhao et al., 1998).

CHAPTER II SOMATOSTATIN-INDUCED PARADOXICAL INCREASE IN INTRACELLULAR Ca^{2+} CONCENTRATION AND INSULIN SECRETION IN THE PRESENCE OF ARGININE VASOPRESSIN IN CLONAL β-CELL HIT-T15

A paper accepted for publication in the Biochemical Journal

Henrique Cheng, Sirintorn Yibchok-anun, Seung-Chun Park and Walter H. Hsu

ABSTRACT

Somatostatin (SRIF), a hormone signals via Gi/Go, usually inhibits intracellular calcium concentration ($[Ca^{2+}]_i$) and insulin release from β-cells. We have found that in the presence of arginine vasopressin (AVP), which signals via Gq, SRIF increased $[Ca^{2+}]_i$ leading to insulin release in HIT-T15 cells. The increase in $[Ca^{2+}]_i$ by SRIF was observed even after 60 min of AVP treatment. SRIF alone failed to increase $[Ca^{2+}]_i$ and insulin release. SRIF induced changes in $[Ca^{2+}]_i$ in a biphasic pattern, characterized by a sharp and transient increase followed by a rapid decline to sub-basal level. Pretreatment with pertussis toxin, which inactivates Gi/Go, abolished the effects of SRIF. U-73122, an inhibitor of phospholipase C, antagonized SRIF-induced increase in $[Ca^{2+}]_i$. In Ca^{2+}-free medium, SRIF still increased $[Ca^{2+}]_i$. Depletion of intracellular Ca^{2+} stores with thapsigargin, a microsomal Ca^{2+} ATPase inhibitor, abolished SRIF's effect. In the presence of bradykinin, another Gq-coupled receptor agonist, SRIF also increased $[Ca^{2+}]_i$, but not in the presence of isoproterenol (a Gs-coupled receptor agonist) or medetomidine (a Gi/Go-coupled receptor agonist). Our findings suggested that SRIF signals through Gi/Go, and involves phospholipase C and Ca^{2+} release from the endoplasmic reticulum. The increase in $[Ca^{2+}]_i$ by SRIF leads to insulin release. This cross-talk is specific to Gq and Gi/Go, and is not limited to the AVP and SRIF receptors.

INTRODUCTION

The hormone insulin is synthesized and released from pancreatic β-cells, and is the most important regulator of elevated blood glucose concentrations. The mechanism that regulates insulin release is rather complex from the endocrine point of view. Although an increase in blood glucose concentrations is one of the most potent stimulators for insulin release, several hormones and neurotransmitters act directly or indirectly in the pancreas to stimulate or inhibit its release. Inhibition of insulin release by somatostatin (SRIF) has been well characterized in studies utilizing the whole pancreas, pancreatic islets and several β-cell lines [1-4]. Arginine vasopressin (AVP), a hormone normally found in the posterior pituitary gland, is also present in the pancreas [5]. We previously demonstrated AVP's ability to stimulate the release of glucagon and insulin from the rat pancreas, and in the α-cell line InR1G9 and β-cell line RINm5F [6,7].

SRIF was initially isolated and identified as an inhibitor of growth hormone release from anterior pituitary cells [8]. In the pancreas, SRIF is synthesized and released from δ-cells, and inhibits both endocrine and exocrine secretions [9,10]. The inhibitory effects of SRIF on insulin release have been associated with decreases in cAMP and intracellular calcium concentration ($[Ca^{2+}]_i$) through inhibition of Ca^{2+} influx via L-type voltage-dependent Ca^{2+} channels [4] and opening ATP-sensitive K^+ channels [11]. High resolution measurements of cell capacitance has also suggested that inhibition of insulin release by SRIF is associated with activation of the Ca^{2+}-dependent protein phosphatase calcineurin, and involves activation of G-proteins but not inhibition of voltage dependent Ca^{2+} currents or adenylate cyclase activity [12]. SRIF receptors are coupled to the pertussis toxin (PTX) sensitive family of G-proteins (Gi/Go) [13]. Binding of SRIF to its receptors leads to conformational changes in G-proteins, where α and βγ subunits assume their active form and dissociate from the receptor. Both PTX-sensitive and -insensitive G-proteins have the ability to transduce signals between receptors and phospholipase C (PLC) [14]. Overall, α and βγ subunits from different Gi/Go-coupled receptors have been shown to activate various target effectors [15,16]. The α subunit can inhibit adenylyl cyclase and Ca^{2+} influx via voltage-dependent Ca^{2+} channels, increase K^+ efflux via ATP-sensitive K^+ channels, and activate cGMP phosphodiesterase, whereas the βγ subunit can activate several enzymes

such as PLC-β, G-protein coupled receptor kinase, phospholipase A_2 and PtdIns 3-kinase [17-20].

An increasing number of cross-talk mechanisms have emerged among several G-protein-coupled receptors, which involve all levels of the signal cascade. Cross-talks between Gq and Gi/Go have been described in human neuroblastoma SH-SY5Y and COS cells [21-23]. In HIT-T15 cells, AVP binds V_{1b} receptors [24], which couples to Gq, thus activating PLC-β through the αq subunit with subsequent hydrolysis of PtdIns(4,5)P_2 to Ins(1,4,5)P_3 and diacylglycerol (DAG) [25]. DAG activates protein kinase C (PKC), while Ins(1,4,5)P_3 promotes Ca^{2+} release from the endoplasmic reticulum (ER), leading to an increase in $[Ca^{2+}]_i$ [7,26]. In SH-SY5Y cells, SRIF and neuropeptide Y (NPY) increase $[Ca^{2+}]_i$ after pretreatment with carbachol, a Gq-coupled receptor agonist [22]. SRIF and NPY alone fail to increase $[Ca^{2+}]_i$. Stimulation of PLC-β by the βγ subunit of different G-proteins has been shown to occur in addition to αq [27]. Studies in COS-1 cells provide further support for the βγ dimer mediation of the cross-talk between the Gq- and Gi-coupled receptors [23]. Enhancement of Gq-dependent signals by Gi-coupled receptors in COS-7 cells requires an activated PLC-β and is mediated by the βγ dimer [21]. In addition, activation of Gi/Go-coupled receptors has been shown to enhance the inositol phosphate signals generated by Gq-coupled receptors [28,29]. Although there are reports of cross-talk where an increase in inositol phosphate mass formation and $[Ca^{2+}]_i$ by Gi/Go occurred after activation of Gq-coupled receptors, our findings represent the first example in an endocrine cell line, and the first example of the cross-talk between SRIF and AVP receptors. The objective of the present study is to provide insights on the mechanism by which SRIF increases $[Ca^{2+}]_i$ and insulin release in the presence of AVP in β-clonal cells HIT-T15.

MATERIALS AND METHODS

Materials

All reagents were purchased from Sigma Chemical Co. (St. Louis, MO, U.S.A.), except that fura-2 acetoxymethyl ester (fura-2AM) was from Molecular Probes (Eugene, OR, U.S.A.), U-73122, 1-[6-[[17β-3-methoxyestra-1,3,5(10)-trien-17-yl]amino]hexyl]-1H-pyrrole,2,5-dione and U-73343, 1-[6-[[17β-3-methoxyestra-1,3,5(10)-trien-17-

yl]amino]hexyl]-2,5-pyrrolidine-dione were from Biomol Research Laboratory (Plymouth Meeting, PA, U.S.A.).

Cell culture

HIT-T15 cells (Simian virus 40-transformed Syrian hamster islets) were maintained in RPMI 1640 with 10 % fetal bovine serum and aerated with 5 % CO_2-95 % air at 37 °C. All experiments were performed using cells from passages 80-90.

$[Ca^{2+}]_i$ measurement in cell suspension

5 x 10^6 cells were grown in 75-cm^2 culture flasks for 5 days until 80-90 % confluency had been reached. Thereafter, the cells were harvested by treatment with trypsin-EDTA and prepared for experiments. Measurement of $[Ca^{2+}]_i$ was accomplished by loading 20 x 10^6 cells with 2 μM fura-2AM for 30 min at 37 °C in Krebs-Ringer bicarbonate buffer (KRB) containing (in mM): NaCl 136; KCl 4.8; $CaCl_2$ 1.2; $MgSO_4$ 1.2; Hepes 10; glucose 4 and 0.1 % BSA, pH 7.4. The loaded cells were centrifuged at 300 x *g* for 2 min and resuspended at a density of 2 x 10^6 cells/ml with KRB. The 340/380 nm fluorescence ratios were monitored by a SLM-8000 spectrofluorometer (SLM instruments, Urbana, IL, U.S.A.). The $[Ca^{2+}]_i$ was calibrated as previously described [4]. Experimental conditions in Ca^{2+}-free medium were created by centrifugation at 300 x *g* for 60 s followed by resuspending the cells in Ca^{2+}-free KRB containing 10 μM EGTA. Depletion of ER Ca^{2+} was accomplished by pretreatment with thapsigargin (TG), a microsomal Ca^{2+} ATPase inhibitor [30], for 30 min prior to SRIF. The involvement of Gi/Go in the SRIF-induced increase in $[Ca^{2+}]_i$ was examined by pretreatment with PTX (100 ng/ml) for 24 h. All experiments were repeated 4 times.

$[Ca^{2+}]_i$ measurement in single cells

1000-2000 cells were grown for 2-3 days on 22-mm^2 glass coverslip inside a 35-mm culture dish under similar conditions as described above. Thereafter, the culture medium was discarded and the cells loaded with fura-2AM for 30 min at 37 °C. Each coverslip was mounted inside a custom-made perfusion chamber, where it was possible to control the exposure of cells to different treatments. Measurement of $[Ca^{2+}]_i$ from single cells was accomplished by mounting the perfusion chamber on the stage of an inverted fluorescence microscope (Carl Zeiss, Thornwood, NY, U.S.A.). The fluorescence images were obtained (excitation 340 and 380 nm; emission 510±20 nm), background subtracted, and divided on a

pixel-by-pixel basis to generate spatially resolved maps of the $[Ca^{2+}]_i$. The emitted signals were digitalized, recorded and processed using the Attofluor Digital Fluorescence Imaging System (Atto Instruments, Rockville, MD, U.S.A.). The $[Ca^{2+}]_i$ was calculated according to a published method [31]. Calibration was performed *in situ* according the procedure provided by Attofluor, using Fura-2 penta K^+ salt as a standard.

Measurement of insulin release under perifusion conditions

The perifusion system used in this study was as previously described [32] with some modifications. HIT-T15 cells were grown in 10-mm round glass coverslips inside a 35-mm culture dish for 3-4 days until reaching confluency (400-700 x 10^3 cells). Each coverslip was then removed from the culture dish and mounted inside a 0.7-ml perifusion chamber (Millipore Swinnex Filter Holders, Waters, Milford, MA, U.S.A.) with cells facing inside of the chamber. Initially, the cells were perifused for a 20-min equilibration period at 37 °C with modified KRB containing (in mM): NaCl 136; KCl 4.8; $CaCl_2$ 2.5; KH_2PO_4 1.2; $MgSO_4$ 1.2; $NaHCO_3$ 5; Hepes 10; glucose 4 and 0.1 % BSA, pH 7.4. The flow rate was adjusted to 0.5 ml/min prior to the experiments and samples collected at a 30-s interval. Each coverslip was exposed to one of four treatments: control, which was treated with KRB; 1 nM AVP; 100 nM SRIF; 1 nM AVP followed by 100 nM SRIF. At the end of each experiment, cells were treated with 20 mM KCl to test their ability to release insulin. Once the experiments had been completed, the glass coverslips were removed from the perifusion chambers and the number of cells quantified. The insulin concentrations of effluent samples were measured by RIA. Each treatment group was replicated four times.

Data analysis

Traces from the $[Ca^{2+}]_i$ measurement are representative of 4 experiments. Results from the insulin release under perifusion conditions are presented as mean ± S.E.M., and were analyzed using analysis of variance (ANOVA) to determine the effect of treatment. Fisher's least significant difference test was used to determine the difference between means for which the ANOVA indicated a significant F ratio ($P < 0.05$).

RESULTS

SRIF-induced increase in $[Ca^{2+}]_i$ in the presence of AVP

In the presence of 1 nM AVP, 100 nM SRIF induced a sharp and transient increase in $[Ca^{2+}]_i$, followed by a rapid decline to the sub-basal level. To determine if this effect was due to hormone treatment, we replaced AVP and SRIF with KRB. SRIF failed to increase $[Ca^{2+}]_i$ in KRB and no further increases in $[Ca^{2+}]_i$ was observed when KRB was added in the presence of AVP. Treatment with SRIF prior to AVP did not enhance AVP-induced increase in $[Ca^{2+}]_i$. The increase in $[Ca^{2+}]_i$ by SRIF in the presence of AVP was still apparent even after 60 min of AVP treatment (Figure 1). The response to 100 nM SRIF gradually increased with a decrease in the AVP concentration from 100 nM to 100 pM. In the presence of 1 nM AVP, 100 nM SRIF caused a near maximal increase in $[Ca^{2+}]_i$. A concentration-dependent response to 100 pM-1 μM SRIF was also observed in the presence of 1 nM AVP, where near maximal response was obtained with 100 nM SRIF (Figure 2). For this reason, we chose 1 nM AVP followed by 100 nM SRIF to investigate the mechanism underlying SRIF-induced increase in $[Ca^{2+}]_i$ and insulin release in HIT-T15 cells.

By measuring $[Ca^{2+}]_i$ in single cells through imaging analysis, we determined if temporary pre-exposure to AVP or its presence was required for the SRIF-induced increase in $[Ca^{2+}]_i$. In the presence of AVP, SRIF increased $[Ca^{2+}]_i$, whereas temporary pre-exposure to AVP, followed by a 5-min washout period abolished the increase in $[Ca^{2+}]_i$ by SRIF (Figure 3).

In addition, we investigated if the rapid decline in $[Ca^{2+}]_i$ to sub-basal levels after the increase by SRIF was due to closure of voltage-dependent Ca^{2+} channels, thereby inhibiting the Ca^{2+} influx, or through efflux from the cytosol through plasma membrane Ca^{2+}-ATPases. Pretreatment with Bay K8644 (1 μM), which opens voltage-dependent Ca^{2+} channels or experiments in Ca^{2+}-free medium failed to alter the decline in $[Ca^{2+}]_i$. Pretreatment with Ca^{2+}-ATPases inhibitors such as sodium orthovanadate (0.01 – 1 mM), eosin Y(0.01 – 1 mM), lanthanum chloride (0.16 – 1 mM), ruthenium red (10 μM), or nickel sulfate (0.01 – 10 mM) also failed to alter the sharp decrease in $[Ca^{2+}]_i$ (data not shown).

SRIF-induced insulin release

We measured insulin release under perifusion conditions to determine if the increase in $[Ca^{2+}]_i$ by SRIF also resulted in insulin exocytosis. Perifusion with KRB or SRIF alone did

not increase insulin release. In the presence of AVP, SRIF induced a significant increase in insulin release, which was also characterized by a sharp peak, followed by a rapid decline to sub-basal levels. The stimulatory effect of SRIF lasted 2-3 min. Treatment with AVP alone induced a gradual increase in insulin release with a lower amplitude and a longer period (Figure 4).

Mediation by PTX-sensitive protein(s) of the SRIF effects

Since SRIF receptors belong to the PTX-sensitive Gi/Go family of G-proteins, we hypothesized that Gi/Go also mediated the increase in $[Ca^{2+}]_i$ by SRIF. Pretreatment of HIT-T15 cells with PTX abolished the increase in $[Ca^{2+}]_i$ by 100 nM SRIF, whereas it did not alter the increase in $[Ca^{2+}]_i$ by 1 nM AVP, which signals via Gq (Figure 5).

Involvement of PLC pathway

We examined if the PLC pathway was also involved in the SRIF signaling by using U-73122, a specific PLC inhibitor [33]. Pretreatment with U-73122 (1-4 μM) for 100 s before 100 nM SRIF (but after 1 nM AVP) inhibited the increase in $[Ca^{2+}]_i$ by SRIF in a concentration-dependent manner (data not shown). U-73122 (4 μM) abolished the increase in $[Ca^{2+}]_i$ by SRIF (Figure 6). Pretreatment with 4 μM U-73343, an inactive analog of U-73122 failed to inhibit the SRIF-induced increase in $[Ca^{2+}]_i$. When U-73122 was given prior to AVP, the responses to AVP and subsequently to SRIF were abolished.

Endoplasmic reticulum as the main source for Ca^{2+} release

Activation of the PLC pathway often leads to the formation of $Ins(1,4,5)P_3$, which increases Ca^{2+} release from the ER by binding to $Ins(1,4,5)P_3$ receptors [34]. We hypothesized that ER was the primary source of Ca^{2+} for the sharp and transient increase in $[Ca^{2+}]_i$ by SRIF. Pretreatment with 1 μM TG after 1 nM AVP abolished the increase in $[Ca^{2+}]_i$ by 100 nM SRIF. In Ca^{2+}-free medium supplemented with 10 μM EGTA, SRIF maintained its ability to increase $[Ca^{2+}]_i$ (Figure 7).

Cross-talk between Gq and Gi/Go

The SRIF-induced increase in $[Ca^{2+}]_i$ and insulin release in the presence of AVP may involve a cross-talk between Gq and Gi/Go. We examined if in the presence of bradykinin (BK), another Gq-coupled receptor agonist [35], and also in the presence of isoproterenol

(Gs-coupled receptor agonist) [36] or medetomidine (Gi/Go-coupled receptor agonist) [37], SRIF would maintain its ability to increase $[Ca^{2+}]_i$. In the presence of BK (1 nM-1 μM BK), 100 nM SRIF increased $[Ca^{2+}]_i$. Similar to AVP, the response to SRIF gradually increased with a decrease in the BK concentration from 1 μM to10 nM. In the presence of 10 μM isoproterenol, which induced a small increase in $[Ca^{2+}]_i$ or 10 μM medetomidine, SRIF failed to increase $[Ca^{2+}]_i$. In the presence of 1 nM AVP, 10 μM medetomidine also increased $[Ca^{2+}]_i$ (Figure 8).

DISCUSSION

The present study demonstrated that in the presence of AVP, SRIF increased $[Ca^{2+}]_i$, which was characterized by a sharp and transient peak followed by a rapid decline to the sub-basal level. Experiments with TG, which depletes Ca^{2+} stores from the ER, suggested that Ca^{2+} released from this organelle is mainly responsible for the sharp and transient increase in $[Ca^{2+}]_i$ by SRIF. Pretreatment with Ca^{2+}-ATPases inhibitors or experiments in Ca^{2+}-free medium failed to alter the rapid decline in $[Ca^{2+}]_i$ to sub-basal level. Further investigation will be needed to determine the mechanism responsible for this sharp decline in $[Ca^{2+}]_i$.

One unexpected finding was the ability of SRIF to increase $[Ca^{2+}]_i$ even after 60 min of AVP treatment. In HIT-T15 cells, the V_{1b} receptor is coupled to Gq, which upon activation stimulates PLC-β through its αq subunit [24]. The hydrolysis of PtdIns(4,5)P_2 by PLC-β results in Ins(1,4,5)P_3 and DAG formation, where DAG activates protein kinase C (PKC) and Ins(1,4,5)P_3 promotes Ca^{2+} release from the ER [7,26,34]. Phosphorylation of AVP receptors and PLC-β by PKC after activation of the AVP receptor occurs during desensitization [38-41]. This event accounts in part for the reduction in the responsiveness of cells to further stimulation by AVP. However, in our system, desensitization of AVP receptors and PLC-β may not be apparent during the stimulation by a small concentration of AVP (1 nM) , since we demonstrated that the presence of AVP is required for SRIF to increase $[Ca^{2+}]_i$ and this increase could be observed even after 60 min of treatment with 1 nM of AVP.

An increase in $[Ca^{2+}]_i$ usually triggers exocytosis [42]. During perifusion experiments, SRIF alone did not increase insulin release, but enhanced the AVP-induced insulin release.

These results were consistent with data on $[Ca^{2+}]_i$, which suggested that the increase in insulin release was mediated by the increase in $[Ca^{2+}]_i$.

Five distinct SRIF receptor subtypes have been characterized and designated as sstr1-5, where two splice variants of the sstr2 exist, sstr2a and sstr2b [43,44]. All 5 receptor subtypes are coupled to Gi/Go. Pretreatment with PTX abolished the increase in $[Ca^{2+}]_i$ by SRIF, suggesting that Gi/Go also mediate the SRIF effects. PTX pretreatment did not alter the increase in $[Ca^{2+}]_i$ by AVP, which signals via Gq, a PTX-insensitive family of G-proteins. The SRIF receptor subtype that mediates the increase in $[Ca^{2+}]_i$ and insulin release remains to be characterized.

Activation of PLC-β frequently leads to an increase in Ins(1,4,5)P_3 mass formation and $[Ca^{2+}]_i$, where the involvement of Gi/Go subunits, mainly the βγ dimer in these increases have been reported by others [17,21,23]. In our study, the increase in $[Ca^{2+}]_i$ by SRIF was inhibited by U-73122, a specific PLC inhibitor, but not by U-73343, an inactive analog of U-73122. These findings suggested that the effects of SRIF are mediated through the PLC pathway. Pretreatment with U-73122 prior to AVP abolished the responses to AVP and subsequently to SRIF, which suggested that activation of PLC-β by AVP is essential for SRIF to increase $[Ca^{2+}]_i$. To date, reports addressing the stimulatory effects of Gi/Go-coupled receptor agonists on the PLC-β pathway have been made through measurement of Ins(1,4,5)P_3 mass formation or using inhibitors/antibodies against PLC [18,21,23], which does not provide evidence to preclude the events occurring prior to activation of PLC-β, such as an increase in the formation of PtdIns(4,5)P_2.

We have demonstrated that the cross-talk is specific to Gq and Gi/Go, although not limited to the AVP and SRIF receptors, since in the presence of BK, SRIF increased $[Ca^{2+}]_i$. After AVP, treatment with medetomidine, an α_2-adrenoceptor agonist that stimulates Gi/Go, also increased $[Ca^{2+}]_i$. When isoproterenol, a β-adrenoceptor agonist that stimulates Gs, or medetomidine was given prior to SRIF, it failed to increase $[Ca^{2+}]_i$.

In summary, our findings suggested that in the presence of AVP, SRIF increased $[Ca^{2+}]_i$ and insulin release from HIT-T15 cells through Gi/Go, which involves the PLC pathway and Ca^{2+} release from the ER. The cross-talk mechanism is specific to Gq and Gi/Go, although it may not be limited only to the G-protein system coupled to the AVP or SRIF receptors. Further work on primary β-cells and islets will be necessary to determine the physiological significance of the present findings.

REFERENCES

1 Alberti, K. G., Christensen, N. J., Christensen, S. E., Hansen, A. P., Iversen, J., Lundbaek, K., Seyer-Hansen, K. and Orskov, H. (1975) Inhibition of insulin release by somatostatin. Lancet **2**, 1299-1301

2 Okamoto, H., Noto, Y., Miyamoto, S., Mabuchi, H. and Takeda, R. (1975) Inhibition by somatostatin of insulin release from isolated pancreatic islets. FEBS Lett. **54**, 103-105

3 Strowski, M. Z., Parmar, R. M., Blake, A. D. and Schaeffer, J. M. (2000) Somatostatin inhibits insulin and glucagon secretion via two receptors subtypes: an in vitro study of pancreatic islets from somatostatin receptor 2 knockout mice. Endocrinology **141**, 111-117

4 Hsu, W. H., Xiang, H. D., Rajan, A. S., Kunze, D. L. and Boyd, A. E. (1991) Somatostatin inhibits insulin secretion by a G-protein-mediated decrease in Ca^{2+} entry through voltage-dependent Ca^{2+} channels in the beta cell. J. Biol. Chem. **266**, 837-843

5 Amico, J. A., Finn, F. M. and Haldar, J. (1988) Oxytocin and vasopressin are present in human and rat pancreas. Am. J. Med. Sci. **296**, 303-307

6 Yibchok-anun, S., Cheng, H., Chen, T. H. and Hsu, W. H. (2000) Mechanisms of AVP-induced glucagon release in clonal α-cells In-R1-G9: involvement of Ca^{2+}-dependent and -independent pathways. Br. J. Pharmacol. **129**, 257-264

7 Chen, T. H., Lee, B. and Hsu, W. H. (1994) Arginine vasopressin-stimulated insulin secretion and elevation of intracellular Ca^{++} concentration in rat insulinoma cells: influences of a phospholipase C inhibitor 1-[6-[[17 β-methoxyestra-1,3,5(10)-trien- 17-yl]amino]hexyl]-1H-pyrrole-2,5-dione (U-73122) and a phospholipase A2 inhibitor N-(p-amylcinnamoyl) anthranilic acid. J. Pharmacol. Exp. Ther. **270**, 900-904

8 Brazeau, P., Vale, W., Burgus, R., Ling, N., Butcher, M., Rivier, J., and Guillemin, R. (1973) Hypothalamic polypeptide that inhibits the secretion of immunoreactive pituitary growth hormone. Science **170**, 77-79

9 Mandarino, L., Stenner, D., Blanchard, W., Nissen, S., Gerich, J., Ling, N., Brazeau, P., Bohlen, P., Esch, F. and Guillemin, R. (1981) Selective effects of somatostatin -14, -25 and -28 on in vitro insulin and glucagon secretion. Nature **291**, 76-77

10 Reichlin, S. (1983) Somatostatin. N. Engl. J. Med. **309**, 1556-1563

11 Ribalet, B. and Eddlestone, G. T. (1995) Characterization of the G protein coupling of a somatostatin receptor to the K^+ ATP channel in insulin-secreting mammalian HIT and RIN cell lines. J. Physiol (Lond.). **485**, 73-86

12 Renstrom, E., Ding, W. G., Bokvist, K. and Rorsman, P. (1996) Neurotransmitter-induced inhibition of exocytosis in insulin-secreting beta cells by activation of calcineurin. Neuron **17**, 513-522

13 Reisine, T., Zhang, Y. L. and Sekura, R. (1985) Pertussis toxin treatment blocks the inhibition of somatostatin and increases the stimulation by forskolin of cyclic AMP accumulation and adrenocorticotropin secretion from mouse anterior pituitary tumor cells. J. Pharmacol. Exp. Ther. **232**, 275-282

14 Sternweis, P. C. and Smrcka, A. V. (1992) Regulation of phospholipase C by G proteins. Trends Biol. Sci. **17**, 502-506

15 Carty, D. J., Padrell, E., Codina, J., Birnbaumer, L., Hildebrandt, J. D. and Iyengar, R. (1990) Distinct guanine nucleotide binding and release properties of the three Gi proteins. J. Biol. Chem. **265**, 6268-6273

16 Linder, M. E., Ewald, D. A., Miller, R. J. and Gilman, A. G. (1990) Purification and characterization of Go α and three types of Gi α after expression in Escherichia coli. J. Biol. Chem. **265**, 8243-8251

17 Clapham, D. E. and Neer, E. J. (1993) New roles for G-protein $\beta\gamma$ dimers in transmembrane signalling. Nature **365**, 403-406

18 Murthy, K. S., Coy, D. H. and Makhlouf, G. M. (1996) Somatostatin receptor-mediated signaling in smooth muscle. Activation of phospholipase C-β3 by G$\beta\gamma$ and inhibition of adenylyl cyclase by Gαi1 and Gαo. J. Biol. Chem. **271**, 23458-23463

19 Lopez-Ilasaca, M., Gutkind, J. S. and Wetzker, R. (1998) Phosphoinositide 3-kinase γ is a mediator of G$\beta\gamma$-dependent Jun kinase activation. J. Biol. Chem. **273**, 2505-2508

20 Myung, C. S. and Garrison, J. C. (2000) Role of C-terminal domains of the G protein β subunit in the activation of effectors. Proc. Natl. Acad. Sci. U S A. **97**, 9311-9316

21 Chan, J. S., Lee, J. W., Ho, M. K. and Wong, Y. H. (2000) Preactivation permits subsequent stimulation of phospholipase C by G(i)-coupled receptors. Mol. Pharmacol. **57**, 700-708

22 Connor, M., Yeo, A. and Henderson, G. (1997) Neuropeptide Y Y_2 receptor and somatostatin sst_2 receptor coupling to mobilization of intracellular calcium in SH-SY5Y human neuroblastoma cells. Br. J. Pharmacol. **120**, 455-463

23 Quitterer, U. and Lohse, M. J. (1999) Crosstalk between $G\alpha_i$- and $G\alpha_q$-coupled receptors is mediated by $G\beta\gamma$ exchange. Proc. Natl. Acad. Sci. USA. **96**, 10626-10631

24 Richardson, S. B., Eyler, N., Twente, S., Monaco, M., Altszuler, N. and Gibson, M. (1990) Effects of vasopressin on insulin secretion and inositol phosphate production in a hamster β cell line (HIT). Endocrinology **126**, 1047-1052

25 Thibonnier, M. (1992) Signal transduction of V_1-vascular vasopressin receptors. Regul. Pept. **3**, 1-11

26 Li, G., Pralong, W. F., Pittet, D., Mayr, G. W., Schlegel, W. and Wollheim, C. B. (1992) Inositol tetrakisphosphate isomers and elevation of cytosolic Ca^{2+} in vasopressin-stimulated insulin-secreting RINm5F cells. J. Biol. Chem. **267**, 4349-4356

27 Offermanns, S. and Simon, M. I. (1995) $G\alpha_{15}$ and $G\alpha_{16}$ couple a wide variety of receptors to phospholipase C. J. Biol. Chem. **270**, 15175-15180

28 Muller, S. and Lohse, M. J. (1995) The role of G-protein βγ subunits in signal transduction. Biochem. Soc. Trans. **23**, 141-148

29 Neer, E. J. (1995) Heterotrimeric G proteins: organizers of transmembrane signals. Cell **80**, 249-257

30 Thastrup, O., Cullen, P. J., Drobak, B. K., Hanley, M. R. and Dawson, A. P. (1990) Thapsigargin, a tumor promoter, discharges intracellular Ca^{2+} stores by specific inhibition of the endoplasmic reticulum Ca^{2+}-ATPase. Proc. Natl. Acad. Sci. U S A. **87**, 2466-2470

31 Grynkiewicz, G., Poenie, M., and Tsien, R. Y. (1985) A new generation of Ca^{2+} indicators with greatly improved fluorescence properties. J. Biol. Chem. **260**, 3440-3450

32 Kikuchi, M., Rabinovitch, A., Blackard, W. G. and Renold, A. E. (1975) Perifusion of pancreas fragments. A system for the study of dynamic aspects of insulin secretion. Diabetes **23**, 550-559

33 Smith, R. J., Sam, L. M., Justen, J. M., Bundy, G. L., Bala, G. A. and Bleasdale, J. E. (1990) Receptor-coupled signal transduction in human polymorphonuclear neutrophils: effects of a novel inhibitor of phospholipase C-dependent processes on cell responsiveness. J. Pharmacol. Exp. Ther. **253**, 688-697

34 Thorn, P. and Petersen, O. H. (1991) Activation of voltage-sensitive Ca^{2+} currents by vasopressin in an insulin-secreting cell line. J. Membr. Biol. **124**, 63-71

35 Saito, Y., Kato, M., Kubohara, Y., Kobayashi, I. and Tatemoto, K. (1996) Bradykinin increases intracellular free Ca^{2+} concentration and promotes insulin secretion in the clonal beta-cell line, HIT-T15. Biochem. Biophys. Res. Commun. **221**, 577-580

36 Walseth, T. F., Zhang, H. J., Olson, L. K., Schroeder, W. A. and Robertson, R. P. (1989) Increase in Gs and cyclic AMP generation in HIT cells. Evidence that the 45-kDa alpha-subunit of Gs has greater functional activity than the 52-kDa alpha-subunit. J. Biol. Chem. **264**, 21106-21111

37 Chen, T. H. and Hsu, W. H. (1994) Inhibition of insulin release by a formamidine pesticide amitraz and its metabolites in a rat beta-cell line: an action mediated by alpha-2 adrenoceptors, a GTP-binding protein and a decrease in cyclic AMP. J. Pharmacol. Exp. Ther. **271**, 1240-1245

38 Innamorati, G., Sadeghi, H. and Birnbaumer, M. (1998) Transient phosphorylation of the V1a vasopressin receptor. J. Biol. Chem. **273**, 7155-7161

39 Birnbaumer, M., Antaramian, A., Themmen, A. P. and Gilbert, S. (1992) Desensitization of the human V2 vasopressin receptor. Homologous effects in the absence of heterologous desensitization. J. Biol. Chem. **267**, 11783-11788

40 Aiyar, N., Nambi, P. and Crooke S. T. (1990) Desensitization of vasopressin sensitive adenylate cyclase by vasopressin and phorbol esters. Cell Signal **2**, 153-160

41 Cantau, B., Guillon, G., Alaoui, M. F., Chicot, D., Balestre, M. N. and Devilliers, G. (1988) Evidence of two steps in the homologous desensitization of vasopressin-sensitive phospholipase C in WRK1 cells. Uncoupling and loss of vasopressin receptors. J. Biol. Chem. **263**, 10443-10450

42 Wollheim, C. B. and Pozzan, T. (1984) Correlation between cytosolic free Ca^{2+} and insulin release in an insulin-secreting cell line. J. Biol. Chem. **259**, 2262-2267

43 Bruno, J. F., Xu, Y., Song, J. and Berelowitz, M. (1992) Molecular cloning and functional expression of a brain-specific somatostatin receptor. Proc. Natl. Acad. Sci. U S A. **89**, 11151-11155

44 Patel, Y. C., Greenwood, M. T., Warszynska, A., Panetta, R. and Srikant, C. B. (1994) All five cloned human somatostatin receptors (hSSTR1-5) are functionally coupled to adenylyl cyclase. Biochem. Biophys. Res. Commun. **198**, 605-612

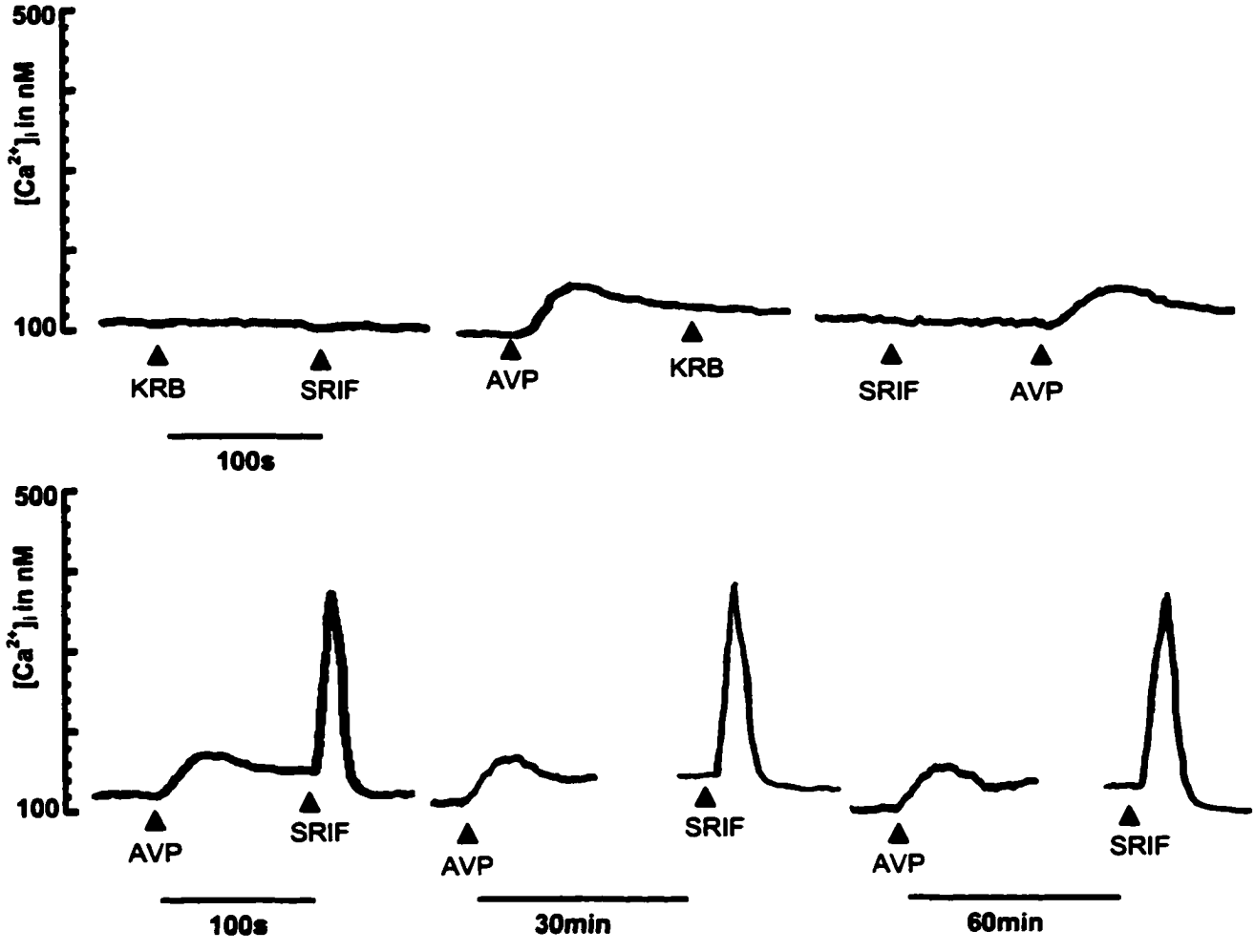

Figure 1 Somatostatin (SRIF)-induced increase in $[Ca^{2+}]_i$ in the presence of AVP
Lower panel: In the presence of 1 nM AVP, 100 nM SRIF increased $[Ca^{2+}]_i$ (right). The increase in $[Ca^{2+}]_i$ by SRIF was observed even after 60 min of AVP treatment (left). Upper panel: The effect of SRIF was confirmed by replacing AVP with working buffer (KRB). No increase in $[Ca^{2+}]_i$ was observed after SRIF treatment (left). When SRIF was replaced by KRB, only the typical increase in $[Ca^{2+}]_i$ by AVP was observed (middle). Treatment with SRIF prior to AVP did not induce further increase in $[Ca^{2+}]_i$ by AVP (Right). Traces are representative of 4 experiments.

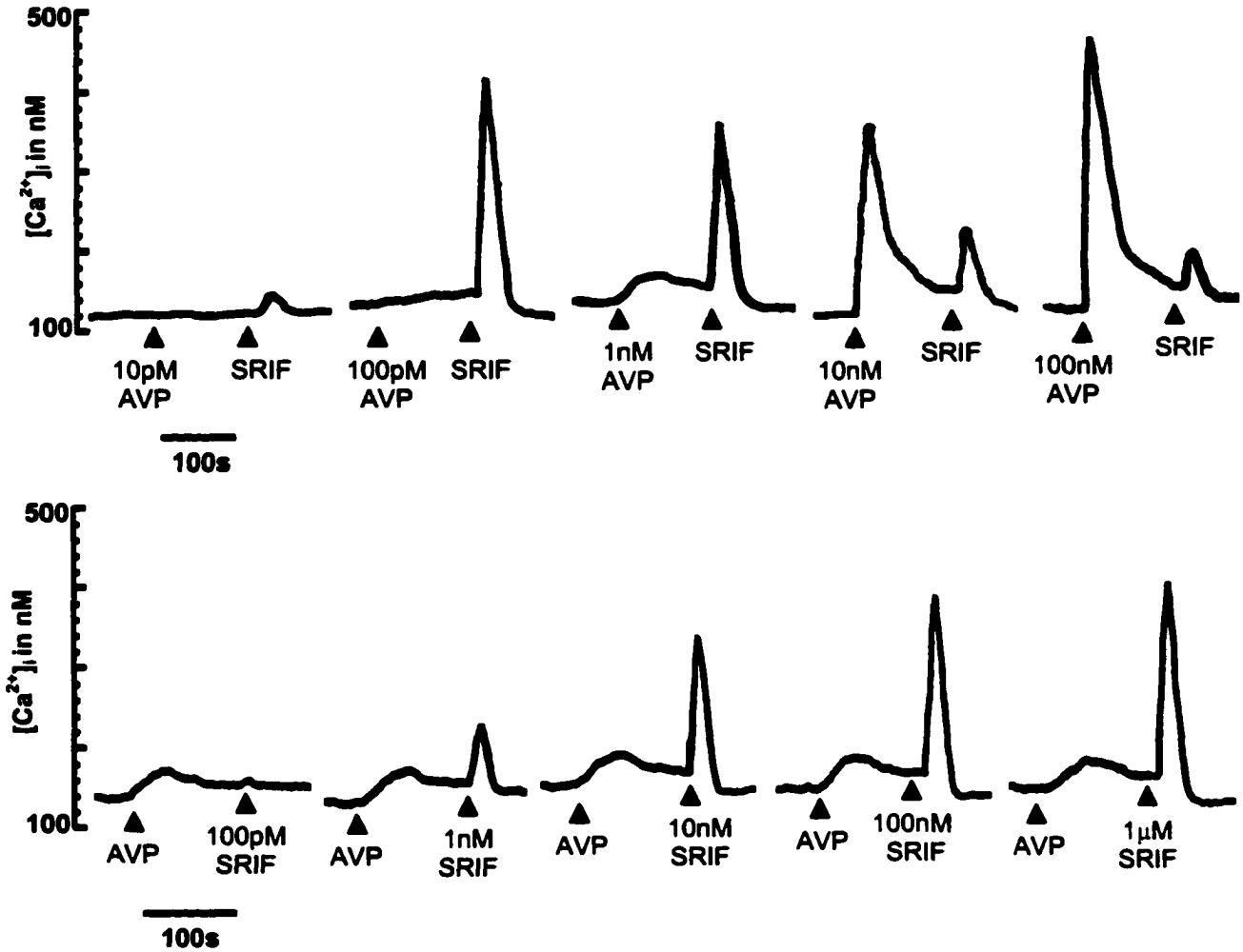

Figure 2 Dose responses to AVP and SRIF

Upper panel: The response to 100 nM SRIF gradually increased with a decrease in the AVP concentration from 100 nM to100 pM, where a near maximal response was obtained in the presence of AVP. Lower panel: A concentration-dependent response to 100 pM -1 μM SRIF was also observed in the presence of 1 nM AVP, where a near maximal response was obtained with 100 nM SRIF. Traces are representative of 4 experiments.

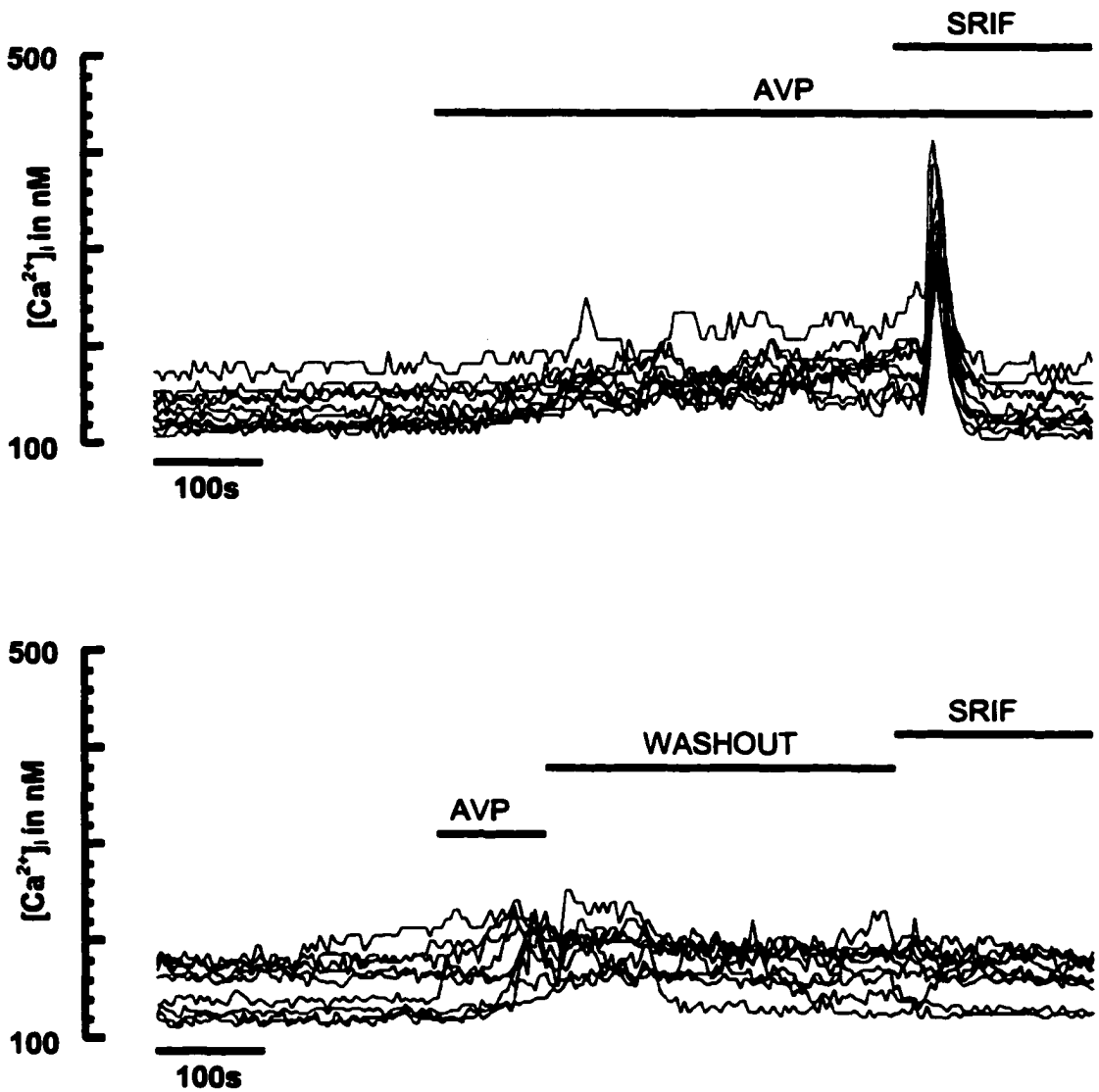

Figure 3 Effect of AVP washout on SRIF-induced increase in $[Ca^{2+}]_i$

Upper panel: In the presence of 1nM AVP, SRIF (100 nM) increased $[Ca^{2+}]_i$ in single cells during Ca^{2+} imaging analysis (n=10 cells). Lower panel: Temporary pre-exposure to AVP, followed by a 5-min washout period, abolished the increase in $[Ca^{2+}]_i$ by SRIF (n=9 cells). Traces are representative of 4 experiments.

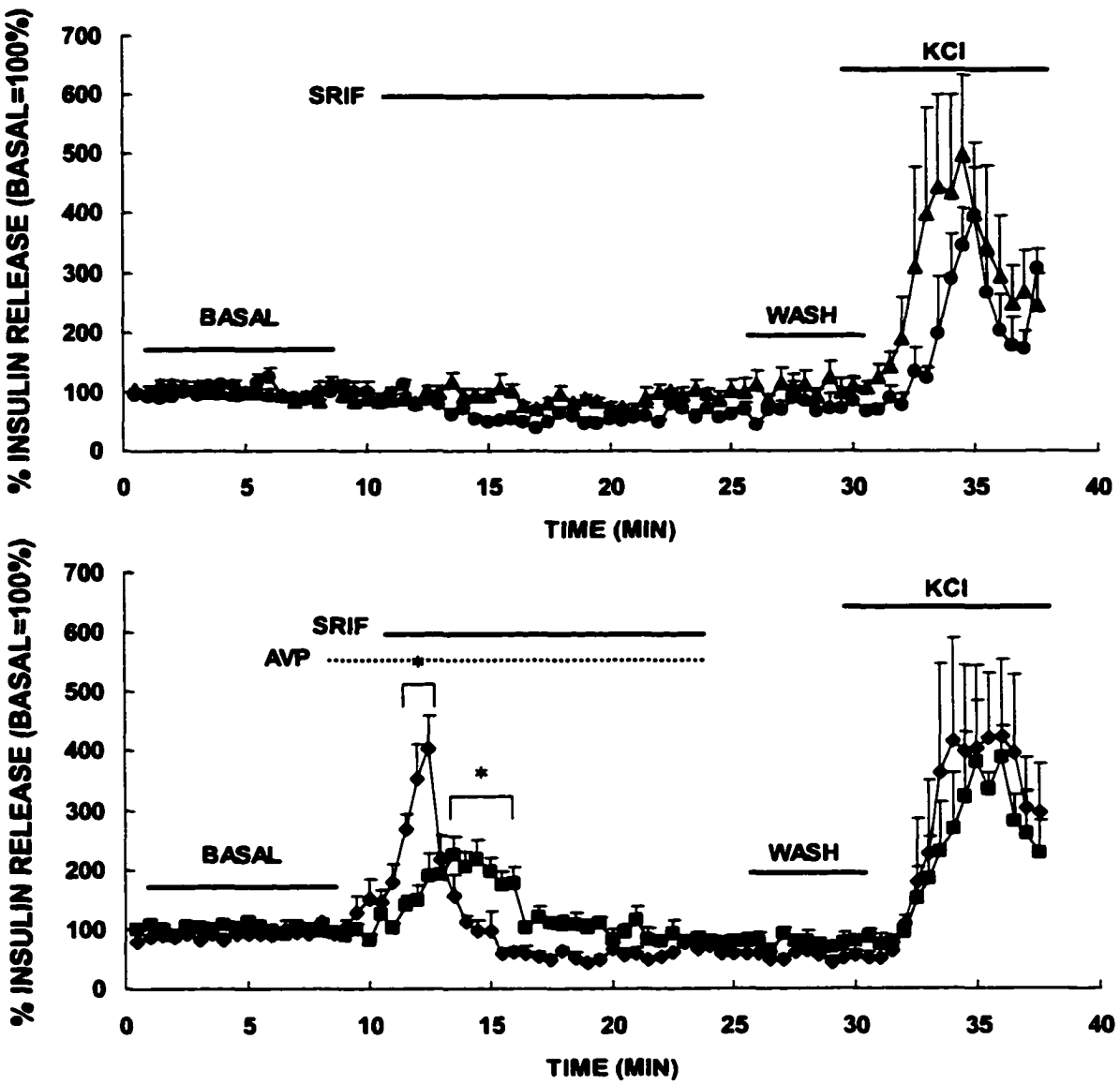

Figure 4 Effect of SRIF on insulin release in the presence of AVP

Upper panel: In control experiments, perifusion with Krebs-Ringer bicarbonate buffer (KRB) (▲) or 100 nM SRIF alone (●) did not increase insulin release. Lower panel: In the presence of 1 nM AVP, SRIF (◆) increased insulin release, which was characterized by a sharp peak, followed by a rapid decline to sub-basal level. Treatment with 1 nM AVP alone (■) induced a gradual increase in insulin release with a lower amplitude but a longer period. Treatment with 20 mM KCl at the end of the perifusion experiments also stimulated insulin release. Each data point represents the mean ± S.E.M. (n=4), $^{*}P < 0.05$ between the AVP and AVP + SRIF treated groups at the corresponding times.

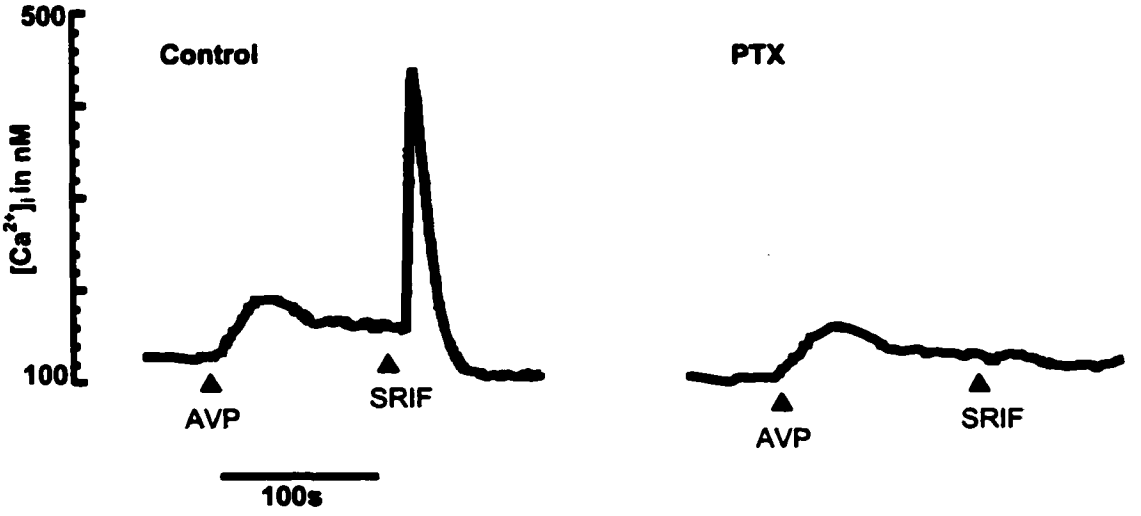

Figure 5 Effect of pertussis-toxin (PTX) on SRIF-induced increase in $[Ca^{2+}]_i$
Pretreatment with PTX (100 ng/ml, 24 h) abolished the increase in $[Ca^{2+}]_i$ by 100 nM SRIF. PTX pretreatment had no effects on the response to 1nM AVP. Traces are representative of 4 experiments.

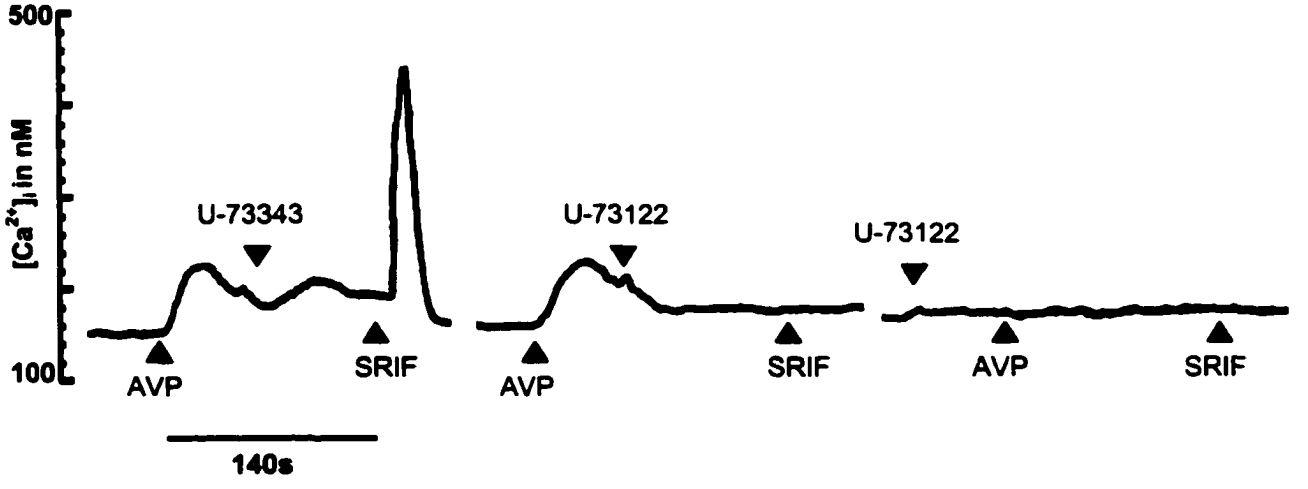

Figure 6 Effects of U-73122 and U-73343 on SRIF-induced increase in $[Ca^{2+}]_i$

Pretreatment with U-73122 (4 μM), a specific PLC inhibitor, after 40 s of 1 nM AVP and 100 s prior to SRIF, abolished the increase in $[Ca^{2+}]_i$ by 100 nM SRIF (middle panel). Pretreatment with U-73122 for 100 s prior to AVP (right panel), abolished the responses to AVP and subsequently to SRIF. Traces are representative of 4 experiments. Pretreatment with 4 μM U-73343 (left panel), an inactive analog of U-73122, failed to inhibit the increase in $[Ca^{2+}]_i$ by SRIF.

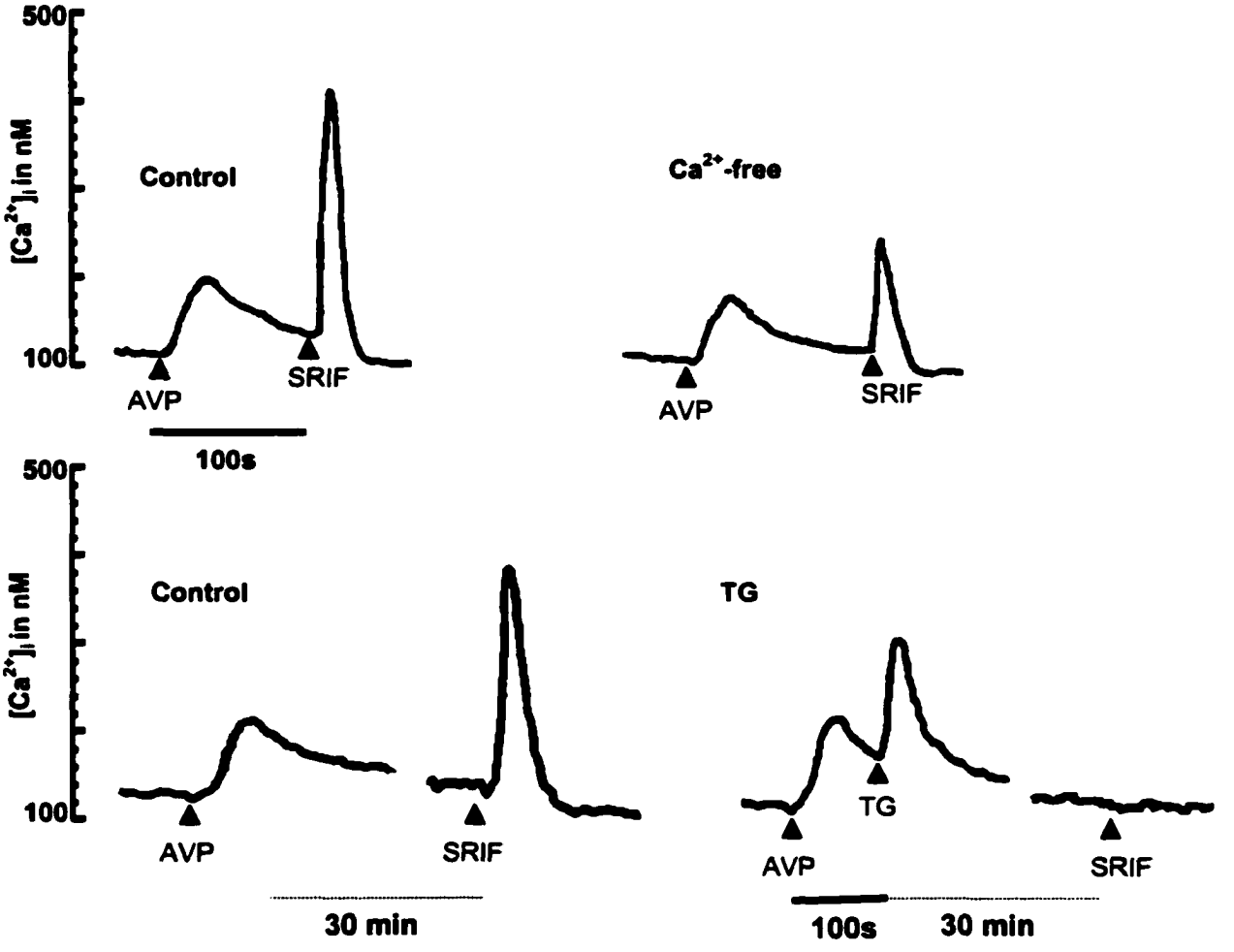

Figure 7 Effects of Ca^{2+}-free environment and thapsigargin (TG) on SRIF-induced increase in $[Ca^{2+}]_i$

Upper panel: In Ca^{2+}-free medium supplemented with 10 μM EGTA, 100 nM SRIF maintained its ability to increase $[Ca^{2+}]_i$ in the presence of AVP. Lower panel: Pretreatment with TG (1 μM), which depletes endoplasmic reticulum Ca^{2+} stores, abolished the increase in $[Ca^{2+}]_i$ by SRIF. Traces are representative of 4 experiments.

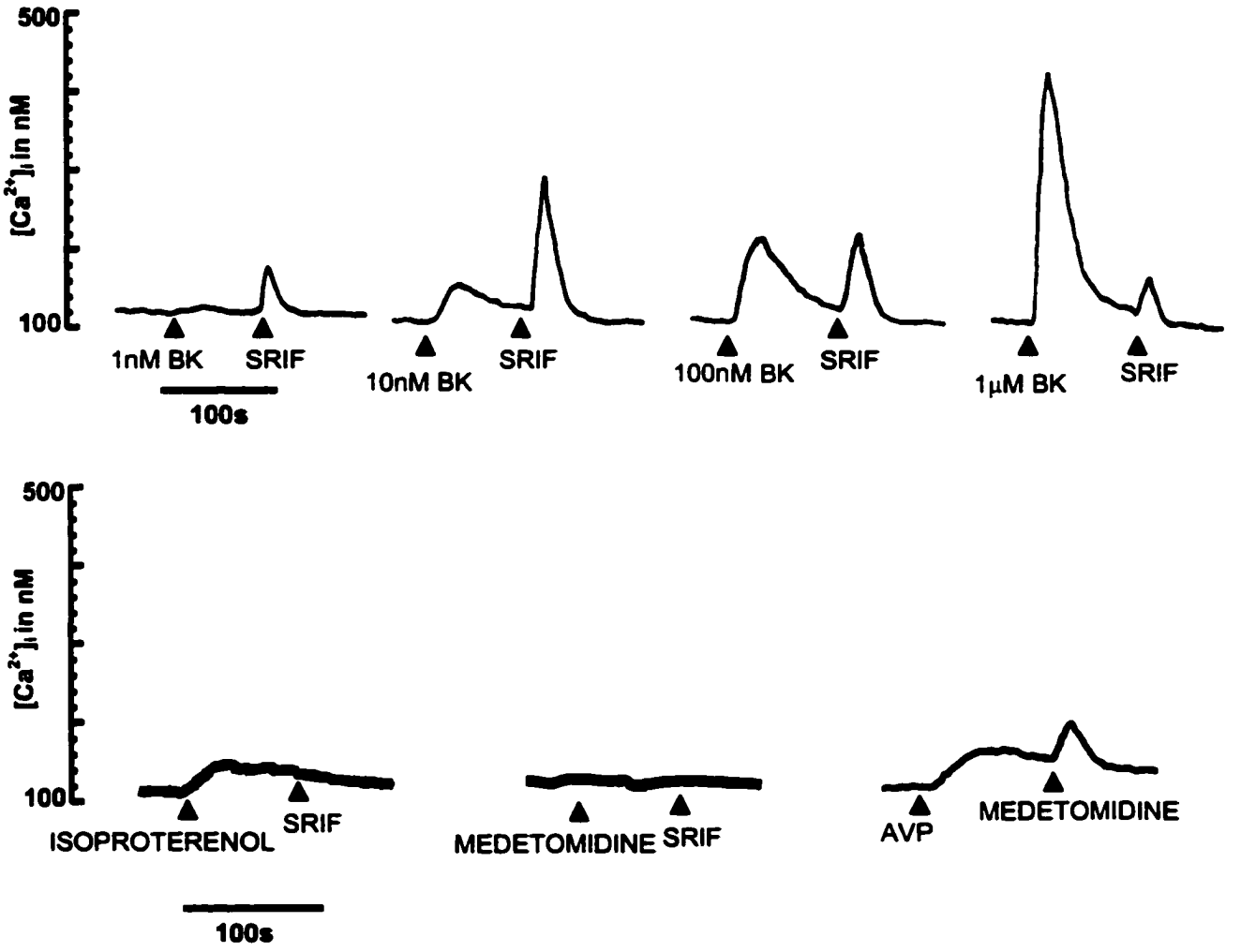

Figure 8 Interactions between other agonists of G-protein-coupled receptors
Upper panel: In the presence of bradykinin, another Gq-coupled receptor agonist, 100 nM SRIF also increased $[Ca^{2+}]_i$. Lower panel: In the presence of isoproterenol (10 μM), a Gs-coupled receptor agonist (left), or medetomidine (10 μM), a Gi/Go-coupled receptor agonist (middle), 100 nM SRIF failed to increase $[Ca^{2+}]_i$. In the presence of 1 nM AVP, medetomidine (10 μM), increased $[Ca^{2+}]_i$ (right). Traces are representative of 4 experiments.

CHAPTER III SSTR2 MEDIATES THE SOMATOSTATIN-INDUCED INCREASE IN INTRACELLULAR Ca^{2+} CONCENTRATION AND INSULIN SECRETION IN THE PRESENCE OF ARGININE VASOPRESSIN IN CLONAL β-CELLS HIT-T15

A paper accepted for publication in Life Sciences

Henrique Cheng, Sirintorn Yibchok-anun, David H. Coy and Walter H. Hsu

ABSTRACT

The effects of somatostatin (SRIF) are mediated through the seven transmembrane receptor family that signals via Gi/Go. To date, five distinct SRIF receptors have been characterized and designated SSTR1-5. We have characterized the SRIF receptor that mediates the increase in $[Ca^{2+}]_i$ and insulin secretion in HIT-T15 cells (Simian virus 40-transformed Syrian hamster islets) using high affinity, subtype selective agonists for SSTR1 (L-797,591), SSTR2 (L-779,976), SSTR3 (L-796,778), SSTR4 (L-803,087), SSTR5 (L-817,818) and PRL-2903, a specific SSTR2 antagonist. In the presence of arginine vasopressin (AVP), SRIF increased $[Ca^{2+}]_i$ and insulin secretion. Treatment with the SSTR2 agonist L-779,976 resulted in similar responses to SRIF. In addition, L-779,976 increased both $[Ca^{2+}]_i$ and insulin secretion in a dose-dependent manner. Treatment with L-779,976 alone did not alter $[Ca^{2+}]_i$ or basal insulin secretion. In the presence of AVP, all other SRIF receptor agonists failed to increase $[Ca^{2+}]_i$ and insulin secretion. The effects of SRIF and L-779,976 were abolished by the SSTR2 antagonist PRL-2903. Our results suggest that the mechanism underlying SRIF-induced insulin secretion in HIT-T15 cells be mediated through the SSTR2.

INTRODUCTION

Somatostatin (SRIF), a tetradecapeptide hormone that has diverse physiological actions, was initially isolated and identified as an inhibitor of growth hormone secretion from anterior pituitary cells [1]. SRIF-containing neurons are found in the central nervous system [2]. In addition, SRIF is also present in the gut, where it promotes smooth muscle

contraction [3]. In the pancreas, SRIF is synthesized and released from δ-cells, which inhibits both endocrine and exocrine secretions [4-6]. The inhibitory effect of SRIF on insulin secretion is well-characterized in the whole pancreas [7-9], pancreatic islets [10,11] and several β-cell lines [12-16]. The inhibitory effect of SRIF on insulin secretion is associated with a decrease in cAMP and a decrease in $[Ca^{2+}]_i$ through inhibiting Ca^{2+} influx via L-type voltage-dependent Ca^{2+} channels [14,17,18] and opening ATP-sensitive K^+ channels [19].

Arginine vasopressin (AVP), a hormone normally present in the posterior pituitary gland, is also found in the pancreas [20]. Previously, we demonstrated that in the presence of AVP, which signals via Gq, SRIF increased $[Ca^{2+}]_i$ leading to insulin secretion in HIT-T15 cells [21,22]. Our findings suggested that the mechanism by which SRIF signals be through Gi/Go, and involve the phospholipase C pathway and mainly Ca^{2+} release from the endoplasmic reticulum. The increase in $[Ca^{2+}]_i$ by SRIF leads to insulin secretion.

Five distinct SRIF receptors have been characterized and designated as SSTR1-5, where two splice variants of the SSTR2 exists, SSTR2a and SSTR2b [23-25]. Studies utilizing rabbit polyclonal antibodies against the human SSTR1-5 and double-label confocal fluorescence immunocytochemistry have demonstrated that all five subtypes are variably expressed in human pancreatic islets, where SSTR1 and SSTR5 are dominant in β-cells [26]. Studies in rat β-cells have provided evidence for the SSTR5 being the mediator for the inhibitory effects of SRIF [27]. This observation has been confirmed in knockout mice, where SSTR5 mediates the inhibitory effect on insulin secretion [28]. However, the receptor subtype that mediates the SRIF effects in HIT-T15 cells remains unknown. The lack of specific antagonists for all five different receptor subtypes makes it impossible to characterize these through antagonism studies. Fortunately, the identification of high-affinity, subtype-selective agonists for SSTR1-5 through combinatorial chemistry [29] now provides a direct approach for the characterization and definition of their physiological roles. The objective of the study is to characterize the SRIF receptor subtype that mediates the increase in $[Ca^{2+}]_i$ leading to insulin secretion in the presence of AVP in HIT-T15 cells.

MATERIALS AND METHODS

Reagents

All reagents were purchased from Sigma Chemical (St. Louis, MO), except that fura-2 acetoxymethyl ester (fura-2AM) was from Molecular Probes (Eugene, OR); The SRIF

receptor subtype-selective agonists: L-797,591 (SSTR1), L-779,976 (SSTR2), L-796,778 (SSTR3), L-803,087 (SSTR4) and L-817,818 (SSTR5) were donated by Merck Research Laboratories (West Point, PA); The SSTR2 antagonist PRL-2903 was synthesized by standard solid phase methodologies, purified and analyzed by mass spectrometry as previously described [30,31].

Cell culture

HIT-T15 cells were maintained in RPMI 1640 with 10 % fetal bovine serum and aerated with 5 % CO_2-95 % air at 37 °C. All experiments were performed using cells from passages 80-90.

$[Ca^{2+}]_i$ measurement in cell suspension

5 x 10^6 cells were grown in 75-cm^2 culture flasks for 5 days until 80-90 % confluency had been reached. Thereafter, the cells were harvested by treatment with trypsin-EDTA and prepared for experiments. Measurement of $[Ca^{2+}]_i$ was accomplished by loading 20 x 10^6 cells with 2 μM fura-2AM for 30 min at 37 °C in Krebs-Ringer bicarbonate buffer (KRB) containing (in mM): NaCl 136; KCl 4.8; $CaCl_2$ 1.2; $MgSO_4$ 1.2; HEPES 10; glucose 4 and 0.1 % BSA, pH 7.4. The loaded cells were centrifuged at 300 x *g* for 2 min and resuspended at a density of 2 x 10^6 cells/ml with dye-free KRB until used. The 340/380 nm fluorescence ratios were monitored by an SLM-8000 spectrofluorometer (SLM instruments, Urbana, IL). The $[Ca^{2+}]_i$ was calibrated as previously described [32]. Experiments with PRL-2903 were done by pretreating HIT-T15 cells with this SSTR2 antagonist for 5 min prior to the $[Ca^{2+}]_i$ measurement. The SRIF receptor subtype-selective agonists were given after 100 s of AVP treatment. All experiments were repeated 4 times.

Measurement of insulin secretion under static incubation conditions

HIT-T15 cells were plated into 24-well plates at ~ 2 x 10^5 cells/well and grown for 3-4 days. Measurement of insulin secretion was accomplished by replacing the culture medium with modified KRB containing (in mM): NaCl 136; KCl 4.8; $CaCl_2$ 2.5; KH_2PO_4 1.2; $MgSO_4$ 1.2; $NaHCO_3$ 5; HEPES 10; glucose 4 and 0.1 % BSA, pH 7.4. After a 15-min equilibration period at 37 °C, the cells were exposed to one the following treatments: (1) AVP; (2) SRIF; (3) AVP followed by SRIF or one of the SRIF receptor subtype-selective agonists (100 s interval); (4) 5 min of PRL-2903 pretreatment followed by AVP and SRIF or L-779,976. The

KRB was collected from each well for insulin RIA [32] 5 min after SRIF or the SRIF receptor subtype-selective agonist treatment. The number of cells from each well was then determined. Each treatment was done in duplicate and all experiments were repeated four times, with the exception of dose-dependent experiments for L-779,976, which were done in triplicate and repeated three times.

Data analysis

Traces from the $[Ca^{2+}]_i$ measurement are representative of 4 experiments. Results from the insulin secretion under static incubation conditions are presented as mean ± SEM, and were analyzed using the SAS PROC MIXED procedure and a randomized block design. There were two factors, treatment and block. Individual mean comparisons were performed using the *F* test. The significance level was set at $P < 0.05$.

RESULTS AND DISCUSSION

Previously, we reported in HIT-T15 cells, SRIF increased $[Ca^{2+}]_i$ leading to insulin secretion in the presence of AVP, whereas treatment with SRIF alone failed to do so [21,22]. The increase in $[Ca^{2+}]_i$ by SRIF was characterized by a sharp and transient increase, followed by a rapid decline to sub-basal levels. Treatment with 100 nM SRIF resulted in a sub-maximal increase in $[Ca^{2+}]_i$ in the presence of 1 nM AVP. In the present study, we characterized the SRIF receptor subtype that mediates the increase in $[Ca^{2+}]_i$ leading to insulin secretion using SRIF receptor subtype-selective agonists and PRL-2903, a specific SSTR2 antagonist.

We demonstrated the ability of 100 nM SRIF to increase $[Ca^{2+}]_i$ in the presence of 1 nM AVP (Fig. 1). Each SRIF receptor subtype-selective agonist was tested at 1 μM concentration in the presence of 1 nM AVP, with the exception of L-817,818 (a SSTR5 agonist), which was tested at 100 nM. L-817,818 itself emitted fluorescence at 1 μM concentration. In the presence of AVP, only L-779,976 (a SSTR2 agonist) increased $[Ca^{2+}]_i$ in a similar manner to SRIF (Fig. 1). All other SRIF receptor agonists failed to increase $[Ca^{2+}]_i$ (Fig. 1). This suggested that the SSTR2 be involved in the SRIF-induced increase in $[Ca^{2+}]_i$.

Next, we measured insulin secretion to determine if the increase in $[Ca^{2+}]_i$ by L-779,976 also lead to insulin exocytosis, since an increase in $[Ca^{2+}]_i$ usually triggers hormone

exocytosis [33]. Under static incubation conditions, 1 μM of each SRIF receptor subtype-selective agonist was tested in the presence of 1 nM AVP. Treatment with AVP alone resulted in ~ 2 fold increase in insulin secretion compared to basal controls ($P < 0.05$). In the presence of 1 nM AVP, both SRIF and L-779,976 further increased insulin secretion ~ 1.5 fold compared to AVP alone ($P < 0.05$) or ~ 3 fold to basal controls ($P < 0.05$). All other SRIF receptor agonists failed to further increase insulin secretion in the presence of AVP. Treatment with SRIF alone did not increase insulin secretion (Fig. 2). In this study, treatment with the SRIF receptor agonists alone did not alter basal $[Ca^{2+}]_i$ or insulin secretion from HIT-T15 cells (data not shown).

In the presence of 1 nM AVP, L-779,976 (10 pM-1μM) increased $[Ca^{2+}]_i$ and insulin secretion in a dose-dependent manner (Fig. 3). Similar to SRIF, 100 nM L-779,976 also resulted in a sub-maximal increase in $[Ca^{2+}]_i$. Results from static incubation experiments suggested that no further increase in insulin secretion be induced by L-779,976 at concentrations greater than 100 nM. This is attributable to the fact that the increase in $[Ca^{2+}]_i$, necessary for maximal insulin secretion, was reached with 100 nM L-779,976.

Finally, we confirmed the involvement of the SSTR2 by pretreatment of HIT-T15 cells with a specific SSTR2 antagonist, PRL-2903 [34], to determine whether it would antagonize the increases in $[Ca^{2+}]_i$ and insulin secretion by both SRIF and L-779,976. Pretreatment with 1 μM PRL-2903 for 5 min abolished the SRIF- and L-779,976-induced increases in $[Ca^{2+}]_i$ (Fig. 4) and insulin secretion (Fig. 5). In addition, PRL-2903 (10 nM-1 μM) inhibited the SRIF- and L-779,976-induced increases in insulin secretion in a dose-dependent manner (Fig. 5). Treatment with PRL-2903 had no effect on basal $[Ca^{2+}]_i$ and insulin secretion or responses to AVP (data not shown).

The SRIF receptor subtype that mediates the inhibitory effects of SRIF in clonal β-cells HIT-T15 has yet to be described. SSTR5 is responsible for the inhibitory effects of SRIF on insulin secretion in rats and mice [27,28]. Since HIT-T15 cells are derived from hamster, there is a possibility that another SRIF receptor subtype, possibly the SSTR2, may mediate the inhibitory effects of SRIF in this cell line [14,17,18]. Although results from our study suggested that the SSTR2 mediate the increase in $[Ca^{2+}]_i$ and insulin secretion by SRIF, a cross-talk between Gq and Gi/Go may account for the differences between the inhibitory and stimulatory effects of SRIF. In the presence of carbachol, which signals via Gq, similar increase in $[Ca^{2+}]_i$ by SRIF is seen in human neuroblastoma SH-SY5Y cells [35]. Additional reports regarding the cross-talk between Gq and Gi/Go have also been described

in COS cells [36,37], where activation of a Gi/Go-coupled receptor increased IP_3 formation after activation of a Gq-coupled receptor. Further studies are warranted to confirm the involvement of the SSTR2 on the inhibitory effects of SRIF.

In summary, our findings suggest that the SSTR2 mediates the SRIF-induced increases in $[Ca^{2+}]_i$ and insulin secretion in the presence of AVP in HIT-T15 cells. This was further confirmed by the ability of L-779,976, a specific SSTR2 agonist, to increase both $[Ca^{2+}]_i$ and insulin secretion in a similar manner to SRIF. In addition, PRL-2903, a specific SSTR2 antagonist, inhibited the SRIF- and L-779,976-induced increases in $[Ca^{2+}]_i$ and insulin secretion. This is the first report in clonal β-cell HIT-T15 describing the involvement of a SRIF receptor subtype on the effects of SRIF on $[Ca^{2+}]_i$ and insulin secretion. The physiological significance of the current finding remains to be determined.

ACKNOWLEDGMENTS

We thank Merck Research Laboratories, West Point, PA for donating the SRIF receptor subtype-selective agonists: L-797,591; L-779,976; L-796,778; L-803,087; L-817,818.

REFERENCES

1. Brazeau, P., Vale, W., Burgus, R., Ling, N., Butcher, M., Rivier, J. and Guillemin, R. Hypothalamic polypeptide that inhibits the secretion of immunoreactive pituitary growth hormone. Science 1973; 170: 77-79.

2. Finley, J. C., Maderdrut, J. L., Roger, L. J. and Petrusz, P. The immunocytochemical localization of somatostatin-containing neurons in the rat central nervous system. Neuroscience 1981; 6: 2173-2192.

3. Murthy, K. S., Coy, D. H. and Makhlouf, G. M. Somatostatin receptor-mediated signaling in smooth muscle. Activation of phospholipase C-β3 by $G_{\beta\gamma}$ and inhibition of adenylyl cyclase by $G_{\alpha i1}$ and $G_{\alpha o}$. J. Biol. Chem. 1996; 271: 23458-23463.

4. Bloom, S. R., Mortimer, C. H., Thorner, M. O., Besser, G. M., Hall, R., Gomez-Pan, A., Roy, V. M., Russell, R. C., Coy, D. H., Kastin, A. J. and Schally A. V. Inhibition of gastrin and gastric-acid secretion by growth-hormone release-inhibiting hormone. Lancet 1974; 2: 1106-1109.

5. Mandarino, L., Stenner, D., Blanchard, W., Nissen, S., Gerich, J., Ling, N., Brazeau, P., Bohlen, P., Esch, F. and Guillemin, R. Selective effects of somatostatin-14, -25 and -28 on in vitro insulin and glucagon secretion. Nature 1981; 291: 76-77.

6. Reichlin, S. Somatostatin. N. Engl. J. Med. 1983; 309: 1556-1563.

7. Alberti, K. G., Christensen, N. J., Christensen, S. E., Hansen, A. P., Iversen, J., Lundbaek, K., Seyer-Hansen, K. and Orskov, H. Inhibition of insulin secretion by somatostatin. Lancet 1975; 2: 1299-1301.

8. Gerich, J. E., Lovinger, R. and Grodsky, G. M. Inhibition by somatostatin of glucagon and insulin release from the perfused rat pancreas in response to arginine, isoproterenol and theophylline: evidence for a preferential effect on glucagon secretion. Endocrinology 1975; 96: 749-754.

9. Basabe, J. C., Cresto, J. C. and Aparicio, N. Studies on the mode of action of somatostatin on insulin secretion. Endocrinology 1977; 101: 1436-1443.

10. Okamoto, H., Noto, Y., Miyamoto, S., Mabuchi, H. and Takeda, R. Inhibition by somatostatin of insulin release from isolated pancreatic islets. FEBS Lett. 1975; 54: 103-105.

11. Strowski, M. Z., Parmar, R. M., Blake, A. D. and Schaeffer, J. M. Somatostatin inhibits insulin and glucagon secretion via two receptors subtypes: an in vitro study of pancreatic islets from somatostatin receptor 2 knockout mice. Endocrinology 2000; 141: 111-117.

12. Sullivan, S. J. and Schonbrunn, A. Characterization of somatostatin receptors which mediate inhibition of insulin secretion in RINm5F insulinoma cells. Endocrinology 1987; 121: 544-52.

13. Ullrich, S., Prentki, M. and Wollheim, C. B. Somatostatin inhibition of Ca^{2+}-induced insulin secretion in permeabilized HIT-T15 cells. Biochem. J. 1990; 270: 273-276.

14. Hsu, W.H., Xiang, H.D., Rajan, A. S., Kunze, D. L. and Boyd, A. E. Somatostatin inhibits insulin secretion by a G-protein-mediated decrease in Ca^{2+} entry through voltage-dependent Ca^{2+} channels in the β cell. J. Biol. Chem. 1991; 266: 837-843.

15. Poitout, V., Stout, L. E., Armstrong, M. B., Walseth, T. F., Sorenson, R.L. and Robertson, R. P. Morphological and functional characterization of βTC-6 cells: an insulin-secreting cell line derived from transgenic mice. Diabetes 1995; 44: 306-313.

16. Abel, K. B., Lehr, S. and Ullrich, S. Adrenaline-, not somatostatin-induced hyperpolarization is accompanied by a sustained inhibition of insulin secretion in INS-1 cells.

Activation of sulphonylurea K^+ ATP channels is not involved. Pflugers Arch. 1996; 432: 89-96.

17. Richardson, S. B., Eyler, N., Twente, S., Monaco, M., Altszuler, N. and Gibson, M. Effects of vasopressin on insulin secretion and inositol phosphate production in a hamster β cell line (HIT). Endocrinology 1990; 126: 1047-1052.

18. Ma, H. T., Kato, M. and Tatemoto, K. Effects of pancreastatin and somatostatin on secretagogues-induced rise in intracellular free calcium in single rat pancreatic islet cells. Regul. Pept. 1996; 61: 143-148.

19. Ribalet, B. and Eddlestone, G. T. Characterization of the G protein coupling of a somatostatin receptor to the K^+ ATP channel in insulin-secreting mammalian HIT and RIN cell lines. J. Physiol. 1995; 485: 73-86.

20. Amico, J. A., Finn, F. M. and Haldar, J. Oxytocin and vasopressin are present in human and rat pancreas. Am. J. Med. Sci. 1988; 296: 303-307.

21. Cheng, H., Yibchok-anun, S. and Hsu, W. H. Somatostatin-induced paradoxical increase in intracellular calcium concentration after arginine vasopressin priming in clonal hamster (HIT) cells. 11th Session of The Iowa Academy of Science, Iowa State University, Ames, IA., IAS suppl. 1999; 1: 20. Abstract 57.

22. Cheng, H., Yibchok-anun, S. and Hsu, W. H. Somatostatin-induced paradoxical increase in intracellular Ca^{2+} concentration and insulin release in the presence of arginine vasopressin in clonal β-cells HIT-T15. Biochem. J. 2001; accepted.

23. Bruno, J. F., Xu, Y., Song, J. and Berelowitz, M. Molecular cloning and functional expression of a brain-specific somatostatin receptor. Proc. Natl. Acad. Sci. U S A. 1992; 89: 11151-11155.

24. Reisine, T., Zhang, Y. L. and Sekura, R. Pertussis toxin treatment blocks the inhibition of somatostatin and increases the stimulation by forskolin of cyclic AMP accumulation and adrenocorticotropin secretion from mouse anterior pituitary tumor cells. J. Pharmacol. Exp. Ther. 1985; 232: 275-282.

25. Patel, Y. C., Greenwood, M. T., Warszynska, A., Panetta, R. and Srikant, C. B. All five cloned human somatostatin receptors (hSSTR1-5) are functionally coupled to adenylyl cyclase. Biochem. Biophys. Res. Commun. 1994; 198: 605-612.

26. Kumar, U., Sasi, R., Suresh, S., Patel, A., Thangaraju, M., Metrakos, P., Patel, S. C. and Patel, Y. C. Subtype-selective expression of the five somatostatin receptors (hSSTR1-5)

in human pancreatic islet cells: a quantitative double-label immunohistochemical analysis. Diabetes 1999; 48: 77-85.

27. Mitra, S. W., Mezey, E., Hunyady, B., Chamberlain, L., Hayes, E., Foor, F., Wang, Y., Schonbrunn, A. and Schaeffer, J. M. Colocalization of somatostatin receptor sst5 and insulin in rat pancreatic β cells. Endocrinology 1999; 140: 3790-3796.

28. Strowski, M. Z., Parmar, R. M., Blake, A. D. and Schaeffer, J. M. Somatostatin inhibits insulin and glucagon secretion via two receptors subtypes: an in vitro study of pancreatic islets from somatostatin receptor 2 knockout mice. Endocrinology 2000; 141: 111-117.

29. Rohrer, S. P., Birzin, E. T., Mosley, R. T., Berk, S. C., Hutchins, S. M., Shen, D. M., Xiong, Y., Hayes, E. C., Parmar, R. M., Foor, F., Mitra, S. W., Degrado, S. J., Shu, M., Klopp, J. M., Cai, S. J., Blake, A., Chan, W. W., Pasternak, A., Yang, L., Patchett, A. A., Smith, R. G., Chapman, K. T. and Schaeffer, J. M. Rapid identification of subtype-selective agonists of the somatostatin receptor through combinatorial chemistry. Science 1998; 282: 737-740.

30. Hocart, S. J., Jain, R., Murphy, W. A., Taylor, J. E., Morgan, B. and Coy, D. H. Highly potent cyclic disulfide antagonists of somatostatin. J. Med. Chem. 1999; 42: 1863-1871.

31. Rossowski, W. J., Cheng, B. L., Jiang, N. Y. and Coy, D. H. Examination of somatostatin involvement in the inhibitory action of GIP, GLP-1, amylin and adrenomedullin on gastric acid release using a new SRIF antagonist analogue. Br. J. Pharmacol. 1998; 125: 1081-1087.

32. Chen, T. H., Lee, B. and Hsu, W. H. Arginine vasopressin-stimulated insulin secretion and elevation of intracellular Ca^{++} concentration in rat insulinoma cells: influences of a phospholipase C inhibitor 1-[6-[[17 β-methoxyestra-1,3,5(10)-trien- 17-yl]amino]hexyl]-1H-pyrrole-2,5-dione (U-73122) and a phospholipase A2 inhibitor N-(p-amylcinnamoyl) anthranilic acid. J. Pharmacol. Exp. Ther. 1994; 270: 900-904.

33. Wollheim, C. B. and Pozzan, T. Correlation between cytosolic free Ca^{2+} and insulin release in an insulin-secreting cell line. J. Biol. Chem. 1984; 259: 2262-2267.

34. Kawakubo, K., Coy, D. H., Walsh, J. H. and Tache, Y. Urethane-induced somatostatin mediated inhibition of gastric acid: reversal by the somatostatin 2 receptor antagonist, PRL-2903. Life Sci. 1999; 65: 115-120.

35. Connor, M., Yeo, A. and Henderson, G. Neuropeptide Y Y_2 receptor and somatostatin sst_2 receptor coupling to mobilization of intracellular calcium in SH-SY5Y human neuroblastoma cells. Br. J. Pharmacol. 1997; 120: 455-463.

36. Quitterer, U. and Lohse, M. J. Crosstalk between $G\alpha_i$- and $G\alpha_q$-coupled receptors is mediated by $G\beta\gamma$ exchange. Proc. Natl. Acad. Sci. U S A. 1999; 96: 10626-10631.

37. Chan, J. S., Lee, J. W., Ho, M. K. and Wong, Y. H. Preactivation permits subsequent stimulation of phospholipase C by G(i)-coupled receptors. Mol. Pharmacol. 2000; 57:700-708.

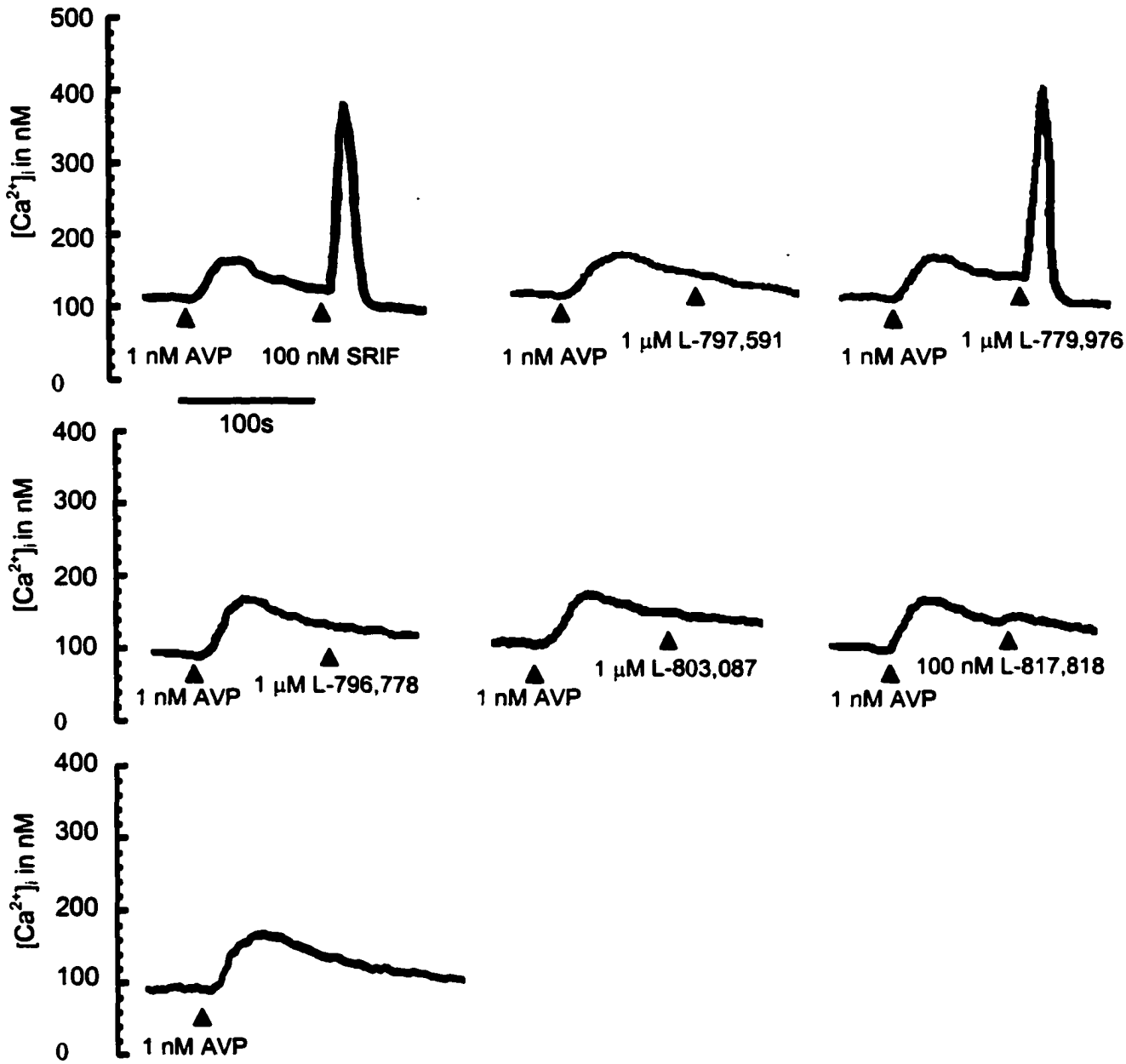

Figure 1 Effect of SRIF receptor subtype-selective agonists L-797,591 (SSTR1), L-779,976 (SSTR2), L-796,778 (SSTR3), L-803,087 (SSTR4) and L-817,818 (SSTR5) on $[Ca^{2+}]_i$. In the presence of AVP, SRIF increased $[Ca^{2+}]_i$ during Ca^{2+} measurement experiments. Treatment with L-779,976 also increased $[Ca^{2+}]_i$ in a similar manner as for SRIF. All other SRIF receptor agonists failed to increase $[Ca^{2+}]_i$ in the presence of AVP. No further increase in $[Ca^{2+}]_i$ was observed with AVP alone after 100 s. Traces are representative of 4 experiments.

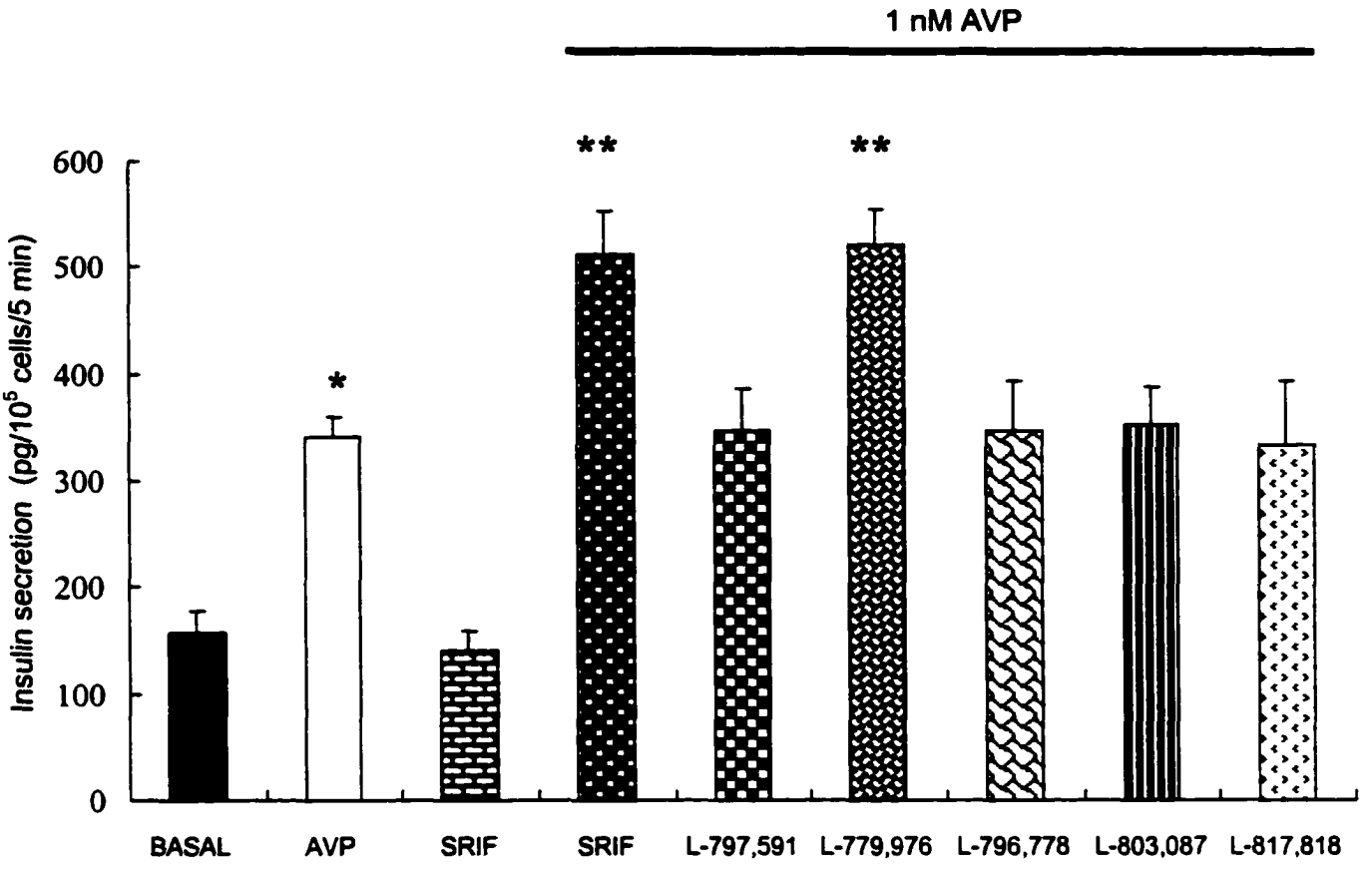

Figure 2 Effect of SRIF receptor subtype-selective agonists L-797,591 (SSTR1), L-779,976 (SSTR2), L-796,778 (SSTR3), L-803,087 (SSTR4) and L-817,818 (SSTR5) on insulin secretion. Under static incubation conditions, treatment with AVP alone increased insulin secretion (*$P < 0.05$ compared to basal controls). In the presence of AVP, both SRIF and L-779,976 further increased insulin secretion compared to AVP alone (**$P < 0.05$). All other SRIF receptor agonists failed to further increase insulin secretion in the presence of AVP. Treatment with SRIF alone did not increase insulin secretion. In this study, treatment with the SRIF receptor subtype-selective agonists alone did not alter basal insulin secretion. Values are mean ± S.E.M. (n = 4 cultures with duplicates).

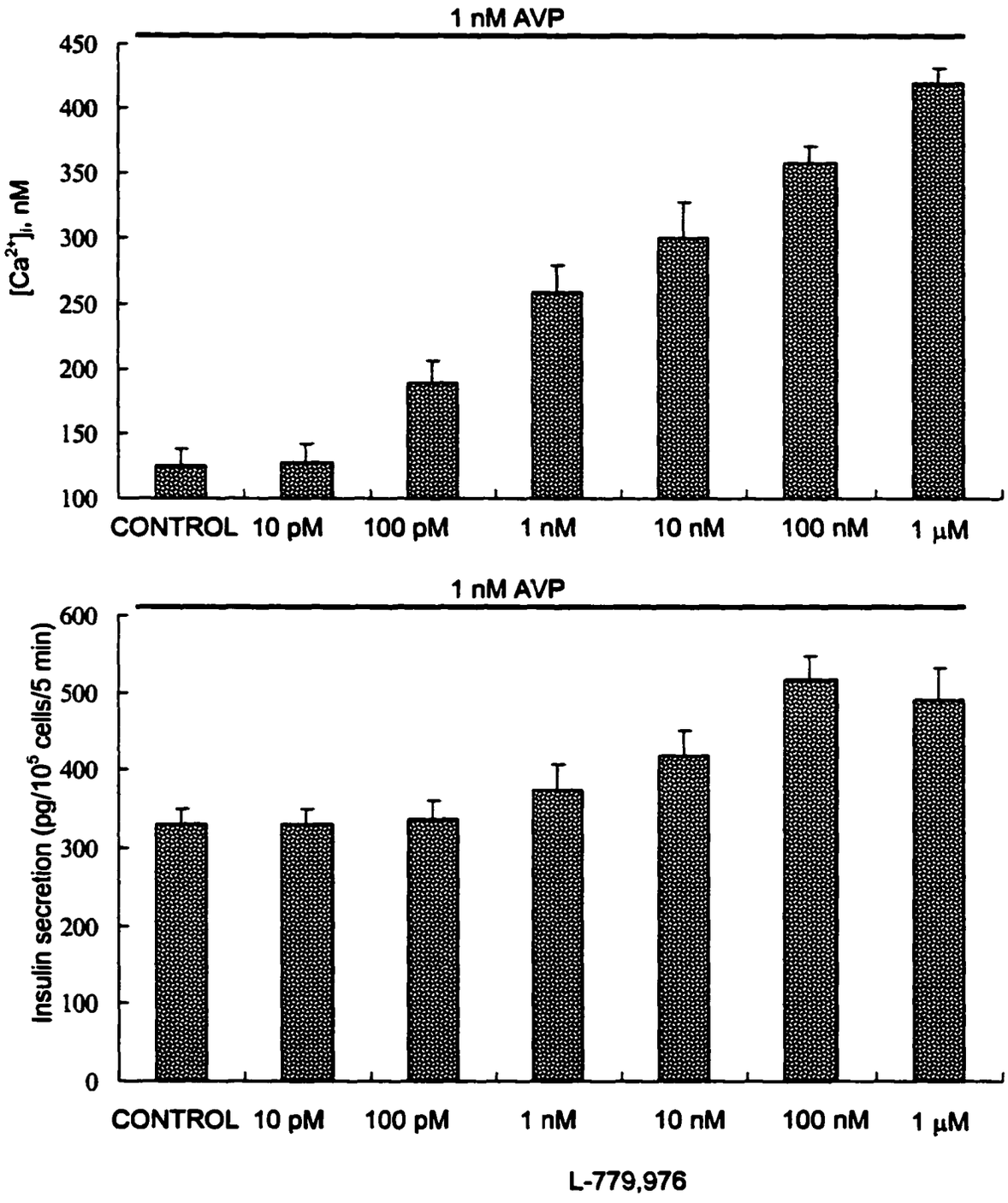

Figure 3 Dose-dependent response to L-779,976, a specific SSTR2 agonist. In the presence of AVP, L-779,976 increased $[Ca^{2+}]_i$ (upper panel/n=4) and insulin secretion (lower panel/n=3 cultures with triplicates) in a dose-dependent manner. Treatment with 100 nM L-779,976 resulted in sub-maximal Ca^{2+} increases and a maximal insulin secretion. Values are mean ± S.E.M.

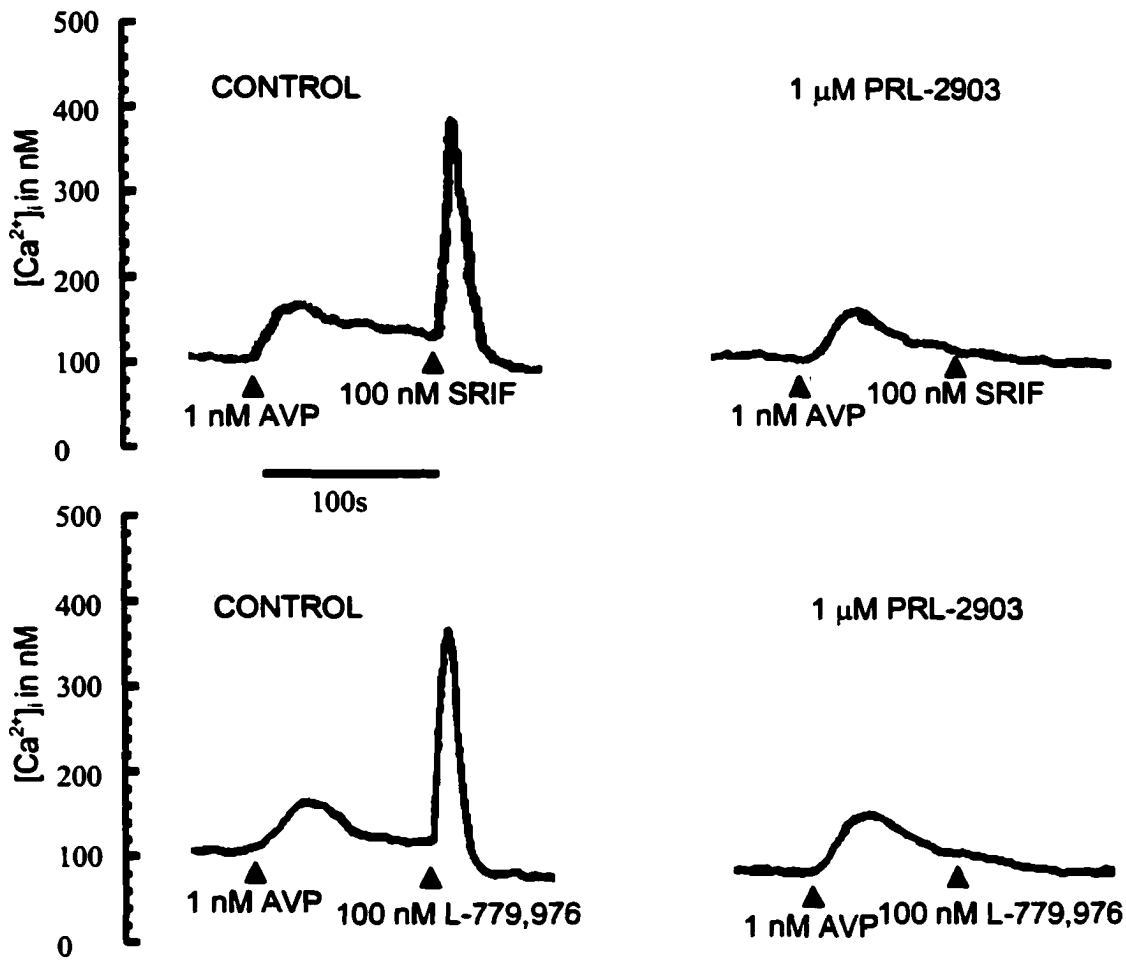

Figure 4 Effect of PRL-2903, a specific SSTR2 antagonist, on SRIF- and L-779,976-induced increases in $[Ca^{2+}]_i$. Pretreatment with PRL-2903 for 5 min prior to SRIF (upper panel) or L-779,976 (lower panel) abolished the increase in $[Ca^{2+}]_i$ by both agonists in the presence of AVP. Traces are representative of 4 experiments.

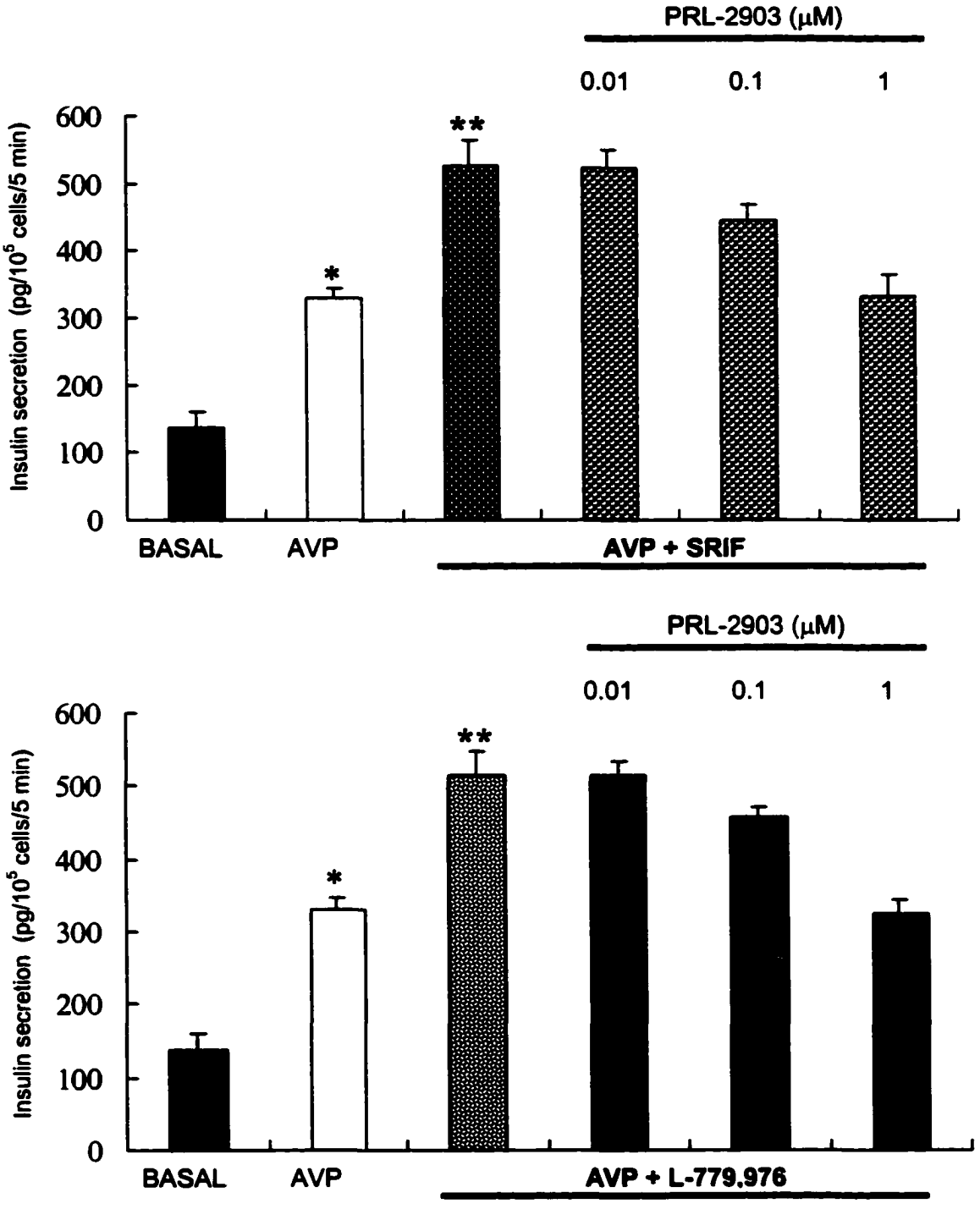

Figure 5 Effect of PRL-2903, a specific SSTR2 antagonist on SRIF- and L-779,976-induced increases in insulin secretion. Pretreatment with PRL-2903 for 5 min prior to SRIF (upper panel) or L-779,976 (lower panel) inhibited further increases in insulin secretion in a dose-dependent manner (*P < 0.05 compared to basal controls; **P < 0.05 compared to 1 μM PRL-2903 or AVP alone group). Values are mean ± S.E.M. (n = 4 cultures with duplicates).

CHAPTER IV SOMATOSTATIN INCREASES PHOSPHATIDYLINOSITOL 4,5-BISPHOSPHATE FORMATION VIA βγ DIMER OF $G_{i/o}$ IN CLONAL β-CELLS HIT-T15: MECHANISMS FOR ITS PARADOXICAL INCREASE IN INSULIN RELEASE

A paper submitted for publication in the Journal of Biological Chemistry

Henrique Cheng, Sirintorn Yibchok-anun, Nipattra Debavalya, Jing Ding, F. Anderson Norris and Walter H. Hsu

ABSTRACT

Phosphatidylinositol 4,5-bisphosphate (PIP_2) is best known for its ability to serve as a precursor for the second messengers inositol 1,4,5-triphosphate (IP_3) and diacylglycerol (DAG), which are generated from the hydrolysis of PIP_2 by phospholipase C (PLC). Previously, we demonstrated that in the presence of arginine vasopressin (AVP), somatostatin (SRIF) increased $[Ca^{2+}]_i$, leading to insulin release from HIT-T15 cells via $G_{i/o}$ and the PLC pathway. Since SRIF alone failed to increase $[Ca^{2+}]_i$, we hypothesized that SRIF increases PIP_2 synthesis, which serves as additional substrate for preactivated PLC-β to generate IP_3. In addition, we determined which G-protein subunit mediates this effect of SRIF. Administration of antibody against the β subunit of $G_{i/o}$ into single cells inhibited the increase in $[Ca^{2+}]_i$ by SRIF, but antibodies against $G_{i\alpha1}/G_{i\alpha2}$ and $G_{i\alpha3}/G_{o\alpha}$ failed to do so. In the presence of AVP, administration of PIP_2 into single cells increased $[Ca^{2+}]_i$, but PIP_2 alone failed to increase $[Ca^{2+}]_i$. SRIF increased PIP_2 synthesis from PIP in the presence or absence of AVP, whereas an increase in IP_3 level was observed only in the presence of AVP. These results suggest that activation of SRIF receptors, which are coupled to $G_{i/o}$, leads to an increase in PIP_2 synthesis through the βγ dimer. The PIP_2 generated by SRIF serves as additional substrate for preactivated PLC-β, which hydrolyzes PIP_2 to form IP_3, leading to an increase in $[Ca^{2+}]_i$ and insulin release in HIT-T15 cells. The regulation of PIP_2 synthesis by a $G_{i/o}$-coupled receptor represents a novel concept in cross-talk between G_q- and $G_{i/o}$-coupled receptors.

INTRODUCTION

Insulin synthesized and secreted from β-cells is the most important regulator of blood glucose levels. Although glucose is the major stimulator for insulin release, several hormones have been shown to inhibit or stimulate its release. SRIF synthesized and secreted from δ-cells, is known for its ability to inhibit insulin release (1-3). In β-cells, AVP binds V_{1b} receptors (4), which are coupled to G_q, thus activating PLC-β (5). Recently, we reported that in the presence of AVP, SRIF paradoxically increased $[Ca^{2+}]_i$ and insulin release from HIT-T15 cells (6). The effects of SRIF were mediated by $G_{i/o}$, the PLC pathway and mainly Ca^{2+} release from the endoplasmic reticulum. The increases in $[Ca^{2+}]_i$ and insulin release by SRIF was due to a cross-talk between G_q and $G_{i/o}$ (6).

Signaling via the large family of G protein-coupled receptors can lead to many cellular responses, ranging from regulation of hormone release to stimulation of gene transcription. PIP_2 plays a critical role in intracellular signaling and is best known for its ability to serve as the precursor for the second messengers IP_3 and DAG, which are generated from the hydrolysis of PIP_2 by PLCs. Production of IP_3 triggers a transient increase in $[Ca^{2+}]_i$, while DAG activates protein kinase C (7, 8). Although activation of G_q-coupled receptors increases $[Ca^{2+}]_i$ via the PLC pathway, and activation of $G_{i/o}$-coupled receptors inhibits adenylyl cyclase (9, 10), there is accumulating evidence that activation of one particular signaling pathway can amplify intracellular signaling within a parallel but separate pathway. For example, activation of $G_{i/o}$-coupled receptors can enhance inositol phosphate signals generated by G_q-coupled receptors (11-13). Enhancement of G_q-dependent signals through an increase in inositol phosphate formation by $G_{i/o}$-coupled receptors requires preactivated PLC-β and is mediated by the βγ dimer (14). Further support for the βγ dimer mediation of the cross-talk between G_q and $G_{i/o}$ has been reported by others (12, 15). In SH-SY5Y cells, SRIF increases $[Ca^{2+}]_i$ after pretreatment with carbachol, a cholinergic agonist, which signals via G_q (16).

To date, studies examining cross-talk signals between G_q- and $G_{i/o}$-coupled receptors have been performed through quantification of inositol phosphates and/or $[Ca^{2+}]_i$ (13-15). In addition, antibodies against PLC-β isozymes (17) or inhibitors such as U-73122 (6) have also been used to investigate the signaling mechanism of $G_{i/o}$-coupled receptors of SRIF. Studies suggest that $G_{i/o}$ is responsible for a direct activation of PLC-β (14, 17). However, treatment with SRIF alone, even at 1 μM failed to increase $[Ca^{2+}]_i$ and insulin

release in our previous study (6). We, therefore, hypothesized that SRIF increases PIP_2 synthesis, thereby increasing the substrate for preactivated PLC-β by AVP.

In the present study, we examined the involvement of $G_{i/o}$ subunits and PIP_2 on SRIF-induced $[Ca^{2+}]_i$ increase in the presence of a low concentration of AVP (1nM) in HIT-T15 cells. Our findings clearly show that SRIF increased IP_3 and $[Ca^{2+}]_i$ through an increase in PIP_2 synthesis by the βγ dimer of $G_{i/o}$.

MATERIALS AND METHODS

Materials - All reagents were purchased from Sigma Chemical (St. Louis, MO), except that fura-2 acetoxymethyl ester (fura-2AM) was from Molecular Probes (Eugene, OR) and rabbit polyclonal antibodies against $G_{i\alpha1}/G_{i\alpha2}$, $G_{i\alpha3}/G_{o\alpha}$, and G_β from Biomol (Plymouth Meeting, PA).

Cell culture - HIT-T15 cells were maintained in RPMI 1640 with 10 % fetal bovine serum and aerated with 5 % CO_2-95 % air at 37 °C. All experiments were performed using cells from passages 80-90.

Measurement of $[Ca^{2+}]_i$ in single cells - $[Ca^{2+}]_i$ was measured as previously described (6, 18). Cells were loaded with 2 μM fura-2AM in Krebs Ringer Bicarbonate buffer containing (in mM): NaCl 136; KCl 4.8; $CaCl_2$ 1.2; $MgSO_4$ 1.2; HEPES 10; glucose 4; 0.1 % bovine serum albumin, pH 7.4 for 30 min at 37°C. Measurement of $[Ca^{2+}]_i$ from single cells was accomplished by mounting the 35-mm culture dishes on the stage of an inverted fluorescence microscope (Carl Zeiss, Thornwood, NY). Fluorescence images were obtained (excitation wavelengths, 340 and 380 nm; emission wavelength, 510 ± 20 nm), background subtracted, and divided on a pixel-by-pixel basis to generate spatially resolved maps of the $[Ca^{2+}]_i$. The emitted signals were digitalized, recorded and processed using Attofluor Digital Fluorescence Imaging System (Atto Instruments, Rockville, MD). The $[Ca^{2+}]_i$ was calculated according to previously published method (19). Calibration was performed according the procedure provided by Attofluor, using fura-2 penta K^+ as a standard.

Microinjection protocol - Single cells were grown for 2 days on a glass coverslip of custom-made 35-mm culture dishes. Thereafter, cells were loaded with fura-2AM, mounted

on the stage of an inverted microscope. Two cells from each dish were injected with intracellular buffer and rabbit polyclonal antibodies respectively, using a disposable glass pipette (VWR Scientific, West Chester, PA) held by a Narishige MW-3 micromanipulator. Pipettes were made by a PE-2 Micropipette Puller (Narishige Scientific Instrument, Tokyo, Japan). All antibodies were diluted at 1:100 with intracellular buffer solution containing (in mM): K_2HPO_4 27; NaH_2PO_4 8; KH_2PO_4 26; pH 7.3. Injection pressure was controlled by a pressure injection system (Picospritzer II, General Valve, Fairfield, NJ). A 30-min incubation period was allowed between the antibody injection and $[Ca^{2+}]_i$ measurement. At the end of each experiment, cells were depolarized with 10 mM KCl to test membrane integrity.

Determination of phophatidylinositol phosphate (PIP) and PIP_2 - PIP and PIP_2 levels were measured using thin layer chromatography as previously described (20). HIT-T15 cells were labeled with 200 μCi/ml of ^{32}P (Perkin Elmer Life Sciences, Boston, MA) in phosphate free KRB for 60 min and washed twice by centrifugation at 300 x *g* for 2 min. For experiments, cells were resuspended at a density of 15 x 10^6 cells/ml/treatment. The reactions were terminated by addition of 1 ml ice cold 1M HCl. Phospholipids were separated by a chloroform:methanol (1:1) mixture. The lower phase was dried under a stream of nitrogen, resuspended in 200-500 μL chloroform:methanol (1:1) mixture, and spotted on silica gel 60 plates (Merck, Gibbstown, NJ). PIP and PIP_2 were identified by comigration with unlabeled standards visualized by iodine staining and radiograph into 1-cm blocks that were scraped and radioactivity quantified by liquid scintillation counting.

Determination of IP_3 - Measurement of inositol phosphates followed modified procedures from those of Hoque et al. (21). Cells were labeled with 20 μCi/ml of myo-[2-^{3}H]inositol (Perkin Elmer Life Sciences, Boston, MA) at 37°C for 90 min and washed twice by centrifugation at 300 x *g* for 2 min. For experiments, cells were resuspended at a density of 20 x 10^6 cells/ml/treatment. The reactions were terminated by addition of 0.5 ml ice cold 10% TCA and samples centrifuged at 3000 x *g* for 20 min at 4°C. The supernatants were passed through a 200-400 mesh Dowex AG1-X 8 in formate form column (Bio-Rad Laboratories, Hercules, CA). Inositol phosphates were eluted by stepwise addition of 0.2, 0.5, and 1 M ammonium formate, which contained IP_1, IP_2, and IP_3 respectively. Radioactivity from each sample was quantified by liquid scintillation counting.

Data analysis - All values are presented as mean ± S.E.M. Results were analyzed using analysis of variance and individual mean comparisons were made using Least Significant Difference test. The significance level was set at $P < 0.05$.

RESULTS

Mediation by βγ dimer of SRIF-induced increase in $[Ca^{2+}]_i$ in the presence of AVP - We determined which subunit of $G_{i/o}$ mediated the SRIF (100 nM)-induced increase in $[Ca^{2+}]_i$ in the presence of 1 nM AVP by microinjecting antibodies against $G_{i/o}$ subunits into single cells. Antibody (1:100) against the β subunit of $G_{i/o}$ reduced the response to SRIF by 89 % ($P < 0.05$). In contrast, antibodies against $G_{i\alpha1}/G_{i\alpha2}$ or $G_{i\alpha3}/G_{o\alpha}$ (1:100) did not significantly change the response to SRIF (Fig. 1).

SRIF-induced increase in PIP_2 synthesis - We hypothesized that SRIF increases PIP_2 synthesis, which in turn serves as additional substrate for preactivated PLC-β by AVP. If this hypothesis is correct, injection of PIP_2 into single cells in the presence of 1 nM AVP should increase $[Ca^{2+}]_i$ in a similar manner to SRIF. Administration of PIP_2 (1.5-50 amol) into single cells increased $[Ca^{2+}]_i$ in the presence of AVP in a concentration-dependent manner. Microinjection of intracellular buffer did not increase $[Ca^{2+}]_i$ in the presence of AVP (Fig. 2). PIP_2 at the highest concentration tested (50 amol), failed to increase $[Ca^{2+}]_i$ in the absence of AVP (data not shown). These results are consistent with our hypothesis that SRIF increases PIP_2 synthesis.

We then determined if SRIF increased PIP_2 and the time course of this increase. In the presence of 1 nM AVP, 100 nM SRIF increased PIP_2 8 s post-SRIF administration ($P < 0.05$). In addition, there was a decrease in PIP levels, the precursor for PIP_2, 8 s post-SRIF administration (Fig. 3). Based on these results, we compared PIP_2 synthesis by SRIF with other treatment groups using the 8-s time frame.

Treatment with 100 nM SRIF increased PIP_2 synthesis in the presence and absence of 1 nM AVP ($P < 0.05$), compared to basal controls. Treatment with AVP alone failed to increase PIP_2 synthesis (Fig. 4A). Treatment with SRIF resulted in a decrease in PIP levels ($P < 0.05$) in the presence and absence of AVP (Fig. 4B).

PIP_2 hydrolysis by PLC-β - We hypothesized that PIP_2 serves as additional substrate for preactivated PLC-β, and thus measured IP_3 levels. In the presence of 1 nM AVP, 100 nM SRIF increased IP_3 levels after 10-12 s of SRIF administration (Fig. 5A, $P < 0.05$). We then utilized the 12-s post-SRIF time frame to compare IP_3 levels among 4 treatment groups.

In the presence of 1 nM AVP, 100 nM SRIF increased IP_3 levels ($P < 0.05$) compared to basal controls. Treatment with SRIF alone failed to increase IP_3 levels. Treatment with AVP for 112 s induced a small, but significant increase in IP_3 levels ($P < 0.05$) compared to basal controls (Fig. 5B).

DISCUSSION

Previously, we reported in HIT-T15 cells that SRIF increased $[Ca^{2+}]_i$ and insulin release in the presence of AVP. These effects of SRIF are due to activation of sst_2 receptors (22), and are attributable to a cross-talk between $G_{i/o}$ and G_q (6). Cross-talk between G_q- and $G_{i/o}$-coupled receptors has been reported in other systems. For example, activation of $G_{i/o}$-proteins coupled to adenosine A1 receptor enhances the stimulation of PLC-β by G_q-coupled receptors such as α_1-adrenergic, bradykinin, histamine H_1, and muscarinic receptors (23). For such a cross-talk, activation of $G_{i/o}$ alone usually has no effect, but it enhances signals generated by G_q, particularly when G_q is activated prior to $G_{i/o}$ (11-13, 16). Activation of $G_{i/o}$-coupled adenosine A1, α_2 adrenergic receptors (12) or δ- or κ-opioid receptors (13) enhances inositol phosphate formation generated by G_q-coupled receptors in COS cells. In CHO cells, neuropeptide Y, a $G_{i/o}$-coupled receptor agonist, enhances inositol phosphate formation generated by ATP, a G_q-coupled receptor agonist (15). In addition, activation of δ-opioid receptors that are coupled to $G_{i/o}$ in SH-SY5Y cells increases $[Ca^{2+}]_i$ after activation of m3 muscarinic receptors that are coupled to G_q (13). SRIF also increases $[Ca^{2+}]_i$ after activation of the G_q-coupled muscarinic receptor in SH-SY5Y cells (16). Studies have suggested that enhancement of G_q signals by $G_{i/o}$ is through activation of PLC (14) or interaction with a step after PLC activation (13), but none of them have attributed the effect of $G_{i/o}$ to a step before PLC activation. In the present study, we have demonstrated for the first time that SRIF can increase PIP_2 synthesis from PIP, which in turn serves as additional substrate for preactivated PLC-β by AVP to generate high levels of IP_3. Without a preactivated PLC-β, SRIF failed to increase IP_3 levels, $[Ca^{2+}]_i$ and insulin

release (6). These findings are further supported by administration of PIP_2 into the cells, in which PIP_2 alone failed to increase $[Ca^{2+}]_i$, whereas PIP_2 in the presence of a small concentration of AVP (1 nM) increased $[Ca^{2+}]_i$.

To date, studies on the cross-talk between G_q and $G_{i/o}$ suggest that the $\beta\gamma$ dimer of $G_{i/o}$ is responsible for the enhancement of G_q-generated signals (12-15). We demonstrated that the antibody against the β subunit of $G_{i/o}$ nearly abolished the SRIF-induced increase in $[Ca^{2+}]_i$, whereas antibodies against $G_{i\alpha1}/G_{i\alpha2}$ and $G_{i\alpha3}/G_{o\alpha}$ failed to do so. Our findings are consistent with the literature, and further suggests that the increases in $[Ca^{2+}]_i$ and insulin released by SRIF are mediated through the $\beta\gamma$ dimer.

Several studies have shown that the $\beta\gamma$ dimer of $G_{i/o}$ can activate a number of enzymes, including PLC-β (24, 25), PLA_2 (26), mitogen-activated protein kinase (27, 28), Raf-1 (29), β-adrenergic receptor kinase (30), phosphatidylinositol 3-kinase (31) and adenylyl cyclase (32). In fact, in intestinal smooth muscle cells, treatment with SRIF alone activates PLC-β_3, thereby increasing IP_3 levels, $[Ca^{2+}]_i$ and contractions through the $\beta\gamma$ dimer of $G_{i/o}$ (17). Since both phosphatidylinositol 4-phosphate (PI4P) 5-kinase and phosphatidylinositol 5-phosphate (PI5P) 4-kinase are involved in the formation of PIP_2 from PIP (33), the $\beta\gamma$ dimer of $G_{i/o}$ may activate one or both enzymes. Although the majority of PIP_2 in cells is produced from PI4P, we cannot preclude PIP_2 synthesis from PI5P pools (34, 35). Further studies are warranted to determine the interaction between the $\beta\gamma$ dimer of $G_{i/o}$ and PI4P 5-kinase or PI5P 4- kinase.

In summary, we have demonstrated that activation of SRIF receptors, which are coupled to $G_{i/o}$, leads to an increase in PIP_2 synthesis through the $\beta\gamma$ dimer of the G-protein. The PIP_2 generated by SRIF serves as additional substrate for preactivated PLC-β, which hydrolyzes PIP_2, thereby increasing IP_3 levels, $[Ca^{2+}]_i$ and insulin release from HIT-T15 cells (Fig. 6). This is the first report regarding SRIF-induced increase in PIP_2 synthesis by activation of $G_{i/o}$.

REFERENCES

1. Alberti, K. G., Christensen, N. J., Christensen, S. E., Hansen, A. P., Iversen, J., Lundbaek, K., Seyer-Hansen, K., and Orskov, H. (1975) *Lancet* **2**, 1299-1301
2. Hsu, W.H., Xiang, H.D., Rajan, A. S., Kunze, D. L., and Boyd, A. E. (1991) *J. Biol. Chem.* **266**, 837-843
3. Ullrich, S., Prentki, M., and Wollheim, C. B. (1990) *Biochem. J.* **270**, 273-276
4. Lee, B., Yang, C., Chen, T. H., Al-Azawi, N., and Hsu, W. H. (1995) *Am. J. Physiol.* **269**, E1095-E1100
5. Thibonnier, M. (1992) *Regul. Pept.* **3**, 1-11
6. Cheng, H., Yibchok-anun, S., and Hsu, W. H. (2002) *Biochem. J.* In Press
7. Berridge, M. J., Heslop, J. P., Irvine, R. F., and Brown, K. D. (1984) *Biochem. J.* **222**, 195-201
8. Nishizuka, Y. (1984) *Nature* **308**, 693-698
9. Rhee, S. G. (2001) *Annu. Rev. Biochem.* **70**, 281-312
10. Patel, Y. C., Greenwood, M. T., Warszynska, A., Panetta, R., and Srikant, C. B. (1994) *Biochem. Biophys. Res. Commun.* **198**, 605-612
11. Muller, S., and Lohse, M. J. (1995) *Biochem. Soc. Trans.* **23**, 141-148
12. Quitterer, U., and Lohse, M. J. (1999) *Proc. Natl. Acad. Sci. U. S.A.* **96**, 10626-10631
13. Yeo, A., Samways, D. S., Fowler, C. E., Gunn-Moore, F., and Henderson, G. (2001) *J. Neurochem.* **76**, 1688-1700
14. Chan, J. S., Lee, J. W., Ho, M. K., and Wong, Y. H. (2000) *Mol. Pharmacol.* **57**, 700-708
15. Selbie, L. A., King, N. V., Dickenson, J. M., and Hill, S. J. (1997) *Biochem. J.* **328**, 153-158
16. Connor, M., Yeo, A., and Henderson, G. (1997) *Br. J. Pharmacol.* **120**, 455-463
17. Murthy, K. S., Coy, D. H., and Makhlouf, G. M. (1996) *J. Biol. Chem.* **271**, 23458-23463
18. ZhuGe, R., and Hsu, W. H. (1995) *J. Pharmacol. Exp. Ther.* **275**, 1077-1083
19. Grynkiewicz, G., Poenie, M., and Tsien, R. Y. (1985) *J. Biol. Chem.* **260**, 3440-3450
20. Norris, F. A., and Majerus, P. W. (1994) *J. Biol. Chem.* **269**, 8716-8720
21. Hoque, K. M., Pal, A., Nair, G. B., Chattopadhyay, S., and Chakrabarti, M. K. (2001) *FEMS Microbiol. Lett.* **196**, 45-50
22. Cheng, H., Yibchok-anun, S., Coy, D., and Hsu, W. H. (2002) *Life Sci.* In Press
23. Selbie, L. A., and Hill, S. J. (1998) *Trends Pharmacol. Sci.* **19**, 87-93

24. Blake, B. L., Wing, M. R., Zhou, J. Y., Lei, Q., Hillmann, J. R., Behe, C. I., Morris, R. A., Harden, T. K., Bayliss, D. A., Miller, R. J., and Siderovski, D. P. (2001) *J. Biol. Chem.* **276**, 49267-49274

25. Murthy, K. S., and Makhlouf, G. M. (1998) *J. Biol. Chem.* **273**, 4695-4704

26. Kim, D., Lewis, D. L., Graziadei, L., Neer, E. J., Bar-Sagi, D., and Clapham, D. E. (1989) *Nature* **337**, 557-560

27. Koch, W. J., Hawes, B. E., Allen, L. F., and Lefkowitz, R. J. (1994) *Proc. Natl. Acad. Sci. U. S. A.* **91**, 12706-12710

28. Hedin, K. E., Bell, M. P., Huntoon, C. J., Karnitz, L. M., and McKean, D. J. (1999) *J. Biol. Chem.* **274**, 19992-20001

29. Pumiglia, K. M., LeVine, H., Haske, T., Habib, T., Jove, R., and Decker, S. J. (1995) *J. Biol. Chem.* **270**, 14251-14254

30. Goldman, P. S., DeMaggio, A. J., Hoekstra, M. F., and Goodman, R. H. (1997) *Biochem. Biophys. Res. Commun.* **240**, 425-429

31. Lopez-Ilasaca, M., Gutkind, J. S., and Wetzker, R. (1998) *J. Biol. Chem.* **273**, 2505-2508

32. Myung, C. S., and Garrison, J. C. (2000) *Proc. Natl. Acad. Sci. U. S. A.* **97**, 9311-9316

33. Rameh, L. E., Tolias, K. F., Duckworth, B. C., and Cantley, L. C. (1997) *Nature* **390**, 192-196

34. Hawkins, P. T., Jackson, T. R., and Stephens, L. R. (1992) *Nature* **358**, 157-159

35. Stephens, L. R., Hughes, K. T., and Irvine, R. F. (1991) *Nature* **351**, 33-39

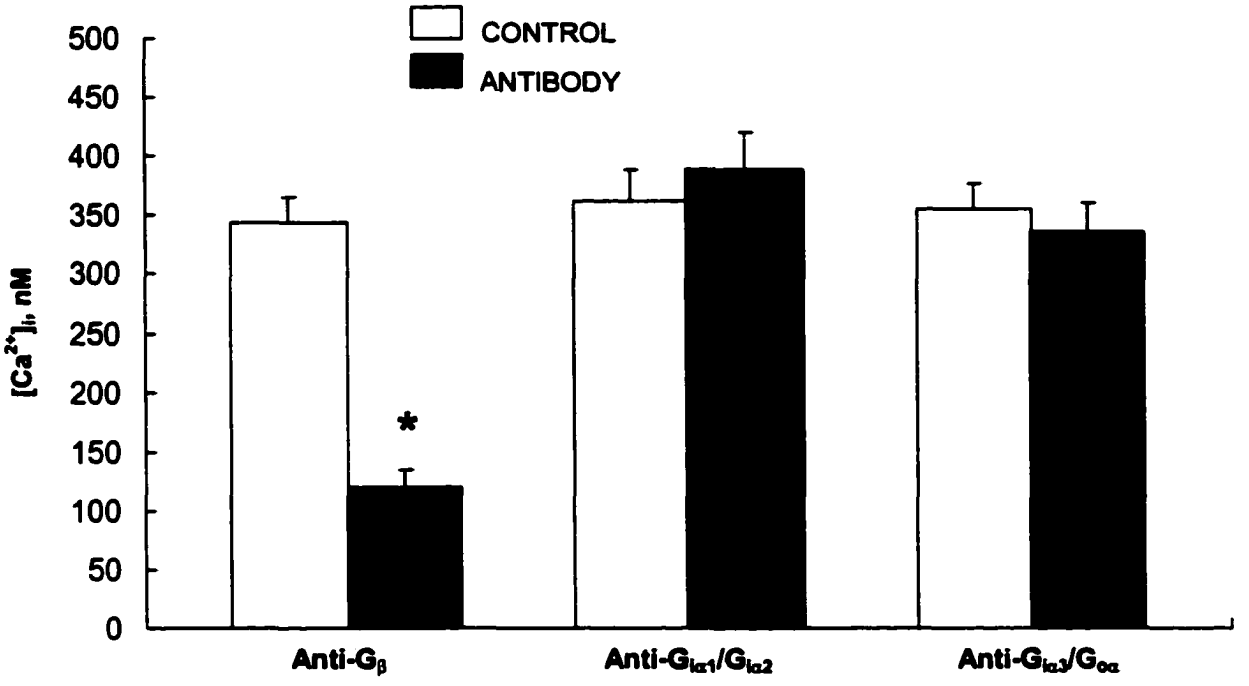

Fig. 1. Effect of antibodies against $G_{i/o}$ subunits on somatostatin (SRIF)-induced increase in $[Ca^{2+}]_i$ in the presence of arginine vasopressin (AVP). Antibodies against G_β, $G_{i\alpha1}/G_{i\alpha2}$, and $G_{i\alpha3}/G_{o\alpha}$ were diluted 1:100 and microinjected into single cells followed by a 30-min incubation period and Ca^{2+} image analysis. 100 nM SRIF was given 100 s following administration of AVP (1 nM). Values are mean ± S.E.M.; n=10 cells/treatment. *$P < 0.05$ compared to SRIF controls.

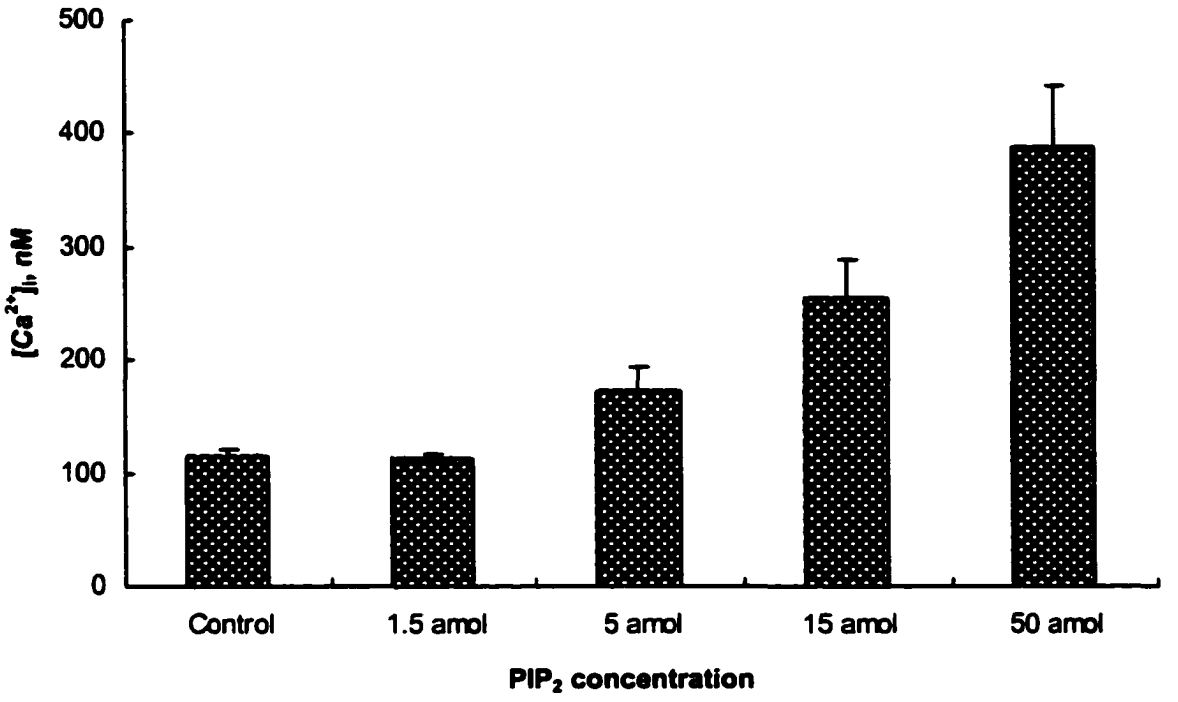

Fig. 2. Effect of PIP_2 microinjection on $[Ca^{2+}]_i$ in the presence of AVP. Administration of PIP_2 (1.5-50 amol) into single cells increased $[Ca^{2+}]_i$ in a concentration-dependent manner after 100 s of AVP (1 nM). Control cells received intracellular buffer alone after AVP. Values are mean ± S.E.M.; n=3 cells/PIP_2 concentration.

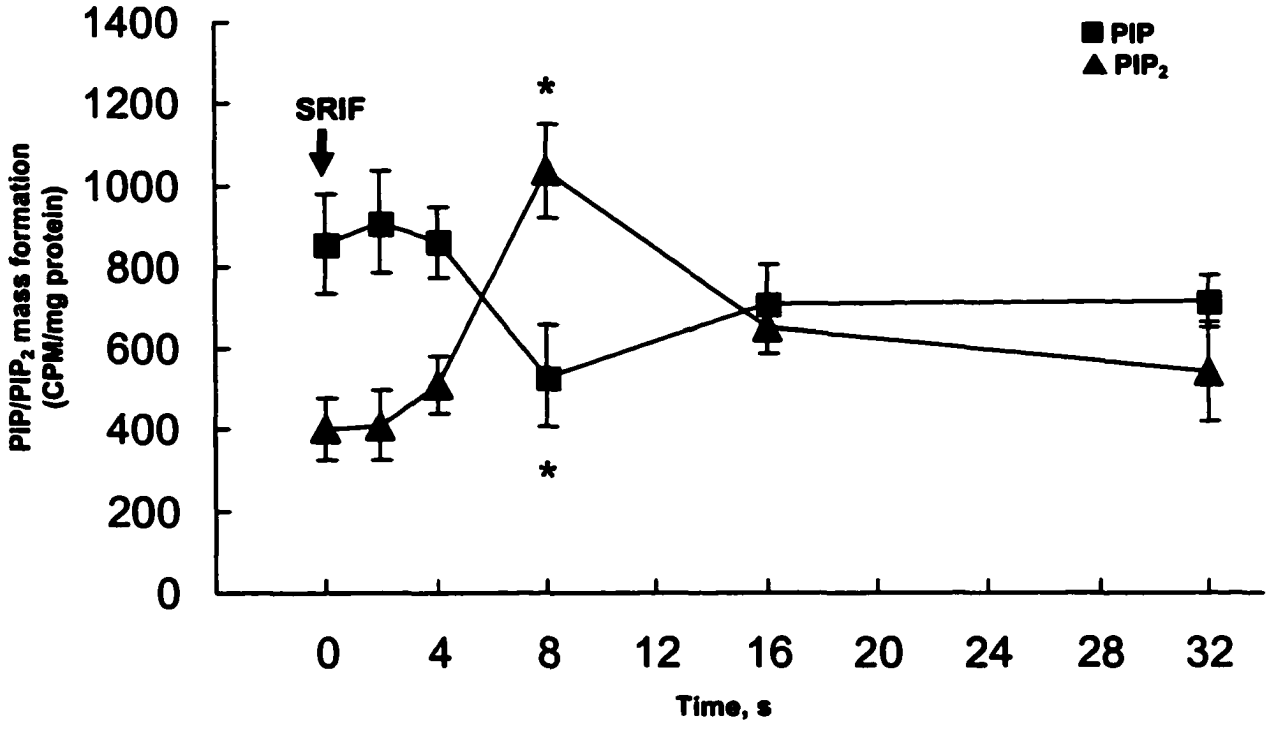

Fig. 3. Time course for PIP_2 synthesis from PIP by SRIF in the presence of AVP. PIP_2 and PIP formation by SRIF after treatment of HIT-T15 cells with AVP, as determined by thin layer chromatography. SRIF (100 nM) was given 100 s after AVP (1 nM) and experiments terminated at the respective time. Values are mean ± S.E.M.; n=3. $^*P < 0.05$ compared to 0 s.

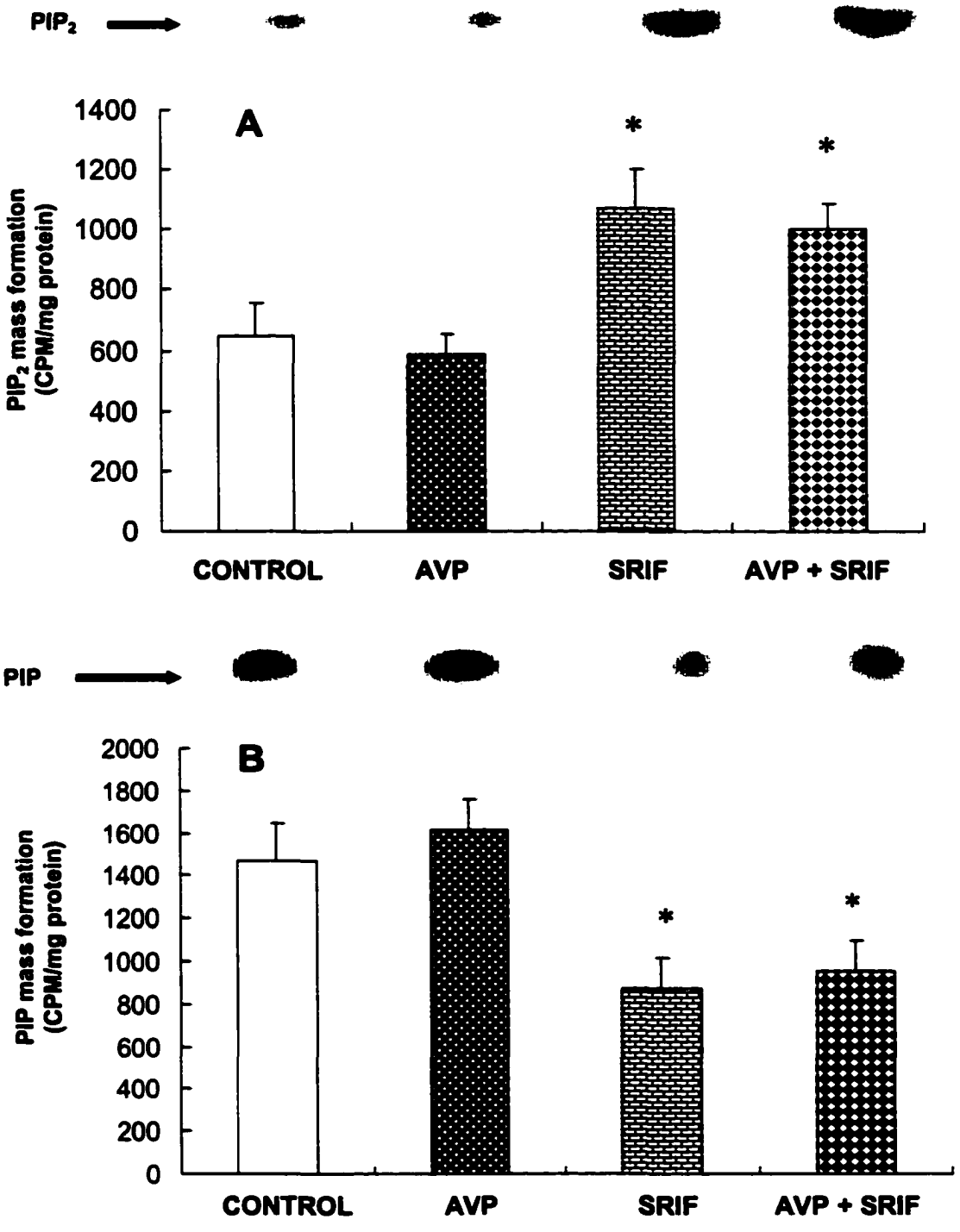

Fig. 4. SRIF-induced increase in PIP_2 synthesis in the presence and absence of AVP. PIP_2 (A) and PIP (B) formation after exposure to different treatments. SRIF (100 nM) was given 100 s after AVP (1 nM) and experiments terminated at 8 s of SRIF treatment. Values are mean ± S.E.M.; n=4. *$P < 0.05$ compared to basal controls.

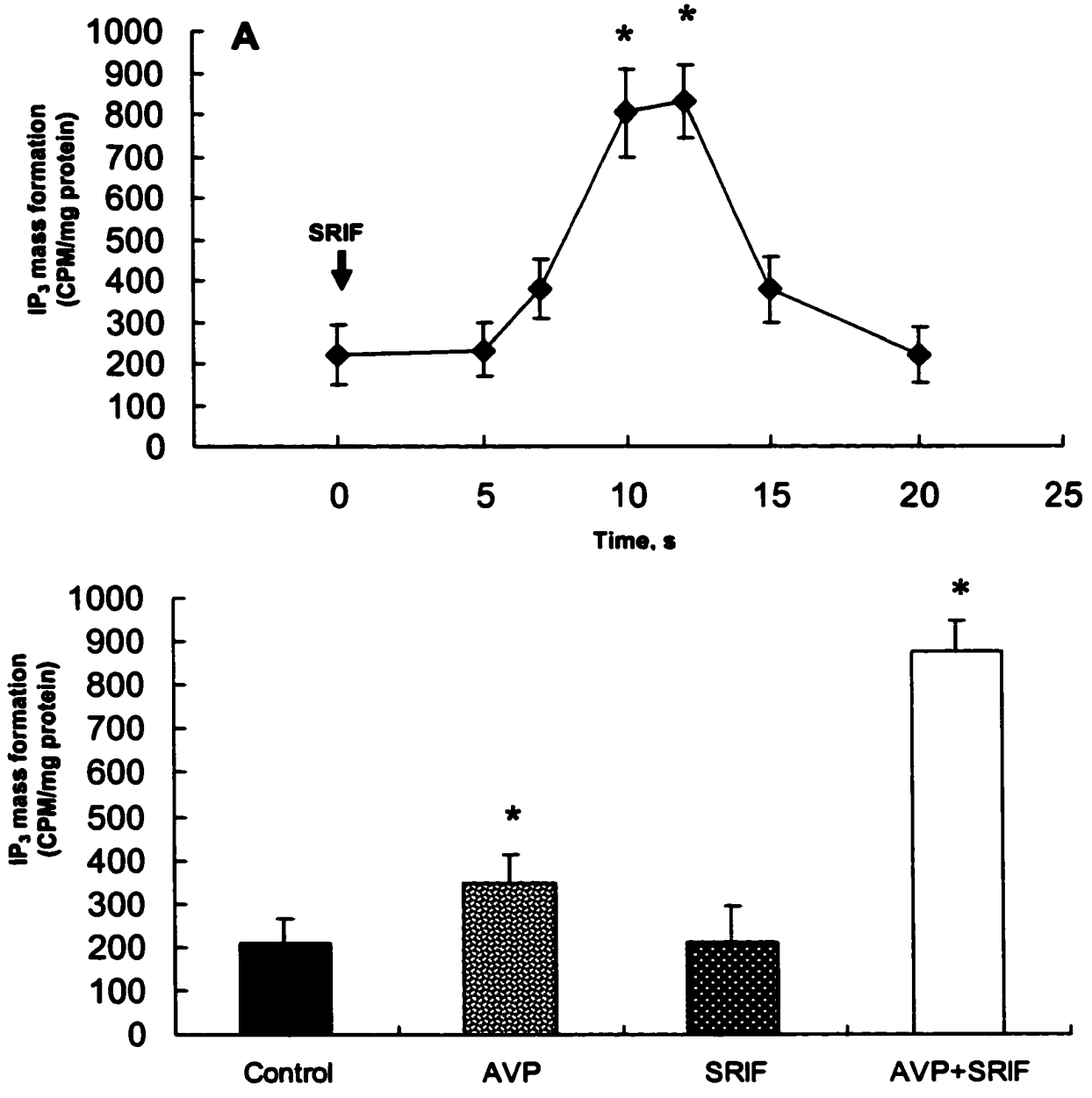

Fig. 5. IP_3 synthesis by SRIF in the presence and absence of AVP. A) Time course of AVP-SRIF induced increase in IP_3 formation, as determined by ion-exchange chromatography. SRIF (100 nM) was given 100 s after AVP (1 nM) and experiments terminated at the respective time; $^*P < 0.05$ compared to 0 s (n=3). B) Measurement of IP_3 formation after exposure to different treatments. SRIF (100 nM) was given 100 s after AVP (1 nM) and experiments terminated at 12 s of SRIF treatment; $^*P < 0.05$ compared to basal controls (n=4). Values are mean ± S.E.M.

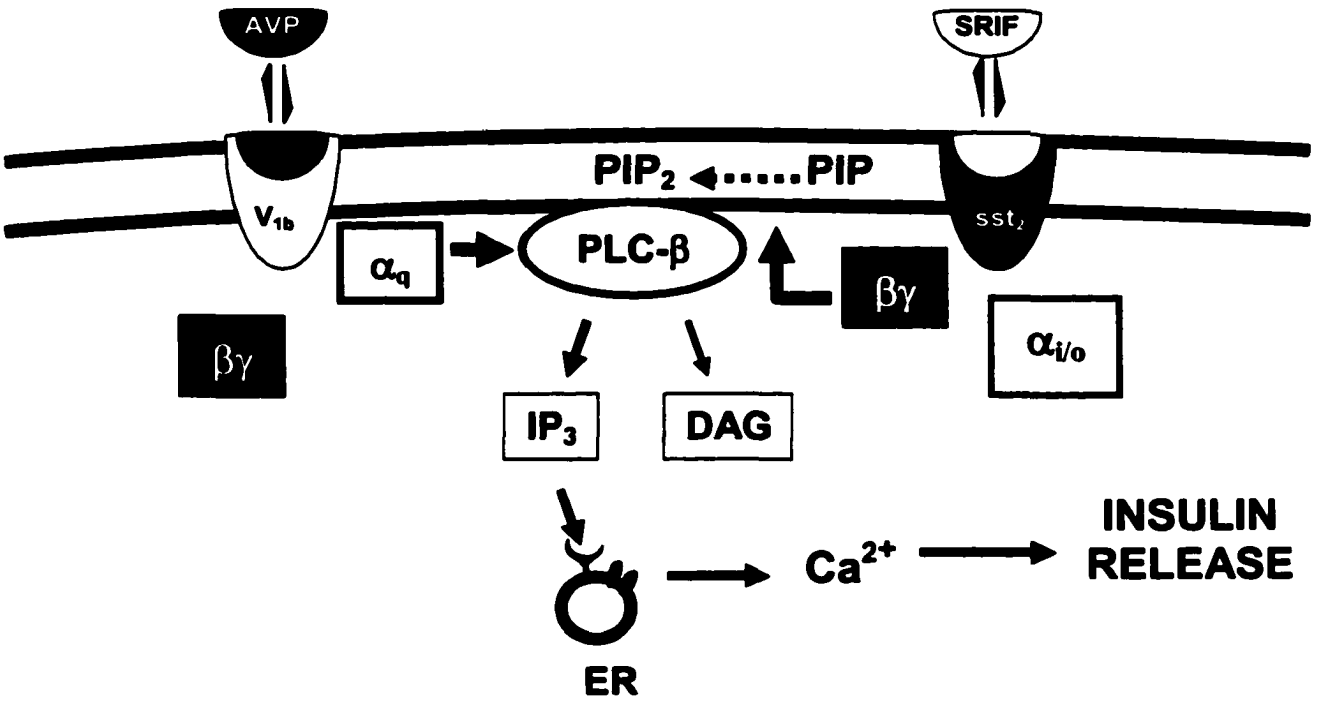

Fig. 6. Summary of SRIF-AVP cross-talk in stimulation of insulin release from HIT-T15 cells. Activation of the $G_{i/o}$-coupled receptor by SRIF increases PIP_2 synthesis from PIP through the βγ dimer of the G-protein. The PIP_2 generated serves as additional substrate for preactivated PLC-β by AVP, which increases IP_3 levels and $[Ca^{2+}]_i$ leading to insulin release. ER: endoplasmic reticulum.

CHAPTER V GENERAL DISCUSSION

The major points pertaining to the findings obtained in this dissertation have already been discussed in the Discussion section of each chapter. An outline of the major conclusions derived from the study and some speculative ideas on further details of the mechanism of insulin release by somatostatin (SRIF) are as follow:

Regulation of $[Ca^{2+}]_i$ and insulin release by SRIF

Ca^{2+} signaling is an important step for hormone exocytosis from endocrine cells. The role of Ca^{2+} in insulin release from β-cells has been demonstrated by several investigators (Henquin et al., 1998; Qian and Kennedy, 2001; Wollheim and Pozzan, 1984). To date, reports on the effects of SRIF on $[Ca^{2+}]_i$ and insulin release have been all inhibitory. For the first time, we describe a stimulatory effect of SRIF on $[Ca^{2+}]_i$ and insulin release in β-cells. This effect requires the presence of a Gq agonist such as AVP, and is mediated through Gi/Go, the PLC pathway and mainly Ca^{2+} release from the ER. The SRIF-induced increase in $[Ca^{2+}]_i$ and insulin release was characterized by a sharp and transient increase followed by a rapid decline to the sub-basal level. Investigation of the Ca^{2+} sources revealed that the ER Ca^{2+} is the main source for the responses to SRIF, since treatment with TG, which depletes Ca^{2+} stores from the ER, abolished this effect. Under Ca^{2+}-free condition, SRIF maintained its ability to increase $[Ca^{2+}]_i$, although the magnitude was lower compared to Ca^{2+}-containing condition. Receptor-activated Ca^{2+} mobilization through the IP_3 cascade can involve two phases: 1) Ca^{2+} release from the ER, and 2) Ca^{2+} influx from the extracellular space (Putney, 1987). Mobilization of Ca^{2+} from intracellular stores by IP_3 promotes Ca^{2+} influx through the opening of Ca^{2+} channels present on the plasma membrane (Icrac) (Voets et al., 2001). It is likely that Icrac is involved in the increases in $[Ca^{2+}]_i$ by SRIF.

In addition, a sharp decrease in $[Ca^{2+}]_i$ to the sub-basal level followed its peak. An increase in mitochondrial Ca^{2+} uptake is triggered by IP_3-induced Ca^{2+} release (Collins et al., 2001). The rate of Ca^{2+} uptake by the mitochondria is greatly increased when $[Ca^{2+}]_i$ reaches ~ 400 nM, which is similar to the increases obtained with SRIF in our study. An alternative mechanism of Ca^{2+} redistribution is by efflux to the extracellular space through ATP-dependent Ca^{2+} pumps present on the plasma membrane (Sorin et al., 1997). In the

present study, pretreatment of HIT-T15 cells with inhibitors of ATP-dependent Ca^{2+} pumps did not alter the sharp decrease in $[Ca^{2+}]_i$, suggesting that Ca^{2+} uptake by the mitochondria maybe responsible for the Ca^{2+} redistribution. Another explanation for this transient increase may be attributable to the transient increase in IP_3 formation.

Phosphorylation leading to desensitization and conformational changes

Exposure of GPCRs to agonists often results in a rapid attenuation of receptor responsiveness. The time frame over which these processes occur range from seconds (phosphorylation) to minutes (endocytosis) and hours (down-regulation). Studies have shown that GPCRs and PLC isozymes can serve as substrates for PKA, PKC, and G-protein-coupled receptor kinase phosphorylation during desensitization (Budd et al., 2000; Francesconi and Duvoisin, 2000; Pitcher et al., 1998). Phosphorylation of the V_{1b} receptor and PLC-β by PKC after receptor activation occurs during desensitization (Aiyar et al., 1990; Birnbaumer et al., 1992; Innamorati et al., 1998). This event accounts in part for the reduction in the responsiveness of cells to further stimulation by AVP.

The ability of SRIF to increase $[Ca^{2+}]_i$ even after 60 min of AVP treatment suggest that desensitization of the V_{1b} receptor and PLC-β may not be apparent during stimulation with a small concentration of AVP (1 nM). Activation of the V_{1b} receptor coupled to Gq, leads to PLC-β activation (Thibonnier et al., 1993), which utilizes PIP_2 as a substrate to generate IP_3 and DAG (Berridge, 1993). Although there are no reports on conformational changes for PLC-β during desensitization, phosphorylation of PLC-γ leads to conformational changes of this isozyme (Smith et al., 2001). Such structural changes could mask the PIP_2 binding sites for additional substrate generated by SRIF. Several PIP_2-regulated actin-binding proteins and PLC isozymes, including PLC-β posses a basic amino acid motif (KxxxKxKK, x = any amino acid), that represents the PIP_2-binding site commonly present in these proteins (Simoes et al., 1995). In our system, the absence of desensitization of PLC-β after activation of the V_{1b} receptor may leave the PIP_2-binding sites exposed to PIP_2 generated by SRIF, and this would explain why SRIF can increase $[Ca^{2+}]_i$ even after 60 min of AVP treatment. Future work on structural analysis of PLC-β may provide insights to the conformational changes and exposure of the binding sites during preactivation by AVP.

SRIF receptors and insulin release

The effects of SRIF are mediated through the seven-transmembrane receptor family that signals via Gi/Go. Five distinct SRIF receptors have been characterized and designated as SSTR1-5, where two splice variants of the SSTR2 exists, SSTR2a and SSTR2b (Bruno et al., 1992; Patel et al., 1994; Reisine and Bell, 1995). Studies utilizing rabbit polyclonal antibodies against the human SSTR1-5 and double-label confocal fluorescence immunocytochemistry have demonstrated that all five subtypes are variably expressed in human pancreatic islets, where SSTR1 and SSTR5 are dominant in β-cells (Kumar et al., 1999). In both human and rat β-cells SSTR5 mediate the inhibitory effects of SRIF (Mitra et al., 1999). However, the receptor subtype that mediates the SRIF effects in HIT-T15 cells remains unknown. We characterized the SRIF receptor subtype that mediates the increase in $[Ca^{2+}]_i$ leading to insulin secretion using subtype-selective agonists for SSTR1-5 and PRL-2903, a specific SSTR2 antagonist. Our results strongly suggest that SSTR2 be involved in the SRIF-induced increase in $[Ca^{2+}]_i$.

SSTR5 is responsible for the inhibitory effects of SRIF on insulin release in rats, mice, and humans (Mitra et al., 1999; Strowski et al., 2002). Since HIT-T15 cells are derived from hamster, there is a possibility that another SRIF receptor subtype, possibly the SSTR2, may mediate the inhibitory effects of SRIF in this cell line. Our recent findings demonstrated that both SRIF and L-779,976, but not other SSTR agonist inhibited KCl-induced increase in insulin release, suggesting that SSTR2 mediates both inhibitory and stimulatory effects of SRIF (unpublished results). A cross-talk between the G-protein system coupled to the V_{1b} receptor and the SSTR2 may account for the differences between inhibition and stimulation of insulin release by SRIF.

Cross-talk between Gq and Gi/Go

Reports of cross-talk between Gq- and Gi/Go-coupled receptors have been described in different cell types (Quitterer and Lohse, 1999; Selbie et al., 1997; Yeo et al., 2001). This particular mode of intracellular signaling has been suggested to be a way through which a G-protein system can be amplified. We demonstrated that SRIF, which is coupled to Gi/Go can increase $[Ca^{2+}]_i$ leading to insulin release after activation of the Gq-coupled V_{1b} receptor. SRIF alone failed to increase $[Ca^{2+}]_i$ and insulin release. This cross-

talk is specific to Gq- and Gi/Go-coupled receptors, although not limited to the AVP and SRIF receptors, since in the presence of BK, another Gq-coupled receptor agonist, SRIF increased $[Ca^{2+}]_i$. In the presence of AVP, medetomidine, an α_2-adrenergic receptor agonist that stimulates Gi/Go, also increased $[Ca^{2+}]_i$. In contrast, activation of Gs with isoproterenol, a non-specific β-adrenergic receptor agonist, or Gi/Go with medetomidine prior to SRIF, did not induce an increase in $[Ca^{2+}]_i$ by SRIF.

During cross-talk with Gq, activation of Gi/Go-coupled receptors often leads to increases in inositol phosphate formation and $[Ca^{2+}]_i$ (Quitterer and Lohse, 1999; Selbie et al., 1997; Yeo et al., 2001). Studies suggest that enhancement of Gq signals by Gi/Go is through activation of PLC-β (Chan et al., 2000) or interaction with a step after PLC activation (Yeo et al., 2001), but none of them have attributed the effect of Gi/Go to a step before PLC activation. We demonstrated that SRIF increased $[Ca^{2+}]_i$ and insulin release by stimulating PIP_2 synthesis through the βγ dimer of Gi/Go. The PIP_2 generated by SRIF serves as additional substrate for preactivated PLC-β, which hydrolyzes PIP_2, thereby increasing IP_3 levels, $[Ca^{2+}]_i$ and insulin release from HIT-T15 cells. It is likely that the βγ dimer activates PI4P 5- and/or PI5P 4-kinase. These enzymes are responsible for the synthesis of PIP_2 from PIP (Rameh et al., 1997). Although the majority of PIP_2 in cells is produced from PI4P (Hawkins et al., 1992; Stephens et al., 1991), we cannot preclude PIP_2 synthesis from PI5P pools. Activation of other kinases by the βγ dimer of Gi/Go such as mitogen-activated protein kinase (Hedin et al., 1999; Koch et al., 1994), phosphatidylinositol 3-kinase (Lopez-Ilasaca et al., 1998) and β-adrenergic receptor kinase (Goldman et al., 1997) has been reported. In addition to the PIP_2 hydrolysis by PLC-β, there are two possible mechanisms involved in the PIP_2 metabolism: 1) phosphorylation by phosphatidylinositol 3-kinase to PIP_3, and 2) dephosphorylation by 5-phosphatase to PIP.

Hydrolysis of PIP_2 by PLC-β increases IP_3 formation. In the presence of AVP, SRIF induced a transient increase in IP_3 formation, which peaked at 12 s of SRIF treatment and returned to basal level within 20 s. Metabolism of IP_3 can occur by two pathways: 1) dephosphorylation by inositol polyphosphate 5-phosphatase to IP_2, and 2) phosphorylation by phosphatidylinositol 3-kinase to IP_4. The increases in PIP_2, IP_3, $[Ca^{2+}]_i$, and insulin release by SRIF are all characterized by transient patterns. In a preliminary study, treatment with LY-294002, a phosphatidylinositol 3-kinase inhibitor did not alter the SRIF-induced sharp decline in $[Ca^{2+}]_i$ (unpublished results). It is possible that dephosphorylation of IP_3 to

IP_2 by the 5-phosphatase is mainly responsible for its transient increase, although we cannot rule out the possibility of conversion of IP_3 to IP_4. An increase in 5-phosphatase activity occurs in *Xenopus laevis* simultanecusly to the increase in IP_3 formation (Sims and Allbritton, 1998).

Since this is the first report of cross-talk between Gq and Gi/Go in an endocrine cell, it is tempting to speculate that a dual-mode of insulin regulation by SRIF exists in β-cells. One in which insulin release is inhibited by SRIF during exposure of β-cells to secretagogues. In the presence of hormones such as AVP (Gq agonists), activation of SRIF receptors would stimulate insulin release. The differences between inhibition and stimulation of insulin release would depend on the presence or absence of a particular hormone that β-cells being exposed to. This cross-talk mechanism may represent another way through which a particular G-protein system can be amplified.

Physiological significance of insulin release by SRIF

Insulin is the most important regulator of elevated blood glucose levels. At the same time, glucose is the major stimulus for insulin release from β-cells. One possible mechanism by which glucose stimulates insulin release is by uptake into β-cells via GLUT2, where it is phosphorylated by glucokinases to glucose 6-phosphate. Glucose 6-phosphate undergoes glycolysis to generate ATP, closing ATP-sensitive K^+ channels leading to depolarization and opening of Ca^{2+} channels. An increase in $[Ca^{2+}]_i$ promotes insulin release into the blood stream (Ashchroft et al., 1984). Insulin exerts its action mainly by promoting glucose uptake into muscles, adipose tissue and liver, where it is stored in form of glycogen. Glucose-stimulated insulin secretion is biphasic, comprising a rapid first phase lasting 5-10 min, followed by a prolonged second phase, that continues for the duration of the stimulus. The shape of the glucose-response curve is determined by the activity of the glucokinase, which dictates the rate-limiting step for glucose metabolism (Van Schaftingen, 1994).

A second mode of insulin release is in a pulsatile manner, where insulin is released in transient bursts with shorter duration than the biphasic pattern described for glucose (Gilon et al., 2002; Song et al., 2002). The mechanisms driving the pulsatility of insulin release are still unclear, but an transient increase in $[Ca^{2+}]_i$ is required for such a pattern (Gilon et al., 2002). It is possible that SRIF may be involved in this mechanism, since transient increases in $[Ca^{2+}]_i$ and insulin release are observed upon activation of SRIF

receptors in HIT-T15 cells during cross-talk with Gq. All studies describing the inhibitory effects of SRIF on insulin release have been done in the absence of Gq agonists (Hsu et al., 1991; Strowski et al., 2000; Ullrich et al., 1990), which does not preclude the interaction between signals generated by Gq and Gi/Go, since under physiological conditions β-cells can simultaneously be exposed to hormones such as AVP and SRIF.

Diabetes mellitus is characterized by chronic hyperglycemia and can be divided into type 1 (insulin-dependent) and type 2 (non-insulin-dependent). In the type 1, insulin deficiency is more severe and acute, involves significant weight loss and spontaneous ketosis can occur. The type 2 is characterized by a combination of insulin resistance and deficiency, whereas insulin deficiency is less severe than in the type 1 and blood insulin levels remain high enough to prevent excessive lipolysis and spontaneous ketosis. The type 2 is present in patients that normally do not require insulin treatment to remain alive, although up to 20 % are treated with insulin to control blood glucose levels. Treatment of diabetic patients with insulin infusions in a pulsatile rather than continuous manner has been shown to be beneficial due to its ability to prevent insulin resistance by demonstrating a greater hypoglycemic effect (Gilon et al., 2002). The observation that type 2 patients have impaired pulsatile insulin release (O'Rahilly et al., 1988; Porksen et al., 2002) suggest that absence of this mode of release contributes to the disease. The transient increases in $[Ca^{2+}]_i$ leading to insulin release by SRIF during cross-talk with Gq-coupled receptors may contribute to the pulsatile pattern of insulin release, which in turn may play a role in the prevention of diabetes type 2.

LITERATURE CITED

Abou-Samra, A., Juppner, H., Force, T., Freeman, M. W., Kong, X., Schipani, E., Urena, P., Richards, J., Bonventre, J. V., Potts Jr, J. T., Kronenberg, H. M. and Segre, G. V. (1992) Expression cloning of a common receptor for parathyroid hormone and parathyroid hormone-related peptide from rat osteoblast-like cells: a single receptor stimulates intracellular accumulation of both cAMP and inositol trisphosphates and increases intracellular free calcium. Proc. Natl. Acad. Sci. USA 89: 2732-2736.

Aguila, M. C., Rodriguez, A. M.,Aguila-Mansilla, H. N., Lee and W. T. (1996) Somatostatin antisense oligodeoxy-nucleotide-mediated stimulation of lymphocyte proliferation in culture. Endocrinology 137: 1585-1590.

Ahren, B. (2000) Autonomic regulation of islet hormone secretion-implications for health and disease. Diabetologia 43: 393-410.

Aiyar, N., Nambi, P. and Crooke S. T. (1990) Desensitization of vasopressin sensitive adenylate cyclase by vasopressin and phorbol esters. Cell Signal 2: 153-160.

Akbar, M., Okajima, F., Tomura, H., Majid, M. A., Yamada, Y., Seino, S. and Kondo, Y. (1994) Phospholipase C activation and Ca^{2+} mobilization by cloned human somatostatin receptor subtypes 1-5 in transfected COS-7 cells. FEBS Lett. 348: 192-196.

Allgeier, A., Offermanns, S., Van Sande, J., Spicher, K., Schultz, G. and Dumont, J. E. (1994) The human thyrotropin receptor activates G-proteins Gs and Gq/11. J. Biol. Chem. 269: 13733-13735.

Anborgh, P. H., Seachrist, J. L., Dale, L. B. and Ferguson, S. S. (2000) Receptor/beta-arrestin complex formation and the differential trafficking and resensitization of beta2-adrenergic and angiotensin II type 1A receptors. Mol. Endocrinol. 14: 2040-2053.

Ashcroft, F. M., Harrison, D. E. and Ashcroft, S. J. H. (1984) Glucose induces closure of single potassium channels in isolated rat pancreatic B cells. Nature 312: 446-448.

Ashcroft, S. J., Hammonds, P. and Harrison, D. E. (1986) Insulin secretory responses of a clonal cell line of simian virus 40-transformed beta cells. Diabetologia 29: 727-733.

Backer, J. M., Schroeder, G. G., Kahn, C. R., Myers, M. G. Jr., Wilden, P. A., Cahill, D. A. and White, M. F. (1992) Insulin stimulation of phosphatidylinositol 3-kinase activity

maps to insulin receptor regions required for endogenous substrate phosphorylation. J. Biol. Chem. 267: 1367-1374.

Barberis, C., Mouillac, B. and Durroux, T. (1998) Structural bases of vasopressin/oxytocin receptor function. J. Endocrinol. 156: 223-229.

Barlic, J., Khandaker, M. H., Mahon, E., Andrews, J., DeVries, M. E., Mitchell, G. B., Rahimpour, R., Tan, C. M., Ferguson, S. S. and Kelvin, D. J. (1999) beta-arrestins regulate interleukin-8-induced CXCR1 internalization. J. Biol. Chem. 274: 16287-16294.

Baron, A. D., Steinberg, H., Brechtel, G. and Johnson, A. (1994) Skeletal muscle blood flow independently modulates insulin-mediated glucose uptake. Am. J. Physiol. 266: E248-253.

Barritt, G. J. (1999) Receptor-activated Ca2+ inflow in animal cells: a variety of pathways tailored to meet different intracellular Ca2+ signaling requirements. Biochem. J. 33: 153-169.

Bass, R. T., Buckwalter, B. L., Patel, B. P., Pausch, M. H., Price, L. A., Strnad, J. and Hadcock, J. R. (1996) Identification and characterization of novel somatostatin antagonists. Mol. Pharmacol. 50: 709-715.

Bauer, W., Briner, U., Doepfner, W., Halber, R., Huguenin, R., Marbach, P., Petcher, T. J. and Pless, J. (1982) SMS201-995: A very potent and selective octapeptide analogue of somatostatin with prolonged action. Life Sci. 31: 1133-1140.

Bazenet, C. E., Ruano, A. R., Brockman, J. L. and Anderson, R. A. (1990) The human erythrocyte contains two forms of phosphatidylinositol-4-phosphate 5-kinase which are differentially active toward membranes. J. Biol. Chem. 265: 18012-18022.

Bell, G. I., Pictet, R. L., Rutter, W. J., Cordell, B., Tischer, E. and Goodman, H. M. (1980) Sequence of the human insulin gene. Nature 284: 26-32.

Berridge, M. J. (1993) Inositol trisphosphate and calcium signalling. Nature 361: 315-325.

Birnbaumer, L., Boulay, G., Brown, D., Jiang, M., Dietrich, A., Mikoshiba, K., Zhu, X. and Qin, N. (2000) Mechanism of capacitative Ca2+ entry (CCE): interaction between IP3 receptor and TRP links the internal calcium storage compartment to plasma membrane CCE channels. Recent Prog. Horm. Res. 55:127-161.

Birnbaumer, M. (2000) Vasopressin receptors. Trends Endocrinol. Metab. 11: 406-410.

Birnbaumer, M., Antaramian, A., Themmen, A. P. and Gilbert, S. (1992) Desensitization of the human V2 vasopressin receptor. Homologous effects in the absence of heterologous desensitization. J. Biol. Chem. 267: 11783-11788.

Bito, H., Mori, M., Sakanaka, C., Takano, T., Honda, Z., Gotoh, Y., Nishida, E. and Shimizu, T. (1994) Functional coupling of SSTR4, a major hippocampal somatostatin receptor, to adenylate cyclase inhibition, arachidonate release and activation of the mitogen-activated protein kinase cascade. J. Biol. Chem. 269: 12722-12730.

Blake, B. L., Wing, M. R., Zhou, J. Y., Lei, Q., Hillmann, J. R., Behe, C. I., Morris, R. A., Harden, T. K., Bayliss, D. A., Miller, R. J. and Siderovski, D. P. (2001) G beta association and effector interaction selectivities of the divergent G gamma subunit G gamma(13). J. Biol. Chem. 276: 49267-49274.

Bonner-Weir, S. and Orci, L. (1982) New perspectives on the microvasculature of the islets of Langerhans in the rat. Diabetes 31: 883-889.

Boronenkov, I. V. and Anderson, R. A. (1995) The sequence of phosphatidylinositol-4-phosphate 5-kinase defines a novel family of lipid kinases.
J. Biol. Chem. 270: 2881-2884.

Boronenkov, I. V., Loijens, J. C., Umeda, M. and Anderson, R. A. (1998) Phosphoinositide signaling pathways in nuclei are associated with nuclear speckles containing pre-mRNA processing factors. Mol. Biol. Cell. 9: 3547-3560.

Bourey, R. E., Koranyi, L., James, D. E., Mueckler, M. and Permutt, M. A. (1990) Effects of altered glucose homeostasis on glucose transporter expression in skeletal muscle of the rat. J. Clin. Invest. 86: 542-547.

Bruno, J. F., Xu, Y., Song, J. and Berelowitz, M. (1992) Molecular cloning and functional expression of a brain-specific somatostatin receptor. Proc. Natl. Acad. Sci. USA 89: 11151-11155.

Bruns, C., Raulf, F., Hoyer, D., Schloos, J., Lubbert, H. and Weckbecker, G. (1996) Binding properties of somatostatin receptor subtypes. Metabolism 45 (Suppl 1): 17-20.

Budd, D. C., McDonald, J. E. and Tobin, A. B. (2000) Phosphorylation and regulation of a Gq/11-coupled receptor by casein kinase 1alpha. J. Biol. Chem. 275:19667-19675.

Cantau, B., Guillon, G., Alaoui, M. F., Chicot, D., Balestre, M. N. and Devilliers, G. (1988) Evidence of two steps in the homologous desensitization of vasopressin-sensitive phospholipase C in WRK1 cells. Uncoupling and loss of vasopressin receptors. J. Biol. Chem. 263: 10443-10450.

Carty, D. J., Padrell, E., Codina, J., Birnbaumer, L., Hildebrandt, J. D. and Iyengar, R. (1990) Distinct guanine nucleotide binding and release properties of the three Gi proteins. J. Biol. Chem. 265: 6268-6273.

Castellino, A. M., Parker, G. J., Boronenkov, I. V., Anderson, R. A. and Chao, M. V. (1997) A novel interaction between the juxtamembrane region of the p55 tumor necrosis factor receptor and phosphatidylinositol-4-phosphate 5-kinase. J. Biol. Chem. 272: 5861-5870.

Cattaneo, M. G., Amoroso, D., Gussoni, G., Sanguini, A. M. and Vincenti, L. M. (1996) A somatostatin analogue inhibits MAP kinase activation and cell proliferation in human neuroblastoma and in human small cell lung carcinoma cell lines. FEBS Lett. 397: 164-168.

Chabre, O., Conklin, B. R., Brandon, S., Bourne, H. R. and Limbird, L. E. (1994) Coupling of the alpha 2A-adrenergic receptor to multiple G-proteins. A simple approach for estimating receptor-G-protein coupling efficiency in a transient expression system. J. Biol. Chem. 269: 5730-5734.

Chan, J. S., Lee, J. W., Ho, M. K. and Wong, Y. H. (2000) Preactivation permits subsequent stimulation of phospholipase C by G(i)-coupled receptors. Mol. Pharmacol. 57: 700-708.

Chen, L., Fitzpatrick, D., Vandlen, R. L. and Tashjian, A. H. (1997) Both overlapping and distinct signalling pathways for somatostatin receptor subtype SSTR1 and SSTR2 in pituitary cells. J. Biol. Chem. 272: 18666-18672.

Chen, T. H., Lee, B. and Hsu, W. H. (1994) Arginine vasopressin-stimulated insulin secretion and elevation of intracellular Ca^{++} concentration in rat insulinoma cells: influences of a phospholipase C inhibitor 1-[6-[[17 β-methoxyestra-1,3,5(10)-trien-17-yl]amino]hexyl]-1H-pyrrole-2,5-dione (U-73122) and a phospholipase A2 inhibitor N-(p-amylcinnamoyl) anthranilic acid. J. Pharmacol. Exp. Ther. 270: 900-904.

Chen, Y., Harry, A., Li, J., Smit, M. J., Bai, X., Magnusson, R., Pieroni, J. P., Weng, G. and Iyengar, R. (1997) Adenylyl cyclase 6 is selectively regulated by protein kinase A phosphorylation in a region involved in Galphas stimulation. Proc. Natl. Acad. Sci. USA 94: 14100-14104.

Cheng, H., Yibchok-anun, S. and Hsu, W. H. (1999) Somatostatin-induced paradoxical increase in intracellular calcium concentration after arginine vasopressin priming in

clonal hamster (HIT) cells. 11th Session of The Iowa Academy of Science, Iowa State University, Ames, IA., IAS suppl. 1: 20. Abstract 57.

Cheng, H., Yibchok-anun, S. and Hsu, W. H. (2002) Somatostatin-induced paradoxical increase in intracellular Ca^{2+} concentration and insulin release in the presence of arginine vasopressin in clonal β-cells HIT-T15. Biochem. J. In Press

Cheng, H., Yibchok-anun, S., Coy, D., and Hsu, W. H. (2002) SSTR2 mediates the somatostatin-induced increase in intracellular Ca^{2+} concentration and insulin secretion in the presence of arginine vasopressin in clonal β-cell HIT-T15. Life Sci. In Press

Chick, W. L., Warren, S., Chute, R. N., Like, A. A., Lauris, V. and Kitchen, K. C. (1977) A transplantable insulinoma in the rat. Proc. Natl. Acad. Sci. USA 74: 628-632.

Clapham, D. E. (1996) The G-protein nanomachine. Nature 379: 297-299.

Clapham, D. E. and Neer, E. J. (1993) New roles for G-protein βγ dimers in transmembrane signalling. Nature 365: 403-406.

Clapham, D. E. and Neer, E. J. (1997) G protein beta gamma subunits. Annu. Rev. Pharmacol. Toxicol. 37: 167-203.

Cole, G. M. and Reed, S. I. (1991) Pheromone-induced phosphorylation of a G protein beta subunit in S. cerevisiae is associated with an adaptive response to mating pheromone. Cell 64: 703-716.

Coleman, D. E., Berghuis, A. M., Lee, E., Linder, M. E., Gilman, A. G. and Sprang, S. R. (1994) Structures of active conformations of Gi alpha 1 and the mechanism of GTP hydrolysis. Science 265: 1405-1412.

Collier, E. and Gorden, P. (1991) O-linked oligosaccharides on insulin receptor. Diabetes 40: 197-203.

Collins, T. J., Lipp, P., Berridge, M. J. and Bootman, M. D. (2001) Mitochondrial Ca^{2+} uptake depends on the spatial and temporal profile of cytosolic Ca^{2+} signals. J. Biol. Chem. 276: 26411-26420.

Conklin, B. R., Farfel, Z., Lustig, K. D., Julius, D. and Bourne, H. R. (1993) Substitution of three amino acids switches receptor specificity of Gq alpha to that of Gi alpha. Nature 363: 274-276.

Connor, M., Yeo, A. and Henderson, G. (1997) Neuropeptide Y Y_2 receptor and somatostatin sst_2 receptor coupling to mobilization of intracellular calcium in SH-SY5Y human neuroblastoma cells. Br. J. Pharmacol. 120: 455-463.

Cordelier, P., Esteve, J-P. and Bousquet, C. (1997) Characterization of the antiproliferative signal mediated by the somatostatin receptor subtype sst5. Proc. Natl. Acad. Sci. USA 94: 9343-9348.

Cukierman, E., Huber, I., Rotman, M. and Cassel, D. (1995) The ARF1 GTPase-activating protein: zinc finger motif and Golgi complex localization. Science 270: 1999-2002.

De Lecea, L., Criado, J. R., Prospero-Garcia, O., Gautvik, K. M., Schweitzer, P., Danielson, P. E., Dunlop, C. L. M., Siggins, G. R., Henriksen, S. J. and Sutcliffe, J. G. (1996) A cortical neuropeptide with neuronal depressant and sleep-modulating properties. Nature 381: 242-245.

Denker, B. M., Neer, E. J. and Schmidt, C. J. (1992) Mutagenesis of the amino terminus of the alpha subunit of the G protein Go. In vitro characterization of alpha o beta gamma interactions. J. Biol. Chem. 267: 6272-6277.

Divecha, N., Truong, O., Hsuan, J. J., Hinchliffe, K. A. and Irvine, R. F. (1995) The cloning and sequence of the C isoform of PtdIns4P 5-kinase. Biochem. J. 309: 715-719.

Dohlman, H. G. and Thorner, J. (1997) RGS proteins and signaling by heterotrimeric G proteins. J. Biol. Chem. 272: 3871-3874.

Drake, P. G., Bevan, A. P., Burgess, J. W., Bergeron, J. J. and Posner, B. I. (1996) A role for tyrosine phosphorylation in both activation and inhibition of the insulin receptor tyrosine kinase in vivo. Endocrinology 137: 4960-4968.

Dubois, M. P. (1975) Immunoreactive somatostatin is present in discrete cells of the endocrine pancreas. Proc. Natl. Acad. Sci. USA 72: 1340-1343.

Duckworth, W. C. (1988) Insulin degradation: mechanisms, products, and significance. Endocr. Rev. 9: 319-345.

Duguid, J. R., Steiner, D. F. and Chick, W. L. (1976) Partial purification and characterization of the mRNA for rat preproinsulin. Proc. Natl. Acad. Sci. USA 73: 3539-3543.

Endemann, G., Dunn, S. N. and Cantley, L. C. (1987) Bovine brain contains two types of phosphatidylinositol kinase. Biochemistry 26: 6845-6852.

Endo, K. and Yawo, H. (2000) mu-Opioid receptor inhibits N-type Ca2+ channels in the calyx presynaptic terminal of the embryonic chick ciliary ganglion. J. Physiol. 524: 769-781.

Epelbaum, J., Dournaud, P., Fodor, M. and Viollet, C. (1994) The neurobiology of somatostatin. Crit. Rev. Neurobiol. 8: 25-44.

Florio, T., Yao, H., Carey, K. D., Dillon, T. J. and Stork, P. J. S. (1999) Somatostatin activation of mitogen-activated protein kinase via somatostatin receptor 1 (SSTR1). Mol. Endocrinol. 13: 24-37.

Francesconi, A. and Duvoisin, R. M. (2000) Opposing effects of protein kinase C and protein kinase A on metabotropic glutamate receptor signaling: selective desensitization of the inositol trisphosphate/Ca2+ pathway by phosphorylation of the receptor-G protein-coupling domain. Proc. Natl. Acad. Sci. USA 97: 6185-6190.

Fuchs, A. R. and Fuchs, F. (1984) Endocrinology of human parturition: A review. Br. J. Obstet. Gynecol. 91: 948-967.

Fukami, K., Furuhashi, K., Inagaki, M., Endo, T., Hatano, S. and Takenawa, T. (1992) Requirement of phosphatidylinositol 4,5-bisphosphate for alpha-actinin function. Nature 359: 150-152.

Ganong, W. F. (1997) Central regulation of visceral function. In Review of Medical Physiology, 18th ed. Lange Medical Publications, 217-239.

Geenan, V., Legros, J. J., Franchimont, P., Baudrihaye, M., Defresne, M. P. and Bonvier, J. (1986) The neuroendrocrine thymus: coexistence of oxytocin and neurophysin in the human thymus. Science 232: 508-511.

Gehrmann, T. and Heilmeyer, L. M. Jr. (1998) Phosphatidylinositol 4-kinases. Eur. J. Biochem. 253: 357-370.

Gilman, A. G. (1987) G proteins: transducers of receptor-generated signals. Annu. Rev. Biochem. 56: 615-649.

Gilon, P., Ravier, M. A., Jonas, J. C. and Henquin, J. C. (2002) Control mechanisms of the oscillations of insulin secretion in vitro and in vivo. Diabetes Suppl 1: S144-151.

Goldman, P. S., DeMaggio, A. J., Hoekstra, M. F. and Goodman, R. H. (1997) The beta-adrenergic receptor kinase interacts with the amino terminus of the G protein beta subunit. Biochem. Biophys. Res. Commun. 240: 425-429.

Goodson, J. L. and Bass, A. H. (2001) Social behavior functions and related anatomical characteristics of vasotocin/vasopressin systems in vertebrates. Brain Res. 35: 246-265.

Grazzini, E., Lodboerer, A. M., Perez-Martin, A., Joubert, D. and Guillon G. (1996) Molecular and functional characterization of V_{1b} vasopressin receptor in rat adrenal medulla. Endocrinology 137: 3906-3914.

Grimelius, L., Polak, J. M., Solcia, E. and Pearse, A. G. E. (1978) The enteroglucagon cell. In: Bloom S. R., ed. Gut Hormones. Edinburgh: Churchhill Livingstone 365-368.

Gu Y-Z and Schonbrunn A. (1997) Coupling specificity between somatostatin receptor sst2A and G proteins: Isolation of the receptor-G protein complex with a receptor antibody. Mol. Endocrinol. 11: 527-537.

Guillon, G., Couraud, P. O., Butlen, D., Cantau, B. and Jard, S. (1980) Size of vasopressin receptors from rat liver and kidney. Eur. J. Biochem. 111: 287-294.

Guldenaar, S. F. E. and Pickering, B. T. (1985) Immunocytochemical evidence for the presence of oxytocin in rat testis. Cell Tissue Res. 240: 485-487.

Guldenaar, S.F.E., Wathes, D.C. and Pickering, B.T. (1984) Immunocytochemical evidence for the presence of oxytocin and neurophysin in the large cells of the bovine corpus luteum. Cell Tissue Res. 237: 349-352.

Hartwig, J. H., Bokoch, G. M., Carpenter, C. L., Janmey, P. A., Taylor, L. A., Toker, A. and Stossel, T. P. (1995) Thrombin receptor ligation and activated Rac uncap actin filament barbed ends through phosphoinositide synthesis in permeabilized human platelets. Cell 82: 643-653.

Hawkins, P. T., Jackson, T. R. and Stephens, L. R. (1992) Platelet-derived growth factor stimulates synthesis of PtdIns(3,4,5)P3 by activating a PtdIns(4,5)P2 3-OH kinase. Nature 358: 157-159.

Hay, J. C., Fisette, P. L., Jenkins, G. H., Fukami, K., Takenawa, T., Anderson, R. A. and Martin, T. F. (1995) ATP-dependent inositide phosphorylation required for Ca(2+)-activated secretion. Nature 374: 173-177.

Hedin, K. E., Bell, M. P., Huntoon, C. J., Karnitz, L. M. and McKean, D. J. (1999) Gi proteins use a novel beta gamma- and Ras-independent pathway to activate extracellular signal-regulated kinase and mobilize AP-1 transcription factors in Jurkat T lymphocytes. J. Biol. Chem. 274: 19992-20001.

Henquin, J. C., Jonas, J. C. and Gilon, P. (1998) Functional significance of Ca2+ oscillations in pancreatic beta cells. Diabetes Metab. 24: 30-36.

Hepler, J. R. and Gilman, A. G. (1992) G proteins. TIBS. 17: 383-387.

Hermans, M. P., Schmeer, V. and Henquin, J. C. (1987) The permissive effect of glucose, tolbutamide and high K^+ on arginine stimulation of insulin secretion. Diabetologia 30: 659-665.

Hilgemann, D. W. and Ball, R. (1996) Regulation of cardiac Na+,Ca2+ exchange and K-ATP potassium channels by PIP2. Science 273: 956-959.

Hobart, P., Crawford, R., Shen, L-P., Pictet, R. and Rutter, W. J. (1980) Cloning and sequencing analysis of cDNAs encoding two distinct somatostatin precursors found in endocrine pancreas of anglerfish. Nature 288: 137-141.

Hocart, S. J., Jain, R., Murphy, W. A., Taylor, J. E., Morgan, B. and Coy, D. H. (1999) Highly potent cyclic disulfide antagonists of somatostatin. J. Med. Chem. 42: 1863-1871.

Hokfelt, T., Effendic, S., Hellerstrom, C., Johansson, O., Luft, R. and Arimura, A. (1975) Cellular localization of somatostatin in endocrine-like cells and neurons of the rat with special references to the A1 cells of the pancreatic islets and to the hypothalamus. Acta Endocrinol. Suppl. 200: 5-41.

Holman, G. D., Kozka, I. J., Clark, A. E., Flower, C. J., Saltis, J., Habberfield, A. D., Simpson, I. A. and Cushman, S. W. (1990) Cell surface labeling of glucose transporter isoform GLUT4 by bis-mannose photolabel. Correlation with stimulation of glucose transport in rat adipose cells by insulin and phorbol ester. J. Biol. Chem. 265:18172-18179.

Homma, K., Terui, S., Minemura, M., Qadota, H., Anraku, Y., Kanaho, Y. and Ohya, Y. (1998) Phosphatidylinositol-4-phosphate 5-kinase localized on the plasma membrane is essential for yeast cell morphogenesis. J. Biol. Chem. 273: 15779-15786.

Hou, C., Gilbert, R. L. and Barber, D. L. (1994) Subtype-specific signalling mechanisms of somatostatin receptors SSTR1 and SSTR2. J. Biol. Chem. 269: 10357-10362.

Howell, S. L. (1984) The mechanism of insulin secretion. Diabetologia 26: 319-327.

Hsu, W. H., Rudolph, U., Sanford, J., Bertrand, P., Olate, J., Nelson, C., Moss, L. G., Boyd, A. E., Codina, J. and Bimbaumer, L. (1990) Molecular cloning of a novel splice variant of the alpha subunit of the mammalian Go protein. J. Biol. Chem. 265: 11220-11226.

Hsu, W. H., Xiang, H. D., Rajan, A. S., Kunze, D. L. and Boyd, A. E. (1991) Somatostatin inhibits insulin secretion by a G-protein-mediated decrease in Ca2+ entry through voltage-dependent Ca2+ channels in the beta cell. J. Biol. Chem. 266: 837-843.

Huang, C. L., Feng, S. and Hilgemann, D. W. (1998) Direct activation of inward rectifier potassium channels by PIP_2 and its stabilization by Gbetagamma. Nature 391: 803-806.

Hughes, S. J. and Ashcroft, S. J. (1988) Effect of secretagogues on cytosolic free Ca2+ and insulin release in the hamster clonal beta-cell line HIT-T15. J. Mol. Endocrinol. 1: 13-17.

Hughes, S. J., Carpinelli, A., Niki, I., Nicks, J. L. and Ashcroft, S. J. (1992) Stimulation of insulin release by vasopressin in the clonal beta-cell line, HIT-T15: the role of protein kinase C. J. Mol. Endocrinol. 8: 145-153.

Hutton, J. C. (1994) Insulin secretory granule biogenesis and the proinsulin-processing endopeptidases. Diabetologia 37: S48-56.

Innamorati, G., Sadeghi, H. and Birnbaumer, M. (1998) Transient phosphorylation of the V1a vasopressin receptor. J. Biol. Chem. 273: 7155-7161.

Ishihara, H., Shibasaki, Y., Kizuki, N., Katagiri, H., Yazaki, Y., Asano, T. and Oka, Y. (1996) Cloning of cDNAs encoding two isoforms of 68-kDa type I phosphatidylinositol-4-phosphate 5-kinase. J. Biol. Chem. 271: 23611-23614.

Itoh, T., Ijuin, T. and Takenawa, T. (1998) A novel phosphatidylinositol-5-phosphate 4-kinase (phosphatidylinositol-phosphate kinase II gamma) is phosphorylated in the endoplasmic reticulum in response to mitogenic signals. J. Biol. Chem. 273: 20292-20299.

Jackson, E. K. (1996) Vasopressin and other agents affecting the renal conservation of water. In Goodman & Gilman The pharmacological basis of therapeutics. 9th ed. McGraw-Hill, New York. pp. 715-731.

Janmey, P. A. and Stossel, T. P. (1987) Modulation of gelsolin function by phosphatidylinositol 4,5-bisphosphate. Nature 325: 362-364.

Jans, D. A., Peters, R. and Fahrenholz F. (1990) Lateral mobility of the phospholipase C-activating vasopressin V1-type receptor in A7r5 smooth muscle cells: a comparison with the adenylate cyclase-coupled V2-receptor. EMBO J. 9: 2693-2699.

Jenkins, G. H., Fisette, P. L. and Anderson, R. A. (1994) Type I phosphatidylinositol 4-phosphate 5-kinase isoforms are specifically stimulated by phosphatidic acid. J. Biol. Chem. 269: 11547-11554.

Jockers, R., Angers, S., Da Silva, A., Benaroch, P., Strosberg, A. D., Bouvier, M. and Marullo, S. (1999) Beta(2)-adrenergic receptor down-regulation. Evidence for a pathway that does not require endocytosis. J. Biol. Chem. 274: 28900-28908.

Jost, M., Simpson, F., Kavran, J. M., Lemmon, M. A. and Schmid, S. L. (1998) Phosphatidylinositol-4,5-bisphosphate is required for endocytic coated vesicle formation. Curr. Biol. 8: 1399-1402.

Karalis, K., Mastrorakos, G., Chrousos, G. P. and Tolis, G. (1994) Somatostatin analogues suppress the inflammatory reaction in vivo. J. Clin. Invest. 93: 2000-2006.

Kawakubo, K., Coy, D. H., Walsh, J. H. and Tache, Y. (1999) Urethane-induced somatostatin mediated inhibition of gastric acid: reversal by the somatostatin 2 receptor antagonist, PRL-2903. Life Sci. 65: 115-120.

Kaziro, Y., Itoh, H., Kozasa, T., Nakafuku, M. and Satoh, T. (1991) Structure and function of signal-transducing GTP-binding proteins. Annu. Rev. Biochem. 60: 349-400.

Kemmler, W., Peterson, J. D., Rubenstein, A. H. and Steiner, D. F. (1972) On the biosynthesis, intracellular transport and mechanism of conversion of proinsulin to insulin and C-peptide. Diabetes 21: 572-81.

Kim, D., Lewis, D. L., Graziadei, L., Neer, E. J., Bar-Sagi, D. and Clapham, D. E. (1989) G-protein beta gamma-subunits activate the cardiac muscarinic K+-channel via phospholipase A2. Nature 337: 557-560.

Kim, Y. H., Park, T. J., Lee, Y. H., Baek, K. J., Suh, P. G., Ryu, S. H. and Kim, K. T. (1999) Phospholipase C-delta1 is activated by capacitative calcium entry that follows phospholipase C-beta activation upon bradykinin stimulation. J. Biol. Chem. 274: 26127-26134.

Kirk, C. J., Rodrigues, L. M. and Hems, D. A. (1979) The influence of vasopressin and related peptides on glycogen phosphorylase activity and phosphatidylinositol metabolism in hepatocytes. Biochem. J. 178: 493-496.

Klein, D. E., Lee, A., Frank, D. W., Marks, M. S. and Lemmon, M. A. (1998) The pleckstrin homology domains of dynamin isoforms require oligomerization for high affinity phosphoinositide binding. J. Biol. Chem. 273: 27725-27733.

Koch, W. J., Hawes, B. E., Allen, L. F. and Lefkowitz, R. J. (1994) Direct evidence that Gi-coupled receptor stimulation of mitogen-activated protein kinase is mediated by G beta gamma activation of p21ras. Proc. Natl. Acad. Sci. U SA 91: 12706-12710.

Komatsuzaki, K., Murayama, Y., Giambarella, U., Ogata, E., Seino, S. and Nishimoto, I. (1997) A novel system that reports the G-proteins linked to a given receptor: A study of type 3 somatostatin receptor. FEBS Lett. 406: 165-170.

Korn, L. J., Siebel, C. W., McCormick, F. and Roth, R. A. (1987) Ras p21 as a potential mediator of insulin action in Xenopus oocytes. Science 236: 840-843.

Kozasa, T. and Gilman, A. G. (1996) Protein kinase C phosphorylates G12 alpha and inhibits its interaction with G beta gamma. J. Biol. Chem. 271: 12562-12567.

Kreienkamp, H. J., Honck, H. H. and Richter, D. (1997) Coupling of rat somatostatin receptor subtypes to a G-protein gated inwardly rectifying potassium channel (GIRK1). FEBS Lett. 419: 92-94.

Kubota, A., Yamada, Y., Kagimoto, S., Yasuda, K., Someya, Y., Ihara, Y., Okamoto, Y., Kozasa, T., Seino, S. and Seino, Y. (1994) Multiple effector coupling of somatostatin receptor subtype SSTR1. Biochem. Biophys. Res. Commun. 204: 176-186.

Kumar, U., Sasi, R., Suresh, S., Patel, A., Thangaraju, M., Metrakos, P., Patel, S. C. and Patel, Y. C. (1999) Subtype-selective expression of the five somatostatin receptors (hSSTR1-5) in human pancreatic islet cells: a quantitative double-label immunohistochemical analysis. Diabetes 48: 77-85.

Lacy, P. E. (1970) Beta cell secretion from the standpoint of a pathobiologist. Diabetes 19: 895-905.

Lamberts, S. W. J., Krenning, E. P. and Reubi, J-C. (1991) The role of somatostatin and its analogs in the diagnosis and treatment of tumors. Endocr. Rev. 12: 450-482.

Lambright, D. G., Noel, J. P., Hamm, H. E. and Sigler, P. B. (1994) Structural determinants for activation of the alpha-subunit of a heterotrimeric G protein. Nature 369: 621-628.

Land, H., Grez, M., Ruppert, S., Schmale, H., Rehbein, M., Richter, D. and Schütz, G. (1983) Deduced amino acid sequence from the bovine oxytocin-neurophysin I precursor cDNA. Nature 302: 342-344.

Lanneau, C., Viollet, C., Faivre-Bauman, A., Loudes, C., Kordon, C., Epelbaum, J., and Gardette, R. (1998) Somatostatin receptor subtypes sst1 and sst2 elicit opposite effects on the response to glutamate of mouse hypothalamic neurones: An electrophysiological and single cell RT-PCR study. Eur. J. Neurosci. 10: 204-212.

Lassing, I. and Lindberg, U. (1988) Specificity of the interaction between phosphatidylinositol 4,5-bisphosphate and the profilin:actin complex. J. Cell Biochem. 37: 255-267.

Lee, B., Yang, C., Chen, T. H., Al-Azawi, N. and Hsu, W. H. (1995) Effect of AVP and oxytocin on insulin release: Involvement of V_{1b} receptors. Am. J. Physiol. 269: E1095-1100.

Li, D., Burch, P., Gonzalez, O., Kashork, C. D., Shaffer, L. G., Bachinski, L. L. and Roberts, R. (2000) Molecular cloning, expression analysis, and chromosome mapping of WDR6, a novel human WD-repeat gene. Biochem. Biophys. Res. Commun. 274: 117-123.

Li, G., Pralong, W. F., Pittet, D., Mayr, G. W., Schlegel, W. and Wollheim, C. B. (1992) Inositol tetrakisphosphate isomers and elevation of cytosolic Ca^{2+} in vasopressin-stimulated insulin-secreting RINm5F cells. J. Biol. Chem. 267: 4349-4356.

Liapakis, G., Haeger, C., Rivier, J. and Reisine, T. (1996) Development of a selective agonist at the somatostatin receptor subtype SSTR1. JPET 276: 1089-1094.

Lifson, N., Lassa, C. V. and Dixit, P. K. (1985) Relation between blood flow and morphology in islet organ of rat pancreas. Am. J. Physiol. 248: E43-E48.

Lin, H. C. and Gilman, A. G. (1996) Regulation of dynamin I GTPase activity by G protein betagamma subunits and phosphatidylinositol 4,5-bisphosphate. J. Biol. Chem. 271: 27979-27982.

Liscovitch, M., Chalifa, V., Pertile, P., Chen, C. S. and Cantley, L. C. (1994) Novel function of phosphatidylinositol 4,5-bisphosphate as a cofactor for brain membrane phospholipase D. J. Biol. Chem. 269: 21403-21406.

Logothetis, D. E., Kurachi, Y., Galper, J., Neer, E. J. and Clapham, D. E. (1987) The beta gamma subunits of GTP-binding proteins activate the muscarinic K+ channel in heart. Nature 325: 321-326.

Lohse, M. J., Benovic, J. L., Caron, M. G. and Lefkowitz, R. J. (1990) Multiple pathways of rapid beta 2-adrenergic receptor desensitization. Delineation with specific inhibitors. J. Biol. Chem. 265: 3202-3211.

Loijens, J. C. and Anderson, R. A. (1996) Type I phosphatidylinositol-4-phosphate 5-kinases are distinct members of this novel lipid kinase family. J. Biol. Chem. 271: 32937-32943.

Loijens, J. C., Boronenkov, I. V., Parker, G. J. and Anderson, R. A. (1996) The phosphatidylinositol 4-phosphate 5-kinase family. Adv. Enzyme Regul. 36: 115-140.

Lolait, S., Carroll, A., Mahan, L., Felder, C., Button, D., Young III, W., Mezey, E. and Brownstein, M. (1995) Extrapituitary expression of the rat V_{1b} vasopressin receptor gene. Proc. Nat. Acad. Sci. USA 92: 6783-6787.

Lomasney, J. W., Cheng, H. F., Wang, L. P., Kuan, Y., Liu, S., Fesik, S. W. and King, K. (1996) Phosphatidylinositol 4,5-bisphosphate binding to the pleckstrin homology

domain of phospholipase C-delta1 enhances enzyme activity. J. Biol. Chem. 271: 25316-25326.

Lopez-Ilasaca, M., Gutkind, J. S. and Wetzker, R. (1998) Phosphoinositide 3-kinase gamma is a mediator of Gbetagamma-dependent Jun kinase activation. J. Biol. Chem. 273: 2505-2508.

Luini, A. and de Matteis, M. A. (1990) Evidence that receptor-linked G protein inhibits exocytosis by a post-second messenger mechanism in AtT-20 cells. J. Neurochem. 54: 30-38.

Lumpin, M. D., Samson, W. K. and McCann, S. M. (1987) Arginine vasopressin as a thyrotropin-releasing hormone. Science 235: 1070-1073.

Luttrell, L. M., Hawes, B. E., van Biesen, T., Luttrell, D. K., Lansing, T. J. and Lefkowitz, R. J. (1996) Role of c-Src tyrosine kinase in G protein-coupled receptor- and Gbetagamma subunit-mediated activation of mitogen-activated protein kinases. J. Biol. Chem. 271: 19443-19450.

Ma, H. T., Kato, M. and Tatemoto, K. (1996) Effects of pancreastatin and somatostatin on secretagogues-induced rise in intracellular free calcium in single rat pancreatic islet cells. Regul. Pept. 61: 143-148.

Maeda, T., Wurgler-Murphy, S. M. and Saito, H. (1994) A two-component system that regulates an osmosensing MAP kinase cascade in yeast. Nature 369: 242-245.

Maratos-Flier, E., Goldstein, B. J. and Kahn, C. R. (1997) The insulin receptor and post receptor mechanisms. In Textbook of diabetes, 2nd ed. Blackwell Science Ltd. 10.1-10.22.

Marinissen, M. J. and Gutkind, J. S. (2001) G-protein-coupled receptors and signaling networks: emerging paradigms. Trends Pharmacol. Sci. 22: 368-376.

McClenaghan, N. H. and Flatt, P. R. (1999) Physiological and pharmacological regulation of insulin release: insights offered through exploitation of insulin-secreting cell lines. Diabetes Obes. Metab. 1: 137-150.

McClenaghan, N. H. and Flatt, P. R. (2000) Metabolic and K(ATP) channel-independent actions of keto acid initiators of insulin secretion. Pancreas 20: 38-46.

McNichol, A. M., Murry, J. E. and McMeekin, W. (1990) Vasopressin stimulation of cell proliferation in the rat pituitary gland in vitro. J. Endocrinol. 126: 255-259.

Meda, P., Perrelet, A. and Orci, L. (1984) Gap junctions and cell to cell coupling in endocrine glands. Mod. Cell Biol. 3: 131-196.

Menard, L., Ferguson, S. S., Zhang, J., Lin, F. T., Lefkowitz, R. J., Caron, M. G. and Barak, L. S. (1997) Synergistic regulation of beta2-adrenergic receptor sequestration: intracellular complement of beta-adrenergic receptor kinase and beta-arrestin determine kinetics of internalization. Mol. Pharmacol. 51: 800-808.

Mignery, G. A. and Sudhof, T. C. (1990) The ligand binding site and transduction mechanism in the inositol-1,4,5-triphosphate receptor. EMBO J. 9: 3893-3898.

Mirmira, R. G. and Tager, H. S. (1991) Disposition of the phenylalanine B25 side chain during insulin-receptor and insulin-insulin interactions. Biochemistry 30: 8222-8229.

Mirotznik, R. R., Zheng, X. and Stanley, E. F. (2000) G-Protein types involved in calcium channel inhibition at a presynaptic nerve terminal. J. Neurosci. 20: 7614-7621.

Mitra, S. W., Mezey, E., Hunyady, B., Chamberlain, L., Hayes, E., Foor, F., Wang, Y., Schonbrunn, A. and Schaeffer, J. M. (1999) Colocalization of somatostatin receptor sst5 and insulin in rat pancreatic β cells. Endocrinology 140: 3790-3796.

Montminy, M. R., Goodman, R. H., Horovitch, S. J. A. and Habener, J. F. (1984) Primary structure of the gene encoding rat preprosomatostatin. Proc. Natl. Acad. Sci. USA 81: 3337-3340.

Muller, S. and Lohse, M. J. (1995) The role of G-protein βγ subunits in signal transduction. Biochem. Soc. Trans. 23: 141-148.

Muller, S., Straub, A., Schroder, S., Bauer, P. H. and Lohse, M. J. (1996) Interactions of phosducin with defined G protein βγ subunits. J. Biol. Chem. 271: 11781-11786.

Murthy, K. S., Coy, D. H. and Makhlouf, G. (1996) Somatostatin receptor-mediated signalling in smooth muscle. J. Biol. Chem. 271: 23458-23463.

Murthy, K. S. and Makhlouf, G. M. (1998) Coexpression of ligand-gated P2X and G protein-coupled P2Y receptors in smooth muscle. Preferential activation of P2Y receptors coupled to phospholipase C (PLC)-beta1 via Galphaq/11 and to PLC-beta3 via Gbetagammai3. J. Biol. Chem. 273: 4695-4704.

Myung, C. S. and Garrison, J. C. (2000) Role of C-terminal domains of the G protein beta subunit in the activation of effectors. Proc. Natl. Acad. Sci. USA 97: 9311-9316.

Neer, E. J. (1997) Intracellular signaling: turning down G-protein signals. Curr. Biol. 7: R31-33.

Neer, E. J. and Smith, T. F. (1996) G protein heterodimers: new structures propel new questions. Cell 84: 175-178.

Offermanns, S. and Simon, M. I. (1995) $G\alpha_{15}$ and $G\alpha_{16}$ couple a wide variety of receptors to phospholipase C. J. Biol. Chem. 270: 15175-15180.

Olson, L. K., Sharma, A., Peshavaria. M., Wright, C. V., Towle, H. C., Rodertson, R. P. and Stein, R. (1995) Reduction of insulin gene transcription in HIT-T15 beta cells chronically exposed to a supraphysiologic glucose concentration is associated with loss of STF-1 transcription factor expression. Proc. Natl. Acad. Sci. USA 92: 9127-9131.

Olson, T. S., Bamberger, M. J. and Lane, M. D. (1988) Post-translational changes in tertiary and quaternary structure of the insulin proreceptor. Correlation with acquisition of function. J. Biol. Chem. 263: 7342-7351.

O'Rahilly, S., Turner, R. C. and Matthews, D. R. (1988) Impaired pulsatile secretion of insulin in relatives of patients with non-insulin-dependent diabetes. N. Engl. J. Med. 318: 1225-1230.

Orci, L. (1985) The insulin factory: a tour of the plant surroundings and a visit to the assembly line. Diabetologia 28: 528-546.

Orci, L., Ravazzola, M., Storch, M. J., Anderson, R. G., Vassalli, J. D. and Perrelet A. (1987) Proteolytic maturation of insulin is a post-Golgi event which occurs in acidifying clathrin-coated secretory vesicles. Cell 49: 865-868.

Pak, Y., O'Dowd, B. F., Wang, J. B. and George, S. R. (1999) Agonist-induced, G protein-dependent and -independent down-regulation of the mu opioid receptor. The receptor is a direct substrate for protein-tyrosine kinase. J. Biol. Chem. 274: 27610-27616.

Patel, Y. C. (1992) General aspects of the biology and function of somatostatin. In: Weil, C., Muller, E. E. and Thorner, M. O., Eds. Basic and Clinical Aspects of Neuroscience. Berlin: Springer-Verlag, Vol. 4: 1-16.

Patel, Y. C. (1997) Molecular pharmacology of somatostatin receptor subtypes. J. Endocrinol. Invest. 20: 348-367.

Patel, Y. C. (1999) Somatostatin and its receptor family. Front. Neuroendocrinol. 20: 157-198.

Patel, Y. C., Greenwood, M. T., Panetta, R., Demchyshyn, L., Niznik, H., Srikant, C. B. (1995) The somatostatin receptor family: A mini review. Life Sci. 57: 1249-1265.

Patel, Y. C., Greenwood, M. T., Warszynska, A., Panetta, R. and Srikant, C. B. (1994) All five cloned human somatostatin receptors (hSSTR1-5) are functionally coupled to adenylyl cyclase. Biochem. Biophys. Res. Commun. 198: 605-612.

Patel, Y. C. and Reichlin, S. (1978) Somatostatin in hypothalamus, extrahypothalamic brain and peripheral tissues of the rat. Endocrinology 102: 523-530.

Patel, Y. C. and Srikant, C. B. (1994) Subtype selectivity of peptide analogs for all five cloned human somatostatin receptors (hsstr1-5). Endocrinology 135: 2814-2817.

Pike, L. J. (1992) Phosphatidylinositol 4-kinases and the role of polyphosphoinositides in cellular regulation. Endocr. Rev. 13: 692-706.

Pitcher, J. A., Freedman, N. J. and Lefkowitz, R. J. (1998) G protein-coupled receptor kinases. Annu. Rev. Biochem. 67: 653-692.

Popova, J. S., Garrison, J. C., Rhee, S. G. and Rasenick, M. M. (1997) Tubulin, Gq, and phosphatidylinositol 4,5-bisphosphate interact to regulate phospholipase Cbeta1 signaling. J. Biol. Chem. 272: 6760-6765.

Porksen, N., Hollingdal, M., Juhl, C., Butler, P., Veldhuis, J. D. and Schmitz, O. (2002) Pulsatile Insulin Secretion: Detection, Regulation, and Role in Diabetes. Diabetes Suppl 1: S245-S254.

Pumiglia, K. M., LeVine, H., Haske, T., Habib, T., Jove, R. and Decker, S. J. (1995) A direct interaction between G-protein beta gamma subunits and the Raf-1 protein kinase. J. Biol. Chem. 270: 14251-14254.

Putney, J. W. Jr. (1987) Formation and actions of calcium-mobilizing messenger, inositol 1,4,5-trisphosphate. Am. J. Physiol. 252: G149-157.

Qian, W. J. and Kennedy, R. T. (2001) Spatial organization of Ca(2+) entry and exocytosis in mouse pancreatic beta-cells. Biochem. Biophys. Res. Commun. 286: 315-321.

Quitterer, U. and Lohse, M. J. (1999) Crosstalk between $G\alpha_i$- and $G\alpha_q$-coupled receptors is mediated by $G\beta\gamma$ exchange. Proc. Natl. Acad. Sci. USA 96: 10626-10631.

Rahier, J. (1988) The diabetic pancreas: a pathologists view. In: Lefèbvre, P. J., Pipeleers, D. G. eds. The Pathology of the Endocrine Pancreas in Diabetes. Berlin: Springer 17-40.

Rameh, L. E., Tolias, K. F., Duckworth, B. C. and Cantley, L. C. (1997) A new pathway for synthesis of phosphatidylinositol-4,5-bisphosphate. Nature 390: 192-196.

Randazzo, P. A. (1997) Functional interaction of ADP-ribosylation factor 1 with phosphatidylinositol 4,5-bisphosphate. J. Biol. Chem. 272: 7688-7692.

Reed, B. C. and Lane, M. D. (1980) Insulin receptor synthesis and turnover in differentiating 3T3-L1 preadipocytes. Proc. Natl. Acad. Sci. USA 77: 285-289.

Reichlin, S. (1983) Somatostatin. N. Engl. J. Med. 309: 1495-1501.

Reisine, T. and Bell, G. I. (1995) Molecular biology of somatostatin receptors. Endocr. Rev. 16: 427-442.

Renstrom, E., Ding, W. G., Bokvist, K. and Rorsman, P. (1996) Neurotransmitter-induced inhibition of exocytosis in insulin-secreting β cells by activation of calcineurin. Neuron 17: 513-522.

Rhee, S. G. and Choi, K. D. (1992) Regulation of inositol phospholipid-specific phospholipase C isozymes. J. Biol. Chem. 267: 12393-12396.

Ribalet, B. and Eddlestone, G. T. (1995) Characterization of the G protein coupling of a somatostatin receptor to the K+ ATP channel in insulin-secreting mammalian HIT and RIN cell lines. J. Physiol. 485: 73-86.

Richardson, S. B., Eyler, N., Twente, S., Monaco, M., Altszuler, N. and Gibson, M. (1990) Effects of vasopressin on insulin secretion and inositol phosphate production in a hamster β cell line (HIT). Endocrinology 126: 1047-1052.

Richter, D., Mohr, E. and Schmale, H. (1990) Molecular aspects of the vasopressin gene family: Evolution, expression and regulation. In S. Jard and R. Jamison, Vasopressin. John Libbey, Montrouge. pp. 3-10.

Robinson, A. G. (1987) The neurohypophysis: recent developments. J. Lab. Clin. Med. 109: 336-345.

Rohrer, S. P., Birzin, E. T., Mosley, R. T., Berk, S. C., Hutchins, S. M., Shen, D. M., Xiong, Y., Hayes, E. C., Parmar, R. M., Foor, F., Mitra, S. W., Degrado, S. J., Shu, M., Klopp, J. M., Cai, S. J., Blake, A., Chan, W. W., Pasternak, A., Yang, L., Patchett, A. A., Smith, R. G., Chapman, K. T. and Schaeffer, J. M. (1998) Rapid identification of subtype-selective agonists of the somatostatin receptor through combinatorial chemistry. Science 282: 737-740.

Roosterman, D., Glassmeier, G., Baumeister, H., Scherubl, H. and Meyerhof, W. (1998) A somatostatin receptor 1 selective ligand inhibits Ca^{2+} currents in rat insulinoma 1046-38 cells. FEBS Lett. 425: 137-140.

Rothenberg, P. L. and Kahn, C. R. (1988) Insulin inhibits pertussis toxin-catalyzed ADP-ribosylation of G-proteins. Evidence for a novel interaction between insulin receptors and G-proteins. J. Biol. Chem. 263: 15546-15552.

Russell, J. T., Brownstein, M. J., and Gainer, H. R. (1980) Biosynthesis of vasopressin, oxytocin and neurophysin: Isolation and characterization of two common precursors (propressophysin and prooxyphysin). Endocrinology 107: 1880-1891.

Saito, M., Sugimoto, T., Tahara, A. and Kawashima, H. (1995) Molecular cloning and characterization of rat V1b vasopressin receptor: evidence for its expression in extra-pituitary tissues. Biochem. Biophys. Res. Commun. 212: 751-757.

Sakisaka, T., Itoh, T., Miura, K. and Takenawa, T. (1997) Phosphatidylinositol 4,5-bisphosphate phosphatase regulates the rearrangement of actin filaments. Mol. Cell Biol. 17: 3841-3849.

Sakmar, T. P. (1998) Rhodopsin: a prototypical G protein-coupled receptor. Prog. Nucleic Acid Res. Mol. Biol. 59: 1-34.

Sanchez-Franco, F., Cacicedo, L., Vasallo, J. L., Blazquez, J. L. and Munoz Barragan, L. (1986) Arginine-vasopressin immunoreactive material in the gastrointestinal tract. Histochemistry 85: 419-422.

Santerre, R. F., Cook, R. A., Crisel, R. M., Sharp, J. D., Schmidt, R. J., Williams, D. C. and Wilson, C. P. (1981) Insulin synthesis in a clonal cell line of simian virus 40-transformed hamster pancreatic beta cells. Proc. Natl. Acad. Sci. USA 78: 4339-4343.

Schofl, C., Rossig, L., Leitolf, H., Mader, T., von zur Muhlen, A. and Brabant, G. (1996) Generation of repetitive Ca2+ transients by bombesin requires intracellular release and influx of Ca2+ through voltage-dependent and voltage independent channels in single HIT cells. Cell Calcium 19: 485-493.

Schwartz, J., Derdowska, I., Sobocinska, M. and Kupryszewski, G. (1991) A potent new synthetic analog of vasopressin with relative agonist specificity for the pituitary. Endocrinology 129: 1107-1109.

Seino, S., Chen, L., Seino, M., Blondel, O., Takeda, J., Johnson, J. H. and Bell, G. I. (1992) Cloning of the alpha 1 subunit of a voltage-dependent calcium channel expressed in pancreatic beta cells. Proc. Natl. Acad. Sci. USA 89: 584-588.

Selbie, L. A. and Hill, S. J. (1998) G protein-coupled-receptor cross-talk: the fine-tuning of multiple receptor-signalling pathways. Trends Pharmacol. Sci. 19: 87-93.

Selbie, L. A., King, N. V., Dickenson, J. M., and Hill, S. J. (1997) Role of G-protein beta gamma subunits in the augmentation of P2Y2 (P2U) receptor-stimulated responses by neuropeptide Y Y1 Gi/o-coupled receptors. Biochem. J. 328: 153-158.

Serventi, I. M., Moss, J. and Vaughan, M. (1992) Enhancement of cholera toxin-catalyzed ADP-ribosylation by guanine nucleotide-binding proteins. Curr. Top. Microbiol. Immunol. 175: 43-67.

Shepherd, P. R. and Kahn, B. B. (1999) Glucose transporters and insulin action-implications for insulin resistance and diabetes mellitus. N. Engl. J. Med. 341: 248-257.

Shen, L. P. and Rutter, W. J. (1984) Sequence of the human somatostatin I gene. Science 224: 168-171.

Shibasaki, Y., Ishihara, H., Kizuki, N., Asano, T., Oka, Y. and Yazaki, Y. (1997) Massive actin polymerization induced by phosphatidylinositol-4-phosphate 5-kinase in vivo. J. Biol. Chem. 272: 7578-7581.

Shimon, I., Taylor, J. E., Dong, J. Z., Bitonte, R. A., Kim, S., Morgan, B., Coy, D. H., Culler, M. D. and Melmed, S. (1997) Somatostatin receptor subtype specificity in human fetal pituitary culture. J. Clin. Invest. 99: 789-798.

Shisheva, A., Sbrissa, D. and Ikonomov, O. (1999) Cloning, characterization, and expression of a novel Zn2+-binding FYVE finger-containing phosphoinositide kinase in insulin-sensitive cells. Mol. Cell Biol. 19: 623-634.

Simoes, A. P., Reed, J., Schnabel, P., Camps, M. and Gierschik, P. (1995) Characterization of putative polyphosphoinositide binding motifs from phospholipase C beta 2. Biochemistry 34: 5113-5119.

Sims, C. E. and Allbritton, N. L. (1998) Metabolism of inositol 1,4,5-trisphosphate and inositol 1,3,4,5-tetrakisphosphate by the oocytes of *Xenopus laevis*. J. Biol. Chem. 273: 4052-4058.

Sivitz, W. I., Herlein, J. A., Morgan, D. A., Fink, B. D., Phillips, B. G. and Haynes, W. G. (2001) Effect of acute and antecedent hypoglycemia on sympathetic neural activity and catecholamine responsiveness in normal rats. Diabetes 50:1119-1125.

Skolnik, E. Y., Batzer, A., Li, N., Lee, C. H., Lowenstein, E., Mohammadi, M., Margolis, B. and Schlessinger, J. (1993) The function of GRB2 in linking the insulin receptor to Ras signaling pathways. Science 260:1953-1955.

Smith, A. J., Surviladze, Z., Gaudet, E. A., Backer, J. M., Mitchell, C. A. and Wilson, B. S. (2001) p110beta and p110delta phosphatidylinositol 3-kinases up-regulate Fc(epsilon)RI-activated Ca2+ influx by enhancing inositol 1,4,5-trisphosphate production. J. Biol. Chem. 276: 17213-17220.

Smith, P. A., Ashcroft, F. M. and Fewtrell, C. M. (1993) Permeation and gating properties of the L-type calcium channel in mouse pancreatic beta cells. J. Gen. Physiol. 101: 767-797.

Snow, B. E., Hall, R. A., Krumins, A. M., Brothers, G. M., Bouchard, D., Brothers, C. A., Chung, S., Mangion, J., Gilman, A. G., Lefkowitz, R. J. and Siderovski, D. P. (1998) GTPase activating specificity of RGS12 and binding specificity of an alternatively spliced PDZ (PSD-95/Dlg/ZO-1) domain. J. Biol. Chem. 273: 17749-17755.

Song, S. H., Kjems, L., Ritzel, R., McIntyre, S. M., Johnson, M. L., Veldhuis, J. D., Butler, P. C. (2002) Pulsatile insulin secretion by human pancreatic islets. J. Clin. Endocrinol. Metab. 87: 213-221.

Sorin, A., Rosas, G. and Rao, R. (1997) PMR1, a Ca2+-ATPase in yeast Golgi, has properties distinct from sarco/endoplasmic reticulum and plasma membrane calcium pumps. J. Biol. Chem. 272: 9895-9901.

Spatz, M., Stanimirovic, D., Bacic, F., Uematsu, S. and McCarron, R.M. (1994) Vasoconstrictive peptides induce endothelin-1 and prostanoids in human cerebromicrovascular endothelium. Am. J. Physiol. 266: C654-660.

Sprang, S. R. (1997) G protein mechanisms: insights from structural analysis. Annu. Rev. Biochem. 66: 639-678.

Stephens, L. R., Hughes, K. T. and Irvine, R. F. (1991) Pathway of phosphatidylinositol (3,4,5)-trisphosphate synthesis in activated neutrophils. Nature 351: 33-39.

Strathmann, M. and Simon, M. I. (1990) G protein diversity: a distinct class of alpha subunits is present in vertebrates and invertebrates. Proc. Natl. Acad. Sci. USA 87: 9113-9117.

Strowski, M. Z., Parmar, R. M., Blake, A. D. and Schaeffer, J. M. (2000) Somatostatin inhibits insulin and glucagon secretion via two receptors subtypes: an in vitro study of pancreatic islets from somatostatin receptor 2 knockout mice. Endocrinology 141: 111-117.

Sturgess, N. C., Kozlowski, R. Z., Carrington, C. A., Hales, C. N. and Ashford, M. L. (1988) Effects of sulphonylureas and diazoxide on insulin secretion and nucleotide-sensitive channels in an insulin-secreting cell line. Br. J. Pharmacol. 95: 83-94.

Takemura, H., Hughes, A. R., Thastrup, O. and Putney, J. W. Jr. (1989) Activation of calcium entry by the tumor promoter thapsigargin in parotid acinar cells. Evidence

that an intracellular calcium pool and not an inositol phosphate regulates calcium fluxes at the plasma membrane. J. Biol. Chem. 264: 12266-12271.

Takenawa, T. and Miki, H. (2001) WASP and WAVE family proteins: key molecules for rapid rearrangement of cortical actin filaments and cell movement. J. Cell Sci. 114: 1801-1809.

Tamaoki, J., Kondo, M., Takeuchi, S., Takemura, H. and Nagai, A. (1998) Vasopressin stimulates ciliary motility of rabbit tracheal epithelium: role of V_{1b} receptor-mediated Ca^{2+} mobilization. Am. J. Respir. Cell. Mol. Biol. 19: 293-299.

Taylor, S. J., Chae, H. Z., Rhee, S. G. and Exton, J. H. (1991) Activation of the beta 1 isozyme of phospholipase C by alpha subunits of the Gq class of G proteins. Nature 350: 516-518.

Thastrup, O. (1990) Role of Ca2(+)-ATPases in regulation of cellular Ca2+ signalling, as studied with the selective microsomal Ca2(+)-ATPase inhibitor, thapsigargin. Agents Actions 29: 8-15.

Thibonnier, M. (1992) Signal transduction of V_1-vascular vasopressin receptors. Regul. Peptides 38: 1-11.

Thibonnier, M., Bayer, A. L. and Leng, Z. (1993) Cytoplasmic and nuclear signaling pathways of V_1-vascular vasopressin receptors. Regul. Peptides 45: 79-84.

Thomas, T. C., Schmidt, C. J. and Neer, E. J. (1993) G-protein alpha o subunit: mutation of conserved cysteines identifies a subunit contact surface and alters GDP affinity. Proc. Natl. Acad. Sci. USA 90: 10295-10298.

Thomas, T. C., Sladek, T., Yi, F., Smith, T. and Neer, E. J. (1993) G protein beta gamma subunit: physical and chemical characterization. Biochemistry 32: 8628-8635.

Thorn, P. and Petersen, O. H. (1991) Activation of voltage-sensitive Ca^{2+} currents by vasopressin in an insulin-secreting cell line. J. Membr. Biol. 124: 63-71.

Tolias, K. F. and Carpenter, C. L. (2000) Enzymes involved in the synthesis of PtdIns(4,5)P_2 and their regulation: PtdIns kinases and PtdInsP kinases. In Biology of Phosphoinositides, Oxford University Press, 109-130.

Tolias, K. F., Rameh, L. E., Ishihara, H., Shibasaki, Y., Chen, J., Prestwich, G. D., Cantley, L. C. and Carpenter, C. L. (1998) Type I phosphatidylinositol-4-phosphate 5-kinases synthesize the novel lipids phosphatidylinositol 3,5-bisphosphate and phosphatidylinositol 5-phosphate. J. Biol. Chem. 273: 18040-18046.

Tsuruzoe, K., Emkey, R., Kriauciunas, K. M., Ueki, K. and Kahn, C. R. (2001) Insulin receptor substrate 3 (IRS-3) and IRS-4 impair IRS-1- and IRS-2-mediated signaling. Mol. Cell Biol. 21: 26-38.

Ueda, N., Iniguez-Lluhi, J. A., Lee, E., Smrcka, A. V., Robishaw, J. D. and Gilman, A. G. (1994) G protein βγ subunits. Simplified purification and properties of novel isoforms. J. Biol. Chem. 269: 4388-4395.

Ullrich, A. and Schlessinger, J. (1990) Signal transduction by receptors with tyrosine kinase activity. Cell 61: 203-212.

Umemori, H., Inoue, T., Kume, S., Sekiyama, N., Nagao, M., Itoh, H., Nakanishi, S., Mikoshiba, K. and Yamamoto, T. (1997) Activation of the G protein Gq/11 through tyrosine phosphorylation of the alpha subunit. Science 276: 1878-1881.

Van Schaftingen, E. (1994) Short-term regulation of glucokinase. Diabetologia 37: S43-47.

Villa-Komaroff, L., Efstratiadis, A., Broome, S., Lomedico, P., Tizard, R., Naber, S. P., Chick, W. L. and Gilbert, W. (1978) A bacterial clone synthesizing proinsulin. Proc. Natl. Acad. Sci. USA 75: 3727-3731.

Voets, T., Prenen, J., Fleig, A., Vennekens, R., Watanabe, H., Hoenderop, J. G., Bindels, R. J., Droogmans, G., Penner, R. and Nilius, B. (2001) CaT1 and the calcium release-activated calcium channel manifest distinct pore properties. J. Biol. Chem. 276: 47767-47770.

Watson, R. T. and Pessin, J. E. (2001) Intracellular organization of insulin signaling and GLUT4 translocation. Recent Prog. Horm. Res. 56: 175-193.

Weckbecker, G., Raulf, F., Stolz, B. and Bruns, C. (1993) Somatostatin analogs for diagnosis and treatment of cancer. Pharmacol. Ther . 60: 245-264.

Weiss, R. E., Reddi, A. H. and Nimni, M. E. (1981) Somatostatin can locally inhibit proliferation and differentiation of cartilage and bone precursor cells. Calcif. Tissue Int. 33: 425-430.

Whitman, M., Downes, C. P., Keeler, M., Keller, T. and Cantley, L. (1988) Type I phosphatidylinositol kinase makes a novel inositol phospholipid, phosphatidylinositol-3-phosphate. Nature 332: 644-646.

Whitman, M., Kaplan, D., Roberts, T. and Cantley, L. (1987) Evidence for two distinct phosphatidylinositol kinases in fibroblasts. Implications for cellular regulation. Biochem. J. 247: 165-174.

Wieland, T., Nurnberg, B., Ulibarri, I., Kaldenberg-Stasch, S., Schultz, G. and Jakobs, K. H. (1993) Guanine nucleotide-specific phosphate transfer by guanine nucleotide-binding regulatory protein beta-subunits. Characterization of the phosphorylated amino acid. J. Biol. Chem. 268: 18111-18118.

Wieland, T., Ronzani, M. and Jakobs, K. H. (1992) Stimulation and inhibition of human platelet adenylylcyclase by thiophosphorylated transducin beta gamma-subunits. J. Biol. Chem. 267: 20791-20797.

Wilkinson, G. F., Feniuk, W. and Humphrey, P. P. A. (1997) Characterization of human recombinant somatostatin sst5 receptors mediating activation of phosphoionositide metabolism. Br. J. Pharmacol. 121: 91-96.

Wollheim, C. B. and Pozzan, T. (1984) Correlation between cytosolic free Ca2+ and insulin release in an insulin-secreting cell line. J. Biol. Chem. 259: 2262-2267.

Wong, S. K. and Ross, E. M. (1994) Chimeric muscarinic cholinergic:beta-adrenergic receptors that are functionally promiscuous among G proteins. J. Biol. Chem. 269: 18968-18976.

Wood, S. P. and Gill, R. (1997) The structure and phylogeny of insulin. In Textbook of diabetes, 2nd ed. Blackwell Science Ltd. 7.2-7.9.

Yawo, H. and Chuhma, N. (1993) Preferential inhibition of omega-conotoxin-sensitive presynaptic Ca2+ channels by adenosine autoreceptors. Nature 365: 256-258.

Yeo, A., Samways, D. S., Fowler, C. E., Gunn-Moore, F. and Henderson, G. (2001) Coincident signalling between the Gi/Go-coupled delta-opioid receptor and the Gq-coupled m3 muscarinic receptor at the level of intracellular free calcium in SH-SY5Y cells.J. Neurochem. 76: 1688-1700.

Yibchok-anun, S., Cheng, H., Chen, T. H. and Hsu, W. H. (2000) Mechanisms of AVP-induced glucagon release in clonal α-cells In-R1-G9: involvement of Ca^{2+}-dependent and -independent pathways. Br. J. Pharmacol. 129: 257-264.

Yibchok-anun, S., Cheng, H., Heine, P. A. and Hsu, W. H. (1999) Characterization of receptors mediating AVP- and OT-induced glucagon release from the rat pancreas. Am. J. Physiol. 277: E56-62.

Yoshitomi, H., Fujii, Y., Miyazaki, M., Nakajima, M., Inagaki, N. and Seino, S. (1997) Involvement of MAP kinase and cfos signalling in the inhibition of cell growth by somatostatin. Am. J. Physiol. 35: E769-E774.

Zhang, J., Barak, L. S., Winkler, K. E., Caron, M. G. and Ferguson, S. S. (1997) A central role for beta-arrestins and clathrin-coated vesicle-mediated endocytosis in beta2-adrenergic receptor resensitization. Differential regulation of receptor resensitization in two distinct cell types. J. Biol. Chem. 272: 27005-27014.

Zhao, A. Z., Zhao, H., Teague, J., Fujimoto, W. and Beavo, J. A. (1997) Attenuation of insulin secretion by insulin-like growth factor 1 is mediated through activation of phosphodiesterase 3B. Proc. Natl. Acad. Sci. USA 94: 3223-3228.

Zhao, K., Wang, W., Rando, O. J., Xue, Y., Swiderek, K., Kuo, A. and Crabtree, G. R. (1998) Rapid and phosphoinositol-dependent binding of the SWI/SNF-like BAF complex to chromatin after T lymphocyte receptor signaling. Cell 95: 625-636.

Zheng, Y., Glaven, J. A., Wu, W. J. and Cerione, R. A. (1996) Phosphatidylinositol 4,5-bisphosphate provides an alternative to guanine nucleotide exchange factors by stimulating the dissociation of GDP from Cdc42Hs. J. Biol. Chem. 271: 23815-23819.

Zunkler, B. J., Lenzen, S., Manner, K., Paten, U. and Trube, G. (1988) Concentration-dependent effects of tolbutamide, meglitinide, glipizide, glibenclamide and diazoxide on ATP-regulated K^+ currents in pancreatic β-cells. Naunyn Schmiedebergs Arch. Pharmacol. 337: 225-230.

ACKNOWLEDGMENTS

I would like to extend my sincere appreciation to my mentor and friend, Dr. Walter Hsu for giving me the opportunity to achieve another goal in my professional career. I will always be thankful for his advice and the research environment based on curiosity, self-motivation, and independent thinking offered by him. Overcoming the many challenges during these years through problem solving approaches and critical thinking has helped me become a better scientist and is something I will always benefit from. I must also thank the members of my POS committee: Drs. Franklin A. Ahrens, Lloyd L. Anderson, Janice E. Buss, Donald C. Dyer, Srdija Jeftinija and Etsuro Uemura for their valuable comments, support, and friendship.

I would like to acknowledge Drs Frank Norris, Seung-Chun Park, Arthi Kanthasamy, and Vellareddy Anantharam for their contribution to my work, and my fellow graduate students Drs. Sirintorn Yibchok-anun, Ehab Abu-Basha, Nipattra Debavalya, Ming-Xu Zhang, Marina Ioudina and Mr. Jing Ding for their friendship and support. Thanks to Mr. Laverne Escher and Mrs. Catherine Martens for their technical assistance and friendship.

Special thanks to Dr. Nani Ghoshal for his guidance and friendship during the time I spent with the anatomy teaching team and Mr. Wolfgang Weber for his friendship. I would also like to thank the BMS Staff for their friendship and for taking care of my paper work during my graduate study.

Finally, and most importantly, I dedicate this dissertation to my lovely wife Helia for her support, understanding, and countless hours alone taking care of our two boys Henrique Jr. and Aaron. You made everything worthwhile.

the MP data to estimate the MVR that was then compared with the literature (MWPS, 1990) recommendation. They found that the literature MVR was 165 to 557% and 20 to 49% higher than their study during the first week and the rest of the brooding period, respectively. Such comparisons have not been made for pullets and layers.

The objectives of this paper were to demonstrate the use of the newly collected HP and MP data by Chepete and Xin (2002a) in designing the ventilation rate for 37-week-old W-36 layers under selected environmental and housing conditions representative of those in Iowa; to compare the results with those derived from literature values; and finally to delineate the effects of reduced stocking density on the ventilation graphs, particularly balance temperature (i.e., outside temperature at or below which supplemental heat would be required to maintain the desired indoor conditions) or supplemental heat need.

MATERIALS AND METHODS

Ventilation for Moisture Control

The selected environmental conditions consisted of outside temperature (t_o) ranging from -25 to 10°C, at 5°C increments. The inside temperature (t_i) was 15, 20 or 25°C. The outside relative humidity (RH_o) ranged from 20 to 70%, at 10% increments. The inside relative humidity (RH_i) was 50, 60, or 70%.

The MVR was calculated as:

$$MVR = \frac{MP}{\rho \cdot (W_i - W_o) \cdot 1000} \quad [1]$$

The new MP data was obtained from Chepete and Xin (2002a) (for W-36 hens) while the 'old' data was obtained from Albright (1990) (for White leghorn hens) and Riskowski et al. (1978) (for W-36 hens). Specific sensible heat (SH) and MP data from the bird only (*bird*

MP) was obtained from Chepete and Xin (2002a) and Riskowski et al. (1978) while that from the birds and surroundings (*room* MP) was obtained from Chepete and Xin (2002a) and Albright (1990). The *room* data from Albright (1990) represent data that are currently used in the ASAE standards and can be compared with the new data by Chepete and Xin (2002a). The *bird* data from Chepete and Xin (2002a) and Riskowski et al. (1978) would demonstrate how the use of *bird* values would impact the ventilation rate as compared to the use of *room* values.

The air density, ρ, based on T_o, was calculated as the inverse of specific volume (v) of moist air, calculated as:

$$v_{moist\ air} = \frac{(1/P_a)R_aT(1+1.6078W)}{1+W} \qquad \text{(Albright, 1990)} \qquad [2]$$

The humidity ratio (W) for the inside or outside air was calculated as:

$$W = 0.62198\left[\frac{Pw}{P_a - Pw}\right] \qquad \text{(Weiss, 1977)} \qquad [3]$$

The partial vapor pressure (P_w) of the inside or outside air was calculated as:

$$P_w = RH \times P_{ws} \qquad [4]$$

The saturation vapor pressure of the inlet or outlet air (P_{ws}), a function of dry bulb temperature, (T_{db}) was calculated as such:

$$P_{ws}(T) = e^{\left[C_1/T + C_2 + C_3\cdot T + C_4\cdot T^2 + C_5\cdot T^3 + C_6\cdot T^4 + C_7\cdot \ln(T)\right]} \qquad \text{(ASHRAE, 2001)} \qquad [5]$$

For $-100 \le T_{db} \le 0$ °C, the constants are:

C_1 = -5.6745359 E+03, C_2 = 6.3925247 E+00, C_3 = -9.677843 E-03,

C_4 = 0.622157 E-06, C_5 = 2.0747825 E-09, C_6 = -0.9484024 E-12

C_7 = 4.1635019 E+00.

For $0 \leq T_{db} \leq 200$ °C, the constants are:

C_1 = -5.8002206 E+03, C_2 = 1.3914993 E+00, C_3 = -4.8640239 E-02,

C_4 = 4.1764768 E-05, C_5 = -1.4452093 E-08, C_6 = 0.0,

C_7 = 6.5459673 E+00.

A convenient look-up table of ventilation rates under the different conditions was prepared based on the new MP obtained from Chepete and Xin (2002a).

Ventilation for Temperature Control

In calculating the ventilation rates for temperature control, contributions of solar heat and heat from lights were ignored and the design was for the typical condition where only animal heat is available to warm the air. The energy balance is:

$$\dot{V}_{temp} = \frac{SH - (\sum UA + FP)(t_i - t_o)}{1006 \cdot \rho \cdot (t_i - t_o)} \qquad [6]$$

A typical commercial high-rise layer house (fig. 1) located in Iowa, having dimensions 131.1m L × 14.6m W × 2.3m H (430' L× 48' W× 7.5' H) with a flat ceiling, was considered. The house has a nominal holding

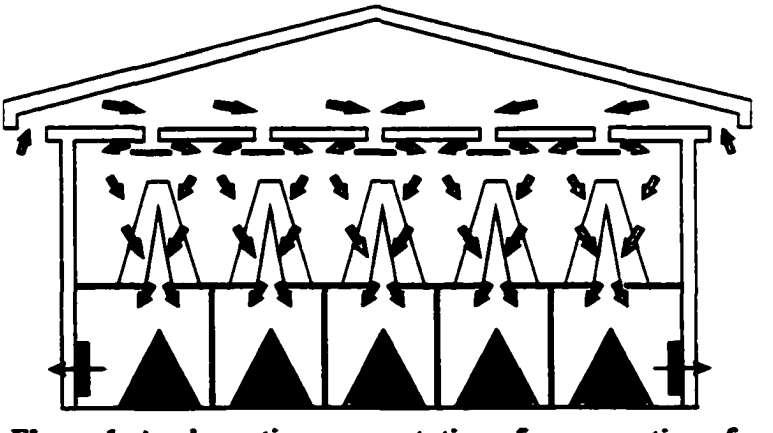

Figure 1. A schematic representation of cross-section of a high-rise layer house with negative pressure ventilation and continuous slot ceiling inlets.

capacity of 84, 000 birds. The new SH data was obtained from Chepete and Xin (2002a) (W-36) while the 'old' data was obtained from Albright (1990) (White leghorn) and Riskowski et al. (1978) (W-36). The inside and outside of the walls and ceiling were covered with 20 gauge tin. The walls were insulated with 0.152 m (6") of fiberglass batt while the ceiling was insulated with 0.303 m (12") of blown-in cellulose. The six walkways were made of 0.019 m (0.75") plywood. The five cage rows had 0.203 m (8") wide opening underneath to allow manure to fall into the storage below. The ΣUA term consisted of contributions from the walls, ceiling and the floor. The perimeter factor (FP) was zero because of the high-rise nature of the house. The t_i and t_o were as previously mentioned. A temperature differential of 5°C between the inside of the house and manure storage space was used as field measurement (Xin, 2002). The air density, ρ, was based on the outside air conditions and was derived from equation [2].

Ventilation curves relating ventilation rate and outside temperature were then generated for both temperature and moisture control under environmental conditions earlier mentioned. Currently, most birds are housed at 0.0355 m^2/bird (55 in^2/bird). Due to animal welfare concerns, a 31% increase in floor space (0.04645 m^2/bird or 72 in^2/bird), has been recommended. This implies a 31% reduction in the total number of birds per house and its effect on ventilation and heating requirement is investigated in this paper.

RESULTS AND DISCUSSIONS

Ventilation Rate Look-up Table

Table 1 shows the ventilation rate or MVR for the 37-week old W-36 birds under different environmental conditions. Higher ventilation rates are associated with lower t_i and RH_i and the opposite is true.

From table 1, it is evident that changes in RH_i directly affect the MVR. For example, an increase in RH_i from 50 to 60% reduced the MVR by 17 to 61% across the different environmental conditions examined. Similarly, when RH was increased from 60 to 70%, the MVR was reduced by 15 to 38%. When RH_i was increased from 50 to 60%, Xin et al. (1998) reported a MVR reduction of 50 to 60% across t_i of 21 to 29 °C, t_o of -23 to 10°C, and RH_o of 20 to 90% on tom turkeys during brooding-growing period. As such, a temporary increase in RH_i would reduce heating and electricity costs on fan operation. However, Xin et al. (1998) cautioned that such practice should be done very carefully as it may result in ammonia build-up, excessive litter moisture and disease problems.

At cold t_o, RH_o had little effect on MVR. For example, at t_o of -5 to -25°C, the MVR values for RH_o of 20 to 70% are within 5% of each other. Xin et al. (1998) reported a 10% variation in MVR for t_o of -15 to -23°C and RH_o of 20 to 90% and they attributed this finding to compliance with thermodynamic properties of air, where, as the air becomes colder its moisture content approaches similarity regardless of RH level.

The MWPS (1990) recommends a value of 0.1 cfm/lb or 0.375 $m^3/(h \cdot kg)$ being the cold weather ventilation rate for layers. Based on this recommended MVR, the MVR based on the new MP data would be 0.56 $m^3/(h \cdot bird)$ (0.33 cfm/bird). On the other hand, the

ventilation rate would be 0.68 m^3/(h·bird) (0.40 cfm/bird). This suggests a 22% over ventilation for modern birds when the MWPS (1990) data are used. The MP data in the MWPS (1990) were based on the 'old' data, as reported in a literature review by Chepete and Xin (2002b), where a significant quantity of the moisture came from wasted drinking water. The MWPS did not define the environmental conditions that constitute a 'cold weather' condition and this may leave room for a wide range of assumptions when designing the MVR. A very convenient look-up table (table 1) provides more information and offers a solution to this discrepancy.

Similar calculations to generate MVR for other birds of different ages can be made by using the relevant MP data.

Ventilation Graphs

The ventilation graphs for temperature and moisture control under different environmental conditions are shown in figures 2 through 13. Figures 2 through 7 are based on a total of 84,000 birds per house while figures 8 through 13 are based on a total of 57, 960 birds per house, a 31% reduction. In order to make comparisons between the graphs, specific SH and MP data from different literature sources, namely, Chepete and Xin (2002a), Albright (1990), and Riskowski et al. (1978), were used. The ventilation rate calculations for both temperature and moisture control were based on bird mass of 1.5 kg.

In all figures, ventilation rate for temperature control derived from *room* SH data by Albright (1990) was 10% higher than that derived from *room* SH data by Chepete and Xin (2002a). This may be due to the higher *room* SH reported by Albright (1990) as compared to that reported by Chepete and Xin (2002a). Specifically, specific *room* SH was 4.02 W/kg for Albright (1990) and 3.70 W/kg for Chepete and Xin (2002a). The ventilation rate derived

from *bird* SH data by Riskowski et al. (1978) was 5% higher than that derived from *bird* SH data by Chepete and Xin (2002a). The *bird* SH used in the case of Riskowski et al. (1978) was 4.40 W/kg while that from Chepete and Xin (2002a) was 4.20 W/kg. The use of *bird* SH in ventilation rate design resulted in higher ventilation rate than when *room* values were used.

The ventilation rate for moisture control based on *room* MP data by Chepete and Xin (2002a) was 22% higher than that based on *room* MP data by Albright (1990). The MP of the *room* was 4.85 g/(h·kg) or 7.28 g/(h·bird) and 3.7 g/(h·kg) or 5.55 g/(h·bird) for Chepete and Xin (2002a) and for Albright (1990), respectively. The higher *room* MP for Chepete and Xin (2002a) may have caused higher ventilation rate when compared to that for Albright (1990). On the other hand, the moisture control curves based on *bird* MP data by Chepete and Xin (2002a) was 134% higher than that derived from *bird* MP data by Riskowski et al. (1978). The *bird* MP used in the case of Chepete and Xin (2002a) was 4.11 g/(h·kg) or 6.17 g/(h·bird) and was 1.76 g/(h·kg) or 2.64 g/(h·bird) for Riskowski et al. (1978). The lower *bird* MP value for Riskowski et al. (1978) may have caused the associated ventilation rate to remain consistently low.

Typically, for a poultry house, the *room* SH and MP data should be used in ventilation rate design because they take into account the effects of moisture evaporation from feces and surroundings. Lower ventilation rates result when *bird* values are used. For example, based on *room* SH and MP data by Chepete and Xin (2002a), the balance point ventilation rate was 2100 m^3/(h·1000hd) (1236 cfm/1000hd) while that based on the corresponding *bird* values was 1200 m^3/(h·1000hd) (706 cfm/1000hd) (fig. 2). Thus, the use of *bird* values underestimated the balance point ventilation rate by 75%.

Effect of increasing RH_i on ventilation rate while holding t_i constant. The ventilation rate and balance temperature were reduced as RH_i was increased. For example, at 15°C room temperature, the balance point ventilation rate or ideal ventilation rate based on *room* SH and MP for Chepete and Xin (2002a) reduced from 2100 to 800 $m^3/(h \cdot 1000hd)$ (1236 to 471 cfm/1000hd) while that by Albright (1990) reduced from 1200 to 600 $m^3/(h \cdot 1000hd)$ (706 to 353 cfm/1000hd) when RH_i was increased from 50% (fig. 2) to 70% (fig. 3). The balance temperature was correspondingly reduced from 8 to -1.5°C, and from 3.5 to -10°C. This agrees well with psychrometric principles (ASHRAE, 2001) that to keep the same temperature in the room while increasing the room RH, colder air should be brought in so as to avoid high room temperature buildup. Air with higher moisture content holds more heat energy than drier one. The MWPS (1990) specifies a minimum t_i of 12.8°C (55F) and RH_i of 50 to 70%.

Similar observations and arguments can be made for other pairs of graphs, namely figures 4 vs. 5; 6 vs 7; 8 vs. 9; 10 vs. 11; and 12 vs. 13. The relative magnitudes of the values would be different between the pairs as different environmental conditions are considered.

Effect of increasing t_i on ventilation rate while holding RH_i constant. In order to illustrate the effect of increasing t_i on ventilation rate while holding RH_i constant, comparisons may be made between figures 2, 4, and 6 at RH_i of 50% and 100% stocking capacity, figures 3, 5, and 7 at RH_i of 70% and 100% stocking capacity; figures 8, 10, and 12 at RH_i of 50% and 69% stocking capacity, and figures 9, 11, and 13 at RH_i of 70% and 69% stocking capacity.

At RH_i of 50% (figures 2, 4, 6, 8, 10, and 12), increasing the room temperature from 15 to 25°C resulted in reduction in the ventilation rate. This is logical because in order to

maintain higher room temperature, the ventilation rate should be reduced in order to minimize sensible heat loss via exhaust air. The greater reduction in moisture control-MVR as a result of maintaining the constant RH_i at a higher t_i led to a lower balance temperature.

Different data used gave different ventilation rates. For example, considering the ventilation curves for moisture and temperature control derived from *room* SH and MP data by Chepete and Xin (2002a) and Albright (1990), the ventilation rates at the balance point were 2100 vs. 1200 $m^3/(h \cdot 1000hd)$ (1236 vs. 706 cfm/1000hd), respectively (fig. 2). This may be a result of modern birds producing lesser SH and more moisture than birds reared several years ago as indicated by comparison of *room* SH and MP reported by Chepete and Xin (2002a) and Albright (1990). The corresponding balance point ventilation rate for 20 and 25°C (figures 4 and 6, respectively) were 940 vs. 600 $m^3/(h \cdot 1000hd)$ (553 vs. 353 cfm/1000hd) and 520 vs. 360 $m^3/(h \cdot 1000hd)$ (306 vs. 212 cfm/1000hd), respectively.

The balance point ventilation rate based on *bird* SH and MP data by Chepete and Xin (2002a) was 1200, 630, and 350 $m^3/(h \cdot 1000hd)$ (706, 371, and 206 cfm/1000hd) at corresponding temperatures of 15, 20, and 25°C and 50% RH (fig. 2, 4, and 6, respectively). Ventilation rate for moisture control based on *bird* MP data by Riskowski et al. (1978) did not coincide with the corresponding temperature control curve. This may be caused by the low *bird* MP value that caused the ventilation rate for moisture control to be consistently low.

For a given t_o, ventilation for temperature control using *room* SH and MP data by Albright (1990) resulted in higher ventilation rate than when the new data by Chepete and Xin (2002a) was used. This suggests potential over ventilation for the modern birds when using the 'old' data and this may lower RH_i and cause dusty conditions that may further cause respiratory disorders in the birds (MWPS, 1990).

For 70% RH_i (figures 3, 5, 7, 9, 11, and 13), similar observations and arguments can be made.

Effect of reducing the stocking capacity by 31% on the ventilation rate. Under similar environmental conditions, the only difference observed between figures 2 through 7 (100% stocking capacity) and figures 8 through 13 (69% stocking capacity) would be due to the different bird numbers resulting in lower net sensible heat when the bird capacity was reduced. For example, comparing results of figure 2 (100% stocking capacity, 50% RH and 15°C temperature) vs. figure 8 (69% stocking capacity, 50% RH and 15°C temperature), the balance point ventilation rate was 2100 vs. 2300 $m^3/(h \cdot 1000hd)$ (1236 vs. 1354 cfm/1000hd), respectively, based on data by Chepete and Xin (2002a), and was 1200 vs. 1300 $m^3/(h \cdot 1000hd)$ (706 vs. 765 cfm/1000hd) based on data by Albright (1990). The corresponding balance temperature was 8.0 vs. 9.0°C and 3.2 vs. 4.5°C. Hence, the reduced number of birds would have rather insignificant effect on the building supplemental heat requirement. This is logical as most of the heat loss is through ventilation pathway that is directly related to moisture control MVR. Similar observations and arguments can be made by comparing figures 3 vs. 9, 4 vs. 10, 5 vs. 11, 6 vs. 12, and 7 vs. 13.

CONCLUSIONS

The use of the newly collected heat and moisture production (HP and MP) data by Chepete and Xin (2002a) in designing the ventilation rate (VR) for 37-week-old W-36 layers under selected environmental and housing conditions representative of those in Iowa has been demonstrated and the results were compared with those derived from the literature. The effects of reduced stocking density on the ventilation graphs, particularly balance

temperature or supplemental heat need have been investigated. The following conclusions have been drawn:

- VR derived from the 'old' literature *room* sensible heat (SH) and MP data was 10% higher or 18% lower for temperature or moisture control, respectively, when compared to that derived from the new data.
- Correspondingly, the VR derived from the 'old' literature *bird* SH and MP data was 5% higher or 57% lower.
- Reducing the bird stocking density by 31% would slightly raise the balance temperature (1.0 to 1.3°C), thereby having little influence on supplemental heat requirement.
- Increasing the inside relative humidity (RH) from 50 to 60% or from 60 to 70% reduced the ventilation rate by 17 to 61% or by 15 to 38%, respectively.
- Under cold outside temperatures of -5 to -25°C, outside RH had little effect on the ventilation rate.

REFERENCES

Albright, L. D. 1990. Environment control for animals and plants. ASAE. St. Joseph, MI.

ASAE Standards, 47th Ed. 2000. EP270.5. Design of ventilation systems for poultry and livestock shelters, 594. St. Joseph, Mich.: ASAE.

ASHRAE Handbook. Fundamentals. 2001. American Society of Heating, Refrigerating and Air Conditioning Engineers, Inc Atlanta, Ga.

Chepete, H. J. and Xin. H. 2002a. Heat and moisture production of poultry and their housing systems: *Pullets and Layers. Transactions of the ASHRAE* (In review).

Chepete, H. J. and Xin. H. 2002b. Heat and moisture production of poultry and their housing systems: *Literature Review. Transactions of the ASHRAE* (In press).

CIGR. 1992. 2nd Ed. *2nd Report of Working Group on Climatization of Animal Houses*, 18-19. Gent, Belgium: Center for Climatization of Animal Houses-Advisory Services, Faculty of Agricultural Sciences, State University of Ghent.

Feddes, J. J. R. and DeShazer J. A. 1988. Feed consumption as a parameter for establishing minimum ventilation rates. *Transactions of the ASAE* 31(2):571-575.

Gates, R. S., Overhults D. G., and Zhang S. H. 1996. Minimum ventilation for modern broiler facilities. *Transactions of the ASAE* 39(3):1135-1144.

MWPS-34. 1990. Heating, Cooling, and Tempering air for Livestock Housing. Ames, Iowa: Iowa State University.

Riskowski, G. L., DeShazer J. A., and Mather F. B. 1978. Heat losses of White Leghorn laying hens as affected by intermittent lighting schedules. *Transactions of the ASAE* 20(4):727-731.

Weiss, A. 1977. Algorithms for the calculation of moist air properties on a hand calculator. *Transactions of the ASAE* 20(4):1133-1136.

Xin, H. 2002. *Personal communication.* Ames, Iowa: Iowa State University.

Xin, H., Chepete H. J., Shao J., and Sell J. L. 1998. Heat and moisture production and minimum ventilation requirements of tom turkeys during brooding-growing period. *Transactions of the ASAE* 41(5):1489-1498.

Xin, H., Berry I. L., and Tabler G. T. 1996. Minimum ventilation requirement and associated energy cost for aerial ammonia control in broiler houses. *Transactions of the ASAE* 39(2):645-648.

NOMENCLATURE

ρ = air density, kg/m^3 (based on outside air temperature)

'$_i$' or '$_o$' = inside or outside

$\dot{V}_{iemp}$ = ventilation rate for temperature control, m^3/s

A = area, m^2

e = base of the natural logarithms, 2.7182818

F = perimeter heat loss factor, $W/(m \cdot °C)$

MP = moisture production rate, g/(kg-h)

MVR = minimum ventilation rate, $m^3/(kg\text{-}h)$

P = perimeter, m

P_a = barometric pressure of ambient air, kPa, assumed to be 101.325 kPa.

P_w = partial vapor pressure of the inside or outside air, kPa

P_{ws} = saturation vapor pressure of the inlet or outlet air, kPa

R_a = dry air gas constant, 287.055 J/(kg·K)

RH = relative humidity, %

SH = specific sensible heat production rate, W/kg

T = absolute dry bulb temperature, K= °C + 273.15

t = dry bulb temperature, °C

U = thermal conductance, $W/(m^2 \cdot °C)$

v = specific volume, m^3/kg

W_i or W_o = humidity ratio for the inside (exhaust) or outside (fresh) air, kg H_2O/kg dry air

Table 1. Minimum ventilation rate (m^3/(h·1000hd) for moisture control for 37-week old W-36 layers with a moisture production rate of 4.85 g/(h·kg) and bird mass of 1.48 kg.

t_o	RH_o	t_i = 15°C			t_i = 20°C			t_i = 25°C		
(°C)	(%)	RH_i (%)			RH_i (%)			RH_i (%)		
		50	60	70	50	60	70	50	60	70
-25	20	837	695	594	578	479	409	403	334	285
-20		861	714	609	593	491	419	413	342	292
-15		890	736	627	610	505	430	424	351	299
-10		925	762	648	630	520	443	436	360	307
-5		972	797	675	656	539	458	451	372	316
0		1038	843	710	689	564	477	469	385	326
5		1125	903	754	731	594	499	491	401	339
10		1255	989	815	789	634	529	520	422	354
-25	30	843	699	596	580	481	410	405	335	286
-20		871	720	614	597	494	421	415	344	293
-15		905	746	635	617	510	434	427	353	301
-10		952	780	661	642	529	449	442	364	310
-5		1017	827	696	676	553	467	460	378	320
0		1117	895	746	723	586	493	485	396	334
5		1260	988	812	786	629	524	516	418	350
10		1504	1137	914	881	692	569	559	447	372
-25	40	848	702	599	583	483	412	406	336	286
-20		880	727	618	601	497	424	417	345	294
-15		922	757	642	624	515	437	431	356	302
-10		980	799	674	655	537	455	448	368	312
-5		1066	859	719	697	567	478	470	385	325
0		1209	953	786	761	611	510	501	407	342
5		1432	1091	881	850	670	552	542	435	363
10		1876	1339	1039	997	761	615	603	475	391
-25	50	854	706	602	585	485	413	407	337	287
-20		890	733	623	606	500	426	419	347	295
-15		938	769	651	632	520	441	435	358	304
-10		1009	819	688	668	546	461	454	372	315
-5		1121	894	743	720	582	488	481	392	330
0		1317	1019	830	802	637	528	519	418	350
5		1659	1218	962	925	716	583	572	454	376
10		2496	1627	1205	1149	847	670	656	507	413

Table 1. (continued)

t_o (°C)	RH_o (%)	t_i = 15°C			t_i = 20°C			t_i = 25°C		
		RH_i (%)			RH_i (%)			RH_i (%)		
		50	60	70	50	60	70	50	60	70
-25	60	860	710	605	588	486	414	408	338	288
-20		900	740	628	611	503	428	422	348	296
-15		956	780	659	640	525	445	438	361	306
-10		1041	839	703	682	555	468	460	377	318
-5		1181	932	769	744	598	499	491	399	335
0		1447	1095	880	849	666	548	538	431	359
5		1972	1379	1059	1015	768	617	605	475	390
10		3729	2074	1435	1356	954	735	718	544	437
-25	70	865	714	608	591	488	416	410	339	288
-20		910	747	633	615	507	430	424	350	297
-15		974	792	667	648	531	449	442	363	308
-10		1074	861	718	696	564	474	467	381	322
-5		1248	973	797	771	615	511	503	406	340
0		1605	1183	936	901	698	569	559	444	368
5		2431	1589	1179	1124	829	656	643	497	405
10		7383	2863	1773	1654	1093	815	795	586	464

t_o = outside temperature; RH_o = outside relative humidity; RH_i = inside relative humidity

t_i = inside temperature; Divide the table values (SI unit) by 1.699 to obtain MVR in cfm (m^3/ft) (IP unit) per 1,000 heads.

The moisture production (MP) used in the calculation of the minimum ventilation rate was calculated from the time-weighted average latent heat production (LHP) rate which included the contribution of moisture evaporation from fecal matter: MP = LHP*3600/2450

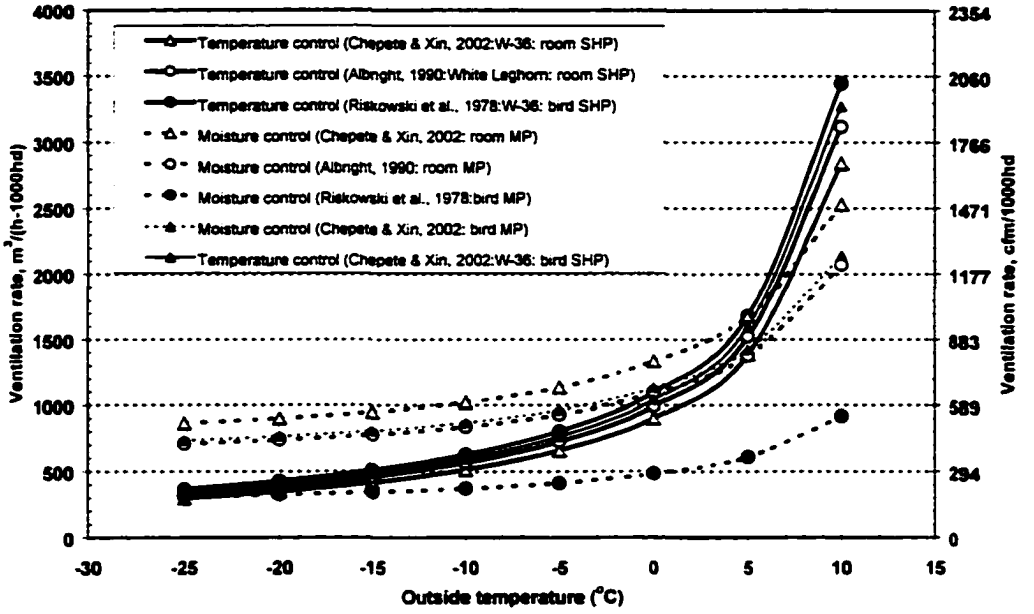

Figure 2. Ventilation graph based on outside air for temperature and moisture control at 100% stocking capacity, inside temperature of 15°C, inside relative humidity (RH) of 50%, and outside RH of 50%. Bird MP or SHP involve moisture effect from birds only; room MP or SHP involve moisture effect from birds and surroundings.

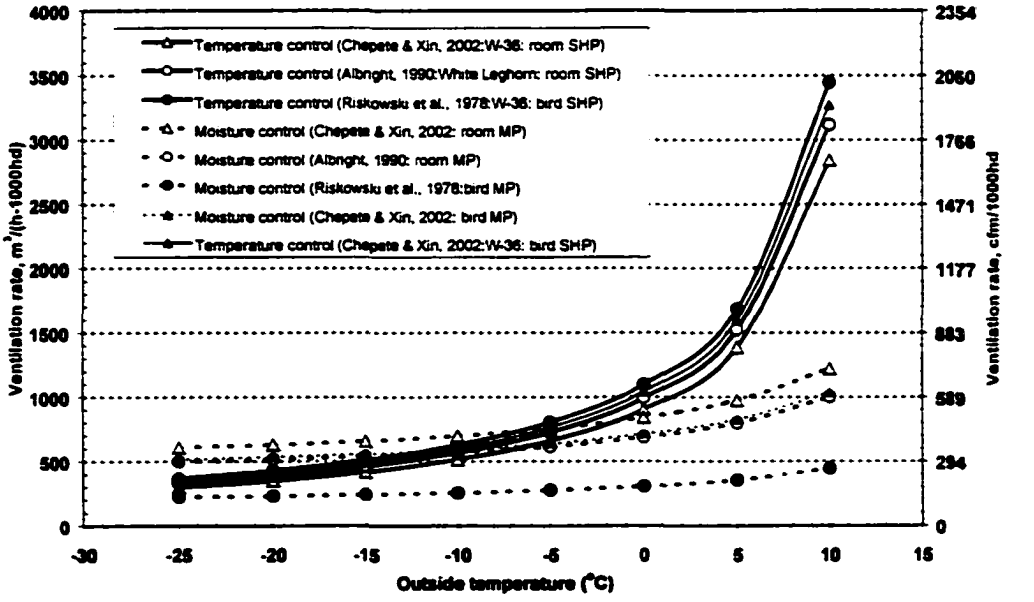

Figure 3. Ventilation graph based on outside air for temperature and moisture control at 100% stocking capacity, inside temperature of 15°C, inside relative humidity (RH) of 70%, and outside RH of 50%. Bird MP or SHP involve moisture effect from birds only; room MP or SHP involve moisture effect from birds and surroundings.

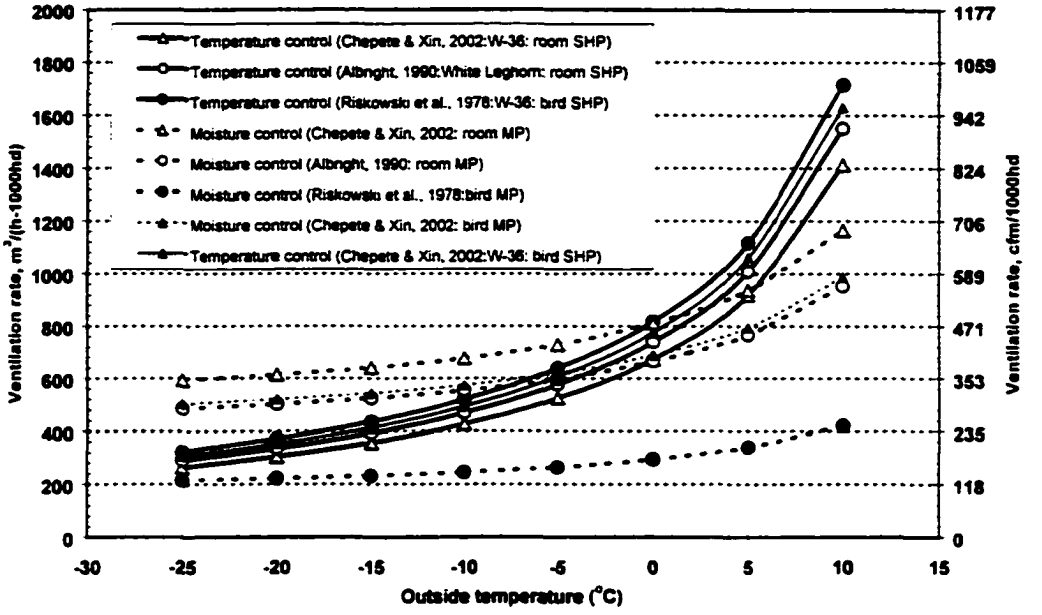

Figure 4. Ventilation graph based on outside air for temperature and moisture control at 100% stocking capacity, inside temperature of 20°C, and inside relative humidity (RH) of 50%, and outside RH of 50%. Bird MP or SHP involve moisture effect from birds only; room MP or SHP involve moisture effect from birds and surroundings.

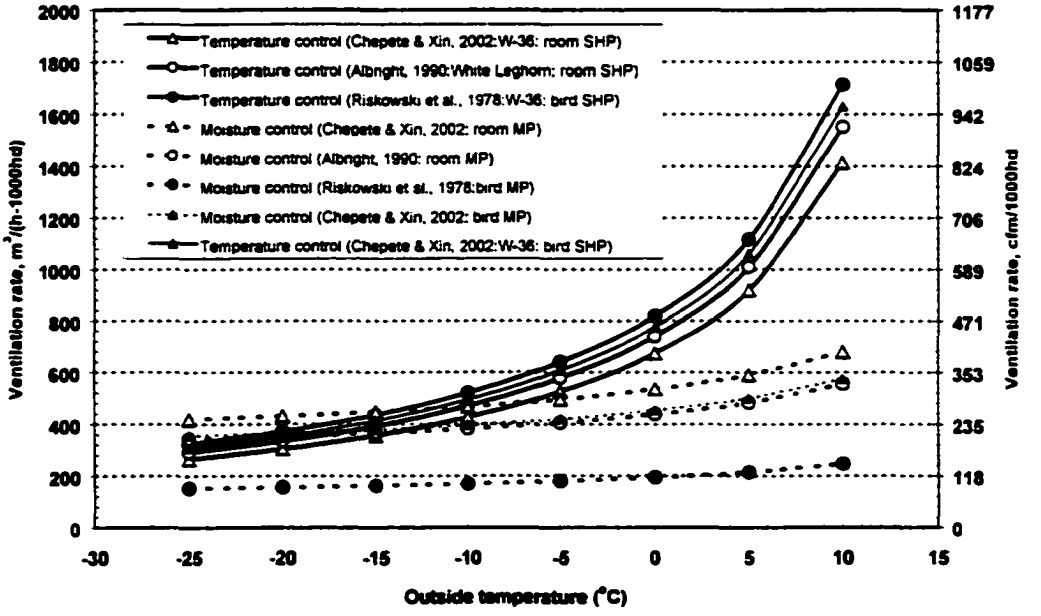

Figure 5. Ventilation graph based on outside air for temperature and moisture control at 100% stocking capacity, inside temperature of 20°C, and inside relative humidity (RH) of 70%, and outside RH of 50%. Bird MP or SHP involve moisture effect from birds only; room MP or SHP involve moisture effect from birds and surroundings.

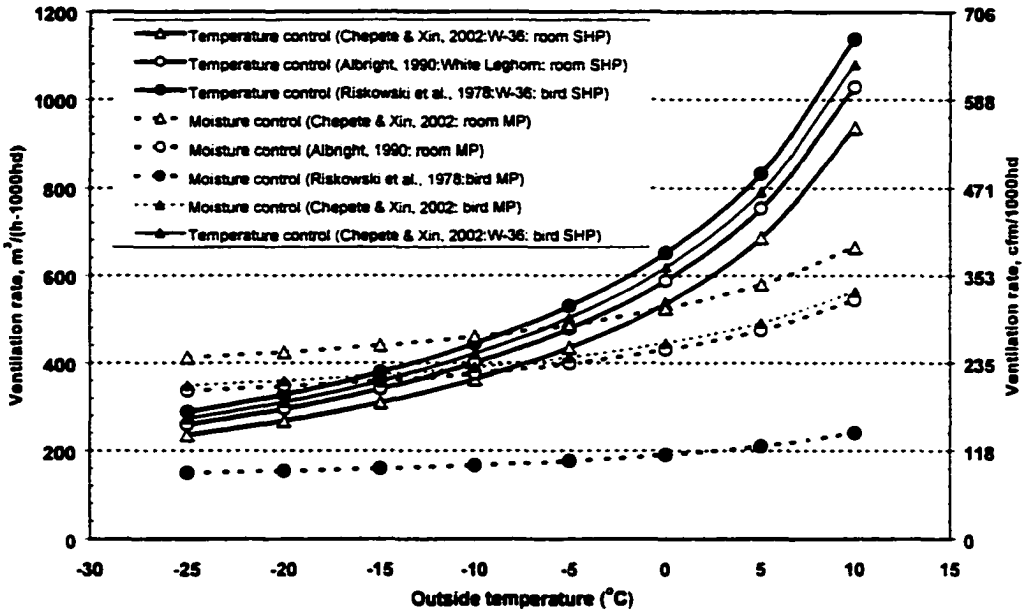

Figure 6. Ventilation graph based on outside air for temperature and moisture control at 100% stocking capacity, inside temperature of 25°C, and inside relative humidity (RH) of 50%, and outside RH of 50%. Bird MP or SHP involve moisture effect from birds only; room MP or SHP involve moisture effect from birds and surroundings.

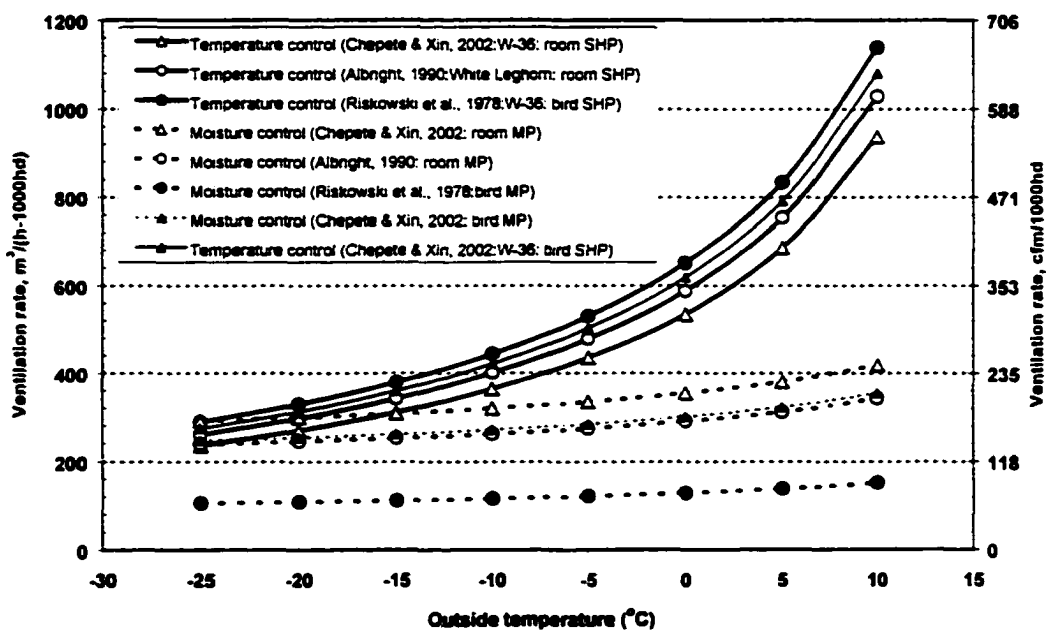

Figure 7. Ventilation graph based on outside air for temperature and moisture control at 100% stocking capacity, inside temperature of 25°C, and inside relative humidity (RH) of 70%, and outside RH of 50%. Bird MP or SHP involve moisture effect from birds only; room MP or SHP involve moisture effect from birds and surroundings.

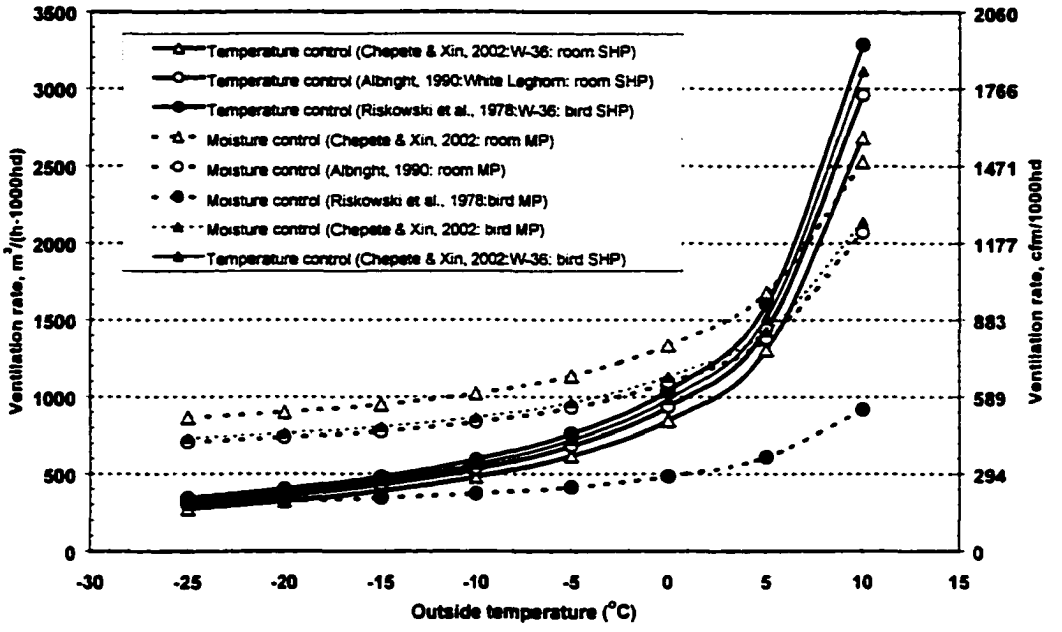

Figure 8. Ventilation graph based on outside air for temperature and moisture control at 69% stocking capacity, inside temperature of 15°C, and inside relative humidity (RH) of 50%, and outside RH of 50%. Bird MP or SHP involve moisture effect from birds only; room MP or SHP involve moisture effect from birds and surroundings.

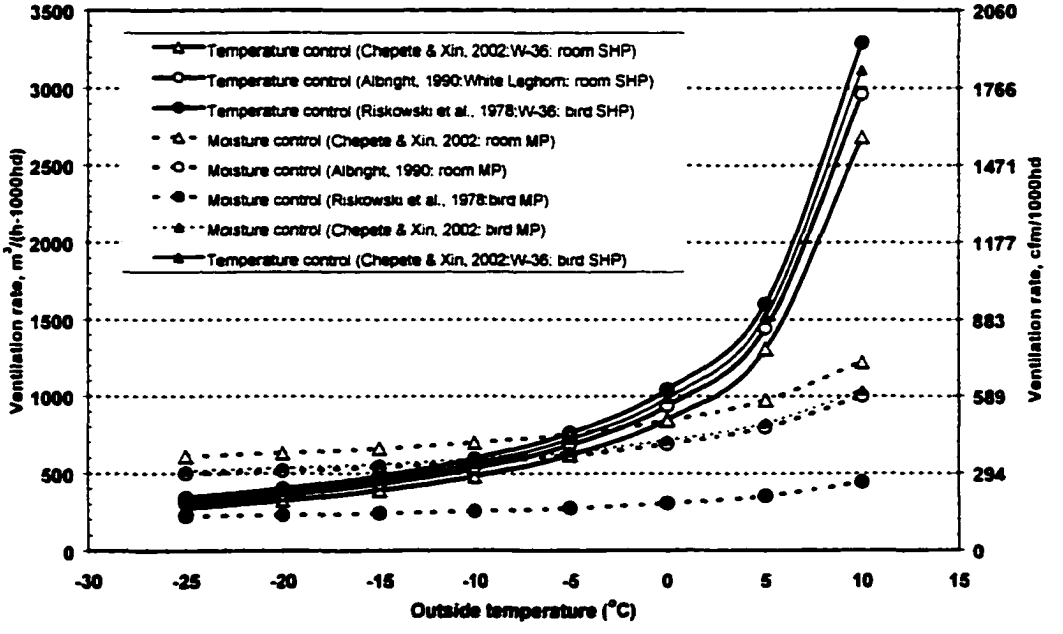

Figure 9. Ventilation graph based on outside air for temperature and moisture control at 69% stocking capacity, inside temperature of 15°C, and inside relative humidity (RH) of 70%, and outside RH of 50%. Bird MP or SHP involve moisture effect from birds only; room MP or SHP involve moisture effect from birds and surroundings.

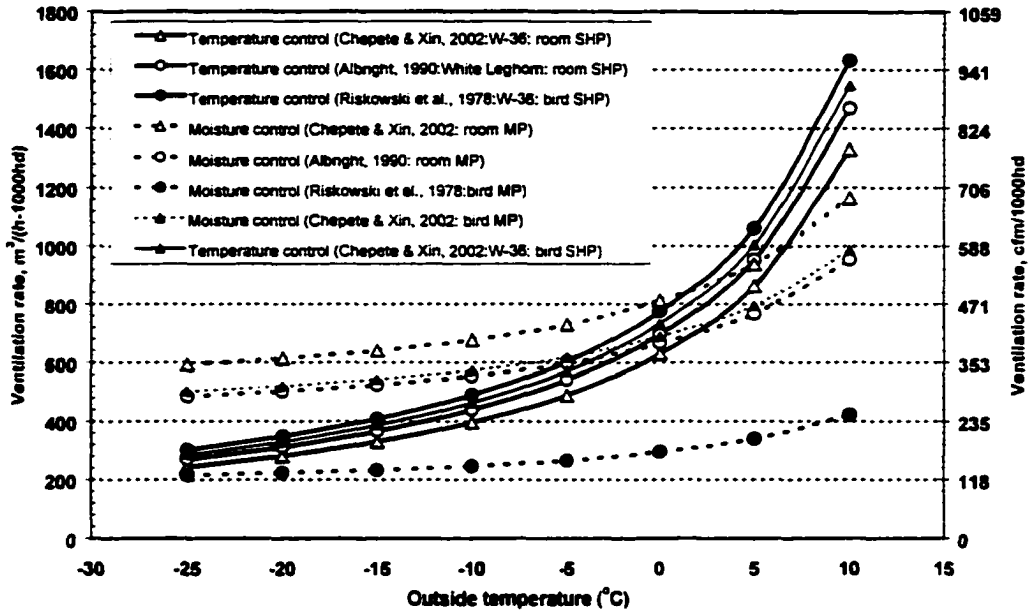

Figure 10. Ventilation graph based on outside air for temperature and moisture control at 69% stocking capacity, inside temperature of 20°C, and inside relative humidity (RH) of 50%, and outside RH of 50%. Bird MP or SHP involve moisture effect from birds only; room MP or SHP involve moisture effect from birds and surroundings.

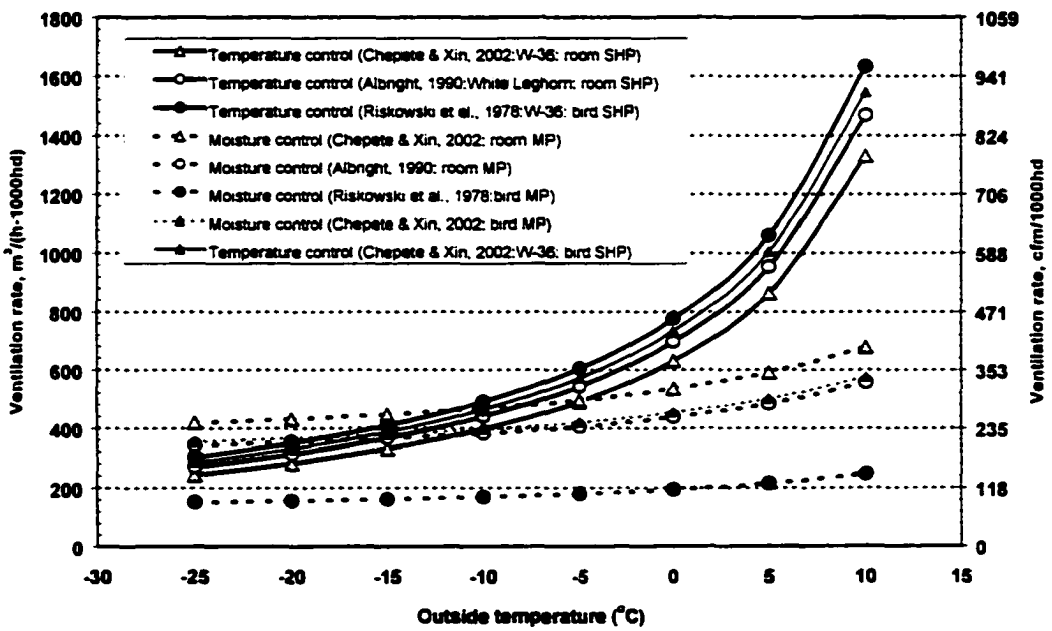

Figure 11. Ventilation graph based on outside air for temperature and moisture control at 69% stocking capacity, inside temperature of 20°C, and inside relative humidity (RH) of 70%, and outside RH of 50%. Bird MP or SHP involve moisture effect from birds only; room MP or SHP involve moisture effect from birds and surroundings.

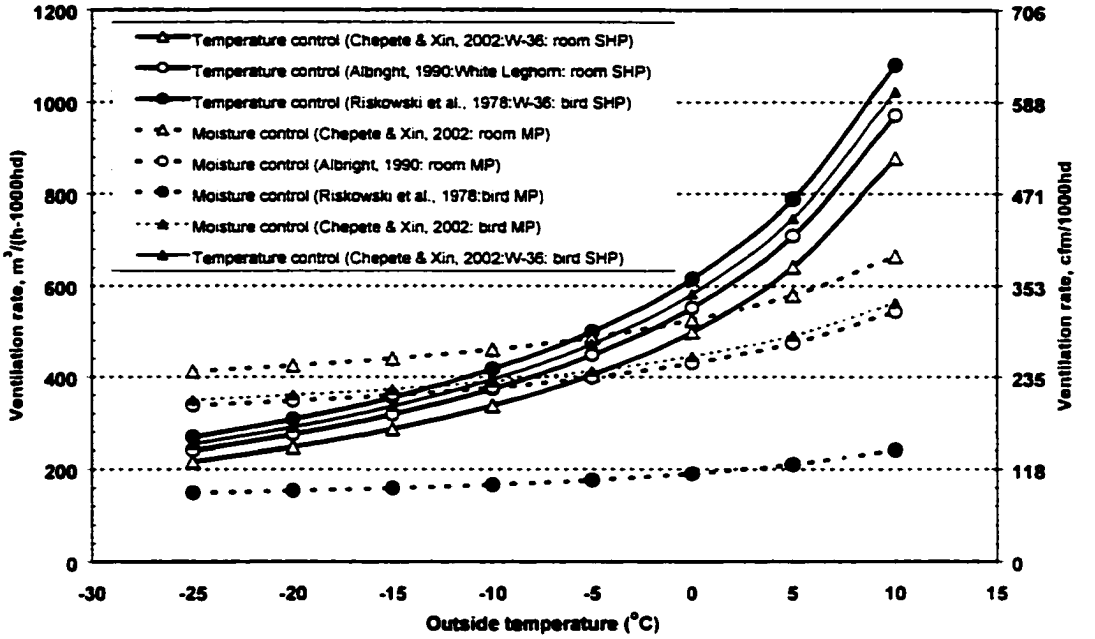

Figure 12. Ventilation graph based on outside air for temperature and moisture control at 69% stocking capacity, inside temperature of 25°C, and inside relative humidity (RH) of 50%, and outside RH of 50%. Bird MP or SHP involve moisture effect from birds only; room MP or SHP involve moisture effect from birds and surroundings.

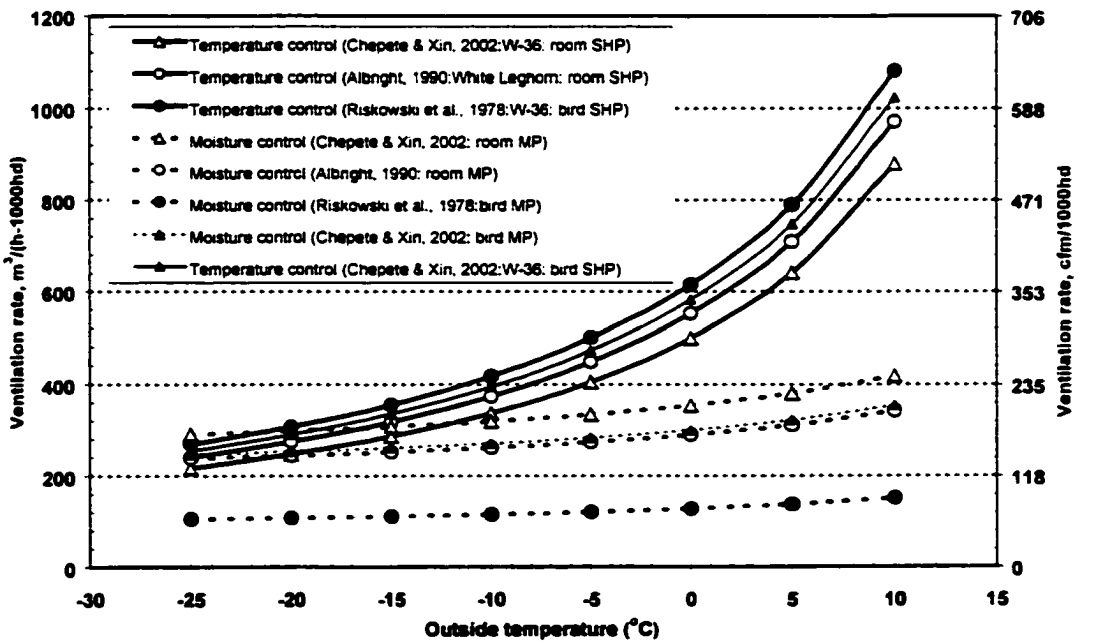

Figure 13. Ventilation graph based on outside air for temperature and moisture control at 69% stocking capacity, inside temperature of 25°C, and inside relative humidity (RH) of 70%, and outside RH of 50%. Bird MP or SHP involve moisture effect from birds only; room MP or SHP involve moisture effect from birds and surroundings.

CHAPTER 6.
GENERAL CONCLUSIONS

1. An extensive literature review and comparative analysis of heat and moisture production (HP, MP) of various poultry types (layers, broilers, and turkeys) and their housing systems indicated that total heat production (THP, W/kg) has increased over the years. Specifically, their increase amounted to about 21 to 44% over a 14-year period (1968 to 1982) for broilers weighing 0.1 to 1.6 kg, 15 to 22% for broilers at 1.4 to 1.6 kg over a 32-year period (1968 to 2000); and 36 to 63% over a 24-year period (1974 to 1998) for tom turkeys weighing 0.4 to 1.0 kg. Data for pullets and layers between 7- and 33- wk old at thermoneutral environment are not available. The metabolic rate equations derived from the literature data were in good agreement with the standard metabolic rate HP (W/bird)= a M^b, where b = 0.66 to 0.75. Specifically, it was 8.55 $M^{0.74}$ (1968) and 10.62 $M^{0.75}$ (1982 to 2000) for broilers; 6.47 $M^{0.77}$ for pullets and layers (1953 to 1990); 7.54 $M^{0.53}$ (1974 to 1977) and 9.86 $M^{0.77}$ (1992 to 1998) for turkeys.

2. HP and MP at *bird* and *room* levels of modern pullets (W-36 at 1-5 and 10 weeks of age and W-98 at 1-5 weeks of age), laying hens (W-36 at 21, 37, and 64 weeks of age), and molting hens (W-36 at 68-75 weeks of age, *room* level only) were measured using large-scale indirect calorimeters that mimic commercial production settings.

Pullets and laying hens. The W-98 and W-36 pullets reached the metabolic peak at 10 and 14 days of age, respectively. The W-98 pullet produced higher THP than the W-36 counterpart. Modern pullets showed higher THP (12-37%) than those 20 to 50 years ago. At the beginning of egg production, THP of the modern layers was 12% higher than that

predicted by the CIGR (1999) model and the difference diminished with time. Evaporation of fecal moisture elevated *room* latent HP (LHP) by 8-38% (light period) or 21-79% (dark period) and reduced the *room* sensible HP (SHP) by 4-17% (light) or 14-33% (dark) with reference to *bird* LHP or SHP. All HP responses were significantly ($P<0.05$) reduced to various degrees (e.g., 23-34% for THP) in the dark as compared to the light period.

Molting hens. LHP and SHP rates measured were for the *room*. THP ranged from 4.4 to 5.6 W/kg, 5.4 to 6.5 W/kg, and 6.7 to 6.9 W/kg during fasting, restricted feeding and post molt periods, respectively. LHP ranged from 1.7 to 2.1 W/kg, 1.5 to 2.0 W/kg, and 2.4 to 2.9 W/kg during the respective periods. The corresponding SHP ranged from 2.6 to 3.5 W/kg, 3.9 to 4.6 W/kg, and 3.9 to 4.4 W/kg, respectively. The corresponding respiratory quotient (RQ) averaged 0.71, 0.76, and 0.92, respectively. HP values during the light period were significantly higher ($P<0.05$) than that during the dark period. LHP as a percentage of THP ranged from 24 to 43% with no significant differences between the light and dark periods.

3. The new data for W-36 layers were used in an example of designing the building ventilation rates for a modern laying hen house in Iowa. Ventilation graphs were developed for a range of outside temperature (t_o) of -25 to 10°C, at 5°C increments, outside relative humidity (RH) of 20 to 70%, and inside RH of 50, 60 and 70%. Comparative ventilation curves based on literature HP and MP data were also presented. The ventilation rate (VR) derived from the 'old' literature *room* sensible heat (SH) and MP data was 10% higher or 18% lower for temperature or moisture control, respectively, than that derived from the new data. Correspondingly, based on *bird* SH and MP data, VR derived from the 'old' literature data was 5% higher or 57% lower. Reducing the number of birds or stocking density by 31% to reflect the new animal welfare guidelines would slightly raise the balance temperature (t_{bal},

1.0 to 1.3°C), thereby having rather negligible influence on the supplemental heat requirement of the house. Increasing the room RH from 50 to 60% or from 60 to 70% reduced the ventilation rate by 17 to 61% or by 15 to 38%, respectively.

4. Results of this study provide an updated thermal load database for design and operation of poultry housing ventilation systems, as well as bioenergetics information for the scientific literature.

APPENDIX 1.

CR10 PROGRAM USED IN THE STUDY

```
Program:
Flag Usage:
Input Channel Usage:
Excitation Channel Usage:
Control Port Usage:
Pulse Input Channel Usage:
Output Array Definitions:


*      1        Table 1 Programs
  01: 2        Sec. Execution Interval

01:  P10       Battery Voltage
  01: 29       Loc [:Bat, Volt]

02:  P86       Do
  01: 1        Call Subroutine 1 [Temp/RH readings & Heater control]

03:  P86       Do
  01: 2        Call Subroutine 2 [Air sampling control]

04:  P26       Timer
  01: 30       Loc [:Timer, s ]

05:  P89       If X<=>F
  01: 30       X Loc Timer, s
  02: 4        <
  03: 301      F
  04: 0        Go to end of Program Table

06:  P86       Do
  01: 3        Call Subroutine 3 [Meter outputs after stabilization]

07:  P34       Z=X+F
  01: 30       X Loc Timer, s
  02: -359     F
  03: 31       Z Loc : Sample if >0

08:  P89       If X<=>F
  01: 31       X Loc
  02: 3        >=
  03: 0        F
  04: 10       Set high Flag 0 (output)

09:  P78       Resolution
  01: 1        High Resolution

10:  P77       Real Time
  01: 110      Day,Hour-Minute

11:  P71       Average
  01: 10       Reps
  02: 1        Loc Temp#0
```

```
Page 2   Table 1

12:  P71        Average
  01: 8         Reps
  02: 20        Loc SLPM#1

13:  P70        Sample
  01: 1         Reps
  02: 28        Loc Sam. Seq.

14:  P89        If X<=>F
  01: 31        X Loc
  02: 3         >=
  03: 0         F
  04: 30        Then Do

15:  P26        Timer
  01: 0         Reset Timer

16:  P32        Z=Z+1
  01: 28        Z Loc [:Sam. Seq.]

17:  P89        If X<=>F
  01: 28        X Loc Sam. Seq.
  02: 3         >=
  03: 5         F
  04: 30        Then Do

18:  P30        Z=F
  01: 0         F
  02: 0         Exponent of 10
  03: 28        Z Loc [:Sam. Seq.]

19:  P95        End

20:  P95        End

21:  P          End Table 1


*     2         Table 2 Programs
  01: 0.0000    Sec. Execution Interval

01:  P          End Table 2


*     3         Table 3 Subroutines
Temp/RH Measurement and Temp Control
Temp and RH Measurement
Heater Control Logic
Air Sampling Control
Analyzer and Flowmeter Output

01:  P85        Beginning of Subroutine
  01: 1         Subroutine Number
```

```
Page 3   Table 3


02:  P11        Temp 107 Probe
  01: 1         Rep
  02: 1         IN Chan
  03: 2         Excite all reps w/EXchan 2
  04: 1         Loc [:Temp#0    ]
  05: 1.8       Mult
  06: 32        Offset

03:  P11        Temp 107 Probe
  01: 4         Reps
  02: 2         IN Chan
  03: 2         Excite all reps w/EXchan 2
  04: 2         Loc [:Temp#1    ]
  05: 1.8       Mult
  06: 32        Offset

04:  P4         Excite,Delay,Volt(SE)
  01: 1         Rep
  02: 25        2500 mV 60 Hz rejection Range
  03: 6         IN Chan
  04: 1         Excite all reps w/EXchan 1
  05: 15        Delay (units .01sec)
  06: 2500      mV Excitation
  07: 6         Loc [:RH#0      ]
  08: 0.1       Mult
  09: 0         Offset

05:  P4         Excite,Delay,Volt(SE)
  01: 4         Reps
  02: 25        2500 mV 60 Hz rejection Range
  03: 7         IN Chan
  04: 1         Excite all reps w/EXchan 1
  05: 15        Delay (units .01sec)
  06: 2500      mV Excitation
  07: 7         Loc [:RH#1      ]
  08: 0.1       Mult
  09: 0         Offset

06:  P87        Beginning of Loop
  01: 0         Delay
  02: 4         Loop Count

07:  P89        If X<=>F
  01: 2--       X Loc Temp#1
  02: 4         <
  03: 69.75     F
  04: 30        Then Do

08:  P30        Z=F
  01: 1         F
  02: 0         Exponent of 10
  03: 11--      Z Loc [:Heater#1 ]

09:  P95        End
```

```
Page 4   Table 3


10:  P89       If X<=>F
  01: 11--     X Loc Heater#1
  02: 2        <>
  03: 0        F
  04: 30       Then Do

11:  P89       If X<=>F
  01: 2--      X Loc Temp#1
  02: 3        >=
  03: 70       F
  04: 30       Then Do

12:  P30       Z=F
  01: 0        F
  02: 0        Exponent of 10
  03: 11--     Z Loc [:Heater#1 ]

13:  P95       End

14:  P94       Else

15:  P30       Z=F
  01: 0        F
  02: 0        Exponent of 10
  03: 11--     Z Loc [:Heater#1 ]

16:  P95       End

17:  P95       End

18:  P104      SDM-CD16
  01: 9        Reps
  02: 0        Address
  03: 11       Loc Heater#1

19:  P95       End

20:  P85       Beginning of Subroutine
  01: 2        Subroutine Number

21:  P89       If X<=>F
  01: 28       X Loc Sam. Seq.
  02: 1        =
  03: 0        F
  04: 30       Then Do

22:  P87       Beginning of Loop
  01: 0        Delay
  02: 5        Loop Count

23:  P30       Z=F
  01: 0        F
  02: 0        Exponent of 10
  03: 15--     Z Loc [:Valve#0  ]
```

```
Page 5   Table 3


24:  P95        End

25:  P30        Z=F
  01: 1         F
  02: 0         Exponent of 10
  03: 15        Z Loc [:Valve#0  ]

26:  P95        End

27:  P89        If X<=>F
  01: 28        X Loc Sam. Seq.
  02: 1         =
  03: 1         F
  04: 30        Then Do

28:  P87        Beginning of Loop
  01: 0         Delay
  02: 5         Loop Count

29:  P30        Z=F
  01: 0         F
  02: 0         Exponent of 10
  03: 15--      Z Loc [:Valve#0  ]

30:  P95        End

31:  P30        Z=F
  01: 1         F
  02: 0         Exponent of 10
  03: 16        Z Loc [:Valve#1  ]

32:  P95        End

33:  P89        If X<=>F
  01: 28        X Loc Sam. Seq.
  02: 1         =
  03: 2         F
  04: 30        Then Do

34:  P87        Beginning of Loop
  01: 0         Delay
  02: 5         Loop Count

35:  P30        Z=F
  01: 0         F
  02: 0         Exponent of 10
  03: 15--      Z Loc [:Valve#0  ]

36:  P95        End

37:  P30        Z=F
  01: 1         F
  02: 0         Exponent of 10
  03: 17        Z Loc [:Valve#2  ]
```

Page 6 Table 3

```
38:  P95        End

39:  P89        If X<=>F
  01: 28        X Loc Sam. Seq.
  02: 1         =
  03: 3         F
  04: 30        Then Do

40:  P87        Beginning of Loop
  01: 0         Delay
  02: 5         Loop Count

41:  P30        Z=F
  01: 0         F
  02: 0         Exponent of 10
  03: 15--      Z Loc [:Valve#0   ]

42:  P95        End

43:  P30        Z=F
  01: 1         F
  02: 0         Exponent of 10
  03: 18        Z Loc [:Valve#3   ]

44:  P95        End

45:  P89        If X<=>F
  01: 28        X Loc Sam. Seq.
  02: 1         =
  03: 4         F
  04: 30        Then Do

46:  P87        Beginning of Loop
  01: 0         Delay
  02: 5         Loop Count

47:  P30        Z=F
  01: 0         F
  02: 0         Exponent of 10
  03: 15--      Z Loc [:Valve#0   ]

48:  P95        End

49:  P30        Z=F
  01: 1         F
  02: 0         Exponent of 10
  03: 19        Z Loc [:Valve#4   ]

50:  P95        End

51:  P104       SDM-CD16
  01: 9         Reps
  02: 0         Address
  03: 11        Loc Heater#1
```

```
Page 7   Table 3

52:  P95        End

53:  P85        Beginning of Subroutine
  01: 3         Subroutine Number

54:  P86        Do
  01: 44        Set high Port 4

55:  P87        Beginning of Loop
  01: 0         Delay
  02: 8         Loop Count

56:  P86        Do
  01: 75        Pulse Port 5

57:  P2         Volt (DIFF)
  01: 1         Rep
  02: 25        2500 mV 60 Hz rejection Range
  03: 6         IN Chan
  04: 40--      Loc [:Flow mV1 ]
  05: 1         Mult
  06: 0         Offset

58:  P95        End

59:  P86        Do
  01: 54        Set low Port 4

60:  P37        Z=X*F
  01: 40        X Loc Flow mV1
  02: 0.6864    F
  03: 32        Z Loc :

61:  P34        Z=X+F
  01: 32        X Loc
  02: -11.537   F
  03: 20        Z Loc [:SLPM#1    ]

62:  P37        Z=X*F
  01: 41        X Loc Flow mV2
  02: 0.6606    F
  03: 33        Z Loc :

63:  P34        Z=X+F
  01: 33        X Loc
  02: 2.3413    F
  03: 21        Z Loc [:SLPM#2    ]

64:  P37        Z=X*F
  01: 42        X Loc Flow mV3
  02: 0.6781    F
  03: 34        Z Loc :
```

```
Page 8   Table 3

65:  P34       Z=X+F
  01: 34       X Loc
  02: 3.1816   F
  03: 22       Z Loc [:SLPM#3    ]

66:  P37       Z=X*F
  01: 43       X Loc Flow mV4
  02: 0.6731   F
  03: 35       Z Loc :

67:  P34       Z=X+F
  01: 35       X Loc
  02: -2.7115  F
  03: 23       Z Loc [:SLPM#4    ]

68:  P37       Z=X*F
  01: 44       X Loc DP mV
  02: 0.0401   F
  03: 36       Z Loc :

69:  P34       Z=X+F
  01: 36       X Loc
  02: -39.635  F
  03: 24       Z Loc [:Dewpt, C ]

70:  P37       Z=X*F
  01: 45       X Loc CO2 mV
  02: 1.2067   F
  03: 48       Z Loc [:CO2, int ]

71:  P34       Z=X+F
  01: 48       X Loc CO2, int
  02: -10.897  F
  03: 25       Z Loc [:CO2, ppm ]

72:  P37       Z=X*F
  01: 46       X Loc O2 mV
  02: 10.104   F
  03: 26       Z Loc [:O2, "ppm"]

73:  P34       Z=X+F
  01: 26       X Loc O2, "ppm"
  02: 832.46   F
  03: 26       Z Loc [:O2, "ppm"]

74:  P37       Z=X*F
  01: 47       X Loc [BP, mV]
  02: 0.184    F
  03: 49       Z Loc [:BP, int   ]

75:  P34       Z=X+F
  01: 49       X Loc BP, int
  02: 600      F
  03: 27       Z Loc [:BP, mbar ]
```

```
Page 9   Table 3

76:  P95        End

77:  P          End Table 3


*      A        Mode 10 Memory Allocation
  01:  50       Input Locations
  02:  64       Intermediate Locations
  03:  0.0000   Final Storage Area 2


*      C        Mode 12 Security
  01:  0        LOCK 1
  02:  0        LOCK 2
  03:  0000     LOCK 3
```

```
Page 10    Input Location Assignments (with comments):

 Key:
 T=Table Number
 E=Entry Number
 L=Location Number

 T:  E:  L:
 3:  2:  1:  Loc [:Temp#0    ]
 3:  3:  2:  Loc [:Temp#1    ]
 3:  4:  6:  Loc [:RH#0      ]
 3:  5:  7:  Loc [:RH#1      ]
 3:  8: 11:  Z Loc [:Heater#1 ]
 3: 12: 11:  Z Loc [:Heater#1 ]
 3: 15: 11:  Z Loc [:Heater#1 ]
 3: 23: 15:  Z Loc [:Valve#0  ]
 3: 25: 15:  Z Loc [:Valve#0  ]
 3: 29: 15:  Z Loc [:Valve#0  ]
 3: 35: 15:  Z Loc [:Valve#0  ]
 3: 41: 15:  Z Loc [:Valve#0  ]
 3: 47: 15:  Z Loc [:Valve#0  ]
 3: 31: 16:  Z Loc [:Valve#1  ]
 3: 37: 17:  Z Loc [:Valve#2  ]
 3: 43: 18:  Z Loc [:Valve#3  ]
 3: 49: 19:  Z Loc [:Valve#4  ]
 3: 61: 20:  Z Loc [:SLPM#1   ]
 3: 63: 21:  Z Loc [:SLPM#2   ]
 3: 65: 22:  Z Loc [:SLPM#3   ]
 3: 67: 23:  Z Loc [:SLPM#4   ]
 3: 69: 24:  Z Loc [:Dewpt, C ]
 3: 71: 25:  Z Loc [:CO2, ppm ]
 3: 72: 26:  Z Loc [:O2, "ppm"]
 3: 73: 26:  Z Loc [:O2, "ppm"]
 3: 75: 27:  Z Loc [:BP, mbar ]
 1: 16: 28:  Z Loc [:Sam. Seq.]
 1: 18: 28:  Z Loc [:Sam. Seq.]
 1:  1: 29:  Loc [:Bat, Volt]
 1:  4: 30:  Loc [:Timer, s ]
 1:  7: 31:  Z Loc : Sample if >0
 3: 60: 32:  Z Loc :
 3: 62: 33:  Z Loc :
 3: 64: 34:  Z Loc :
 3: 66: 35:  Z Loc :
 3: 68: 36:  Z Loc :
 3: 57: 40:  Loc [:Flow mV1 ]
 3: 70: 48:  Z Loc [:CO2, int ]
 3: 74: 49:  Z Loc [:BP, int  ]
```

Page 11 Input Location Labels:

1:Temp#0	14:Heater#4	27:BP, mbar	40:Flow mV1
2:Temp#1	15:Valve#0	28:Sam. Seq.	41:Flow mV2
3:Temp#2	16:Valve#1	29:Bat, Volt	42:Flow mV3
4:Temp#3	17:Valve#2	30:Timer, s	43:Flow mV4
5:Temp#4	18:Valve#3	31:_____	44:DP mV
6:RH#0	19:Valve#4	32:_____	45:CO2 mV
7:RH#1	20:SLPM#1	33:_____	46:O2 mV
8:RH#2	21:SLPM#2	34:_____	47:_____
9:RH#3	22:SLPM#3	35:_____	48:CO2, int
10:RH#4	23:SLPM#4	36:_____	49:BP, int
11:Heater#1	24:Dewpt, C	37:_____	50:
12:Heater#2	25:CO2, ppm	38:_____	51:_____
13:Heater#3	26:O2, "ppm"	39:	52:_____

APPENDIX 2.

LINEAR FUNCTIONS OBTAINED FROM CALIBRATION OF INSTRUMENTS

1. **Mass flow meters (SLPM = standard liter per minute)**

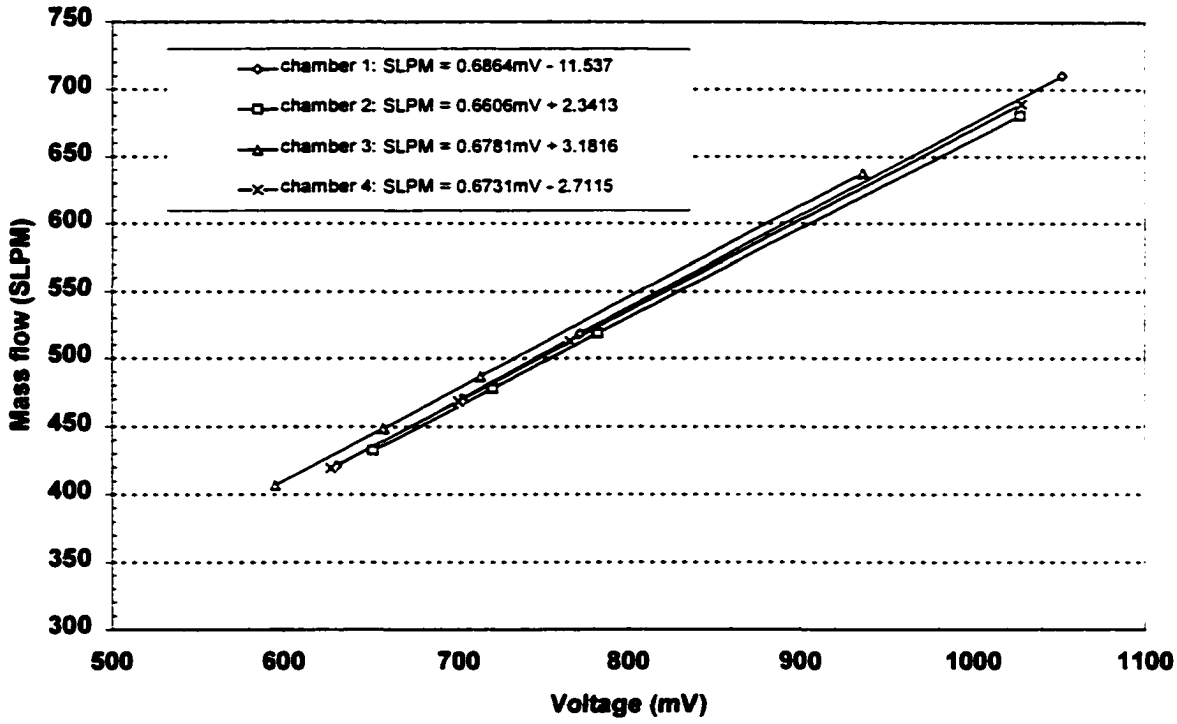

Mass flow as a function of voltage for the four calorimeter chambers. $R^2 = 1$ for all the functions.

2. Oxygen analyzer

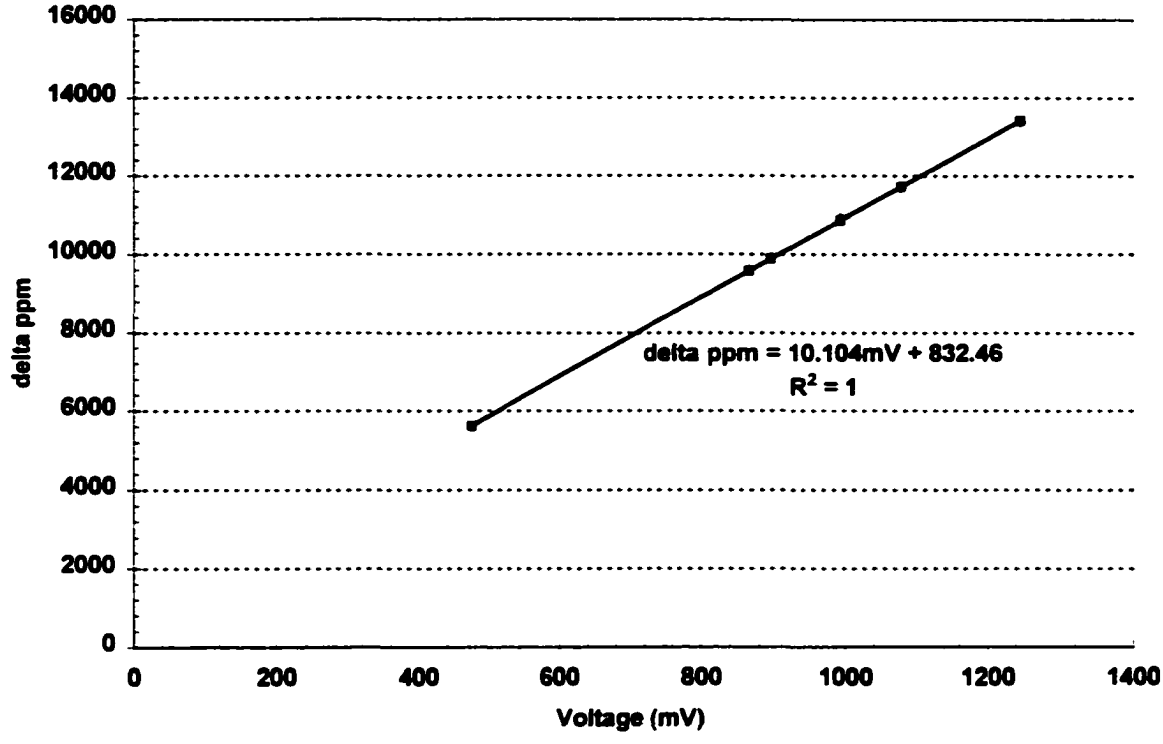

Delta ppm as a function of voltage for the paramagnetic oxygen analyzer

3. Carbon dioxide analyzer

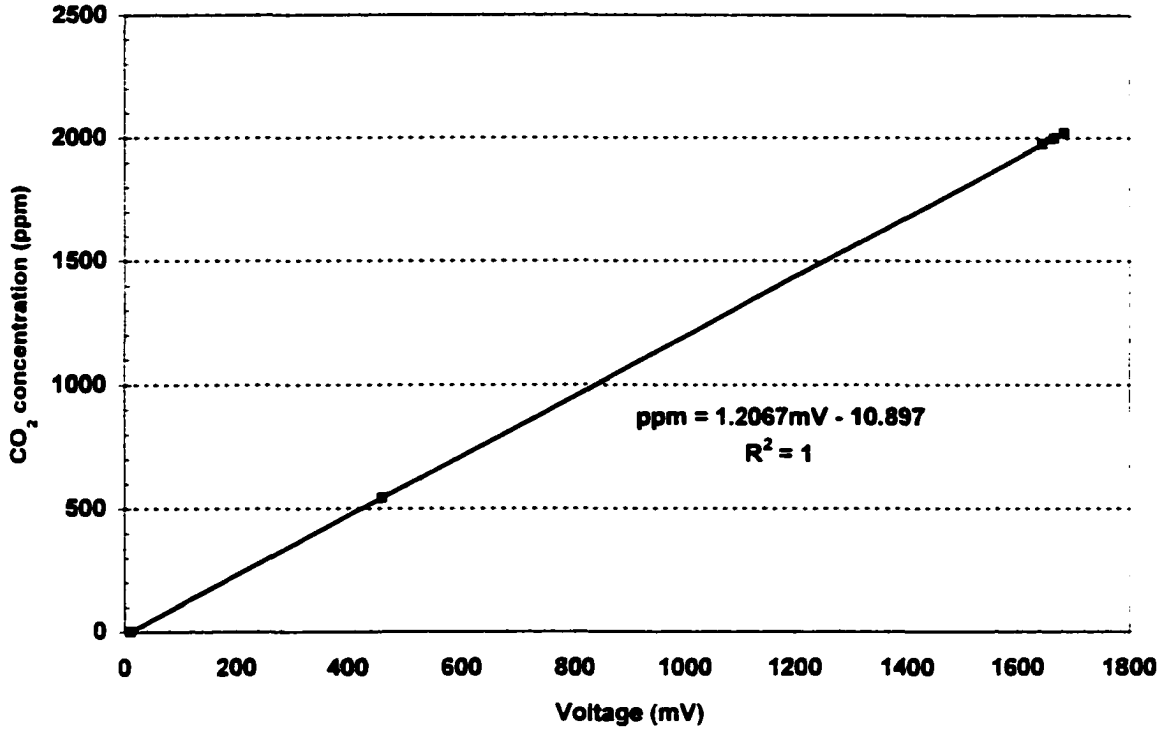

Carbon dioxide concentration (CO_2, ppm) as a function of voltage for the CO_2 analyzer

4. Dew point hygrometer

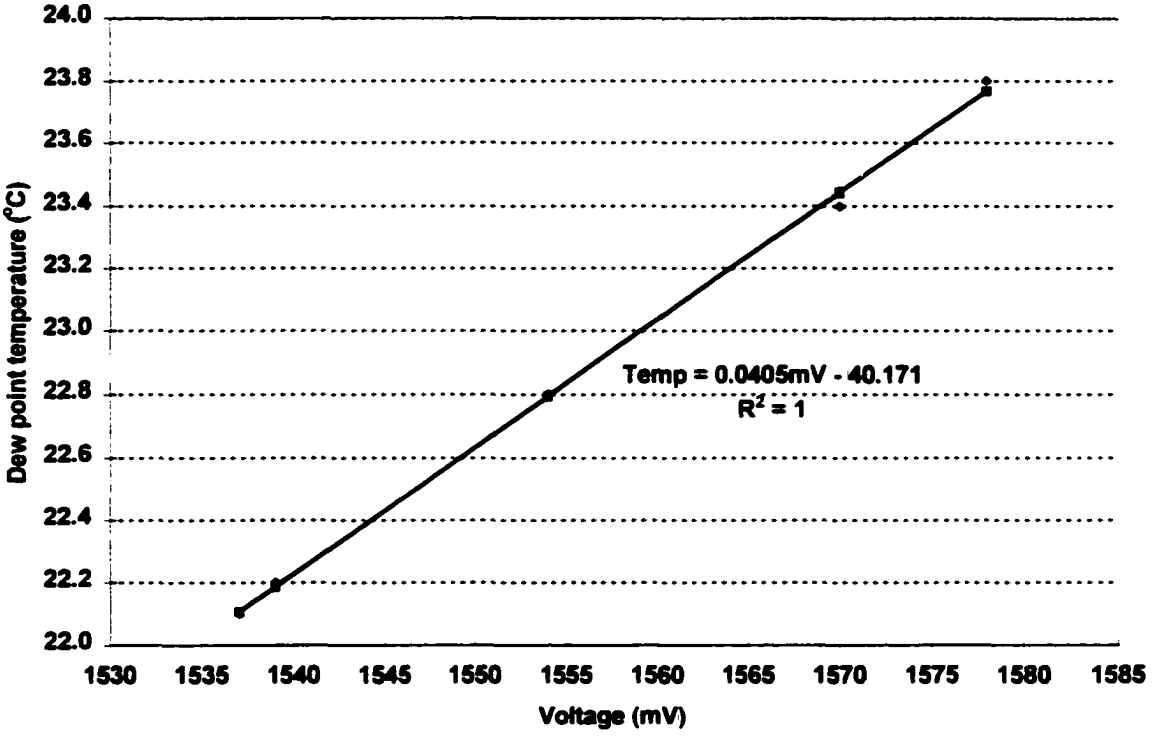

Dew point temperature as a function of voltage for the dew point hygrometer

APPENDIX 3

DYNAMIC BEHAVIOR OF DAILY CALIBRATION OF THE OXYGEN AND CARBON DIOXIDE GAS ANALYZERS DURING THE COURSE OF SOME TRIALS

1. Oxygen analyzer

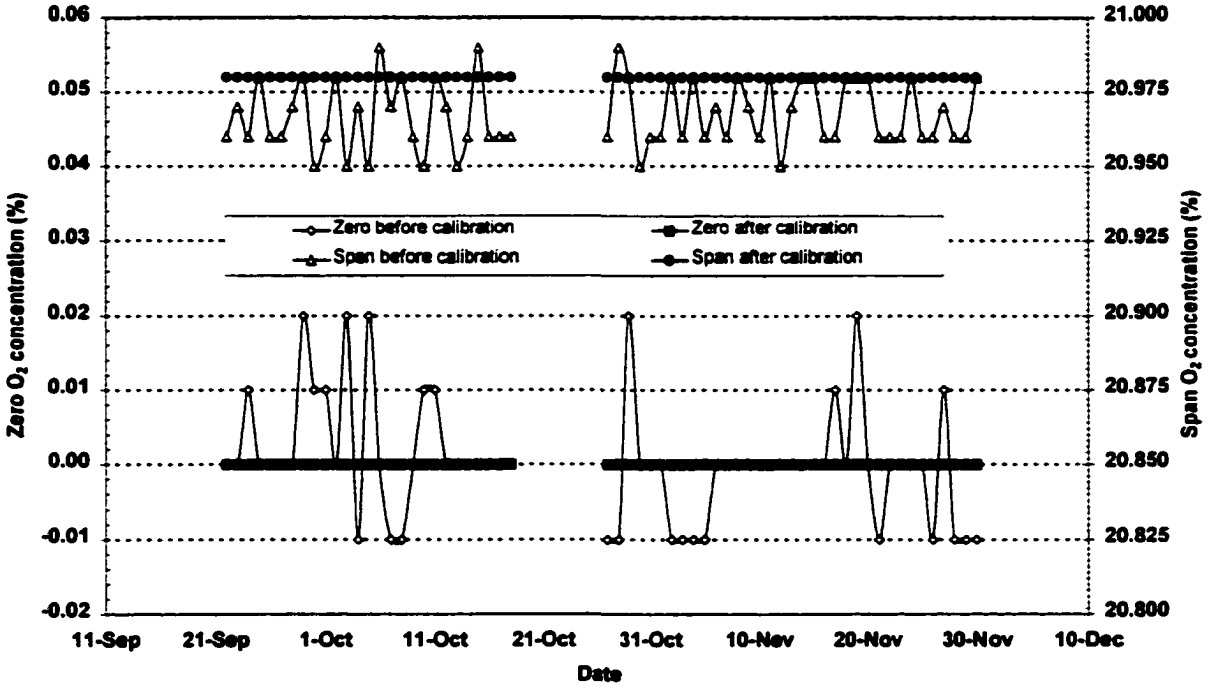

Behavior of the oxygen (O_2) analyzer during zero (99.999% nitrogen) and span (20.98% oxygen) gas calibrations during the course of experiments. The expected readings after zero and span gas calibrations were 0 and 20.89%, respectively.

Oxygen analyzer

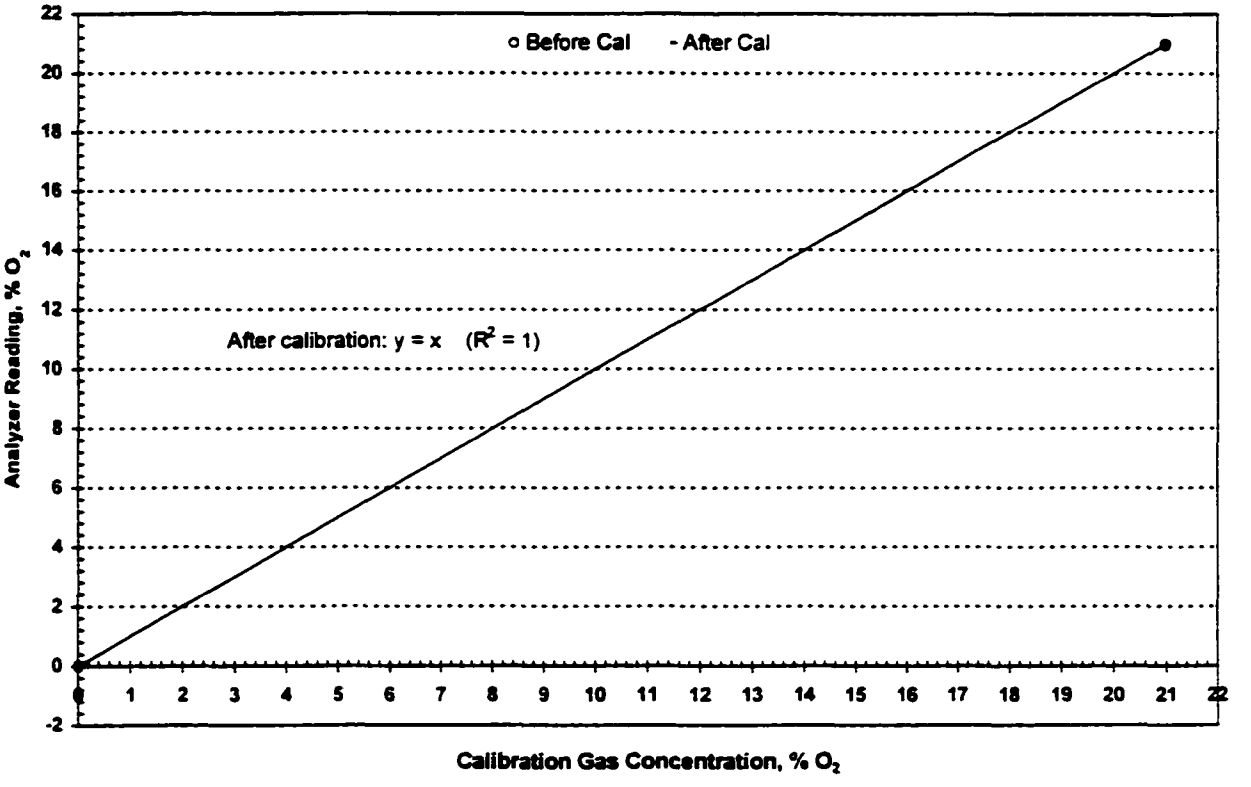

Relationship between the analyzer readings and calibration gas or reference (0% O_2 for zero gas and 20.98% O_2 for span gas) before and after calibration during the course of experiments. The two lines overlap.

2. Carbon dioxide analyzer

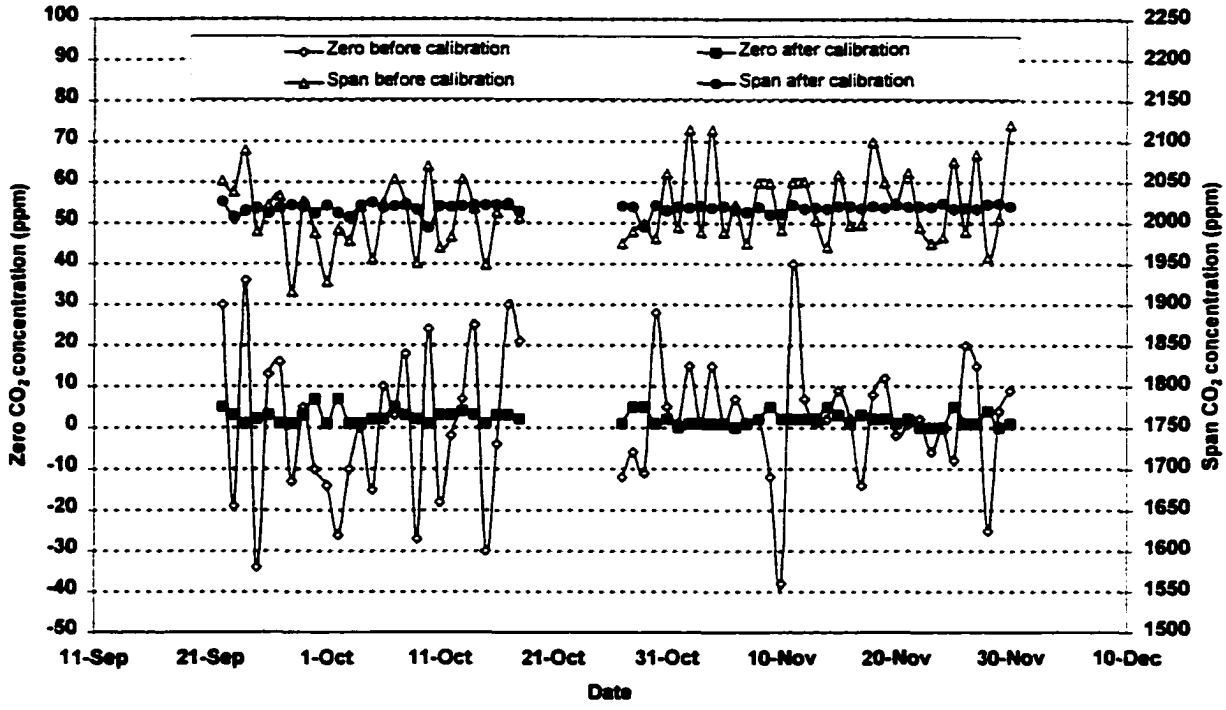

Behavior of the carbon dioxide (CO_2) analyzer during zero (99.999% nitrogen) and span (2019 ppm CO_2 and nitrogen balance) gas calibrations during the course of experiments. The expected readings after zero and span gas calibrations were 0 and 2019 ppm, respectively.

Carbon dioxide analyzer

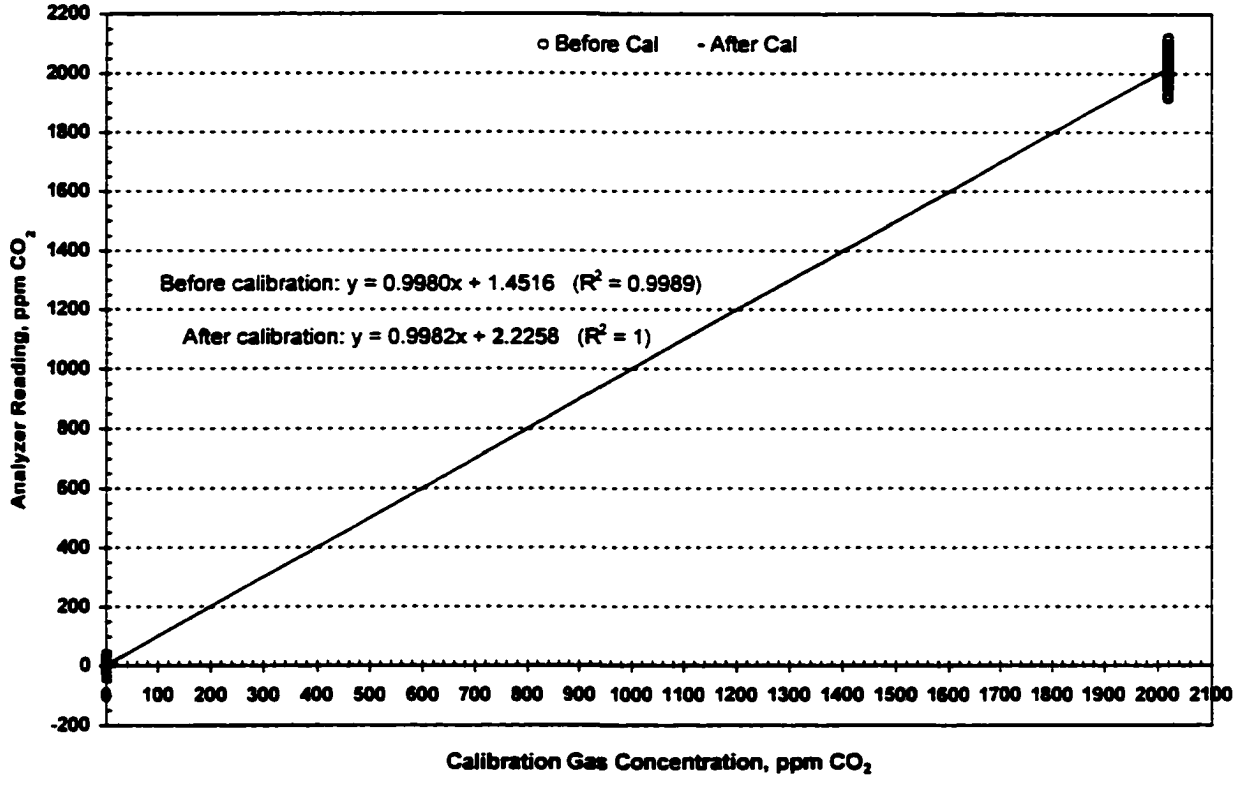

Relationship between the analyzer readings and calibration gas or reference (0 ppm CO_2 for zero gas and 2019 ppm CO_2 for span gas) before and after calibration during the course of experiments. The two lines overlap.

APPENDIX 4.

DYNAMIC PROFILES OF HEAT AND MOISTURE PRODUCTION OF PULLETS AND LAYERS DURING VARIOUS SELECTED TRIALS

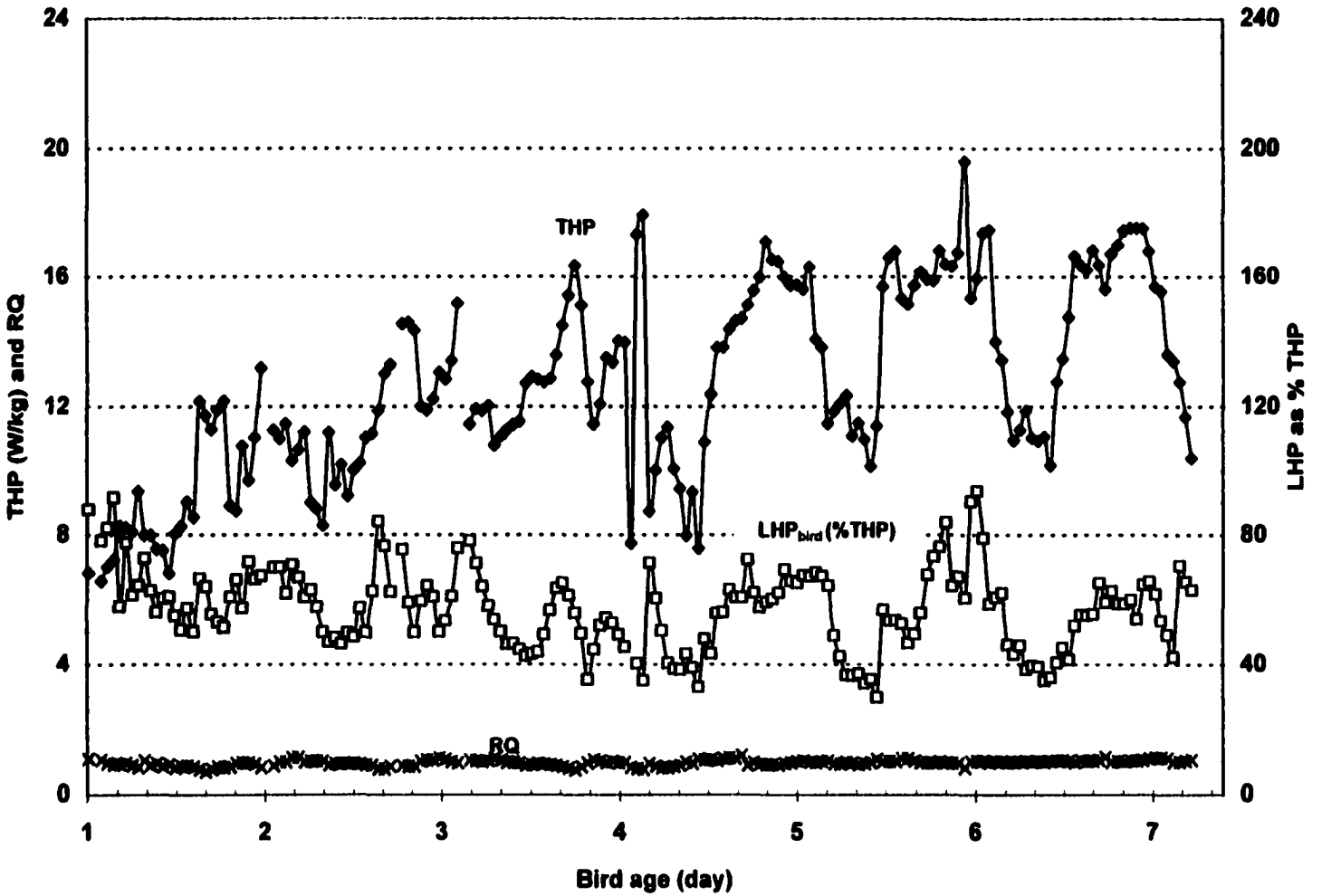

Dynamic profiles of total heat production rate (THP), respiratory quotient (RQ), and latent heat production rate of the *bird* (LHP_{bird}) as % THP for ad-lib fed 1-week old W-36 pullets under 30-32°C temperature and 35-50% relative humidity. Birds had water from nipple drinkers. THP and RQ are averaged over four chambers while LHP_{bird} is averaged over two chambers.

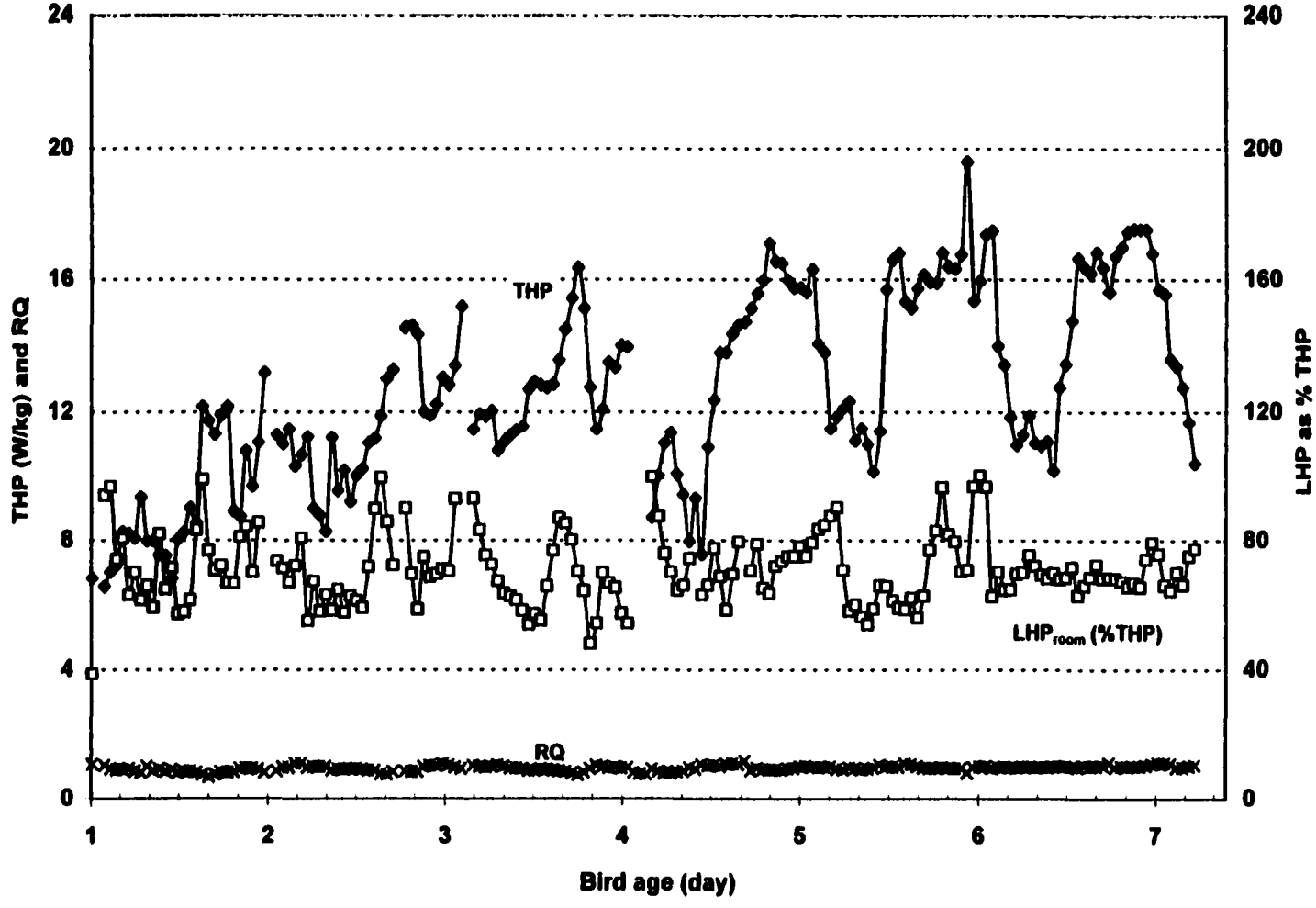

Dynamic profiles of total heat production rate (THP), respiratory quotient (RQ), and latent heat production rate of the *room* (LHP_{room}) as % THP for ad-lib fed 1-week old W-36 pullets under 30-32°C temperature and 35-50% relative humidity. Birds had water from nipple drinkers. THP and RQ are averaged over four chambers while LHP_{room} is averaged over two chambers.

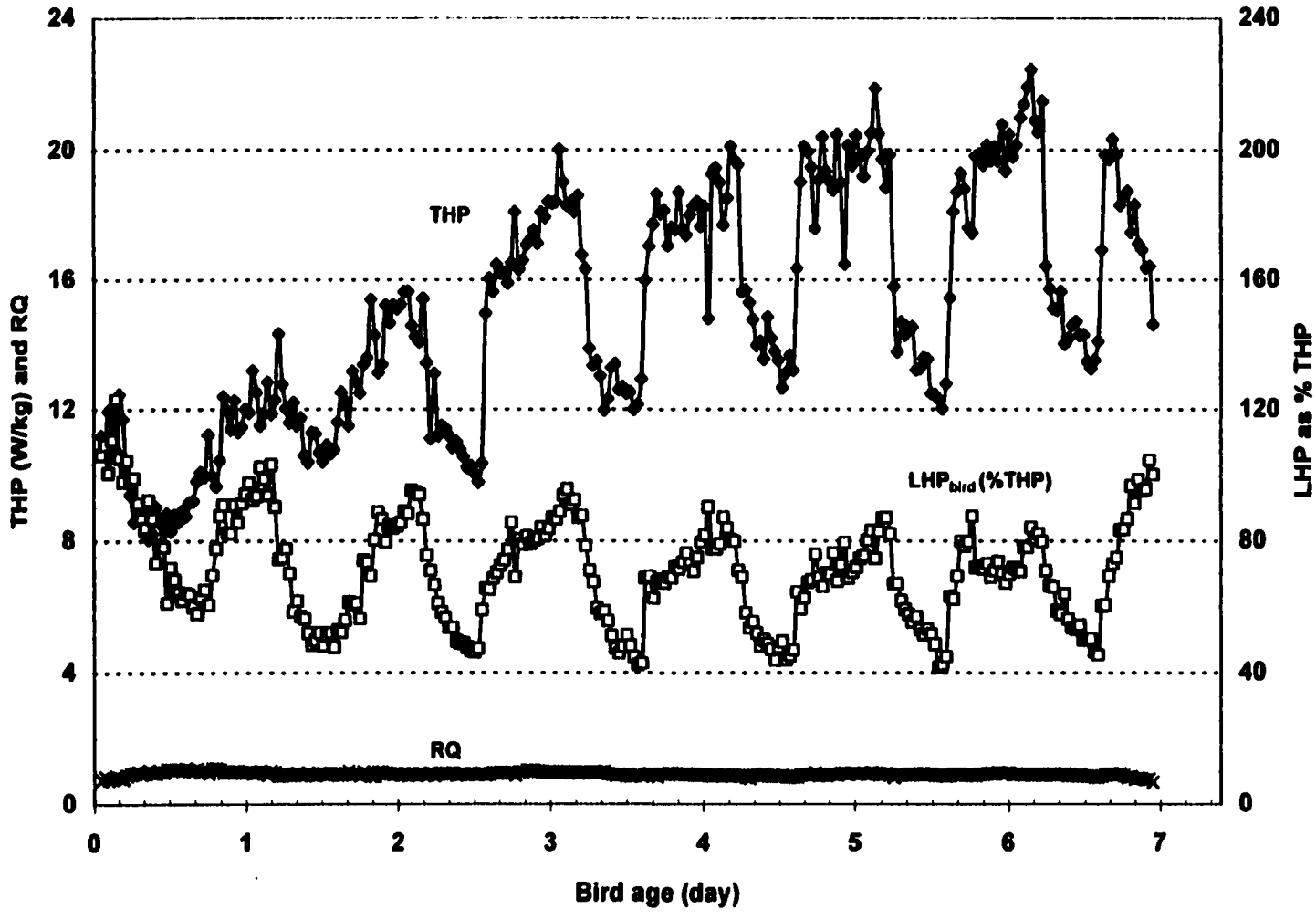

Dynamic profiles of total heat production rate (THP), respiratory quotient (RQ), and latent heat production rate of the *bird* (LHP_{bird}) as % THP for ad-lib fed 1-week old W-98 pullets under 30-32°C temperature and 35-50% relative humidity. Birds had water from nipple drinkers. THP and RQ are averaged over four chambers while LHP_{bird} is averaged over two chambers.

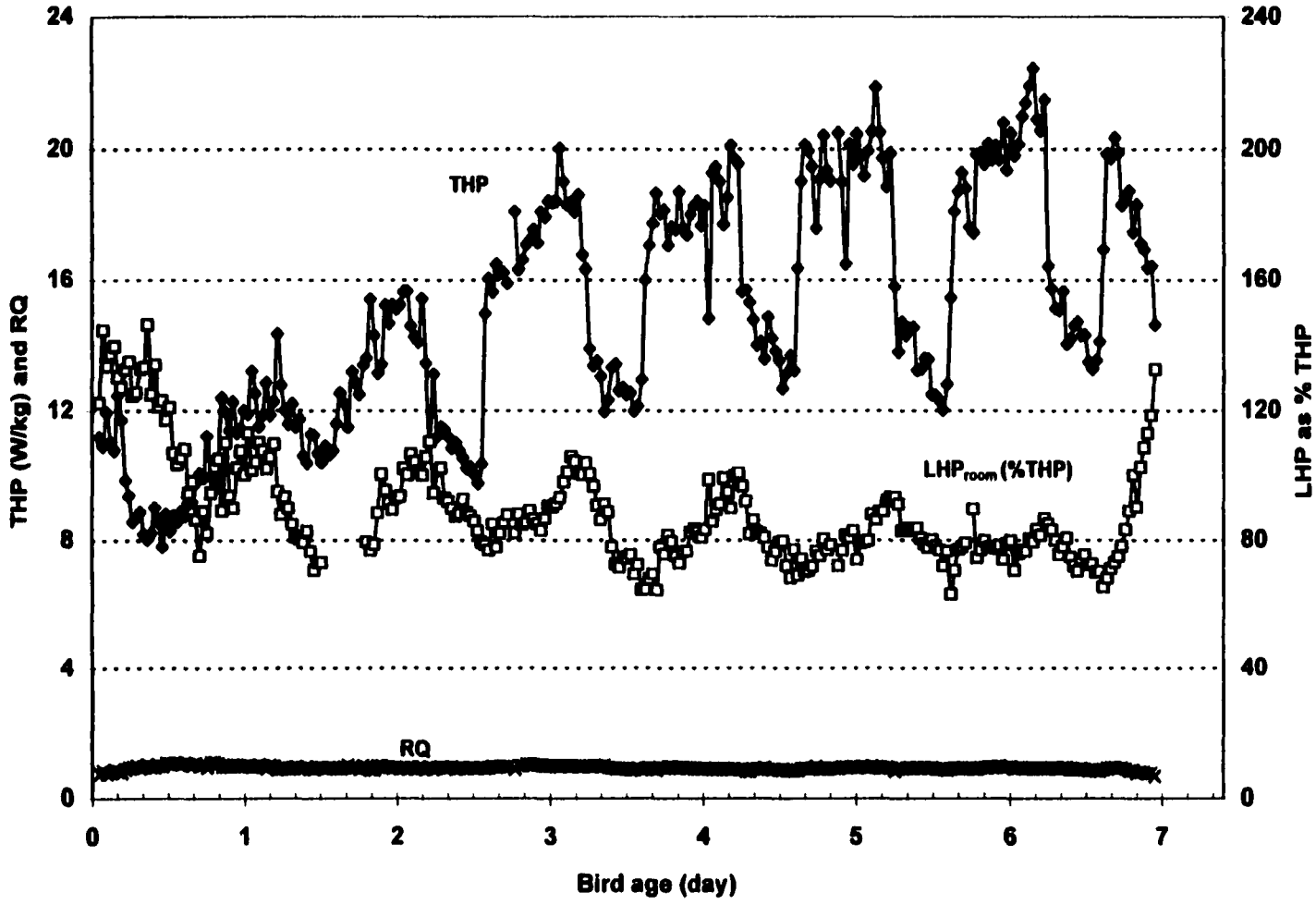

Dynamic profiles of total heat production rate (THP), respiratory quotient (RQ), and latent heat production rate of the *room* (LHP_{room}) as % THP for ad-lib fed 1-week old W-98 pullets under 30-32°C temperature and 35-50% relative humidity. Birds had water from nipple drinkers. THP and RQ are averaged over four chambers while LHP_{room} is averaged over two chambers.

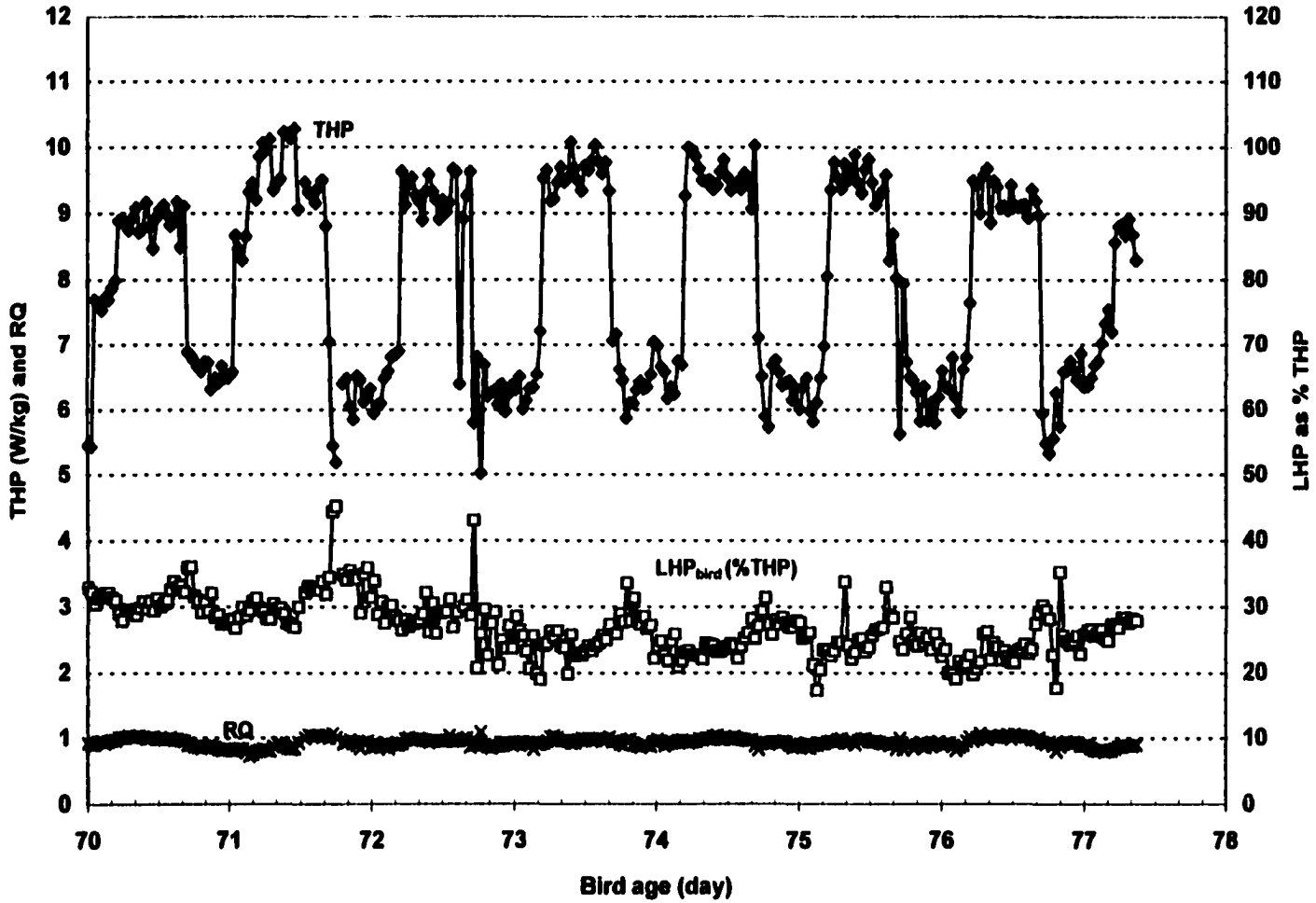

Dynamic profiles of total heat production rate (THP), respiratory quotient (RQ), and latent heat production rate of the *bird* (LHP_{bird}) as % THP for ad-lib fed 10-week old W-36 pullets under 21°C temperature and 35-50% relative humidity. Birds had water from nipple drinkers. THP and RQ are averaged over four chambers while LHP_{bird} is averaged over two chambers.

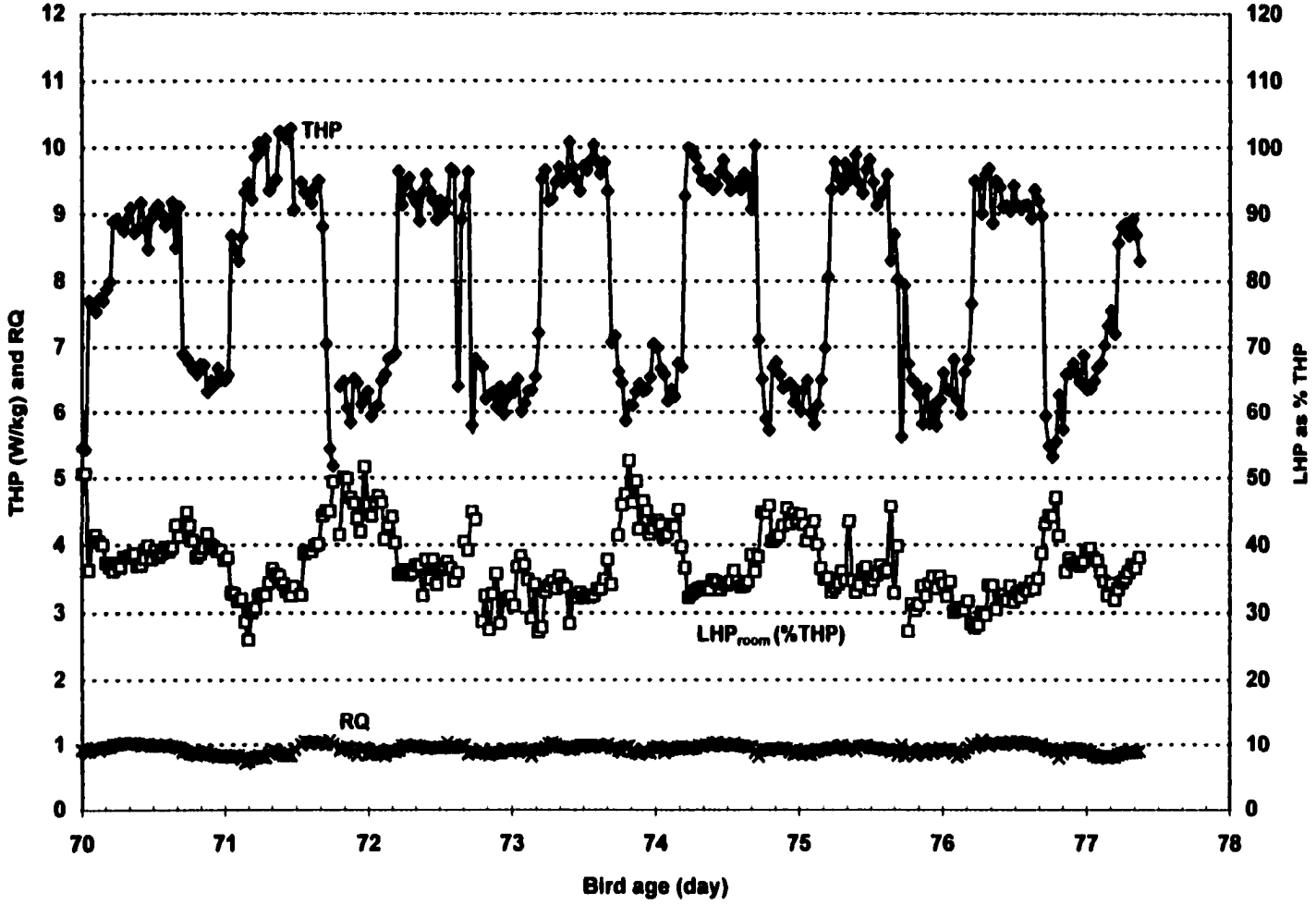

Dynamic profiles of total heat production rate (THP), respiratory quotient (RQ), and latent heat production rate of the *room* (LHP_{room}) as % THP for ad-lib fed 10-week old W-36 pullets under 21°C temperature and 35-50% relative humidity. Birds had water from nipple drinkers. THP and RQ are averaged over four chambers while LHP_{room} is averaged over two chambers.

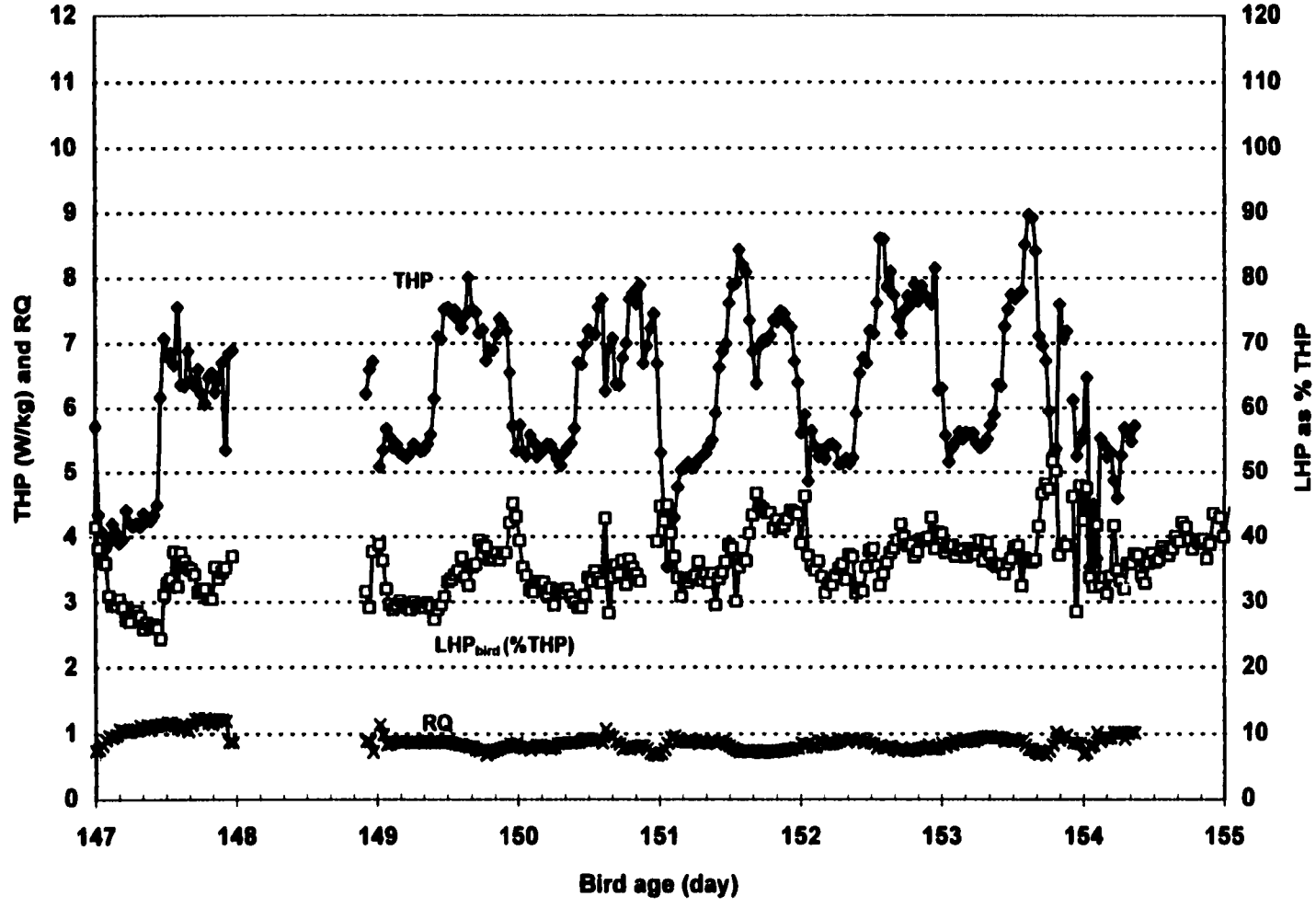

Dynamic profiles of total heat production rate (THP), respiratory quotient (RQ), and latent heat production rate of the *bird* (LHP_{bird}) as % THP for ad-lib fed 21-week old W-36 layers under 24°C temperature and 35-50% relative humidity. Birds had water from nipple drinkers. THP and RQ are averaged over four chambers while LHP_{bird} is averaged over two chambers.

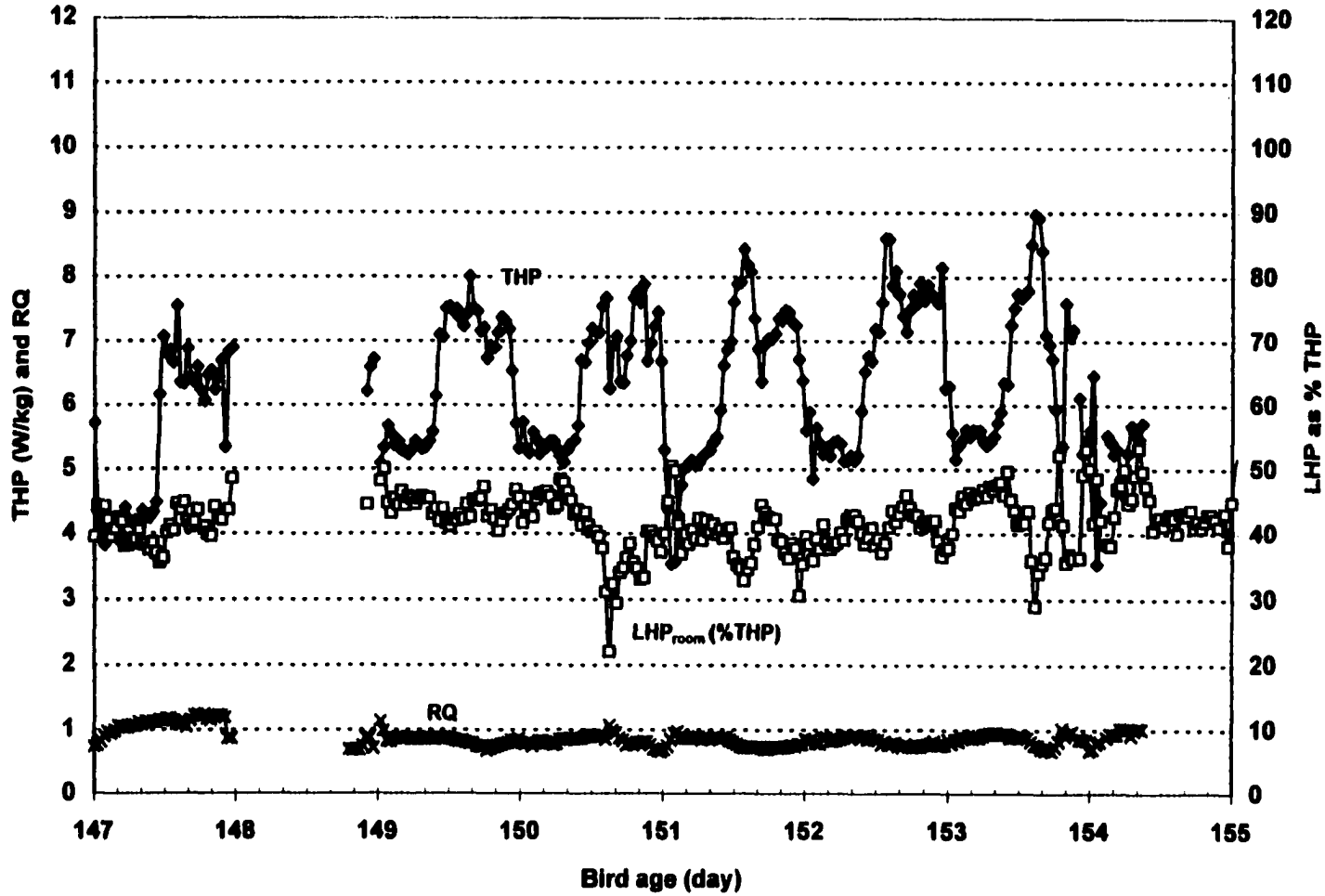

Dynamic profiles of total heat production rate (THP), respiratory quotient (RQ), and latent heat production rate of the *room* (LHP_{room}) as % THP for ad-lib fed 21-week old W-36 layers under 24°C temperature and 35-50% relative humidity. Birds had water from nipple drinkers. THP and RQ are averaged over four chambers while LHP_{room} is averaged over two chambers.

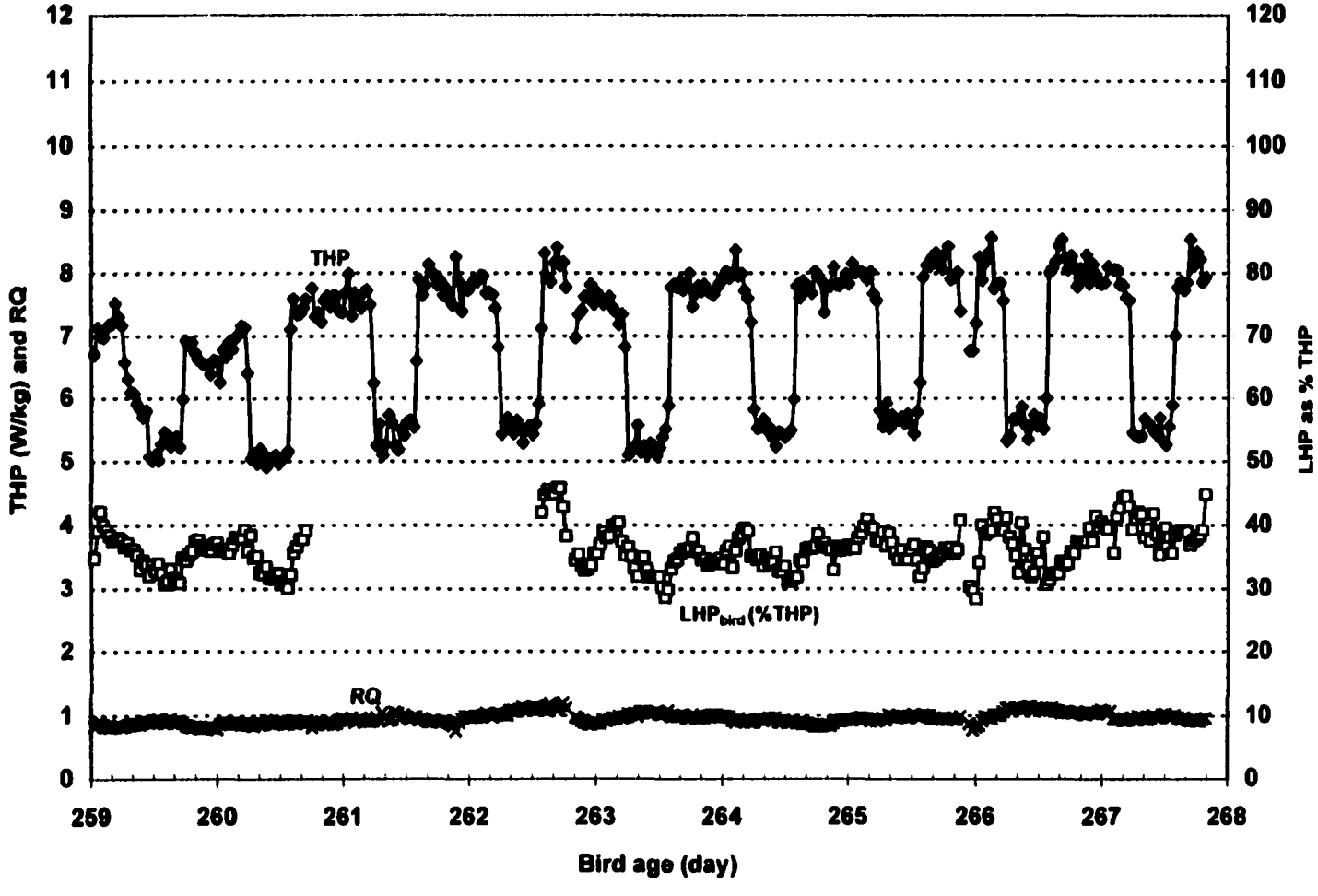

Dynamic profiles of total heat production rate (THP), respiratory quotient (RQ), and latent heat production rate of the *bird* (LHP_{bird}) as % THP for ad-lib fed 37-week old W-36 layers under 24°C temperature and 35-50% relative humidity. Birds had water from nipple drinkers. THP and RQ are averaged over four chambers while LHP_{bird} is averaged over two chambers.

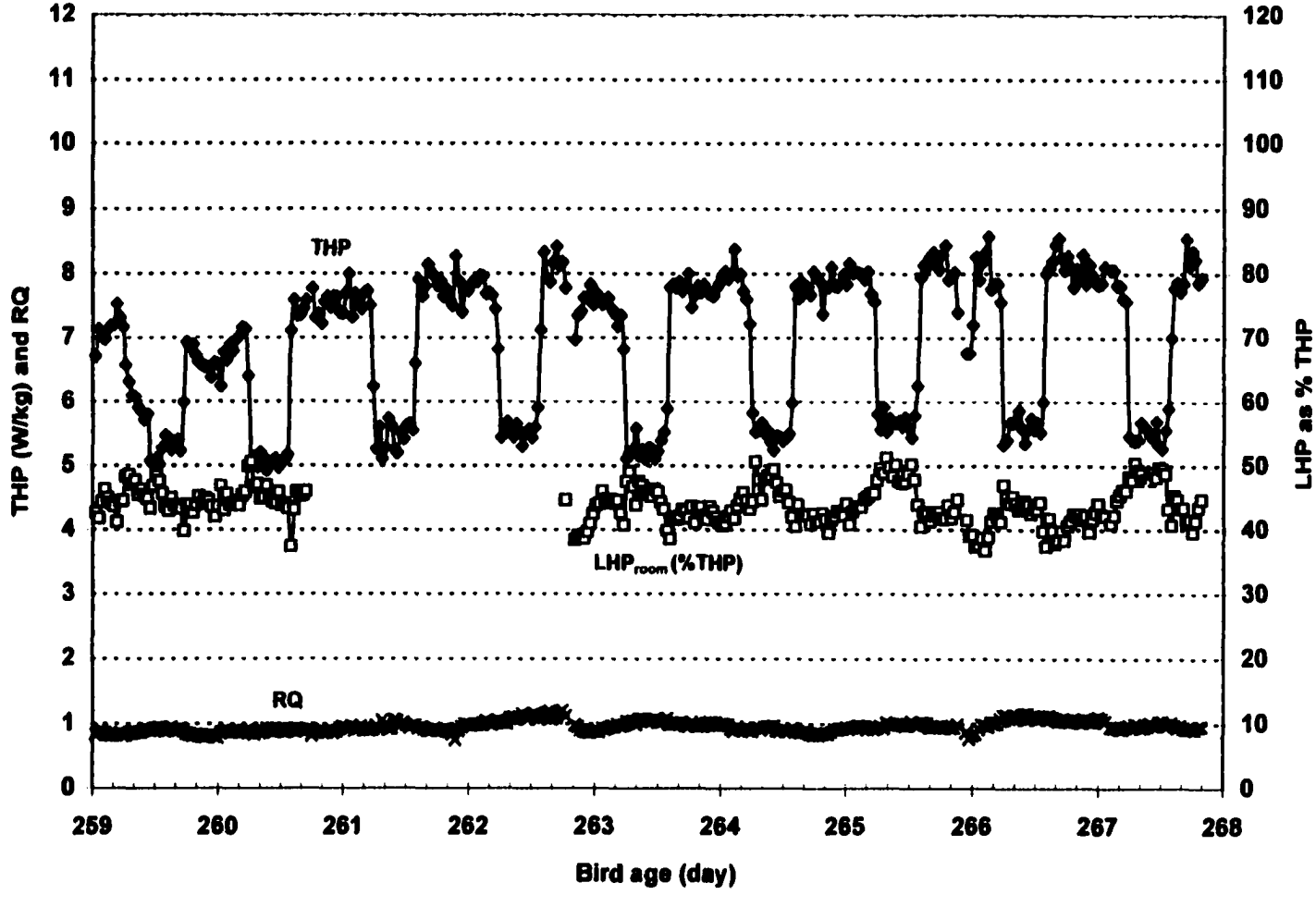

Dynamic profiles of total heat production rate (THP), respiratory quotient (RQ), and latent heat production rate of the *room* (LHP_{room}) as % THP for ad-lib fed 37-week old W-36 layers under 24°C temperature and 35-50% relative humidity. Birds had water from nipple drinkers. THP and RQ are averaged over four chambers while LHP_{room} is averaged over two chambers.

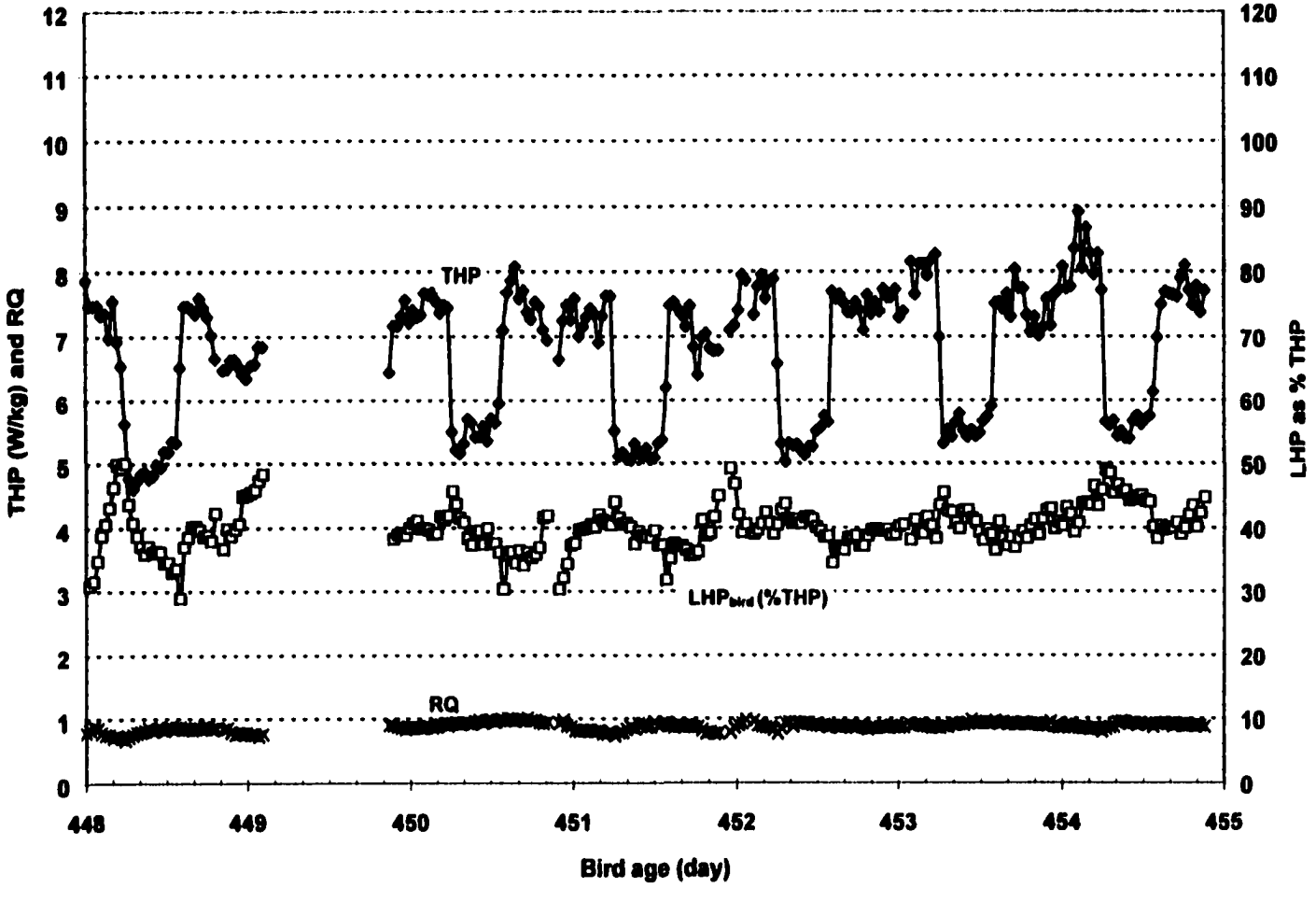

Dynamic profiles of total heat production rate (THP), respiratory quotient (RQ), and latent heat production rate of the *bird* (LHP_{bird}) as % THP for ad-lib fed 64-week old W-36 layers under 24°C temperature and 35-50% relative humidity. Birds had water from nipple drinkers. THP and RQ are averaged over four chambers while LHP_{bird} is averaged over two chambers.

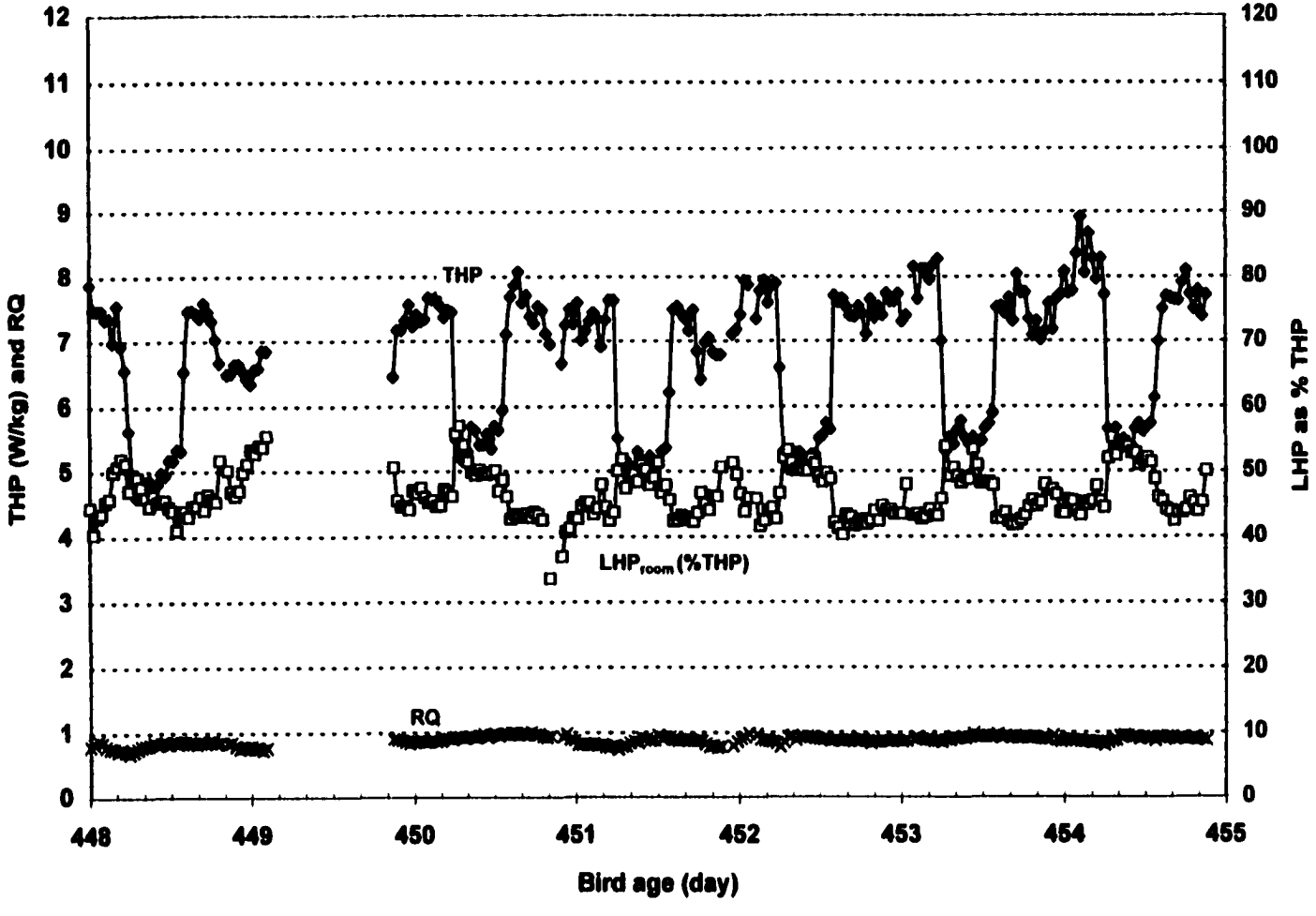

Dynamic profiles of total heat production rate (THP), respiratory quotient (RQ), and latent heat production rate of the *room* (LHP_{room}) as % THP for ad-lib fed 64-week old W-36 layers under 24°C temperature and 35-50% relative humidity. Birds had water from nipple drinkers. THP and RQ are averaged over four chambers while LHP_{room} is averaged over two chambers.

AKNOWLEDGEMENTS

Great support, inspiration and contribution from several people have enabled me to accomplish the work contained in this dissertation. I wish to express my sincere gratitude to my major professor, Dr. Hongwei Xin, for the professional guidance and friendship exercised throughout the course of my Ph.D program. He has undoubtedly empowered me with knowledge and skills through his tireless professional guidance.

I would also like to thank my entire Program of Study team who advised and guided me towards attaining quality education: Drs. Ron Nelson; Steven Hoff; Yuhong Yang and Jay Harmon. Your patience in reading this manuscript and advancing constructive suggestions is highly appreciated. I would like to thank Dr. Manuel Puma and Mr. Nelson S. Kabomo for giving me help when I needed it most during various aspects of my research work. The American Society of Heating, Refrigeration and Air-conditioning Engineers (ASHRAE) is acknowledged with gratitude for funding the research project. Farmegg Products, Humboldt, Iowa, is recognized and thanked for providing birds and feed. I cannot fail to recognize the Agricultural and Biosystems Engineering Department for giving me the opportunity to pursue my studies with Iowa State University.

Lastly, I would like to thank my fiancee, Keneilwe Tawana, for her patience throughout my studies. I would also like to thank my parents, brothers, sisters and friends, whose love and support gave me the all-time courage.